

Exhaled breath analysis in exercise and health

by

Liam Michael Heaney

A Doctoral Thesis

Submitted in partial fulfilment of the requirements for the award of
Doctor of Philosophy of Loughborough University

March 2016

© by Liam Michael Heaney (2016)

ABSTRACT

Research in the field of exhaled breath analysis is developing rapidly and is currently focussed on disease diagnosis and prognosis. The ability to identify early onset of life-threatening diseases, by a subtle change in exhaled profile that is picked up through a non-invasive measure, is of clinical interest. However, implementation of exhaled breath analysis can extend further beyond disease diagnosis and/or management. Using a non-invasive and rapid sample collection with high sensitivity, breath analysis may be seen to have potential benefit to the wider community. This research describes preliminary investigations into exhaled breath in exercise-based scenarios that aims to translate current breath analysis methodologies into a sport and exercise medicine context.

An adaptive absorbent-based breath sampling methodology was used to collect a total of 220 breath samples from 54 participants over 3 studies. Breath volatiles were analysed using thermal desorption-gas chromatography-mass spectrometry. Data were analysed with targeted, and multivariate metabolomics-based approaches.

Potential health impacts to high performance and recreational swimmers exposed to chlorinated water was studied. Following preliminary and scoping studies, 19 participants were sampled before a 30 min swim, and a further 5 times for 10 hrs after swimming. Environmental and control samples were also collected. Concentrations of chlorine-based disinfection by-products were observed to increase by up to a median of 121-fold, and take up to 8.5 hrs to return to pre-swimming levels. Metabolomic profiling identified the monoterpene geranylacetone to be a discriminant variable in samples taken 10 hrs after swimming. Geranylacetone is associated with membranes and extracellular fluids and an upregulated trend was observed across the five sampling time points post-swimming. Further research with an appropriately stratified and powered cohort ($n=38$) was recommended.

The effects of intense exercise on breath profiles was explored for the possible use of breath analysis for exercise science with elite performance-based medicine. Twenty-nine participants provided exhaled breath samples before

undergoing a maximal oxygen uptake (fitness) test and then provided 2 additional samples over the following 1 hr period. High and low fitness groupings, deemed by oxygen uptake values, were compared for exhaled metabolites. Lower exhaled acetone and isoprene were observed in participants with greater absolute oxygen uptake leading to a hypothesis for a non-invasive breath based fitness test.

Finally, an interface for breath-by-breath analysis using a transportable mass spectrometer was developed. A controlled change in exhaled profiles was achieved through the ingestion of a peppermint oil capsule. Menthone was measured on-line and monitored for up to 10 hrs post-administration. Sixteen participants enabled the system to be demonstrated as exhaled menthone was at elevated concentrations for at least 6 hrs. Validation against thermal desorption-gas chromatography-mass spectrometry confirmed the system to be detecting metabolites at the sub- $\mu\text{g L}^{-1}$ range.

One journal article has been published for the work detailed from Chapter 6 in this thesis:

Heaney LM, Ruszkiewicz DM, Arthur KL, Hajithekli A, Aldcroft C, Lindley MR, Thomas CLP, Turner MA, Reynolds JC. Real-time monitoring of exhaled breath volatiles using atmospheric pressure chemical ionization on a compact mass spectrometer. *Bioanalysis* 2016;doi: 10.4155/bio-2016-0045

ACKNOWLEDGMENTS

It is true to say that the work completed and contained in this thesis could not have been achieved without the continued help from a variety of individuals.

Firstly, I would like to thank my supervisors Professor Paul Thomas and Dr Martin Lindley for providing me with the opportunity to complete this course of study. Although there have been some tough scenarios, at all times it has prevailed and the research continued. The Graduate School at Loughborough University must also be thanked, without the PhD studentship award and the associated funding I would have never been able to fulfil my potential and continue into a, hopefully, extensive and successful academic career.

Perhaps the most important part of my time during doctoral training was the support that came from my close friends. It is undoubtable that I would not have got through some of the tough periods without the presence of Caitlyn Da Costa in the lab with me, especially toward the end where we bludgeoned our way to the finish line. However, all of my fellow lab colleagues deserve thanks for their help, especially in my first years of learning new techniques. In addition to my lab friends, all of my friends I have met over the years at conferences and events, you made it all the more worthwhile!

To name all that were additive to my experience would require too many pages to pay for printing! I would like to personally thank Benjamin Michael Kelly for his dry wit and terrible humour, the constant reminder of being in the North West was always well received. A thank you must also be given to all of those from the SSEHS PhD cohort, including all the guys I lived with at 10 Adam Dale over the years. Lastly, a thank you to every lad I've played rugby with over my entire lifetime, it built me to be the man I am now and helped me get through to the end.

A special thank you must also be extended to each and every participant that gave up their precious time to help me fulfil my research goals.

To finish, a massive thank you to all my family.

I dedicate this thesis to those who were not able to see me finish it:

My grandparents;

Alan Brooke

1929 – 2012

Bronwen Brooke

1931 – 2012

My friend;

Ben Smith

1987 – 2015

Altrincham Grammar School for Boys class of 2006

Loughborough University class of 2009

And my kitten;

Freddie

November 2015 – May 2016

Forever missed, never forgotten.

If— by Rudyard Kipling

If you can keep your head when all about you
Are losing theirs and blaming it on you,
If you can trust yourself when all men doubt you,
But make allowance for their doubting too;
If you can wait and not be tired by waiting,
Or being lied about, don't deal in lies,
Or being hated, don't give way to hating,
And yet don't look too good, nor talk too wise:

If you can dream - and not make dreams your master;
If you can think - and not make thoughts your aim;
If you can meet with Triumph and Disaster
And treat those two impostors just the same;
If you can bear to hear the truth you've spoken
Twisted by knaves to make a trap for fools,
Or watch the things you gave your life to, broken,
And stoop and build 'em up with worn-out tools:

If you can make one heap of all your winnings
And risk it on one turn of pitch-and-toss,
And lose, and start again at your beginnings
And never breathe a word about your loss;
If you can force your heart and nerve and sinew
To serve your turn long after they are gone,
And so hold on when there is nothing in you
Except the Will which says to them: 'Hold on!'

If you can talk with crowds and keep your virtue,
'Or walk with Kings - nor lose the common touch,
If neither foes nor loving friends can hurt you,
If all men count with you, but none too much;
If you can fill the unforgiving minute
With sixty seconds' worth of distance run,
Yours is the Earth and everything that's in it,
And - which is more - you'll be a Man, my son!

TABLE OF CONTENTS

Chapter one: General introduction and thesis direction	1
1.1 Scope of doctoral thesis	1
1.2 The premise of exhaled breath analysis	1
1.3 Exhaled breath in sport and exercise	3
1.3.1 The importance of sport and exercise science	3
1.3.2 Current uses of exhaled breath with exercise	4
Maximal oxygen uptake	4
Exhaled breath condensate	8
Exhaled nitric oxide	9
Exhaled volatilome	10
Metabolomics	11
Chlorine related insults to swimmers and swimming pool staff	12
1.3.3 Potential uses for exhaled breath analysis in exercise science	14
1.4 References	15
Chapter two: Physiological and analytical theory	25
2.1 Respiratory physiology and VOC exchange	25
2.1.1 Structure and function of the lungs	25
Airflow through the lung	25
Mechanics of breathing	26
The blood-gas interface	28
Respiratory responses to exercise	30
2.2 Exhaled VOC breath analysis	30
2.2.1 The modern era	30
2.2.2 Considerations with exhaled breath	31
2.2.3 Current uses of exhaled breath analysis	33

2.2.4	Sample collection and analysis methods.....	34
	Exhaled breath gases	34
	Adaptive breath sampler for alveolar air.....	35
	Collection and analysis of VOCs using thermal desorption technologies	36
	Solid-phase micro extraction.....	36
2.3	Gas chromatography-mass spectrometry in exhaled breath analysis	38
2.3.1	Introduction	38
2.3.2	Separation, elution and efficiency	39
2.3.3	The rate theory of chromatography	42
	The van Deemter equation.....	42
	The Golay equation	46
	van Deemter plots	46
	Kovats retention index.....	48
	Resolution	48
	Open tubular (capillary) columns.....	49
	Programmed temperature in gas chromatography	50
2.3.4	Mass spectrometry	51
	Sample ionisation	52
	Mass analysers in mass spectrometry	53
	Quadrupole mass filter	54
	Quadrupole ion trap.....	56
	Ion detection	58
2.4	Thermal desorption-gas chromatography-mass spectrometry.....	59
2.5	Proposed experiments.....	59
2.6	References	60
Chapter three: General methods		65
3.1	Exhaled VOC sampling.....	65

3.1.1	Exhaled VOC sampling mask preparation	65
3.1.2	Thermal desorption tube preparation	65
3.2	Breath sampling protocol	66
3.2.1	Air supply to the participant.	66
3.2.2	Sampling procedure.	67
	Exhaled breath sampling.....	67
	Environmental sampling.....	68
3.3	Exhaled VOC sample analysis	69
3.3.1	Analytical methods.....	69
	Pre-analysis preparation.....	70
	Thermal desorption.....	70
	Gas chromatography	73
	Mass spectrometry	73
3.3.2	Daily quality control procedures	73
	Instrument checks	73
3.3.3	Data processing	75
	Targeted GC-MS compounds	75
	Metabolomic profiling of GC-MS compounds	75
3.3.4	Statistical analyses	80
	Targeted analyses.....	80
	Multivariate metabolomic profiling.....	80
	Scaling	81
	Preliminary principal components analysis (PCA)	81
	Orthogonal partial least squares-discriminant analysis (OPLS-DA).....	81
3.3.5	Analysis of target components – candidate biomarkers	82
3.4	Acknowledgments.....	82
3.5	References	82

3.6	Appendix 1: details of portable breath sampler	84
Chapter four: Exhaled breath monitoring in healthy participants after exercise in a swimming pool environment: a targeted and metabolomics approach		
4.1	Introduction	86
4.2	Study aims:.....	87
4.2.1	Primary aim	87
4.2.2	Secondary aim:	88
4.3	Methods.....	88
4.3.1	Ethical approval	88
4.3.2	Characterisation of swimming pool environment.....	88
4.3.2	Preliminary study	89
4.3.2	Refinement study.....	92
4.4	Main experiment.....	95
4.4.1	Experimental design	95
4.4.2	Participant information.....	96
4.4.3	Exercise protocol.....	97
4.4.4	Sampling protocol	97
4.4.5	Sampling methods.....	97
	Exhaled breath VOCs	97
	Environmental VOCs	97
	VOC sample analysis	98
4.4.6	Statistical analyses	98
4.4.7	Calibration of target DBPs.....	99
4.4.8	Data processing.....	102
	Targeted compounds.....	102
	Metabolomic profiling.....	102
4.5	Results.....	102

4.5.1	Exercise performance and environmental conditions.....	102
4.5.2	DBP standard calibrations	102
4.5.3	DBPs in exhaled VOC samples.....	105
	Variations in elimination profiles.....	105
	Delayed elimination	106
	First-order elimination	106
4.5.4	Metabolomic profiling of exhaled VOCs.....	113
4.6	Discussion	121
4.7	Follow on research.....	124
4.8	Acknowledgments.....	126
4.9	References	126
4.10	Appendix 1: certificate of analysis for disinfection by-product standard mixture.....	130
4.11	Appendix 2: additional figure	131
Chapter five: Exhaled breath profiles and intense exercise		132
5.1	Introduction	132
5.2	Methods.....	135
5.2.1	Ethical clearance	135
5.2.2	Participant information.....	135
5.2.3	Experimental design	135
5.2.4	Exhaled VOC collection	136
5.2.5	Maximal oxygen uptake ($\dot{V}O_{2max}$) test protocol.....	136
5.2.6	VOC sample analysis	137
5.2.7	Statistical analyses	138
5.3	Results.....	138
5.3.1	Exercise testing.....	138
5.3.2	Metabolomic profiling analyses	142

High vs low relative VO _{2max} groups	142
High vs low absolute VO _{2max} groups	143
Candidate biomarker analysis	145
5.3.3 Predictors of fitness.....	146
5.3.4 Changes in exhaled VOCs after exercise.....	149
5.3.5 Isoprene across exercise stages.....	151
5.4 Discussion	152
5.5 References	154
Chapter six: Development of an atmospheric pressure ionisation interface for on-line, quadrupole mass spectrometric exhaled breath analysis.....	156
6.1 Introduction	156
6.2 Experimental objectives	158
6.3 Methods.....	159
6.3.1 Ethical clearance	159
6.3.2 Capsule details and mass spectral behaviour.....	159
6.3.3 Instrumentation	161
6.3.4 Preliminary GC-MS characterisation.....	162
6.3.5 Menthone elimination experiment with CMS.....	163
6.3.6 Statistical analyses	164
6.4 Results.....	164
6.4.1 GC-MS analysis of exhaled peppermint oil VOCs.....	164
6.4.2 CMS analysis of exhaled peppermint oil VOCs	168
Comparison of breathing profiles using APCI-MS and breath mask pressure	168
VOC profiles.....	169
Menthone emergence and elimination	170
Continuous real-time monitoring	170

Extended protocol	172
6.5 Discussion	174
6.6 Acknowledgments.....	176
6.7 References	176
Chapter seven: General discussion	180
7.1 Review of swimming impacts on breath profiles.....	180
7.1.1 Summary of findings.....	180
7.1.2 Recommendations for follow on studies.....	181
Relocate on-site sampling station	181
Management of exercise intensity.....	182
7.2 Review of fitness prediction breath test.....	183
7.2.1 The prospect of rapid assessment of physical fitness	183
7.2.2 Recommendations for future studies.....	184
Incorporate a longitudinal research design	184
Baseline repository	184
VOC profiles from a maximally exercised metabolism.	185
The need for on-line measurements	185
7.3 Increased cohort size	185
7.4 An on-line breath analyser for breath-by-breath monitoring.....	186
7.5 Concluding remarks.....	187
7.6 Conclusion	189
7.7 References	189

CHAPTER ONE: GENERAL INTRODUCTION AND THESIS DIRECTION

1.1 Scope of doctoral thesis

This research sought to explore the potential of the analysis of exhaled volatile organic compounds (VOCs) as a research methodology in sport and exercise science. The studies undertaken highlight the potential uses for exhaled breath analysis with athletes to assess their health and current performance capabilities, with the view to possible use of assays for personalised and/or stratified training protocols. A central aim of this research was to reflect on the prospects for breath analysis to improve health and performance monitoring as part of an exercise science routine. In addition, any beneficial advances for elite sport could translate into a wider remit of public health and treatments involving exercise. Therapy and training associated with managing chronic disease, maintaining good health and preparing elite athletes for competition is generally time constrained and so a focus on rapid analysis is required. These works aim to potentiate the development and introduction of exhaled breath analyses into exercise and health.

1.2 The premise of exhaled breath analysis

Exhaled breath is predominantly comprised of mixture of nitrogen (N₂), oxygen (O₂), carbon dioxide (CO₂), inert gases and water vapour. However, trace amounts of volatile compounds have been observed at parts per million ($> 0.1 \text{ g m}^{-3}_{(g)}$, ppm_(v/v)), parts per billion ($1 \text{ } \mu\text{g m}^{-3}_{(g)}$ to $0.1 \text{ g m}^{-3}_{(g)}$, ppb_(v/v)) and parts per trillion ($< 1 \text{ } \mu\text{g m}^{-3}_{(g)}$, ppt_(v/v)) concentrations [1,2]. Endogenous VOCs are produced during metabolic processes, transported in the circulatory system and enter the air in the lungs across the alveolar membrane. Various diseases result in disrupted metabolic pathways and it has been suggested that such changes would be apparent in the concentration of VOCs in exhaled breath. It has been proposed that, through further

research, exhaled breath analysis can be used as a non-invasive clinical diagnostic method to help assess health status [3].

The notion of exhaled breath investigation has been evident across two millennia. In circa 400 BC Hippocrates used the aroma of exhaled breath to diagnose illness in his patients, before it was known that specific volatile compounds are associated with certain diseases. For example, diabetic patients have an increased level of acetone in their breath, which holds a characteristic sweet smell [4,5]. Insulin deficiency means they are unable to metabolise glucose efficiently, so metabolism shifts toward the oxidation of fat. This action increases ketoacidosis, and acetone is formed by hepatocytes in the decarboxylation of acetoacetate (a derivative of lipolysis) under conditions of excess Acetyl-CoA [1]. These blood-borne VOCs equilibrate with the gases in the small airways of the lung, diffusing across the blood-alveoli barrier, causing them to be detectable in exhaled air.

The continuous development and enhancement of analytical technologies has allowed the capture and detection of a variety of exhaled compounds to be achieved routinely. Consequently, the use of exhaled breath analysis is being adopted by an increasing number of researchers, and the prospect of breath analysis providing the early-onset diagnosis of health conditions is one of widespread interest. The premise is that disrupted metabolism, resulting from the deterioration of cells or the growth of tumours, alters the types and concentrations of volatile compounds that can ultimately pass into the alveoli and be exhaled. The focus of this research was not to use exhaled breath for diagnostic purposes, but instead to begin the exploration of possible uses of exhaled VOC analysis in sport-and/or exercise-based situations. The underlying premise of this work is that exhaled breath analyses, with extensive development, could show utility for the monitoring of elite athletes and provide valuable information on rehabilitation from illness and/or injury for both athletes and the general population alike. Although the use of exhaled breath is common in exercise testing, with the measurement of inhaled/exhaled O₂ and CO₂ to estimate O₂ utilisation, little has been done to study exhaled VOCs; only 14 research articles that assess exhaled VOCs in an exercise environment have been published [6-19].

1.3 Exhaled breath in sport and exercise

1.3.1 The importance of sport and exercise science

It has long been established that exercise generates adaptations within the biological system, with significant increases in exercise output ability following periods of repeated exercise training. Understanding of how these adaptations occur, and the underlying mechanisms that result in improved performance characteristics, such as strength and endurance, is continually increasing as the field of sport and exercise science/medicine grows. Better characterisation of the preferential adaptations that occur as a result of different exercise interventions, i.e. training regimes, results in more sophisticated and better targeted programmes. This could benefit individuals of different phenotypes, who may fall into disparate groups of exercise capability. For elite sports people it is important to focus on sport-specific training and to push the adaptations that confer the greatest competitive advantage for each individual. Such training regimes may be focussed toward strength, for example weightlifters and power sports such as rugby, or more toward endurance, for long distance runners and cyclists. The research conducted in these areas allows these athletes, and their coaches, to adopt strategies that match the results of their exercise adaptations to the requirements of their sport or event. Such advances go beyond competitive benefits to the prevention of injury and illness and accelerated recovery from sporting injuries.

Sports science yields many benefits to public health that go beyond the sphere of elite exercise and sport. Exercise is beneficial to everyone, and the American College of Sports Medicine provides detailed recommendations for exercise testing and prescription [20] to improve general public health by increasing the exercise output of 'the masses'. The primary aim of these recommendations is to increase energy output with a hope to reduce conditions, such as type II diabetes mellitus, associated with overweight or obese individuals. Exercise is also beneficial to individuals recovering from illnesses, especially those with cardiovascular perturbations. Exercise during rehabilitation from acute episodes of conditions such as heart failure, can reduce recovery periods and ultimately improve prognosis for

the individual (see Wilson *et al.* for a review on the science behind the cardiovascular benefits of exercise [21]). The general benefit of sport is taken a step further and examined more specifically in sports and exercise/medicine. The associated underpinning science offers benefit across all sectors of society, from elite competitive sport to leisure and general well-being, and the vitally important challenges of promoting well-being and reducing exacerbations of chronic illnesses and hospital admissions in an aging population.

1.3.2. Current uses of exhaled breath with exercise

Maximal oxygen uptake

Breath analysis is used widely within research and elite sport. It is used to measure an individual's fitness level by calculating their maximal O₂ uptake, referred to as $\dot{V}O_{2max}$: the gold standard method of assessing fitness. $\dot{V}O_{2max}$ is a measure of the working muscles' ability to use the O₂ that is inhaled and transported by the circulatory system. As the body's capability of utilising O₂ increases, it allows the individual to work for longer, or at higher intensity, and is described as an improvement in the 'fitness level' for this person. Calculating the amount of O₂ that is utilised during different exercise outputs is possible due to the ratios of inspired and expired O₂ and CO₂ [22]. O₂ and CO₂, along with N₂, are the most abundant molecules present in exhaled breath and are the foundation of the majority of laboratory fitness assessments, having shaped research into exercise interventions over many decades.

The $\dot{V}O_{2max}$ test measures an individual's systemic aerobic respiration (O₂ consumption) during exercise. The test increases exercise intensity, and thus O₂ consumption, in an incremental manner with ¹stepped increases every 3 or 4 min. This allows the participant to equilibrate with the exercise intensity and reach a

¹ Some protocols implement a more gradual, but constant positive gradient of exercise intensity, often leading to shorter test times but may be argued is more amenable to individuals of a low fitness level, or with more fundamental health issues.

steady-state of O₂ consumption, provided the exercise level is below the participant's aerobic limitations.

With stepped increments, the steady state O₂ consumption will be linearly related to increases in exercise intensity. It is most important that the participant does not come to a point of volitional fatigue associated with psychological factors. An accurate result of O₂ uptake ($\dot{V}O_2$) requires exercising until the physical maximum. This linear relationship of $\dot{V}O_2$ across the test allows for calibration of an individual's $\dot{V}O_{2max}$. This provides a means to a stratified exercise training regime, i.e. directing an athlete to work for 30 min at 70 % of their aerobic maximum. To achieve maximum intensity there is an element of coercion (usually through jeers, praise and active encouragement) to motivate and/or persuade participants to continue the test for as long as is possible. By ensuring the individual exercises until their absolute maximum, an accurate result of $\dot{V}O_2$ can be achieved.

A common method to calculate $\dot{V}O_{2max}$ uses a cycle ergometer with total exhaled breath collected for 60 s into a pre-evacuated Douglas bag at the end of each incremental step. Exhaled air is analysed for O₂ and CO₂ content and total exhaled volume measured.

Environmental sampling allows calculation of inhaled and, therefore, exhaled fractions of N₂, O₂ and CO₂. To calculate $\dot{V}O_2$ several values must be known. A step-by-step calculation process is described below.

Firstly, the total exhaled air, or ventilatory equivalent, under ambient conditions (V_{EATPS}) is calculated and normalised to a 1 min collection (Equation 1).

$$V_{EATPS} (L) = \frac{V_t (L)}{t_T (s)} \times 60 (s) \quad \text{Equation 1}$$

Where V_t is total volume collected and t_T is total time of collection.

To convert this value to standardised temperature and pressure (V_{ESTPD}), V_{EATPS} is multiplied by a conversion factor. Under these conditions one mole of gas occupies 22.4 L. Table 1 indicates the conversion factor value across a common range of laboratory temperatures and pressures. For a more comprehensive table see [23].

Table 1 Table to show multiplication factors for converting volume at ambient conditions to standard pressure, temperature and humidity values; adapted from [23].

Barometric pressure (mm Hg)	Ambient temperature / °C						
	19	20	21	22	23	24	25
740	0.887	0.883	0.878	0.874	0.869	0.864	0.860
742	0.890	0.885	0.881	0.876	0.871	0.867	0.862
744	0.892	0.888	0.883	0.878	0.874	0.869	0.864
746	0.895	0.890	0.886	0.884	0.876	0.872	0.867
748	0.897	0.892	0.888	0.883	0.879	0.874	0.869
750	0.900	0.895	0.890	0.886	0.881	0.876	0.872
752	0.902	0.897	0.893	0.888	0.883	0.879	0.874
754	0.904	0.900	0.895	0.891	0.886	0.881	0.876
756	0.907	0.902	0.898	0.893	0.888	0.883	0.879
758	0.909	0.905	0.900	0.896	0.891	0.886	0.881
760	0.912	0.907	0.902	0.898	0.893	0.888	0.883
762	0.914	0.910	0.905	0.900	0.896	0.891	0.886
764	0.916	0.912	0.907	0.903	0.898	0.893	0.888
766	0.919	0.915	0.910	0.905	0.900	0.896	0.891
768	0.922	0.917	0.912	0.908	0.903	0.898	0.893
770	0.924	0.919	0.915	0.910	0.905	0.901	0.896

Inhaled ventilatory equivalent (V_i) for 1 min must be calculated by Equation 2. For the test performed in Chapter 5, exhaled air was collected for 60 s and therefore the units do not need conversion to $L \text{ min}^{-1}$.

$$V_{I(L.min^{-1})} = \frac{F_{EN_2}(\%) \times V_{ESTPD(L.min^{-1})}}{F_{IN_2}(\%)} \quad \text{Equation 2}$$

Where: F_{IN_2} and F_{EN_2} are the inhaled and exhaled fractional values of N_2 , respectively.

$\dot{V}O_2$ can then be calculated using Equation 3.

$$\dot{V}O_{2(L.min^{-1})} = \frac{V_I(L.min^{-1}) \times F_I O_2(\%)}{100} - \frac{V_E STPD(L.min^{-1}) \times F_E O_2(\%)}{100} \quad \text{Equation 3}$$

Where $F_I O_2$ and $F_E O_2$ are the fractional values of inhaled and exhaled O_2 , respectively.

This provides an absolute uptake of oxygen in litres per minute. For data obtained from the final stage of the exercise test, this equals $\dot{V}O_{2max}$. Normalisation against body mass can be performed using Equation 4 to give a reading in $mL(O_2) kg^{-1} min^{-1}$.

$$\dot{V}O_{2max(mL.kg^{-1}.min^{-1})} = \frac{\dot{V}O_{2(L.min^{-1})}}{body\ mass(kg)} \times 1000 \quad \text{Equation 4}$$

Table 2 summarises 'normative' data values for $\dot{V}O_{2max}$ for males and females [24].

Table 2 Normative maximal oxygen uptake ($\dot{V}O_{2max}$) data for males (top) and females (bottom) for an age range of 20 to 79 years old; adapted from [24].

Male, $\dot{V}O_{2max} / mL(O_2) kg^{-1} min^{-1}$					
Age	Poor	Fair	Good	Excellent	Superior
20 - 29	< 42	42 - 45	46 - 50	51 - 55	> 55
30 - 39	< 41	41 - 43	44 - 47	48 - 53	> 53
40 - 49	< 38	38 - 41	42 - 45	46 - 52	> 52
50 - 59	< 35	35 - 37	38 - 42	43 - 49	> 49
60 - 69	< 31	31 - 34	35 - 38	39 - 45	> 45
70 - 79	< 28	28 - 30	31 - 35	36 - 41	> 41

Female, $\dot{V}O_{2max} / mL(O_2) kg^{-1} min^{-1}$					
Age	Poor	Fair	Good	Excellent	Superior
20 - 29	< 36	36 - 39	40 - 43	44 - 49	> 49
30 - 39	< 34	34 - 36	37 - 40	41 - 45	> 45
40 - 49	< 32	32 - 34	35 - 38	39 - 44	> 44
50 - 59	< 25	25 - 28	29 - 30	31 - 34	> 34
60 - 69	< 26	26 - 28	29 - 31	32 - 35	> 35
70 - 79	< 24	24 - 26	27 - 29	30 - 35	> 35

Exhaled breath condensate

Exhaled breath condensate (EBC) is collected by cooling exhaled water vapour and collecting the resultant liquid. Figure 1 shows an example instrument (known commercially as the R Tube®) for the collection of EBC. This medium allows the collection of non-volatile compounds such as isoprostanes and leukotrienes. These molecules are considered as some of the most important intermediates in the inflammatory response [25]. Oxidative stress markers are thought to be present during airway inflammation and have shown to be significantly elevated after a single swimming session by competitive swimmers [26] and in asthmatic patients post-exercise [27]. Additionally, researchers have reported the alteration of pH in EBC at the onset of exercise-induced bronchoconstriction [28], which may be due to the release of molecules such as hydrogen peroxide [29]. The majority of the current work centred on EBC and exercise focuses on inflammatory responses in exercise-induced respiratory conditions. The current study has not located reports or papers on investigations into EBC analysis for exercise-based performance or monitoring. Because EBC collects non-volatile compounds, it was not utilised and is therefore outside of the scope of this research.



Figure 1

A photograph of an exhaled breath condensate collection device. The participant exhales through the mouthpiece at the lower left and exhaled breath passes into the chamber above where it is cooled (cooling jacket not shown). Cooled air condenses and collects into a vial that is attached at the lower end.

Exhaled nitric oxide

Nitric oxide (NO) forms as a free radical gas in the airways, when L-arginine is oxidised to L-citrulline [30], and is expired in the breath. NO is continuously produced in the body, and the lower airways provide the major contribution to increased concentrations in the breath of asthmatics [31]. Increases are likely due to activation of nitrogen oxide synthase 2 in airway epithelial cells [32,33]. It is predominately measured by the detection of photons when NO reacts with ozone in a chemiluminescence assay. Figure 2 shows commercially available exhaled NO (eNO) analysers. Investigations have reported that, in healthy participants, eNO levels reduce after a bout of exercise [34], with no differences in rates of reduction in cold [35] and high altitude [36] environments. Asthmatic individuals showed similar reductions in eNO to healthy controls [37] but, interestingly, chronic systolic heart failure patients showed an increased in eNO post-exercise [38]. These data suggest that an increase in post-exercise eNO due to inflammation does not occur when localised to the respiratory system, but is seen when systemic inflammation is present.

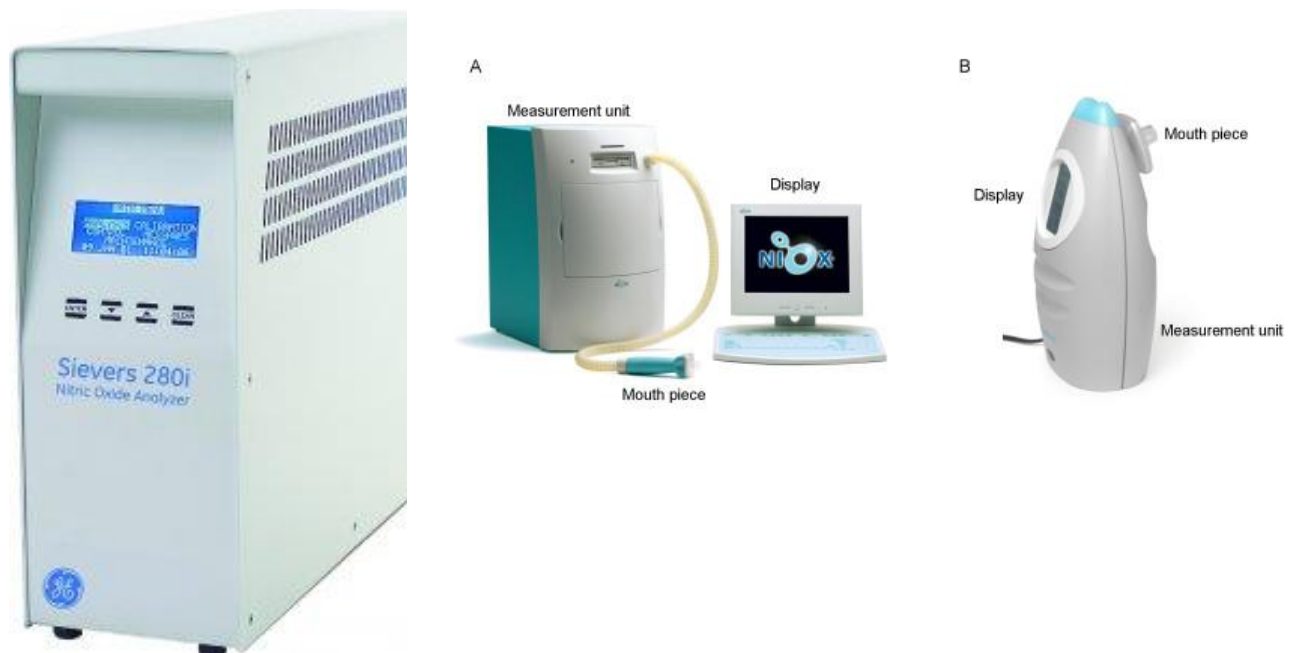


Figure 2 Commercially available exhaled nitric oxide analysers to quantify exhaled concentrations.

Exhaled volatilome

One area of interest within breath analysis is the exhaled volatilome [see 2 for a review on all aspects of the human volatilome]. This refers to the large variety of VOCs that are present in exhaled breath that can be collected and analysed, predominantly by gas chromatography-mass spectrometry (GC-MS) techniques [39]. It has proved a widely-used technique for the non-invasive measurement of potential biomarkers in health and disease [40] and samples are commonly analysed using highly efficient chromatographic runs. These runs can take up to 90 min, however, they are able to separate many hundreds of VOCs present at low levels (less than $1 \text{ mg m}^{-3}(\text{g})$) (and therefore improving analyte identification). Subsequent mass spectrometric analysis provides data for multivariate analysis of exhaled profiles. Multivariate data analysis identifies statistically significant differences in VOC profiles between set groupings; for example, Turner *et al.* [41] were able to differentiate between participants when in a state of calm and after artificial induction of psychological stress.

Changes in exhaled acetone and isoprene during light exercise (75 W) on a cycle ergometer have been previously reported [9]. Acetone and isoprene concentrations rose during exercise with isoprene spiking and tailing over the period of exertion. Acetone concentrations in a single participant rose from approximately 750 to 1000 ng mL^{-1} during exercise, with near complete reversal during the intermediary rest period ($\sim 800 \text{ ng mL}^{-1}$). Resting levels of isoprene were recorded at around 100 ng mL^{-1} and underwent a sharp 4-fold increase ($\sim 400 \text{ ng mL}^{-1}$) at the beginning of exercise, with a gradual decrease toward resting values during the exercise period. Conversely, methane concentrations have been observed to reduce during exercise [17]. Further investigation into exhaled acetone concentrations at different exercise intensities showed that levels continued to rise with work output up to $990 \text{ kg-m min}^{-1}$ (around 161 W). It should be noted that this is low-intensity exercise and is not representative of the work-rate of an able sportsperson [10].

Investigation of exhaled VOCs in conjunction with exercise has provided no exploration into possible alterations that physical activity can produce on the overall exhaled volatilome signature. Overall breath 'smellprints' have been noted as

altered during exercise [16], however, there was no indication of what changes occurred.

Metabolomics

The human volatilome contains volatile small molecules and is an example sample medium suitable for metabolomics analysis. Metabolomics is the study of metabolites present in tissues and bio fluids that represent the end stage molecules of metabolic processes occurring within a living organism. Experiments carrying the '*omics*' label may employ targeted analyses with the intention to identify a specific process, processes or pathway(s) that contribute to a biological function of interest. Conversely, non-targeted methods can be applied which prospect for novel (bio)markers that are indicative of a specific predefined state (e.g. differences between diseased and healthy individuals). The premise of metabolomics is that the small metabolites present within fluids and cells are indicative of physiological changes within an organism and can be assigned as candidate molecules to aid in measurement of health status or implemented for diagnostic, prognostic and therapeutic purposes. These identified metabolites may show causative and/or associative relationships with the physiological state being investigated. In 2007, the Human Metabolome Database (HMDB) was first published [42] and has since been updated, with the latest version published in 2013 [43]. The HMDB is a free-to-access resource that details information about small molecule metabolites that have been identified as present within the human biological system. There are currently 41,993 metabolites present in the database and are represented as a 'metabocard' that details chemical, clinical, biochemical and enzymatic data associated with the metabolite of interest and provide links to website resources for additional information on the molecule [44]. Examples of additional fields that implement this approach, and are encompassed with the '*omics*' remit, include the study of proteins/peptides (proteomics/peptidomics), lipids (lipidomics), RNA (transcriptomics) and DNA (genomics).

Chlorine related insults to swimmers and swimming pool staff

The association of respiratory disorders and the repeated exposure to chlorinated swimming pool environments has been studied [e.g. 45-48], and has led to the hypothesis that disinfection by-products (DBPs) are producing harmful chemicals to swimmers and swimming pool staff. Data show that cumulative life exposure to a chlorinated pool environment is associated with new onset or current asthma, with increased prevalence in those grouped into high cumulative exposure [47,49-51]. Similar findings are also seen in an outdoor chlorinated pool environment [52], suggesting that increased ventilation does not eliminate the association of DBPs with respiratory symptoms. Associated respiratory symptoms have not been observed when assessing children that swam in copper-silver disinfected pools [49].

Chlorination is a common method of disinfection for swimming pool water as it adequately removes microbial pathogens that may be present. The mostly used methods mix chlorine gas ($\text{Cl}_{2(g)}$) or sodium hypochlorite solution ($\text{Na}^+(\text{OCl}_2^-)$) into the water. Chlorine reacts with aqueous organic matter to form DBPs, such as trihalomethanes (THMs), haloacetonitriles, haloacetic acids (HAAs) and haloamines [53]. The main source for the organic matter is from the bathers themselves, this comes in the form of bodily secretions (for example, urine and sweat which contain ammonia and high levels of nitrogen-containing amino acids) and externally applied lotions and cosmetics [54]. Swimmers are estimated to excrete 50 mL of urine and 100 mL of sweat per swimming hour [55]. The most abundant formations of DBPs are THMs, with chloroform (CHCl_3) generally present in the greatest concentration, and HAAs of which di and trichloroacetic acid (CHCl_2COOH and CCl_3COOH , respectively) are in the greatest abundance [53]. If inorganic bromine is present in the water, reactions occur that produce brominated by-products such as bromoform (CHBr_3). Additionally to organic DBPs, inorganic haloamines are produced through reaction of chlorine/bromine and hydrolysed ammonia. Trichloramine, or nitrogen trichloride, (NCl_3) is commonly measured in the air surrounding swimming pools [e.g. 45,46], has been described as a “volatile, irritant compound of penetrating odour” [56] and, therefore, has been identified as being responsible for the ‘chlorine odour’ of swimming pools [57,58]. NCl_3 is highly volatile and is a respiratory irritant in mice [59]. Pool air measurements show relationships with

respiratory irritation symptoms [45,60,61], see Table 3 for a list of predominant chemical disinfectants and their associated DBPs. Swimmers are exposed to these halogenated compounds via ingestion (water swallowed during swimming), dermal absorption (absorbed through the skin barrier) or, most importantly for respiratory irritation, inhalation of VOCs present on and above the surface of the water.

Table 4 utilises data from Richardson *et al.* [62] to highlight the levels of a selection of DBPs in swimming pools in Spain, and more details can be found in Chapter 4 that address this subject.

Table 3 A list of common swimming pool disinfection methods and their associative disinfection by-products; adapted from [53].

Disinfectant	Disinfection by-products
Chlorine/hypochlorite	trihalomethanes, mainly chloroform haloacetic acids haloacetonitriles haloketones trichloroacetaldehyde trichloronitromethane cyanogen chloride chlorate chloramines
Ozone	bromate aldehydes ketones ketoacids carboxylic acids bromoform brominated acetic acids
Chlorine dioxide	chlorite chlorate
Bromine/hypochlorite	trihalomethanes, mainly bromoform bromal hydrate bromate bromamines

Table 4 Concentrations of swimming pool disinfection by-products measured from swimming pools in Spain; adapted from [62].

Chemical	Chlorinated pool			Brominated pool		
	Mean (SD)	Min	Max	Mean (SD)	Min	Max
Free chlorine (mg L ⁻¹)	1.28 (0.43)	0.52	2.35	0.50 (0.16)	0.32	0.70
Monochloramine (mg L ⁻¹)	0.29 (0.11)	0.10	0.64	0.27 (0.03)	0.24	0.30
Dichloramine (mg L ⁻¹)	0.38 (0.14)	< 0.01	0.65	< 0.01	< 0.01	< 0.01
Trichloramine (mg L ⁻¹)	< 0.10	< 0.10	< 0.10	< 0.10	< 0.10	< 0.10
Chloroform (µg L ⁻¹)	15.4 (3.5)	8.4	20.8	0.2 (0.1)	0.1	0.3
Bromodichloromethane (µg L ⁻¹)	14.2 (4.2)	9.3	26.8	0.4 (0.2)	0.2	0.7
Dibromochloromethane (µg L ⁻¹)	12.8 (4.4)	6.5	22.6	2.4 (0.2)	2.1	2.7
Bromoform (µg L ⁻¹)	7.2 (3.2)	3.0	16.5	57.2 (4.4)	54.4	67.2

Note: SD = standard deviation

1.3.3 Potential uses for exhaled breath analysis in exercise science

Exhaled VOC analysis enables a wide range of analytes and their relationships with underlying biological mechanisms to be studied; albeit with complications from environmental factors such as diesel fumes and other pollutants. This offers the prospect of developing breath tests that can aid athletes in their daily training by providing information that may only have been previously possible after completion of time-consuming and physically exertive tests. Breath tests may offer valuable and timely information for athletes, and their coaches, about stress, fatigue, onset of illnesses (e.g. upper respiratory tract infections) and indication of current fitness level. The adoption of such technologies by elite sport, regardless of their success in a research environment, will take many years and proven competitive benefits before being accepted widely and used regularly. The development of rapid, non-invasive methods of screening for VOCs in sport and exercise are applicable to non-laboratory based testing with high-performance sportspeople would be advantageous. For example, a major concern for athletes is their susceptibility to infections, with epidemiological evidence to suggest that although exercise provides a protective mechanism, this protection is lost when regular heavy training outputs are performed [63,64]. For top performing athletes, missing training or competition due to illness can cause ramifications on their current and future careers, with potential loss of earnings. Current monitoring often requires invasive methods such

as measuring immune system status through blood sampling, or time-consuming collection of non-invasive techniques that some individuals can find difficult to perform (e.g. saliva sampling). These are often accompanied by expensive analytical processes, e.g. enzyme-linked immunosorbent assays for measurement of immunoglobulin from passive drool saliva [65], and limited to targeted analysis without the ability for full screening.

The experiments designed for this doctoral study represent an initial step in the use of exhaled breath analysis with exercise, and are intended as a pathfinder study for other researchers to follow to further the understanding of this under-explored field.

1.4 References

1 Miekisch W, Schubert JK, Noeldge-Schomburg GFE. Diagnostic potential of breath analysis – focus on volatile organic compounds. *Clin. Chim. Acta* 2004;347:25-39

2 Amann A, de Lacy Costello B, Miekisch W, Schubert J, Buszewski B, Pleil J, Ratcliffe N, Risby T. The human volatilome: volatile organic compounds (VOCs) in exhaled breath, skin emanations, urine, feces and saliva. *J. Breath Res.* 2014;8:034001

3 Wang T, Pysanen A, Dryahina K, Spaněl P, Smith D. Analysis of breath, exhaled via the mouth and nose, and the air in the oral cavity. *J. Breath Res.* 2008;2:037013

4 Deng C, Zhang Z, Yu X, Zhang W, Zhang X. Determination of acetone in human breath by gas chromatography-mass spectrometry and solid-phase microextraction with on-fiber derivatization. *J. Chromatogr. B* 2004;810:267-75

- 5 Righettoni M, Tricolo A, Pratsinis SE. Si:WO₃ sensors for highly selective detection of acetone for easy diagnosis of diabetes by breath analysis. *Anal. Chem.* 2010;82:3581-7
- 6 Aggazzotti G, Fantuzzi G, Righi E, Predieri G. Environmental and biological monitoring of chloroform in indoor swimming pools. *J. Chromatogr. A* 1995;710:181-90
- 7 Lindstrom AB, Pleil JD, Berkoff DC. Alveolar breath sampling and analysis to assess trihalomethane exposures during competitive swimming training. *Environ. Health Perspect.* 1997;105:636-42
- 8 Aggazzotti G, Fantuzzi G, Righi E, Predieri G. Blood and breath analyses as biological indicators of exposure to trihalomethanes in indoor swimming pools. *Sci. Total Environ.* 1998;217:155-63
- 9 Solga SF, Mudalel M, Spacek LA, Lewicki R, Tittel FK, Loccioni C, Russo A, Ragnoni A, Risby TH. Changes in the concentration of breath ammonia in response to exercise: a preliminary investigation. *J. Breath Res.* 2014;8:037103
- 10 King J, Kupferthaler A, Unterkofler K, Koc H, Teschl S, Teschl G, Miekisch W, Schubert J, Hinterhuber H, Amann A. Isoprene and acetone concentration profiles during exercise on an ergometer. *J. Breath Res.* 2009;3:027006
- 11 Yamai K, Ohkuwa T, Itoh H, Tamazaki Y, Tsuda T. Influence of cycle exercise on acetone in expired air and skin gas. *Redox Rep.* 2009;14:285-9

12 King J, Koc H, Unterkofler K, Mochalski P, Kupferthaler A, Teschl G, Teschl S, Hinterhuber H, Amann A. Physiological modelling of isoprene dynamics in exhaled breath. *J. Theor. Biol.* 2010;267:626-37

13 King J, Mochalski P, Kupferthaler A, Unterkofler K, Koc H, Filipiak W, Teschl S, Hinterhuber H, Amann A. Dynamic profiles of volatile organic compounds in exhaled breath as determined by a coupled PTR-MS/GC-MS study. *Physiol. Meas.* 2010;31:1169-84

14 Font-Ribera L, Kogevinas M, Zock JP, Gómez FP, Barreiro E, Nieuwenhuijsen MJ, Fernandez P, Lourencetti C, Pérez-Olabarría M, Bustamante M, Marcos R, Grimalt JO, Villanueva CM. Short-term changes in respiratory biomarkers after swimming in a chlorinated pool. *Environ. Health Perspect.* 2010;118:1538-44

15 Bikov A, Lazar Z, Schandl K, Antus BM, Losonczy G, Horvath I. Exercise changes volatiles in exhaled breath assessed by an electronic nose (abstract). *Acta Physiol. Hung.* 2011;98:321-8

16 Schwoebel H, Schubert R, Sklorz M, Kischkel S, Zimmermann R, Schubert JK, Miekisch W. Phase-resolved real-time breath analysis during exercise by means of smart processing of PTR-MS data. *Anal. Bioanal. Chem.* 2011;401:2079-91

17 Caro J, Gallego M. Alveolar air and urine analyses as biomarkers of exposure to trihalomethanes in an indoor swimming pool. *Environ. Sci. Technol.* 2008;42:5002-7

18 Szabó A, Ruzsanyi V, Unterkofler K, Mohácsi A, Tuboly E, Boros M, Szabó G, Hinterhuber H, Amann A. Exhaled methane concentration profiles during exercise on an ergometer. *J. Breath Res.* 2015;9:016009

19 Krug S, Kastenmüller G, Stückler F, Rist MJ, Skurk T, Sailer M, Raffler J, Römisch-Margl W, Adamski J, Prehn C, Frank T, Engel KH, Hofmann T, Luy B, Zimmermann R, Moritz F, Schmitt-Kopplin P, Krumsiek J, Kremer W, Huber F, Oeh U, Theis FJ, Szymczak W, Hauner H, Suhre K, Daniel H. The dynamic range of the human metabolome revealed by challenges. *FASEB J.* 2012;26:2607-19

20 Thompson PD, Arena R, Riebe D, Pescatello LS; American College of Sports Medicine. ACSM's new participation health screening recommendations from ACSM's guidelines for exercise testing and prescription, ninth edition. *Curr. Sports Med. Rep.* 2013;12:215-7

21 Wilson MG, Ellison GM, Cable NT. Basic science behind the cardiovascular benefits of exercise. *Heart* 2015;101:758-65

22 Aitken JC, Thompson J. The respiratory VCO_2/VO_2 exchange ratio during maximal exercise and its use as a predictor of maximal oxygen uptake. *Eur. J. Appl. Physiol.* 1988;57:714-19

23 Metabolic computation in open-circuit spirometry.

<http://www.uni.edu/dolgener/Instrumentation/Repeating%20material/VO2%20Computation.pdf> [accessed 20 February 2016]

24 Heywood V. The physical fitness specialist manual, The Cooper Institute for Aerobics Research, Dallas TX, revised 2005. In: Heywood, V. Advanced fitness assessment and exercise prescription [5th ed]. Champaign, IL: Human Kinetics: 2006

25 Kubáň P, Foret F. Exhaled breath condensate: determination of non-volatile compounds and their potential for clinical diagnosis and monitoring. A review. *Anal. Chim. Acta* 2013;805:1-18

26 Morissette MC, Murray N, Turmel J, Milot J, Boulet LP, Bougault V. Increased exhaled breath condensate 8-isoprostane after a swimming session in competitive swimmers. *Eur. J. Sports Sci.* 2016;16:569-76

27 Bikov A, Gajdócsi R, Huszár É, Szili B, Lázár Z, Antus B, Losonczy G, Horváth I. Exercise increases exhaled breath condensate cysteinyl leukotriene concentration in asthmatic patients. *J. Asthma* 2010;47:1057-62

28 Bikov A, Galffy G, Tamasi L, Bartusek D, Antus B, Losonczy G, Horvath I. Exhaled breath condensate pH decreases during exercise-induced bronchoconstriction. *Respirology* 2014;19:563-9

29 Marek E, Volke J, Mückenhoff K, Platen P, Marek W. Exercise in cold air and hydrogen peroxide release in exhaled breath condensate. *Adv Exp Med Biol* 2013;756:167-77

30 Gaston B, Drazen JM, Loscalzo J, Stamler JS. The biology of nitrogen oxides in the airways. *Am. J. Respir. Crit. Care Med.* 1994;149:538-51

31 Kharitonov SA, Chung FJ, Evans DJ, O'Connor BJ, Barnes PJ. The elevated level of exhaled nitric oxide in asthmatic patients is mainly derived from the lower respiratory tract. *Am. J. Respir. Crit. Care Med.* 1996;153:1773-80

32 Hamid Q, Springall DR, Riveros-Moreno V, Chanez P, Howarth P, Redington A, Bousquet J, Godard P, Holgate S, Polak JM. Induction of nitric oxide synthase in asthma. *Lancet* 1993;342:1510-3

33 Saleh D, Ernst P, Lim S, Barnes PJ, Giaid A. Increased formation of the potent oxidant peroxynitrite in the airways of asthmatic patients is associated with induction of nitric oxide synthase: effect of inhaled glucocorticoid. *FASEB J.* 1998;12:929-37

34 Evjenth B, Hansen TE, Holt J. Exhaled nitric oxide decreases during exercise in non-asthmatic children. *Clin. Resp. J.* 2013;7:121-7

35 Stensrud T, Stang J, Thorsen E, Bråten V. Exhaled nitric oxide concentration in the period of 60 min after submaximal exercise in the cold. *Clin. Physiol. Funct. Imaging* 2016;36:85-91

36 Stang J, Bråten V, Caspersen C, Thorsen E, Stensrud T. Exhaled nitric oxide after high-intensity exercise at 2800 m altitude. *Clin. Physiol. Funct. Imaging* 2015;35:338-43

37 Tufvesson E, Svensson H, Ankerst J, Bjermer L. Increase of club cell (Clara) protein (CC16) in plasma and urine after exercise challenge in asthmatics and healthy controls, and correlations to exhaled breath temperature and exhaled nitric oxide. *Respir. Med.* 2013;107:1675-81

38 Schuster A, Thakur A, Wang Z, Borowski AG, Thomas JD, Tang WH. Increased exhaled nitric oxide levels after exercise in patients with chronic systolic heart failure with pulmonary venous hypertension. *J. Card. Fail.* 2012;18:799-803

39 Basanta M, Koimtzis T, Singh D, Wilson I, Thomas CL. An adaptive breath sampler for use with human subjects with an impaired respiratory function. *Analyst* 2007;132:153-63

40 Boots AW, van Berkel JJ, Dallinga JW, Smolinska A, Wouters EF, van Schooten FJ. The versatile use of exhaled volatile organic compounds in human health and disease. *J. Breath Res.* 2012;6:027108

41 Turner MA, Bandelow S, Edwards L, Patel P, Martin HJ, Wilson ID, Thomas CL. The effect of a paced auditory serial addition test (PASAT) intervention on the profile of volatile organic compounds in human breath: a pilot study. *J. Breath Res.* 2013;7:017102

42 Wishart DS, Tzur D, Knox C, Eisner R, Guo AC, Young N, Cheng D, Jewell K, Arndt D, Sawhney S, Fung C, Nikolai L, Lewis M, Coutouly M-A, Forsythe I, Tang P, Shrivastava S, Jeroncic K, Stothard P, Amegbey G, Block D, Hau DD, Wagner J, Miniaci J, Clements M, Gebremedhin M, Guo N, Zhang Y, Duggan GE, MacInnis GD, Weljie AM, Dowlatabadi R, Bamforth F, Clive D, Greiner R, Li L, Marrie T, Sykes BD, Vogel HJ, Querengesser L. HMDB: the human metabolome database. *Nucleic Acids Res.* 2007;35:D521-6

43 Wishart DS, Jewison T, Guo AC, Wilson M, Knox C, Liu Y, Djoubou Y, Mandal R, Aziat F, Dong E, Bouatra S, Sinelnikov I, Arndt D, Xia J, Liu P, Yallou F, Bjorn Dahl T, Perez-Pineiro R, Eisner R, Allen F, Neveu V, Greiner R, Scalbert A. HMDB 3.0 – the human metabolome database in 2013. *Nucleic Acids Res.* 2013;41:D801-7

44 The human metabolome database. <http://www.hmdb.ca/> (accessed 6 June 2016)

45 Massin N, Bohadana AB, Wild P, Héry M, Toamain JP, Hubert G. Respiratory symptoms and bronchial responsiveness in lifeguards exposed to nitrogen trichloride in indoor swimming pools. *Occup. Environ. Med.* 1998;55:258-63

46 Carbonnelle S, Francaux M, Doyle I, Dumont X, de Burbure C, Morel G, Michel O, Bernard A. Changes in serum pneumoproteins caused by short-term exposures to nitrogen trichloride in indoor chlorinated swimming pools. *Biomarkers* 2002;7:464-78

47 Ferrari M, Schenk K, Mantovani W, Papadopoulou C, Posenato C, Ferrari P, Poli A, Tardivo S. Attendance at chlorinated indoor pools and risk of asthma in adult recreational swimmers. *J. Sci. Med. Sport* 2011;14:184-9

48 Helenius IJ, Ryttilä P, Metso T, Haahtela T, Venge P, Tikkanen HO. Respiratory symptoms, bronchial responsiveness, and cellular characteristics of induced sputum in elite swimmers. *Allergy* 1998;53:346-52

49 Bernard A, Nickmilder M, Voisin C, Sardella A. Impact of chlorinated swimming pool attendance on the respiratory health of adolescents. *Pediatrics* 2009;124:1110-8

50 Bernard A, Carbonnelle S, Michel O, Higuët S, de Burbure C, Buchet J-P, Hermans C, Dumont X, Doyle I. Lung hyperpermeability and asthma prevalence in school children: unexpected associations with the attendance at indoor chlorinated swimming pools. *Occup. Environ. Med.* 2003;60:385-94

51 Bernard A, Carbonnelle S, de Burbure C, Michel O, Nickmilder M. Chlorinated pool attendance, atopy, and the risk of asthma during childhood. *Environ. Health Prospect.* 2006;114:1567-73

52 Bernard A, Nickmilder M, Voisin C. Outdoor swimming pools and the risks of asthma and allergies during adolescence. *Eur. Respir. J.* 2008;32:979-88

53 Kim H, Shim J, Lee S. Formation of disinfection by-products in chlorinated swimming pool water. *Chemosphere* 2002;46:123-30

54 World Health Organisation. Guidelines for safe recreational water environments. Volume 2: swimming pools and similar environments. 2006. http://www.who.int/water_sanitation_health/bathing/srwe2full.pdf (accessed 22 November 2015)

55 Judd SJ, Bullock G. The fate of chlorine and organic materials in swimming pools. *Chemosphere* 2003;51:869-79

56 Schmalz C, Wunderlich HG, Heinze R, Frimmer FH, Zwiener C, Grummt T. Application of an optimized system for the well-defined exposure of human lung cells to trichloramine and indoor pool air. *J. Water Health* 2011;9:586-96

57 Weng S, Blatchley III ER. Disinfection by-product dynamics in a chlorinated, indoor swimming pool under conditions of heavy use: National swimming competition. *Water Res.* 2011;45:5241-8

58 Bougault V, Boulet L-P. Airway dysfunction in swimmers. *Br. J. Sports Med.* 2012;46:402-6

59 Gagnaire F, Azim S, Bonnet P, Hecht G, Hery M. Comparison of the sensory irritation response in mice to chlorine and nitrogen trichloride. *J. Appl. Toxicol.* 1994;14:405-9

60 Bowen AB, Kile JC, Otto C, Kazerouni N, Austin C, Blount BC, Wong H-N, Bleach MJ, Fry AM. Outbreaks of short-incubation ocular and respiratory illness following exposure to indoor swimming pools. *Environ. Health Perspect.* 2007;115:267-71

61 Dang B, Chen L, Mueller C, Dunn KH, Almaguer D, Roberts JL, Otto CS. Ocular and respiratory symptoms among lifeguards at a hotel indoor waterpark resort. *J Occup. Environ Med.* 2010;52:207-13

62 Richardson SD¹, DeMarini DM, Kogevinas M, Fernandez P, Marco E, Lourencetti C, Ballesté C, Heederik D, Meliefste K, McKague AB, Marcos R, Font-Ribera L, Grimalt JO, Villanueva CM. What's in the pool? A comprehensive identification of disinfection by-products and assessment of mutagenicity of chlorinated and brominated swimming pool water. *Environ. Health Perspect.* 2010;118:1523-30

63 Nieman DC. Exercise, upper respiratory tract infection, and the immune system. *Med. Sci. Sports Exerc.* 1994;26:128-39

64 Gleeson M, Bishop NC, Stensel DJ, Lindley MR, Mastana SS, Nimmo MA. The anti-inflammatory effects of exercise: mechanisms and implications for the prevention and treatment of disease. *Nat. Rev. Immunol.* 2011;11:607-15

65 Gleeson M, McDonald WA, Pyne DB, Cripps AW, Francis JL, Fricker PA, Clancy RL. Salivary IgA levels and infection risk in elite swimmers. *Med. Sci. Sports Exerc.* 1999;31:67-73

CHAPTER TWO: PHYSIOLOGICAL AND ANALYTICAL THEORY

2.1 Respiratory physiology and VOC exchange

2.1.1 *Structure and function of the lungs*

Respiration is the act of breathing and is achieved through a controlled set of muscular movements, creating a mechanical stimulus for the inhalation and exhalation of gases. Gases diffuse across the blood-lung barrier, transferring oxygen (O_2) to the blood and removing by-products of metabolism, such as carbon dioxide (CO_2), from the body.

Airflow through the lung

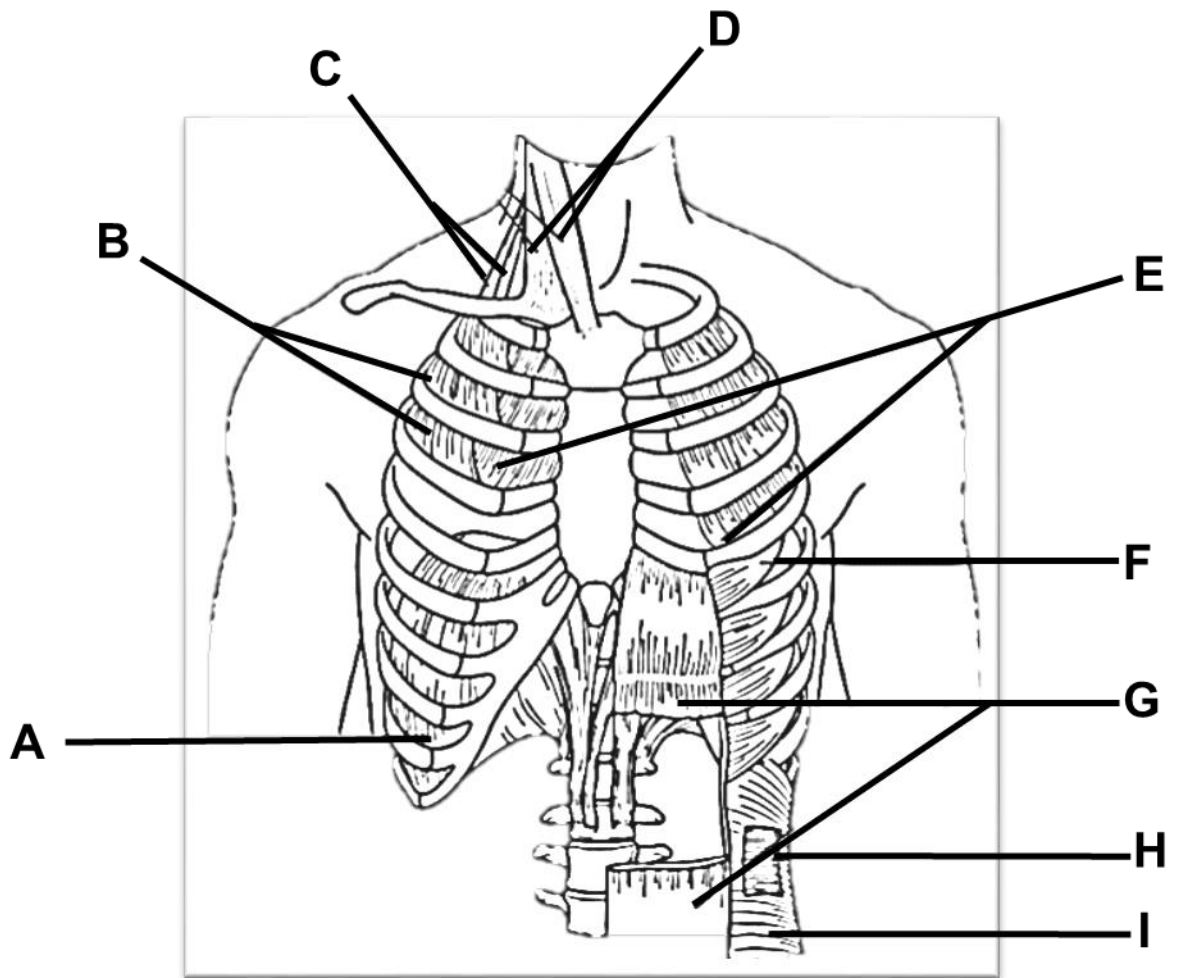
The human respiratory system is a series of airways that decrease in bore and increase in quantity as they pass deeper into the lung. The largest airway, the trachea, bifurcates into the left and right bronchi, which progressively split until the terminal bronchioles. These airways are the conducting airways, taking no part in gaseous exchange. Because of this, air found in this region (which equates to approximately 150 mL [1]) is termed 'dead-space'. The dead-space (D) is calculated using Bohr's method, as the entirety of carbon dioxide (CO_2) exhaled comes from the alveolar gas rather than from D , Equation 5. Terminal bronchioles divide into respiratory bronchioles, which contain some alveoli attached to their walls, and lead to the alveolar ducts, containing alveolar sacks. Alveolar sacks are small hollow structures that have a rich capillary blood supply. They have a thin (0.2 to 2.5 μm) semi-permeable wall allowing gaseous molecules to pass between the air space and blood supply. Respiratory bronchioles and alveolar ducts are termed as the respiratory zone and usually have a volume of 2.5 to 3 L.

$$\frac{V_D}{V_T} = \frac{PA_{(CO_2)} + PE_{(CO_2)}}{PA_{(CO_2)}} \quad \text{Equation 5}$$

Where V_D is the dead volume; V_T is the total volume of the airways, $PA_{(CO_2)}$ refers to partial pressure of CO_2 in alveolar air; and, $PE_{(CO_2)}$ to to partial pressure of CO_2 in mixed-expired air.

Mechanics of breathing

Air is drawn into the lungs by reducing the thoracic cavity pressure, causing air to enter via the mucosal and nasal cavities to equilibrate the negative pressure. This occurs by contraction of the diaphragm and intercostal muscles. The diaphragm is a dome shaped muscle that inserts into the lower ribs and when contracted it flattens and increases the thoracic cavity volume, thereby decreasing its pressure. Intercostal muscles are situated in between ribs and contract to lift the rib cage upwards and outwards, further elevating the cavity volume. During exhalation, the diaphragm and external intercostal muscles passively relax, and the lung returns to the pre-inspiratory volume by elasticity, forcing excess air out of the lungs. During normal at-rest breathing, processes are sufficient for ventilation of required volumes (approximately 500 mL per inhalation). However, when forced inspiratory and/or expiratory actions are required (with up to several litres of air inhaled per breath in intense exercise) further processes are implemented. Heavy inspiration recruits the sternocleidomastoid and scalene muscles which lift the sternum plate and ribs, increasing the total inspired volume. Forced expiration is produced through contraction of the rectus abdominis, internal and external obliques and transverse abdominis. This causes an increase in intra-abdominal pressures, forcing the diaphragm upwards and expelling air. Furthermore, internal intercostal muscles may be recruited to forcefully depress the rib cage and increase the velocity of exhalation (see Figure 3 for a diagram of respiratory muscles [2]).



Inspiratory muscles		Expiratory muscles	
A	Diaphragm	E	Internal intercostals
B	External intercostals	F	External oblique
C	Scalene	G	Rectus abdominis
D	Sternocleidomastoids	H	Transverse abdominis
		I	Internal oblique

Figure 3 A diagram to show the muscles in the upper torso responsible for the mechanics of breathing; adapted from [2].

An adult resting breath usually consists of approximately 500 mL of air entering and exiting the lung (known as tidal volume). However, a person can forcefully inhale greater volumes (around 4 to 4.5 L) and, when combined with a forceful and complete exhalation, is called the vital capacity (approximately 6.5 to 7 L). Air that remains in the lungs after forceful expiration is the residual volume, and remains in order to maintain structure and prevent any collapse that may cause damage to the tissues, see Figure 4 [3].

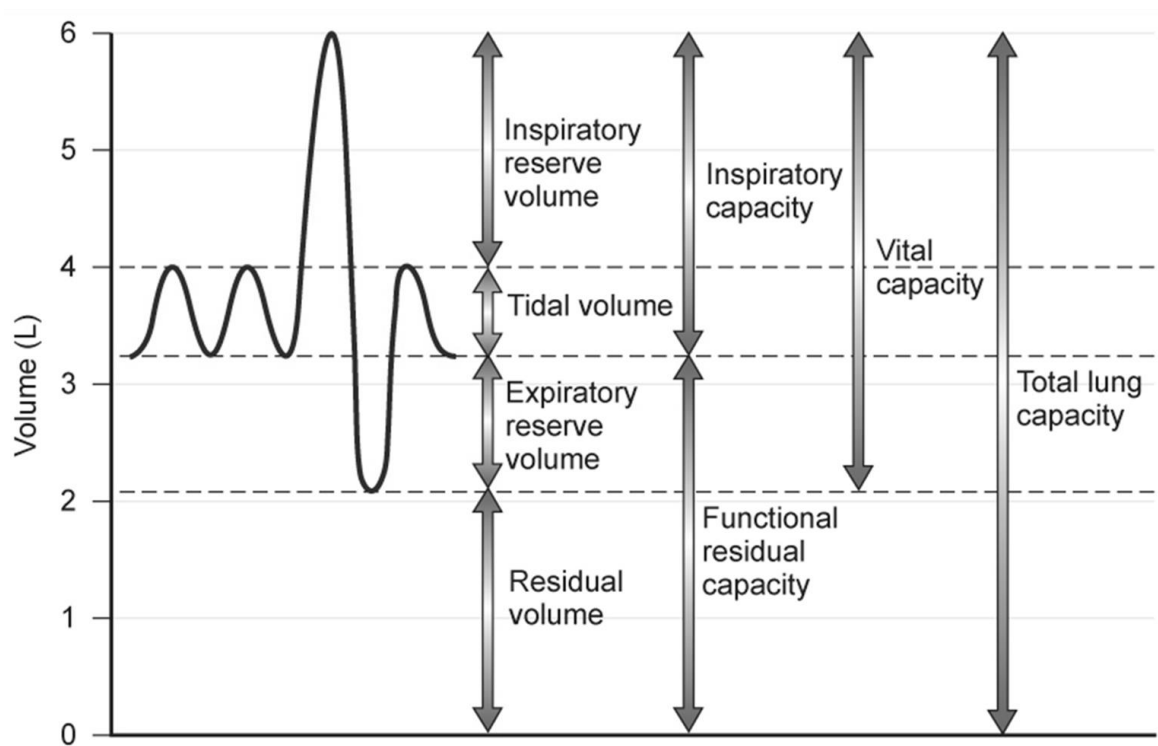


Figure 4 A diagram to indicate the different partitions of the lung and their relative volumes compared to the total lung capacity; adapted from [3].

The blood-gas interface

O₂ and CO₂ pass between the alveoli and bloodstream via diffusion from areas of high to low partial pressures. Fick's Law of Diffusion (Equation 6) states that flux of gas across a permeable membrane is proportional to the area (A) of the membrane, but inversely proportional to its thickness (x).

$$\frac{dV}{dt} = \frac{A}{x} \cdot D \cdot (P_1 - P_2)$$

Equation 6

Where dV is the change in volume of gas across the membrane and dt the change in time, A is the area of the membrane and x is its thickness. D is the diffusion constant, or permeability coefficient, and P_1 and P_2 are the partial pressures of the gases on either side of the membrane. Fick's Law was originally expressed in terms of concentrations but this version has been adapted for the study of partial pressures of gaseous molecules.

Diffusion happens rapidly across the thin blood-alveolar barrier, which has a surface area of 50 to 100 m². This large area is achieved by enclosing millions of sacks with capillary blood supply. Rapid exchange of O₂ and CO₂ occur during every breath, even at high ventilation rates produced during exercise or at high altitudes. Each red blood cell spends around 3 to 4 s in the pulmonary capillary network and is subject to gas exchange with 2 or 3 alveoli; this period is sufficient for almost complete equilibrium of the gases across the membrane [4]. VOCs are transported into exhaled breath following the same principle (see Figure 5).

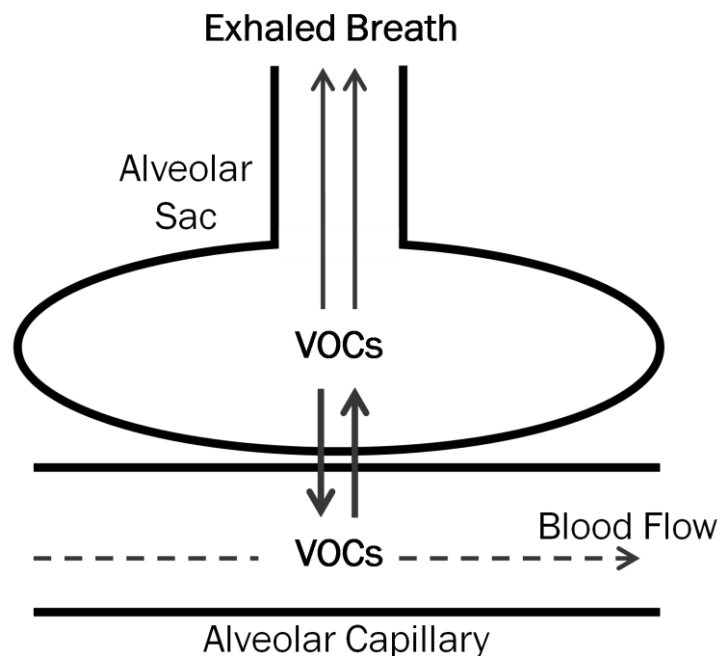


Figure 5 A simplified schematic of the gaseous exchange of volatile molecules between the pulmonary blood supply and the alveolar sacs of the lungs.

Respiratory responses to exercise

During exercise, ventilation rates increase rapidly to supply elevated demand for O₂ delivery and CO₂ removal. Resting ventilation in healthy adults is around 7.5 L min⁻¹ rising to 120 L min⁻¹ during exercise [4]. This substantial increase in air ventilation mechanically stresses the airways and causes high levels of disturbance.

In addition to raised ventilation, exercise causes a rise in the rate of diffusion of molecules across the blood-alveolar barrier. This is due to changes in both the diffusing capacity of the membrane, which typically increases by 3-fold or more [4], and the enlarged volume of blood supplied to pulmonary capillaries. Additionally to the distension of pulmonary capillaries, further blood vessels are recruited to augment diffusion. This is an important consideration for the analysis of metabolites in breath, particularly if exercise is performed.

2.2 Exhaled VOC breath analysis

2.2.1 *The modern era*

Molecular breath analysis began in the early 20th century when JS Haldane and colleagues collected exhaled air to monitor the absorption dissociation of CO₂ in human blood [5]. Research into breath analysis using gas chromatography research began in 1971, when Linus Pauling (winner of Nobel Prizes in both Chemistry (1954) and Peace (1962)) identified 250 compounds present in breath. He did this by trapping VOCs on a coiled stainless steel tube. The tube was cooled in an isopropyl alcohol dry ice bath [6], and VOCs were then passed through a gas chromatography column. Almost three decades later, Phillips *et al.* [7] used gas chromatography coupled with mass spectrometry to isolate a total of 3,481 different VOCs from the breath of 50 participants, with only 27 VOCs that were observed universal to all participants (Table 5). These results define the inter-person variability and significant challenge of using exhaled biomarkers to diagnose diseases and characterise health conditions.

Table 5 A list of 27 volatile organic compounds (VOC) found to be present in all of 50 exhaled breath VOC collections by Phillips *et al.* [7].

VOC	Mean alveolar gradient
Isoprene	60.34
Benzene, (1-methylethenyl)-	4.77
Naphthalene	4.07
2,5-Cycohexadiene-1,4-dione, 2,6-bis(1,1,-dimethyleythyl)	0.61
Naphthalene, 1-methyl-	0.54
Butane, 2-methyl-	0.33
Tetradecane	0.23
Pentodecane	0.10
Dodecane	0.02
Benzene	-0.48
Benzene, 1-ethyl-2-methyl-	-10.09
Benzene, ethyl	-1.73
Benzene, methyl	-7.27
Benzene, propyl	-1.72
Cyclohexane, methyl	-0.75
Decane	-0.28
Heptane	-1.25
Heptane, 2-methyl-	-0.89
Heptane, 3-methyl-	-0.83
Hexane	-0.79
Hexane, 3-methyl-	-1.02
Nonane	-0.44
Pentane, 2,3,4-trimethyl-	-0.26
Pentane, 2-methyl-	-0.43
Pentane, 3-methyl-	-0.59
Propane, 2-methoxy-2-methyl-	-9.44
Undecane	-0.52

2.2.2 Considerations with exhaled breath

The major advantage for breath analysis is the non-invasive collection procedure. Many current methods in medical diagnostics are uncomfortable for the patient,

with even the basic 'gold standard' blood analysis via venepuncture providing levels of discomfort and increased risk of infection.

A major complication of breath sampling is that expired air is not homogenous throughout different sections of respiratory vessels. Upper airways (pharynx, larynx, trachea and bronchi) contain dead space gas and do not contain VOCs diffused from the blood. However, inflammation and damage to these tissues does result in VOC release. Lower airways (bronchioles and alveolar sacks) contain air that has equilibrated with circulating blood. Air from this region allows a better representation of VOCs with blood borne origin that are present in the lungs. Due to physiological differences, mix-exhaled [e.g. 8], distal [e.g. 9] and rebreathed air [e.g. 10 in rats] samples have been used to collect exhaled breath VOCs.

Mixed-exhaled air contains gases from all lung sections. No selective collection is required with all exhaled gases being collected and analysed. Distal air, or 'alveolar air', is exhaled toward the end of each breath. Although gases pass through the dead space, it demonstrates a clearer picture of the compounds present in alveolar sacks, and consequently systemic circulation. When collecting alveolar air from a single exhalation, holding the breath before sampling produces increases concentration and repeatability of VOC measurements. Twenty seconds of breath holding can significantly increase the sampled concentrations of some molecules [1]. However, such breathing manoeuvres lower pH, affect the partitioning of many VOCs into the gas phase and may have impacts on lung metabolism.

The respiratory cycle can be divided into four different phases (Figure 6) as follows:

- *Phase I* – exhalation of the anatomical dead space (gases in this phase would not typically contain any endogenous VOCs);
- *Phase II* – exhaled breath contains a mixture of dead space and alveolar air;
- *Phase III* – this portion of exhaled breath is a result of alveolar emptying and therefore most reflects the characteristics of air in the lower airways;
- *Phase IV* – exhalation ceases, inhalation begins and the cycle is repeated.

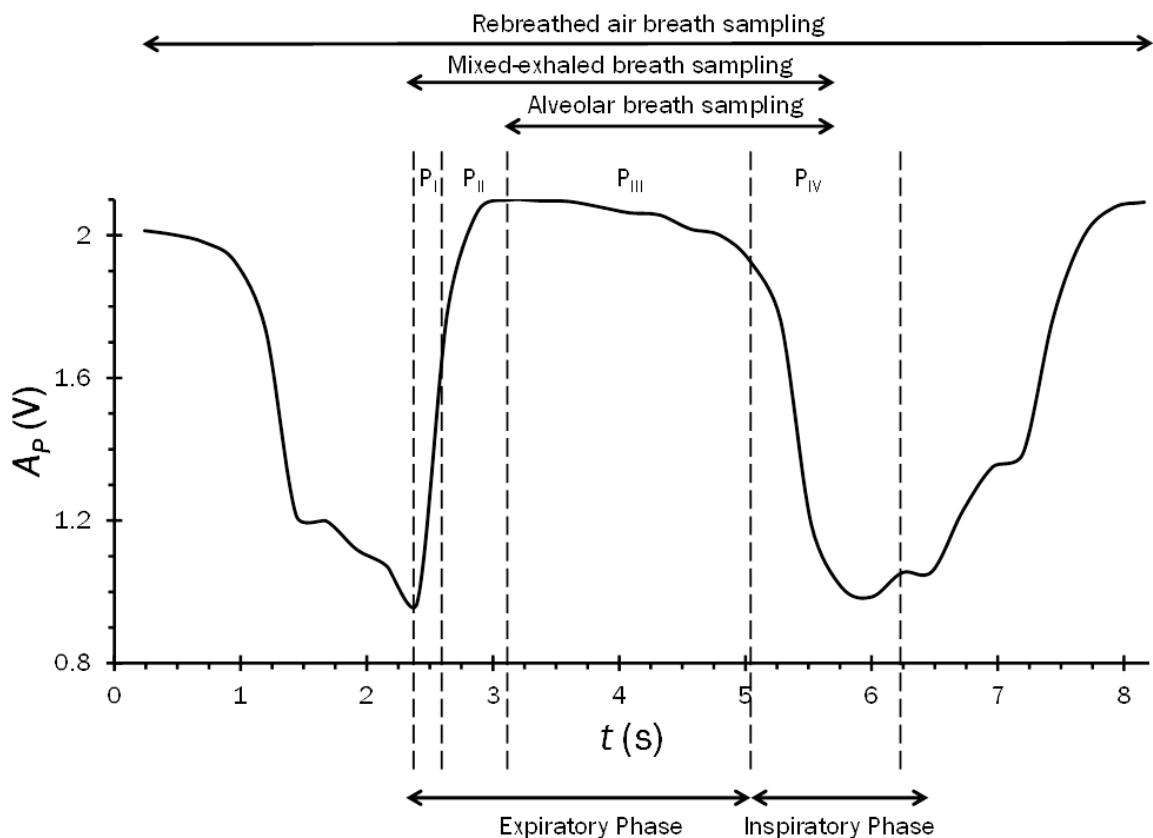


Figure 6 Example of a typical exhaled breath profile of one complete respiratory cycle illustrating the increase in exhaled gas pressure amplitude (A_P) and detailing the fractions of rebreathed, mixed-exhaled and alveolar air used in sample capture. Note: P_* refer to different phases of the respiratory cycle; t = time

Rebreathed air consists of air that has been exhaled into a collection bag, re-inhaled and again exhaled. This allows the concentrations of VOCs in the bag to equilibrate with the gases in the airways. In rats, this technique produced a strong correlation ($r=0.96$) of ethanol in the breath with ethanol in arterial blood [10].

2.2.3 Current uses of exhaled breath analysis

Exhaled ethanol is used as a measure for blood ethanol concentrations by law agencies across the world. Breath ethanol testers (known commonly as breathalysers) were introduced into the UK police force in the 1960s and have been used to give preliminary information on whether a person is driving under the

influence of alcohol. The breath alcohol limit in the UK is set at $35 \mu\text{g } 100\text{ml}^{-1}_{(\text{g})}$ ($35 \text{ mg m}^{-3}_{(\text{g})}$).

eNO is also implemented for general use. The National Institute for Health and Care Excellence (NICE) recommends eNO as an option to diagnose asthma in those who, after initial examination, are considered to have an *intermediate probability* of the condition. It is recommended as a complementary analysis, therefore a negative result does not rule out asthma [11].

Future implications for breath testing are currently in development. Phillips *et al.* [12,13] reported a breath test capable of providing information to predict the rejection of a heart allograft transplant. This test is currently in clinical development in a number of sites across the United States of America [14].

Additionally, *Helicobacter pylori* (*H. pylori*) infection is detected by the presence of carbon labelled urea tests (^{13}C), with breath tests acting as a sensitive and non-invasive sampling method.

2.2.4 Sample collection and analysis methods

Exhaled breath gases

Exhaled breath gases are most commonly collected using Tedlar bags [e.g. 15], breath canisters [e.g. 8] and adsorbent tubes [e.g. 16]. Tedlar bags and breath canisters (BCs) collect mixed-exhaled air and require little training and/or technical equipment. Tedlar bags have low stability for VOC retention (< 2 hrs), require long desorbing time periods and are fragile, leaving them susceptible to leaks and loss of samples. Stainless steel BCs are more robust and have higher stability than the Tedlar bag, but they share also a long desorbing time and are more costly. Adsorbent tubes focus the gases through a metallic mesh and retain volatiles onto adsorbents such as Tenax (for C_6 to C_{30} compounds) and Carbograph (for C_6 to C_{14} compounds). They are relatively inexpensive and can be reconditioned for repeated use. The stability of adsorbent tubes over long storage durations is poorly understood. A gradual loss of some volatiles has been reported over 24 hrs [17],

with another report indicating that transport and storage did not affect diagnostic accuracy after a 14 day period in others [18].

Adaptive breath sampler for alveolar air

Basanta *et al.* [9] described the use of a breath sampling unit that uses a purified medical air supply to produce reproducible, large volume samples of exhaled VOCs in human subjects. Purified air is supplied to a breathing mask through a one-way non-rebreathing valve, and a central control unit monitors exhaled pressure to allow selective sampling of expired air onto an adsorbent trap. Each exhalation is sampled in this manner until a suitable volume has passed through the adsorbent trap, typically around 2 L. This allows enrichment of VOCs present at low concentrations in alveolar air. A schematic drawing of the sampler can be seen in Figure 7.

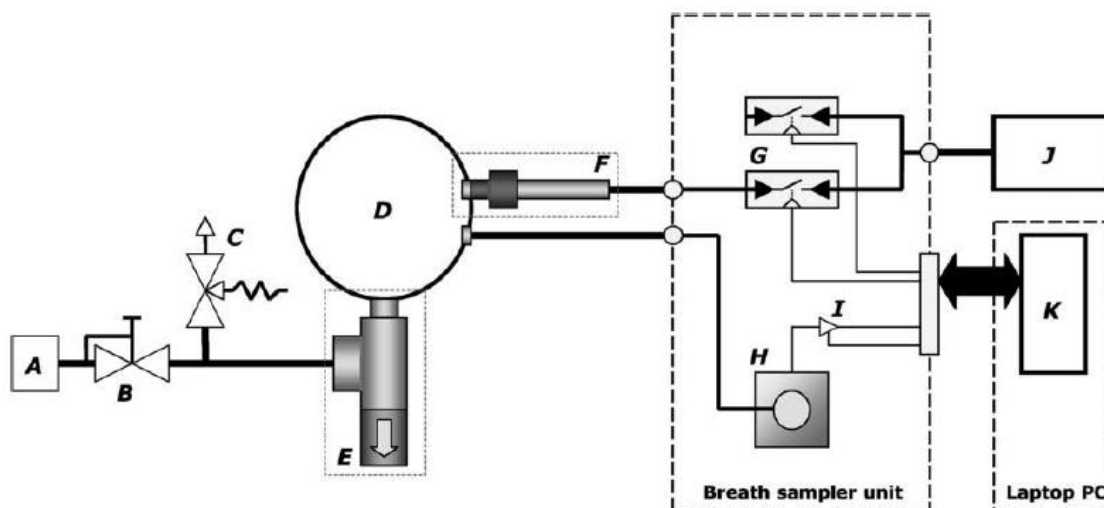


Figure 7 Schematic diagram of the main components of a breath sampling system designed by Basanta *et al.* [9]. Legend: (A) purified air supply; (B) pressure regulator; (C) pressure relief valve; (D) breathing mask; (E) mask air supply assembly; (F) adsorbent sampler assembly; (G) balanced and matched micro-control valves; (H) pressure transducer connected to mask; (I) electronics interface; (J) precision air sampling pump; and, (K) laptop with sampling software; reproduced from [9] with permission from the Royal Society of Chemistry.

Collection and analysis of VOCs using thermal desorption technologies

Although each breath may contain high quantities of VOCs, concentrations of individual compounds may be below limits of detection, or masked by other, more prominent analytes. Use of adsorbent samplers enables thermal desorption (TD) to provide enriched profiles of and therefore, in theory, a wider concentration range for potential biomarker exploration.

Analysis of VOCs from adsorbent traps occurs at concentrations down to pg L^{-1} levels [19], through the use of a pre-concentration step. In TD, the adsorbent tube is heated at a fast rate, causing VOCs to desorb from the surface while a flow of inert gas passes through the tube, carrying the now volatilised compounds. VOCs travel through a flow-path to a second tube, known as the cold trap. This has identical adsorbents packed into a smaller volume and held at sub-zero centigrade, known as cryofocussing. Recovered VOCs are frozen and focussed into the volume of the cold trap, then the cold trap is flash heated under a flow of carrier gas, injecting VOCs into the analytical system. This process allows an enrichment up to 5×10^4 (Figure 8).

Solid-phase micro extraction

Solid-phase micro extraction (SPME) uses a coated fibre that enables different analytes (volatile and non-volatile) to be extracted and concentrated. The extracting phase can be a liquid polymer, a solid sorbent or a combination of the two [21]. For breath investigations, the gases surround the fibre and compounds are retained to maintain an equilibrium. This system allows the pre-concentration and direct desorption to a chromatographic system, without the need for cryofocussing. Fibres are reusable, low cost, simple to use and portable for use outside of laboratory conditions.

SPME utilises a non-quantitative tracking mechanism as it relies on creating an equilibrium with the sample and, therefore, cannot be used for repeated breath exhaled sampling. SPME is suitable for stored breath samples, such as Tedlar bags, canisters and syringes. These methods of collection do not provide a stable sample and, consequently are not suitable for non-targeted discovery studies, where

sample storage and degradation artefacts may mask important underlying trends. For these reasons SPME was not performed and therefore will not be addressed further.

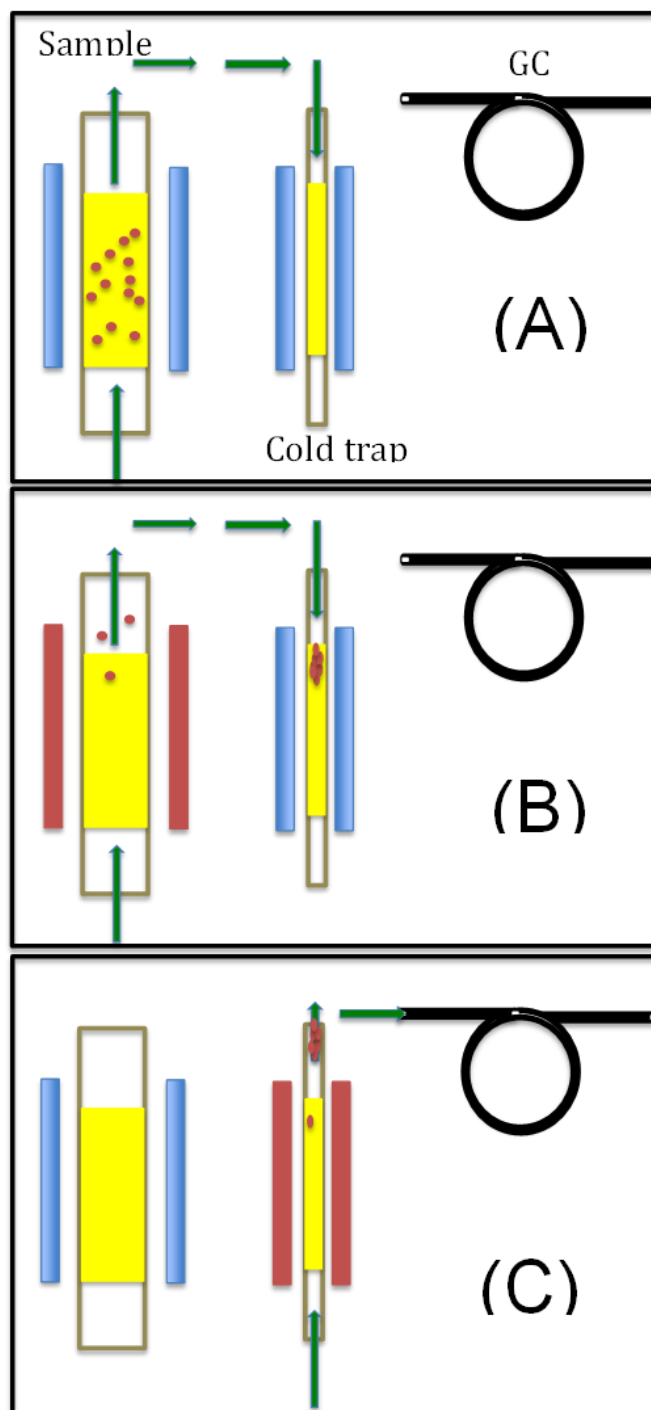


Figure 8 Schematic diagrams to show (A) the presence of collected VOCs on the adsorbent powder of the thermal desorption (TD) tube, (B) the TD of these VOCs from the tube to focus on a cooled cold trap and (C) the rapid heating of the cold trap and ejection of these VOCs off the cold trap and into the gas chromatograph (GC) analytical system; reproduced with permission from [20].

2.3 Gas chromatography-mass spectrometry in exhaled breath analysis

2.3.1 Introduction

Chromatography originates from the early 1900's where Russian botanist Mikhail Semenovich Tswett used an early form of liquid-solid chromatography to separate plant pigments. He termed the process chromatography from the Greek for colour (chroma) and to write (graphein). In 1952, James and Martin [22] were the first to demonstrate gas chromatography (GC) as an analytical tool, when they used it to separate fatty acids.

GC is a physical separation method where a gaseous mixture of compounds is transported along a chromatography column by a carrier gas, and molecules are subject to stationary and mobile phases. The basic GC system (Figure 9) consists of a pressurised and regulated inert gas supply that is mixed with an injected gaseous sample. This mixture passes into a temperature controlled oven containing a column which is internally coated with the stationary phase compound. The carrier gas transports the molecules through the column and out to a detector that is connected to software to plot the peaks that elute. A comprehensive explanation of the theory of GC can be found in chapter 2 of Practical Gas Chromatography by Dettmer-Wilde and Engewald [23].

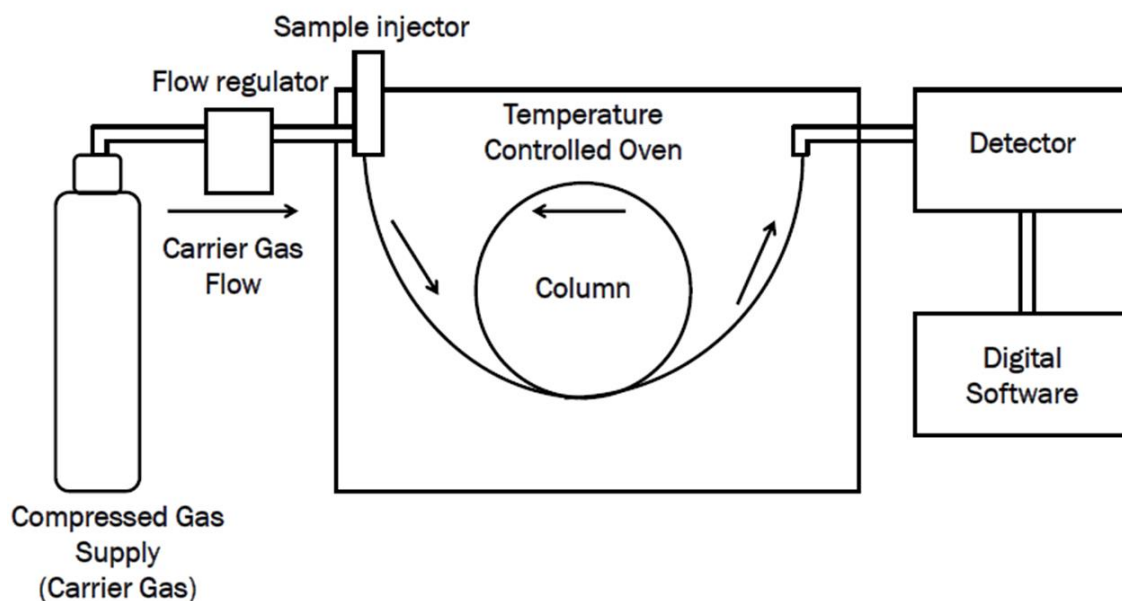


Figure 9 A schematic to illustrate a basic gas chromatography system.

2.3.2 Separation, elution and efficiency

Molecules are separated based on their relative vapour pressures and partition coefficients with the stationary phase, causing the molecules to elute at the end of the column onto the detector at different time intervals, known as the retention time (t_r). The t_r of a molecule depends on its partition coefficient (K_C), with lower K_C values eluting from the column first. Equation 7 defines K_C in terms of the ratio of concentrations of a solute (A) in the stationary phase (s) and the mobile phase (m) at equilibrium.

$$K_C = \frac{[A]_s}{[A]_m} \quad \text{Equation 7}$$

Elution development occurs as the sample moves through the column, consisting of series of adsorption-desorption processes where compounds are distributed between the two phases; this process is always thermodynamically driven towards equilibrium. However, as the gaseous mobile phase is in constant flow in a definite direction, displacement of the concentration of solute in the gas

mobile phase occurs along the column. As the concentration of the mobile phase increases further along the column, the stationary phase concentration falls and the analytes return to the gas phase. They are then carried further along the tube to create equilibrium at the next step. This process repeats throughout the chromatography column and determines t_r (Figure 10).

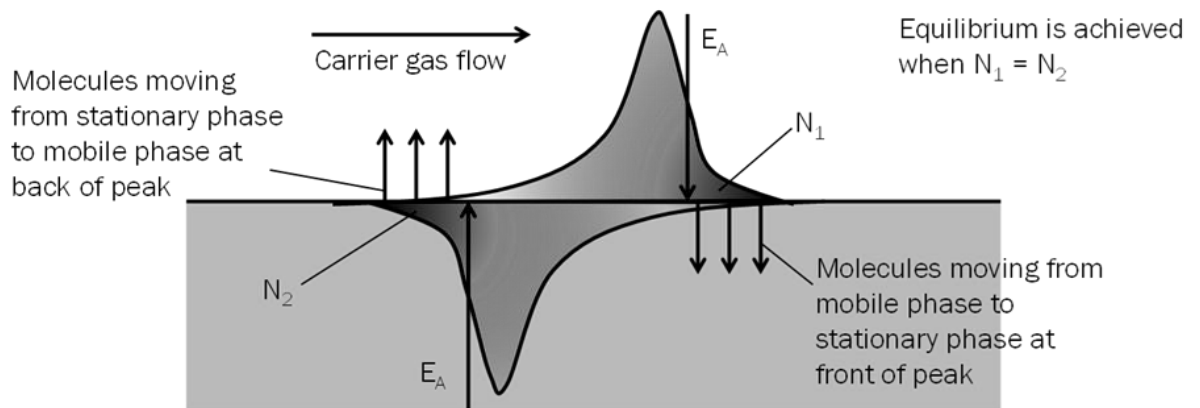


Figure 10 An illustration to show the distribution of the solute between the mobile and stationary phases in a chromatographic column with the influence of a uni-directional carrier gas. EA = region in equilibrium

Figure 11 illustrates samples A and B being introduced into a GC column in a mixed gas. They pass through the column alternating between the stationary and mobile phase at different rates to each other. Sample A passes through the column more rapidly, i.e. shorter t_r , eluting earlier than B, producing two distinct peaks in the chromatogram.

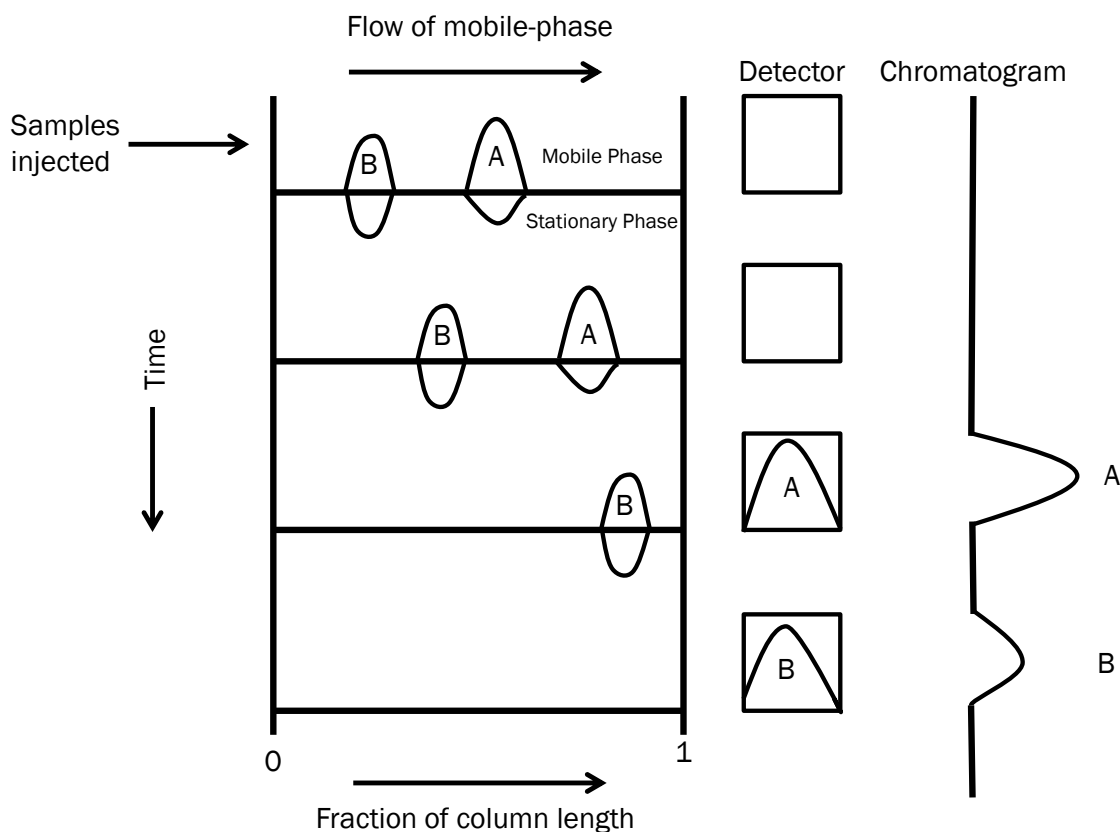


Figure 11 Schematic representation of the chromatographic process; adapted from [23].

Gas chromatography columns consist of two designs; packed and capillary. Packed columns are typically glass or stainless steel tubes that are filled with the stationary phase, or with a packing material that is coated in the stationary phase. Capillary columns are thin fused-silica tubes that have the stationary phase coated on the inner surface. Capillary columns are usually much longer than packed columns and have an internal diameter of 100 to 500 μm , as opposed to mm. Capillary columns produce greater separation efficiency but can be easily overloaded with excessive sample injection. Stationary phases used within these columns are most commonly a mixture of polysiloxanes with differing substituent groups, to change polarity of the phase. Cross-linking of the polymer coated on the column wall or packing material increases thermal stability, and reduces phase break down and bleeding from the column.

Chromatographic column efficiency can be related to the theoretical plate model. The column is modelled as a large number of separate layers (theoretical

plates), where equilibrations of the sample between the stationary and mobile phase occur. The carrier gas transfers the compounds down the column from one plate to the next. The larger the number of theoretical plates (N), the more efficient the column separation. Efficiency can also be stated by the Height Equivalent to a Theoretical Plate (HETP), with a smaller value indicated greater efficiency. The number of theoretical plates is calculated by examining a chromatographic peak after elution, using Equation 8 where $w_{1/2}$ is peak width at half height, and 5.54 is the constant where the base of the peak is 4σ . HETP is then calculated using Equation 9, where L is the length of the column.

$$N = \frac{5.54 t_R^2}{w_{1/2}^2} \quad \text{Equation 8}$$

$$HETP = \frac{L}{N} \quad \text{Equation 9}$$

Values for N are not fixed. Operating conditions are optimised to generate the highest practicable value for N for a given set of compounds. Furthermore, N is compound specific and varies between different species.

2.3.3 *The rate theory of chromatography*

The van Deemter equation

van Deemter *et al.* [24] identified three effects that contribute to peak dispersion. As a sample travels through the column it will begin to randomly disperse and spread, eluting to form a Gaussian shape. The smaller the peak dispersion, the greater level of separation. An example of this is shown in Figure 12.

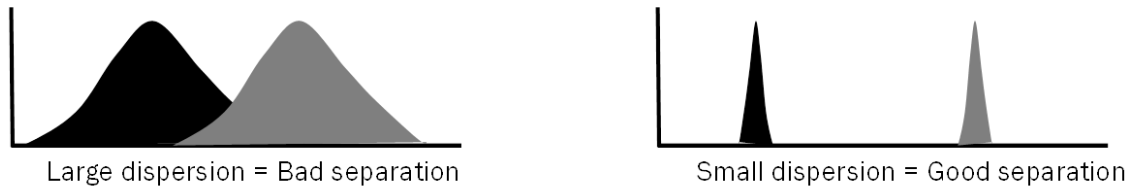


Figure 12 A representation of broad (left) and narrow (right) peaks illustrating the differing dispersion of chromatographic peaks and the effect on separation efficiency.

van Deemter developed the rate theory which identifies three factors that control peak dispersion. These are:

- i) The A-term – eddy diffusion (or multipath dispersion): molecules travel through a packed column and take random paths through the stationary phase. Molecules on a long path take more time to travel through the column and fall behind those on a shorter path, causing dispersion (Figure 13). Equation 10 was derived for multipath dispersion (A), where λ is the packing factor and D_p is the particle diameter of the packed column;

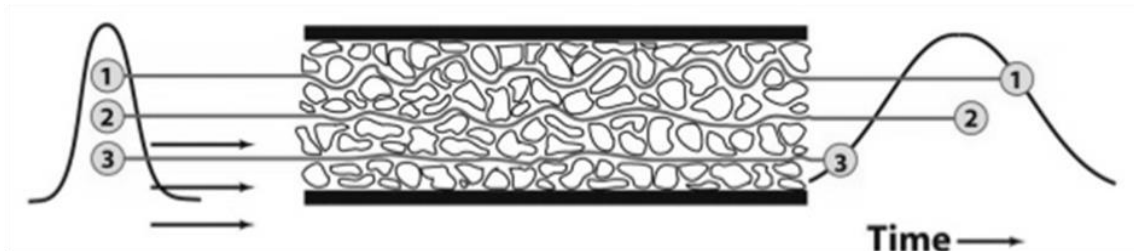


Figure 13 A representation of three identical molecules (1, 2 and 3) taking different paths through a packed column and therefore dispersing the peak on elution; adapted from [25].

$$A = 2\lambda D_p$$

Equation 10

- ii) The B-term – longitudinal diffusion: the concentration of analyte is less at the edges of the band than at its centre. The analyte diffuses out from

the centre toward the edges, producing band broadening. High velocity mobile phase reduces this effect (Figure 14). Equation 11 was derived for longitudinal diffusion (B), where γ is the packing factor, D_m is the diffusivity of the solute in the mobile phase, and \bar{u} is the average linear gas velocity.

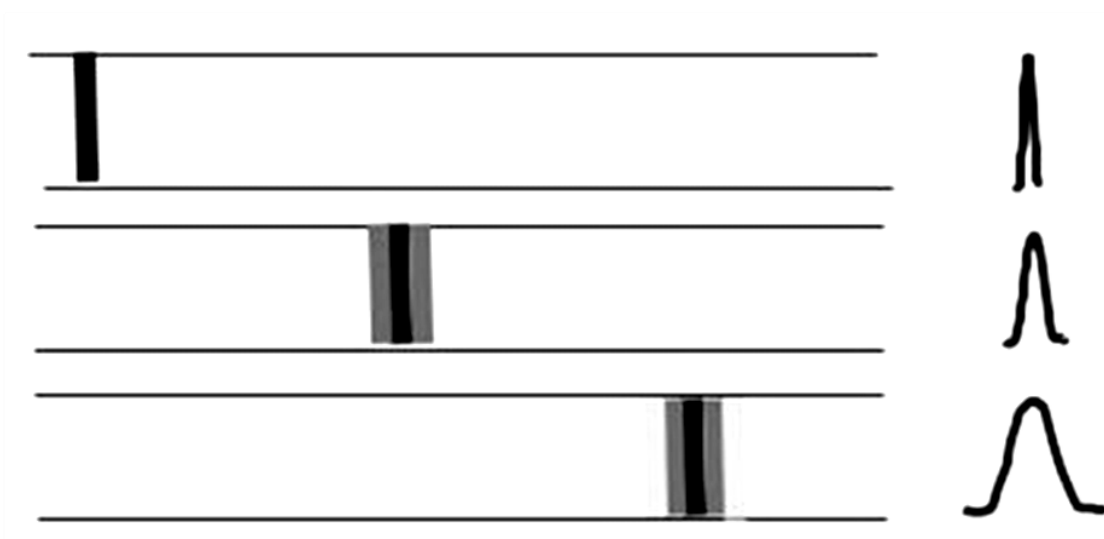


Figure 14 Representation of band broadening through longitudinal diffusion; adapted from [26].

$$B = \frac{2\gamma D_m}{\bar{u}}$$

Equation 11

- iii) The C-term – resistance to mass transfer: an analyte takes a certain time to equilibrate between the stationary and mobile phases. If the velocity of the mobile phase is high, and the analyte has a strong affinity for the stationary phase, the analyte in the mobile phase will move ahead of that in the stationary phase, broadening the band (Figure 15). Equation 12 was derived for resistance to mass transfer (C) where f_1 and f_2 are constants, k' is the capacity ratio of the solute, $d_{p/f}$ is the effective thickness of the mobile/stationary phase, $D_{m/s}$ is the diffusivity of the

solute in mobile/stationary phase and \bar{u} is the average linear gas velocity.

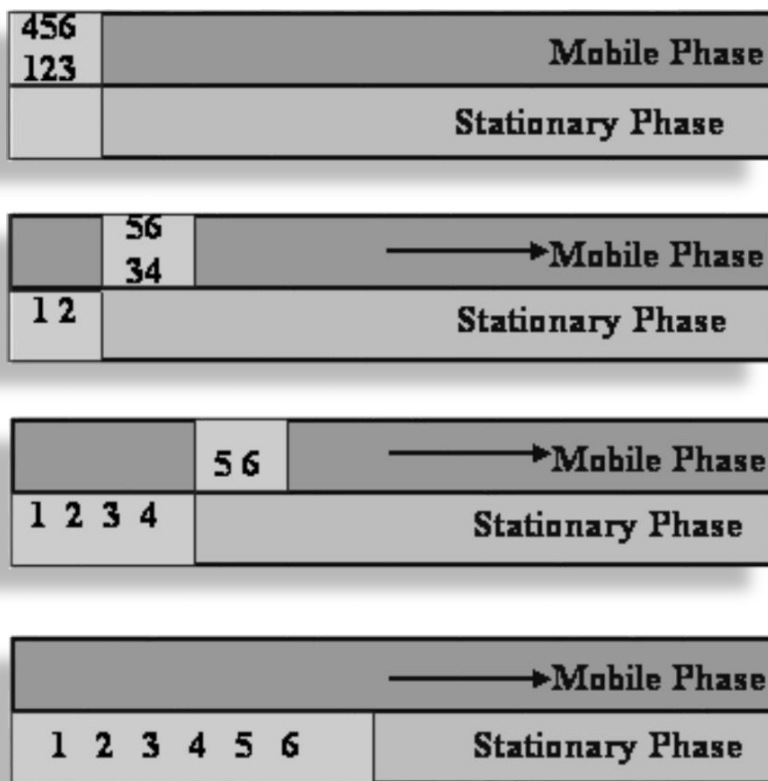


Figure 15 A schematic to illustrate a compound with high affinity to the stationary phase and therefore peak broadening due to the molecules in the mobile phase moving ahead of those in the stationary phase; adapted from [27].

$$C = \frac{f_1 k' d_p^2}{D_m} \bar{u} + \frac{f_2 k' d_f^2}{D_s} \bar{u} \quad \text{Equation 12}$$

These three factors can be integrated together to give the final van Deemter equation (Equation 13).

$$HETP = 2\lambda d_p + \frac{2\gamma D_m}{\bar{u}} + \frac{f_1 k d_p^2 \bar{u}}{D_m} + \frac{f_2 k d_f^2 \bar{u}}{D_s} \quad \text{Equation 13}$$

The Golay equation

Capillary columns are commonly used in modern day GC. There is no A-term as the stationary phase is coated to the internal walls of the column. Golay [28] proposed a new term to satisfy the diffusion process in the gas phase of open tubular columns. The equation (Equation 14) has two C-terms, one for mass transfer of the mass in the stationary phase (C_s) and one for the mobile phase (C_M), where r_c is the column radius, D_m is the diffusion coefficient of the solute in the carrier gas, and K is the distribution coefficient of the solute between the two phases. The simplified Golay equation has a B-term which accounts for molecular diffusion, along with the simplified C_s and C_M (Equation 15).

$$HETP = \frac{2D_m}{\bar{u}} + \frac{f_1 k r_c^2 \bar{u}}{K^2 D_s} + \frac{f_2 k r_c^2 \bar{u}}{D_m} \quad \text{Equation 14}$$

$$HETP = \frac{B}{\bar{u}} + (C_s + C_M)\bar{u} \quad \text{Equation 15}$$

van Deemter plots

When the rate equation is plotted (HETP vs. \bar{u}) a non-symmetrical hyperbola shape is formed (Figure 16). This curve has a minimum point (H_{min}), and is the optimum velocity for the highest efficiency and smallest plate height.

It is possible to use this understanding of the HETP to choose a suitable carrier gas for a GC system. Figure 17 shows the rate equations for Nitrogen, Helium and Hydrogen, when carrying a C_{17} molecule. A higher molecular weight gas will generate more plates since the diffusivity (B-term) is minimised, and therefore will have a lower H_{min} . However, if speed optimisation is required it is more efficient to choose a lighter gas such as helium or hydrogen. The lighter carrier gases have a shallower slope. This means that with an increased flow rate, the loss in column efficiency can be offset with the speed of analysis. If column length can be optimised then the lighter carrier gases would be able to provide the maximum number of plates per second, allowing the fastest analysis times. It is also advantageous to have smaller diameter columns (r_c) as this minimises the C_M term.

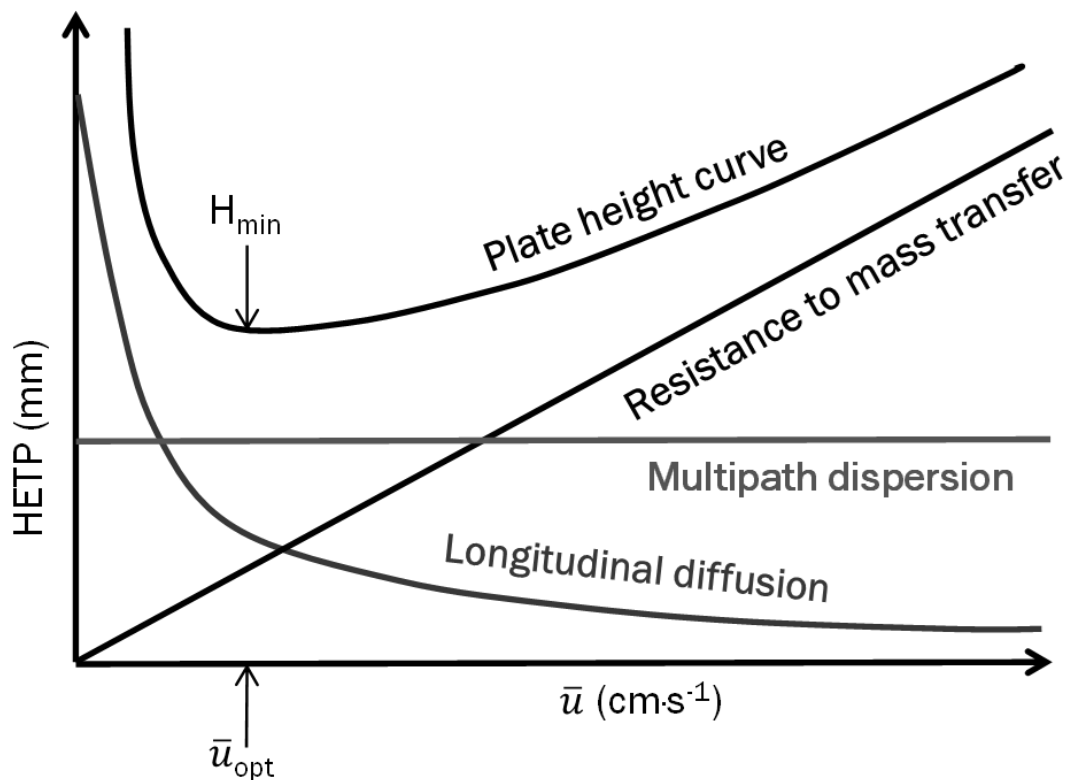


Figure 16 van Deemter plot showing the three factors involved in the rate theory along with a typical plate height curve illustrating the lowest point (H_{\min}) and the optimum velocity through the column (\bar{u}_{opt}).

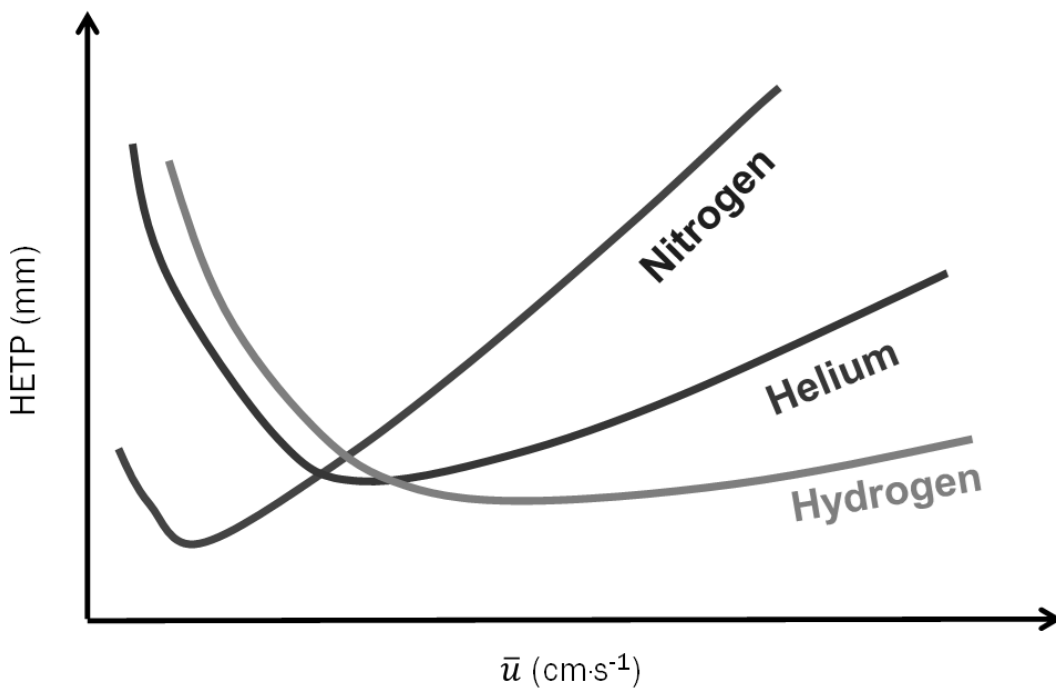


Figure 17 van Deemter plots for three common carrier gases in gas chromatography.

Kovats retention index

Kovats [29] defined a retention index of compounds that were relative to the use of a homologous series of *n*-alkanes. These were used based on their low polarity and freedom from hydrogen bonding. Kovats retention index (*I*) gives a value to each *n*-alkane that is 100x their carbon number. A homologous series of hydrocarbons will have relatively constant intermolecular forces, and so separation occurs primarily due to differences in boiling points (i.e. vapour pressures). A logarithmic relationship is seen, and is linearised by plotting the log of the adjusted retention time (or volume) against *I*. *I* is calculated by running an analyte under the same conditions as the series of *n*-alkanes, and determined from the plotted graph. It is also calculated using Equation 16, where V_N is the adjusted retention time or volume, subscript *u* is used for the unknown analyte and subscript *x/x+1* for the number of carbons in the paraffin series that elutes before and after the unknown.

$$I = \left[\frac{\log(V_N)_u - \log(V_N)_x}{\log(V_N)_{x+1} - \log(V_N)_x} \right] + 100x \quad \text{Equation 16}$$

Resolution

Column efficiency is also determined by the resolution of eluting peaks (R_S). Resolution describes the degree in which adjacent peaks are separated. Equation 17 illustrates how this is determined in chromatography using the distance between the two peaks (*A/B*) of two solutes (*d*), and the width at the base of the two peaks (w_b).

$$R_S = \frac{\frac{(t_R)_B - (t_R)_A}{(w_b)_A + (w_b)_B}}{2} = \frac{2d}{(w_b)_A + (w_b)_B} \quad \text{Equation 17}$$

If adjacent peaks are of equal area and so have the same peak widths; the equation can be simplified to Equation 18.

$$R_S = \frac{d}{w_b} \quad \text{Equation 18}$$

This formula can only be used when the peak heights of the two solutes are equal. Figure 18 shows an example of overlapping peaks, and the sections used to calculate the resolution. The higher the resolution the better the separation, a full baseline separation requires a resolution of ≥ 1.5 .

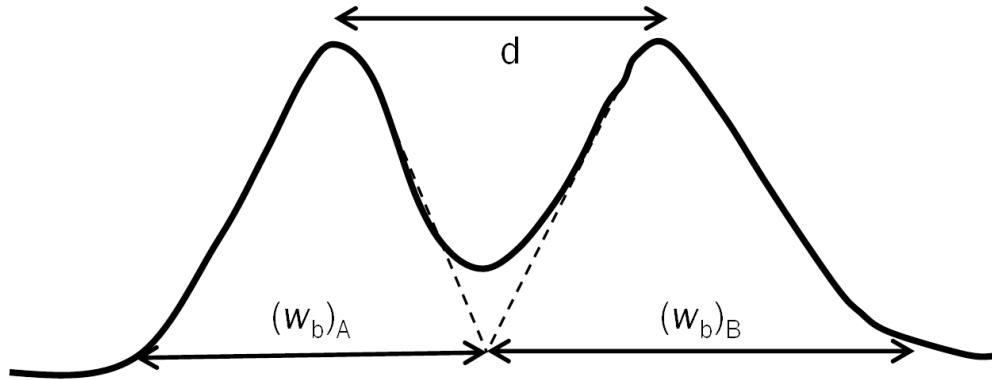


Figure 18 An example of two co-eluting solutes illustrating the distance between peak maxima (d) and the base width (w_b) of the two peaks used to calculate the resolution number.

Open tubular (capillary) columns

Open tubular, or capillary, columns are the most commonly used in modern periods. They are a long, thin and open tube containing no packing material. Most capillary columns exist as a wall-coated open tubular column (WCOT). Tubing is made from glass, stainless steel or fused-silica, with the latter being the most widely used at present. WCOTs consist of a tube diameter from 0.10 to 0.53 mm, and a thin film of liquid phase coated on the inner walls of the column. Due to its open nature, very low flow resistances are recorded. Film thickness varies from 0.1 to 5.0 μm , with thinner films allowing faster analysis times and higher resolution, but with less overall sample capacity. Capillary columns have little loss of pressure throughout the length and a very high efficiency, with 3000 to 5000 theoretical plates per metre being common. Columns are often regularly seen up to 60 m in length, and long paths create very efficient separations in complex mixtures of analytes.

Other forms of capillary columns are:

- i) Support-coated open tubular (SCOT) – containing an absorbed layer of support solid coated with a liquid phase. SCOTs were originally popular due to their ability to hold higher levels of liquid phase, however, the development of cross-linking techniques has allowed stable WCOT films to be produced. These are now only available commercially as stainless steel tubes.

- ii) Porous layer open tubular (PLOT) – containing a porous layer of solid absorbent and are well suited for analysis of light fixed gases.

Programmed temperature in gas chromatography

Programming column temperature to increase through a GC run can optimise analytical output. Distribution constants are temperature dependent, and therefore retention time is inversely proportional to temperature. Gradients can improve separation in complex mixed samples as some compounds may not be separable during isothermal temperature analysis. Increasing temperatures during a GC run allows analytes that are still in the column to have a reduced partition coefficient speeding up their movement and decreasing total analysis time. Additional advantages are: better separation for complexes with analytes of wide boiling point range and improved detection limits, peak shapes and precision. Temperature can increase linearly, or there can be ramps of increasing temperatures at given time points. During this process the temperatures at the injector and detector must remain constant, requiring specialised equipment with three separate ovens for the injector, column and detector. A disadvantage of this technique is that more noise is commonly recorded at higher temperatures.

If sample matrix is screened using programmed temperature gradients, optimum temperature of a single analyte for an isothermal GC run can be calculated. This is known as the significant temperature and is calculated by subtracting 45 from the final temperature at which the analyte eluted in the graduated run.

2.3.4 Mass spectrometry

Mass spectrometry (MS) is a technique used to identify compounds based on their mass to charge ratio (m/z). MS requires multiple processes in order to obtain a measurement of the analyte(s) of interest. A generalised step-by-step approach is as follows (Figure 19):

- i) a gaseous sample is introduced to the system (known as the source). This step can occur by direct infusion of the sample or after separation processes such as liquid and gas chromatography;
- ii) analytes present in the sample undergo ionisation which can occur at atmospheric pressure (e.g. electrospray ionisation) or at vacuum (e.g. electron ionisation);
- iii) after ionisation, the analytes are transferred into a mass analyser under vacuum conditions. In the mass analyser, ions are manipulated by ion optics, and electrical and/or magnetic fields, which separate the ions dependent on their m/z ratio;
- iv) the ions are focussed by the mass analyser onto a detector producing an current for each measured ion;
- v) the detector relays a signal to a digital data system which plots the spectrum using specialised instrument software.

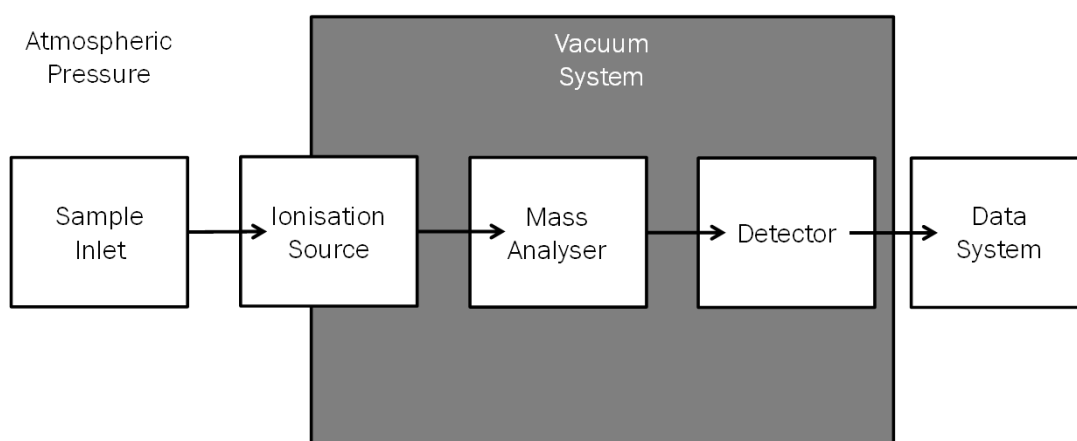


Figure 19 A schematic of the typical processes involved in producing mass spectra.

Sample ionisation

A traditional and widely employed ionisation technique used in organic MS for gaseous samples is electron ionisation (EI). EI is a destructive method, as typically fragmentation of the parent molecule occurs meaning that the molecular ion is not always observed. An advantage is that it leads to reproducible and characteristic fragment patterns in mass spectra. As fragmentation patterns are known within this system, it is possible to create a library of spectra for compounds, allowing identification of unknowns within a sample by comparison.

EI sources consist of a heated filament, which emits electrons focussed into a beam using a magnet (Figure 20). Electrons are accelerated toward the anode at ~ 70 eV and interact with the gaseous molecules. Radical molecular ions or positively charged fragments are created due to the wavelength (λ) of the free e^- . At 70 eV, λ is 1.4 \AA and close to the lengths of the bonds present in the molecules, leading to wave disturbance. If one of the frequencies has an energy corresponding to a transition in the molecule, an energy transfer that leads to excitations can occur. If this energy is sufficient an electron can be expelled [30]. Approximately 10eV is required to ionise most organic compounds and so excess energy provided by the EI source leads to the near complete fragmentation.

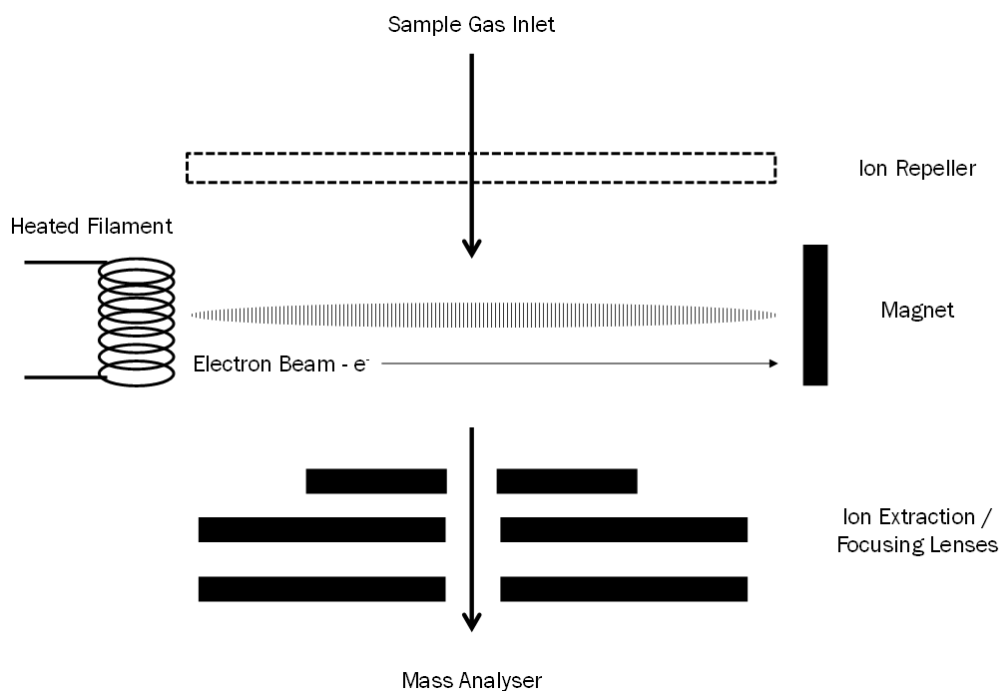


Figure 20 Schematic representation of an electron ionisation source.

Atmospheric pressure chemical ionisation (APCI) is an alternative method of ionisation. APCI is a softer ionisation technique to EI, and usually produces a protonated, intact compound ion for analysis (i.e. $[M+H]^+$). The analyte is directed into the ionisation source and subjected to a corona discharge, causing molecules to ionise and subsequently be analysed in the mass spectrometer.

Mass analysers in mass spectrometry

Mass analysers are used to separate ionised molecules into m/z values and focus them onto the detector. Like ionisation techniques, many different forms have been developed. In this section only quadrupoles and quadrupole (3D) ion traps will be discussed. Other examples of mass analysers include 2D ion traps, time-of-flight, and Orbitrap.

Mass analysers focus ions onto a small area and limit the ions that arrive at the detector to a specific mass or energy. The moving ion passes across an electrical or magnetic field, and is deflected from its original path. A mathematical formula is used to calculate the radial path (r) of the ion due to its mass (m), charge (z), and its interaction with the potential (E) and magnetic field (B) that it passes through (Equation 19).

$$r = \left(\frac{1}{B}\right) \left(2E \frac{m}{z}\right)^{1/2} \quad \text{Equation 19}$$

Detector and exit slits are in a fixed location and applied voltage is generally held constant. Therefore deflection of the ion is dependent on its m/z ratio, which produces a mass spectrum. The mass analyser operates under a vacuum system in the mass spectrometer through the combined use of oil and turbomolecular pumps.

Quadrupole mass filter

Quadrupole mass filters operate without a magnet and separation is performed by using time-varying electric field effects. Four metal rods are aligned in parallel with diagonally positioned rods with identical potentials (direct current, DC), and each pair having opposite polarities. A beam of ions pass through the centre of the rods and a radiofrequency (RF) alternating current potential is superimposed on the static DC potential, inhibiting the ions from colliding with the rods (Figure 21). This causes the ion to follow an oscillating path along the rods, with each m/z having a unique path allowing detection. Only one m/z can be measured at any given time; due to this characteristic, quadrupoles have good sensitivity when selected ion monitoring (SIM) is required. SIM is where a target m/z is applied and the quadrupole is tuned to only allow this ion to pass through to the detector. More than one quadrupole can be used in series to perform MS/MS experiments. For example when using three quadrupoles, the first filters a single m/z value, the second is used as a collision cell causing fragmentation, and the third selectively monitors a target fragment. This method allows a very sensitive and selective analysis of a targeted ion and is known as selective (singular), or multiple, reaction monitoring (SRM/MRM).

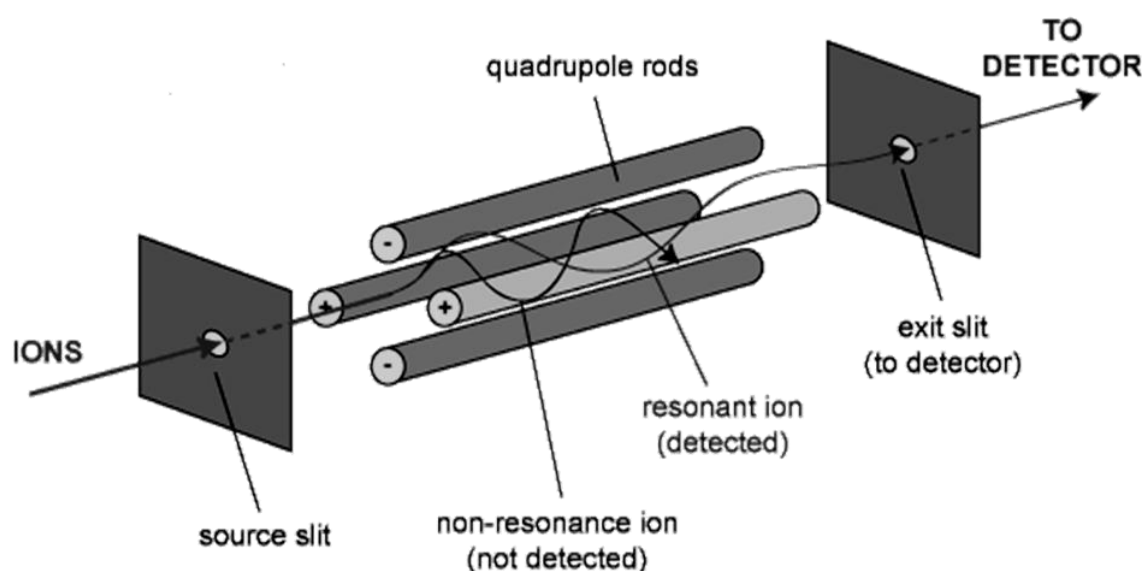


Figure 21 A graphical representation of the four charged rods in a quadrupole mass filter mass analyser and the path taken by the ions as they pass through; adapted from [31].

Selection of masses in the quadrupole filter is achieved through altering the stability of ions as they pass through the ion flight path. In order to reach the detector the ion must be stable across both the x and y axes. As the radius of the quadrupole is constant due to the parallel rods, the DC potential and the RF field are the variables that are manipulated to allow m/z selection. The stability of an ion passing through a quadrupole mass analyser is dependent on the function of the two imposed potentials. As the product of this function increases, stable trajectories favour larger m/z values and an ion of a given m/z will retain a stable flight path until reaching its stability threshold, and therefore no longer able to maintain its path to the detector. Analysis that prospects a wide m/z scan window will employ a change in DC potential as a linear function of the RF field, allowing analysis of ions with successive m/z values (Figure 22). The steeper the slope of the linear function of DC/RF potentials gives a higher resolution, however, the resolution of a quadrupole mass analyser does not allow for elementary analysis and is operated at unit resolution – i.e. at a resolution sufficient to separate peaks one mass unit apart [30].

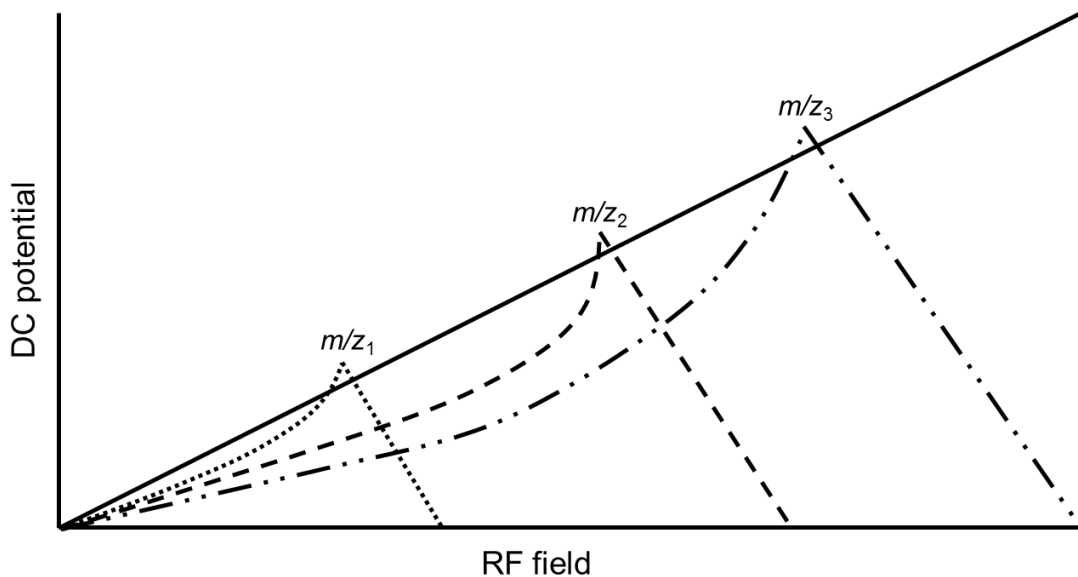


Figure 22 A graphical representation of the stability areas of increasing mass to charge values (m/z_{1-3}). Increasing the function of the direct current (DC) and radiofrequency (RF) field linearly allows for successive analysis of ions with increasing m/z value. An ion shows instability in the system when its stability area passes above the line representing the function of the DC and RF potentials.

Quadrupole ion trap

Quadrupole ion traps store ions with a broad range m/z by causing them to move in stable trajectories. They do this between a ring-shaped electrode and two end caps (Figure 23), accumulating ions with masses extending over several thousand m/z units simultaneously. Ions are subject to an oscillating field, which keeps them situated in the centre of the ion trap. Ions of a specific mass are ejected for detection by increasing the radiofrequency field in the direction of the end caps, causing the ions to become unstable within the electrical field. As they near the edge of stability, the ions are pulsed out of the trap and onto the detector.

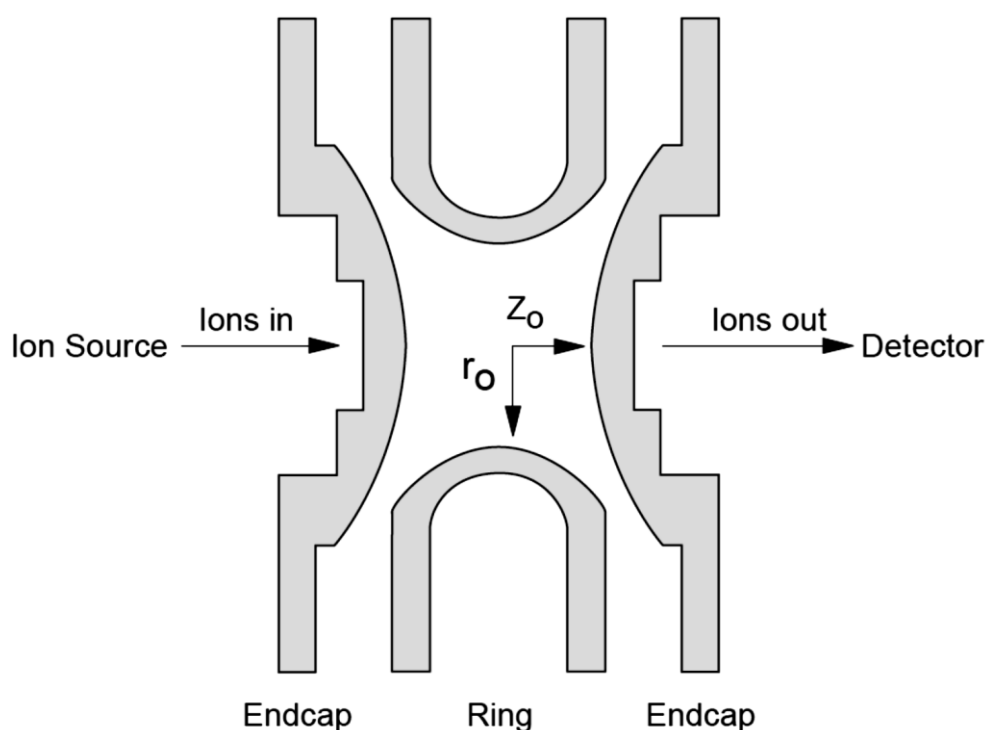


Figure 23 A graphical representation of a cross-sectional slice of a quadrupole ion trap mass analyser. The device is radially symmetrical, and z_0 and r_0 represent its size; adapted from [32].

For a quadrupole ion trap, no DC potential is applied and therefore the ejection of ions occurs due to the imposed RF field. At a given RF potential, ions can be found to lie along a line (q_z) that crosses the stability area. Lower m/z values are situated closer to the point of instability. As the RF field is increased, the q_z for each ion is increased. When the q_z value of an ion reaches a point >0.908 and is outside of the stability region (a value >1), the ion reaches its limit of stability and is ejected on the z axis to the detector Figure 24.

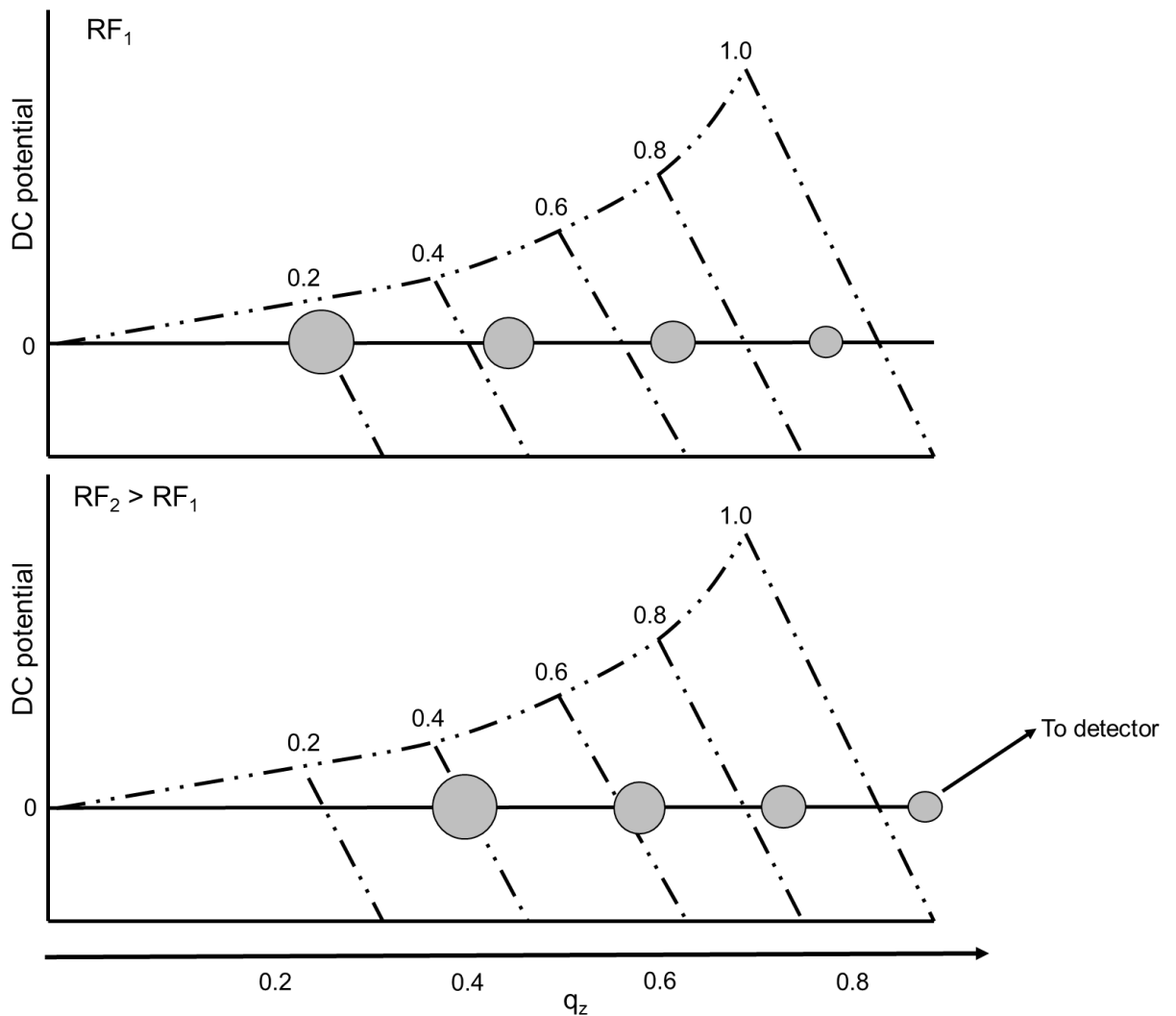


Figure 24 A graphical representation of the stability of increasing m/z values in a quadrupole ion trap. As the RF field is increased the ions are shifted along q_z toward an area of instability. Once an ion is situated outside of the stability area it is ejected out of the quadrupole ion trap along the z axis, causing 50 % of the ions of a single m/z to be directed toward the detector.

Ion detection

The only detector that will be covered in this section is the electron multiplier (EM); the most widely used detector in MS. An EM works by having ions accelerated towards it at a very high velocity, colliding with a conversion dynode (held at a polarity opposite to that of the ions). Here there is an emission of a secondary set of electrons. Electrons are then multiplied through a cascade effect in the EM to produce a current. This cascade occurs due to electrons continually striking the dynode along a curved wall, producing further increased numbers of electrons as they accelerate toward the end of the detector (Figure 25). Finally, a metal anode collects the electron stream and a current is measured.

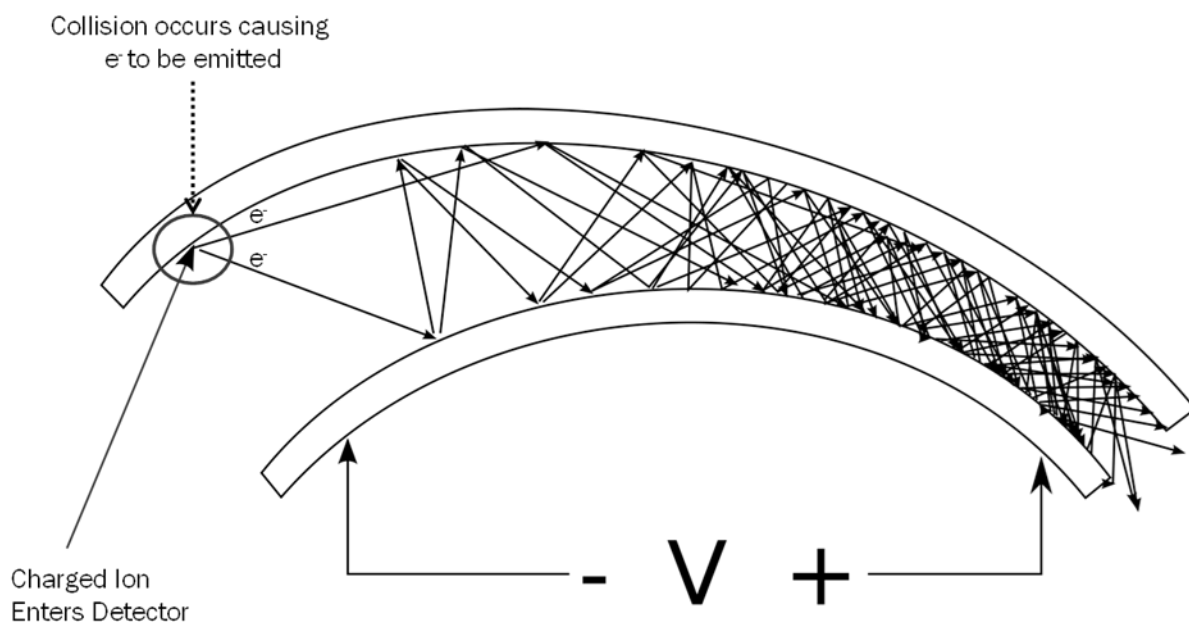


Figure 25 A graphical representation of a charged ion colliding with the dynode of an electron multiplier causing a cascade of secondary electrons; adapted from [33].

2.4 Thermal desorption-gas chromatography-mass spectrometry

A mass spectrometer can be used as a detector for GC analysis. Coupling analytical instruments together allows for a very powerful analytical tool of separation and identification, especially when combined with a method of pre-concentration. This method is extremely sensitive when measuring volatile compounds from breath that have been desorbed onto sorbent tubes. Figure 26 shows a layout of the processes involved for a TD-GC-MS exhaled breath analysis.

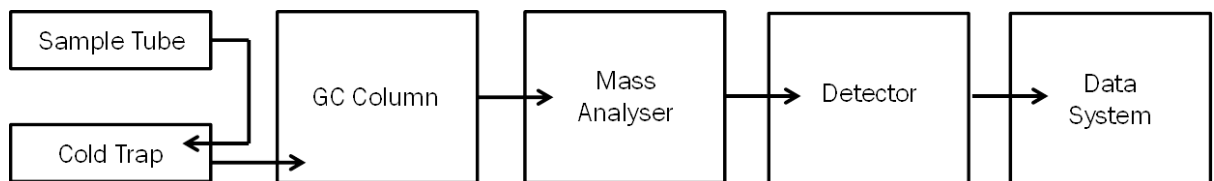


Figure 26 A layout of the process involved in a typical thermal desorption-gas chromatography-mass spectrometry analysis.

2.5 Proposed experiments

In order to explore the potential of breath analysis in sport science, three studies were undertaken:

- i) the analysis of exhaled breath of recreational swimming to track elimination of disinfection by-products, and to apply discovery metabolomic methods to test for detectable signs of inflammation;
- ii) the analysis of exhaled breath in conjunction with a maximal oxygen uptake test, to establish if metabolomic methods were able to identify “fitness markers”;
- iii) the development and preliminary testing of an interface to enable breath-by-breath mass spectrometry of exhaled breath for use during exercise interventions.

2.6 References

- 1 Levitt MD, Ellis C, Furne J. Influence of method of alveolar air collection on results of breath tests. *Drug Dis. Sci.* 1998;43:1938-45
- 2 McConnell A. *Breath strong, perform better.* Champaign, IL: Human Kinetics; 2011:16
- 3 Gildea TR, McCarthy K. Pulmonary function testing.
<http://www.clevelandclinicmeded.com/medicalpubs/diseasemanagement/pulmonary/pulmonary-function-testing> (accessed 18 October 2015)
- 4 West JB. *Respiratory physiology: the essentials [6th ed].* Philadelphia, PA: Wolters Kluwer Health/Lippincott Williams & Wilkins; 2008
- 5 Christiansen J, Douglas CG, Haldane JS. The absorption and dissociation of carbon dioxide by human blood. *J. Physiol.* 1914;48:244-71
- 6 Pauling L, Robinson AB, Teranishi R, Cary P. Quantitative analysis of urine vapour and breath by gas-liquid partition chromatography. *Proc. Nat. Acad. Sci.* 1971;68:2374-6
- 7 Phillips M, Herrer J, Krishnan S, Zain M, Greenberg J, Cataneo RN. Variation in volatile organic compounds in the breath of normal humans. *J. Chromatogr. B* 1999;729:75-88

8 Pleil DJ, Lindstrom AB. Measurement of volatile organic compounds in exhaled breath as collected in evacuated electropolished canisters. *J. Chromatogr. B* 1995;665:271-9

9 Basanta M, Koimtzis T, Singh D, Wilson I, Thomas CL. An adaptive breath sampler for use with human subjects with an impaired respiratory function. *Analyst* 2007;132:153-63

10 Hiltunen AJ, Järbe TU, Hellström-Lindahl E, Croon LB, Jones AW. Concentrations of ethanol in rebreathed air of rats: correlation with the discriminative stimulus effects of ethanol. *Alcohol* 1989;6:39-43

11 National Institute for Health and Care Excellence. NICE diagnostics guidance [DG12]: Measuring fractional exhaled nitric oxide concentration in asthma: NIOX MINO, NIOX VERO and NObreath. National Institute for Health and Care Excellence 2014

12 Phillips M, Boehmer JP, Cataneo RN, Cheema T, Eisen HJ, Fallon JT, Fisher PE, Gass A, Greenberg J, Kobashigawa J, Mancini D, Rayburn B, Zucker MJ. Heart allograft rejection: detection with breath alkanes in low levels (the HARDBALL study). *J. Heart Lung Transplant* 2004;23:701-8

13 Phillips M, Boehmer JP, Cataneo RN, Cheema T, Eisen HJ, Fallon JT, Fisher PE, Gass A, Greenberg J, Kobashigawa J, Mancini D, Rayburn B, Zucker MJ. Prediction of heart transplant rejection with a breath test for markers of oxidative stress. *Am. J. Cardiol.* 2004;94:1593-4

14 Menssana Research Inc. Point-of-care breath test - Heart Transplant Rejection (Heartsbreath™).

http://www.menssanaresearch.com/products_Heartsbreath_heart_transplant_rejection_Menssana.html (accessed 14 February 2016)

15 Caldeira M, Barros AS, Bilelo MJ, Parada A, Câmara JS, Rocha SM. Profiling allergic asthma volatile metabolic patterns using a headspace-solid phase microextraction/gas chromatography based methodology. *J. Chromatogr. A* 2011;1218:3771-80

16 Turner MA, Gullar-Hoyas C, Kent AL, Wilson ID, Thomas CLP. Comparison of metabolomics profiles obtained using chemical ionization and electron ionization MS in exhaled breath. *Bioanalysis* 2011;3:2731-8

17 Mochalski P, Wzorek B, Sliwka I, Amann A. Improved pre-concentration and detection methods for volatile sulphur breath constituents. *J. Chromatogr. B Analyt. Technol. Biomed. Life Sci.* 2009;877:1856-66

18 van der Schee MP, Fens N, Brinkman P, Bos LD, Angelo MD, Nijssen TM, Raabe R, Knobel HH, Vink TJ, Sterk PJ. Effect of transportation and storage using sorbent tubes of exhaled breath samples on diagnostic accuracy of electronic nose analysis. *J. Breath Res.* 2013;7:016002

19 Miekisch W, Schubert JK. From highly sophisticated analytical techniques to life-saving diagnostics: Technical developments in breath analysis. *Trends in Anal. Chem.* 2006;25:665-73

20 Turner MA. Boundaries in volatile organic compounds in human breath. PhD thesis. Loughborough, Loughborough University; 20163

21 Amorim LCA, de L Cardeal Z. Breath air analysis and its use as a biomarker in biological monitoring of occupational and environmental exposure to chemical agents. *J. Chromatogr. B* 2007;853:1-9

22 James AT, Martin JP. Gas-liquid partition chromatography: the separation and micro-estimation of volatile fatty acids from formic acid to dodecanoic acid. *Biochem. J.* 1952;50:679-90

23 Miller JM. *Chromatography: concepts and contrasts* 2nd ed. Hoboken, NJ, USA: John Wiley & Sons; 2009

24 van Deemter JJ, Zuiderweg FJ, Klinkenberg A. Longitudinal diffusion and resistance to mass transfer as causes of nonideality in chromatography. *Chem. Eng. Sci.* 1956;5:271-89

25 Harris D. *Quantitative chemical analysis*. New York, NY: W.H. Freeman; 1999

26 Chromatography Online. Ion chromatography – multi-path diffusion. <http://www.chromatography-online.org/ion-chromatography/Column-Efficiency/Multi-path-Diffusion.php> (accessed 18 October 2015)

27 Chromatography Online. Ion chromatography - dispersion by resistance to mass transfer in the mobile phase. <http://www.chromatography-online.org/ion-chromatography/Column-Efficiency/Resistance-to-Mass-Transfer-in-the-Mobile-Phase.php> (accessed 18 October 2015)

28 Golay MJE. *Gas chromatography*. Desty DH [ed]. London, UK: Butterworths; 1958

29 Kovats E. Gas-chromatographische charakterisierung organischer verbindungen. Teil 1: Retentionsindices aliphatischer halogenide, alkohole, aldehyde und ketone. Helv. Chim. Acta 1958;41:1915-32

30 de Hoffmann E, Stroobant V. Mass spectrometry: principles and applications [3rd ed]. Chichester UK: John Wiley & Sons Ltd: 2007

31 Gates P. Gas Chromatography Mass Spectrometry (GC/MS). <http://www.bris.ac.uk/nerclsmsf/techniques/gcms.html> (accessed 10 October 2015)

32 Wong PSH, Cooks RG. Ion trap mass spectrometry. Curr. Sep. 1997;16:85-92

33 Egmaison. The continuous electron multiplier. https://en.wikipedia.org/wiki/Electron_multiplier#/media/File:Electron_multiplier.svg (accessed 10 October 2015)

CHAPTER THREE: GENERAL METHODS

3.1 Exhaled VOC sampling

3.1.1 *Exhaled VOC sampling mask preparation*

Face masks were cleaned, sterilised and conditioned to remove VOC contaminants after each use. Masks were dismantled and all parts were soaked in disinfectant solution (Milton Baby Care, Newmarket, UK) following manufacturer's instructions. Once disinfected, items were rinsed in clean, cold water for 5 min and air dried before vacuum conditioning at 40 °C and 0.7 mBar for at least 15 hrs. This final step removed VOC residues formed on the mask parts during sterilisation. After vacuum conditioning, mask parts were organised into complete sets and transferred to an airtight sealed plastic box for storage. The following items were present:

- Main full-face mask body.
- Silicone pillow and positioning clip.
- Forehead support and silicone cushion.
- Custom built T-piece with positioning clip and air inlet adapter.
- Adjustable clip harness.
- One-way non-rebreathing valve (single use).

3.1.2 *Thermal desorption tube preparation*

Adsorbent sampling tubes were supplied by Markes International (Llantrisant, UK). All tubes were industry standard stainless steel tubes packed with a hydrophobic dual-bed absorbent mixture of Tenax TA and Carbograph 1TD (Part code C2-AXXX-5032).

Adsorbent tubes were conditioned before use by back-flushing with purified nitrogen at 300 °C for a minimum of 3 hrs, followed by 'thermal polishing' under a

flow of helium at 300 °C for 20 min in a Unity thermal desorption unit (Markets Int., Llantrisant, UK). Once conditioned and prepared for use, adsorbent sample tubes were sealed with airtight caps and stored in a sealed plastic container at 4 °C. Clean white cotton gloves were used to handle thermal desorption (TD) tubes at all times.

3.2 Breath sampling protocol

3.2.1 Air supply to the participant.

Exhaled breath VOCs were sampled using a portable adaptation of a previously described protocol [1]. Compressed ambient air was supplied by a marine diaphragm pump (HIBLOW linear air pump HP-200, Techno Takatsuki, Osaka, Japan) to a three-stage purification process, before being fed to supply the sampling mask. Air supply connections were push-fit silicon tubing, and were regularly conditioned in a vacuum oven.

Compressed air was dehumidified by passing it through a custom made stainless steel vessel containing a molecular sieve (Acros Organics, Fisher Scientific, Loughborough, UK). Then artefact VOCs were removed by passing the air through a bed of granular activated charcoal 4 to 8 mesh (Sigma-Aldrich, Gillingham, UK), housed in a stainless steel vessel. The final stage was a respirable dust and particulate filter. A detailed schematic and list of components for the portable sample can be found in Appendix 1 (Section 3.6).

Regular maintenance ensured the air supplied to the face mask during exhaled VOC sampling was safe and free from contamination. Blank samples were checked after each participant, and the air purification system dismantled and all the components conditioned when required. The large stainless steel unit containing the molecular sieve was connected to a purified nitrogen supply and back flushed for a minimum of 15 hrs at 300 °C. Activated charcoal was removed from its holder and transferred to a clean glass beaker and placed in a vacuum oven. Stainless steel fittings, including the filter, were dismantled, cleaned and

placed into the vacuum oven alongside the beaker of charcoal. These components were then heated to 170 °C at 0.7 mBar for at least 15 hrs. Once complete and all items had cooled to < 40 °C, items were removed from vacuum, reassembled and re-attached immediately to the air supply unit. Final checks assured the air supply was without leaks and supplied flow to the sampling mask was sufficient. Clean white cotton inspection gloves were worn when handling the purified air supply hardware.

3.2.2 Sampling procedure.

Exhaled breath sampling

Purified air was supplied to the sampling mask using silicone tubing connected to an inlet on a PTFE custom made T-piece. This was fitted with a disposable one-way non-rebreathing valve that allowed the inhalation of purified air only, and suppressed the ingress of ambient air contamination into the breath mask. Supply flow was a minimum of 30 L min⁻¹. The mask was fitted to the participant and secured by an adjustable clip harness. Participants were encouraged to relax and breathe in a natural manner. Five minutes of equilibration time was allowed for each participant prior to sampling. The mask was connected by silicone tubing to a pressure sensor located in the central control unit. A virtual instrument ([1]) analysed the pressure signal and displayed a recording of the breath profile, sending trigger control pulses to micro-valves that switched to allow the sample pump (Escort Elf, Zefon Int., Ocala, FL, USA) to withdraw a portion of exhaled breath. The sample programme was set to ensure that distal, i.e. alveolar, air was sampled.

A custom built connection housing a silico-steel sampling capillary (Figure 27) was connected to a luer fitting on the main body of the mask, and an adsorbent sampling tube was connected in-line with the sampling capillary. The rear end of the adsorbent tube was connected by silicone tubing to the switching micro-valve mentioned above (see Figure 28 for an example of the sampling equipment fitted to a participant).

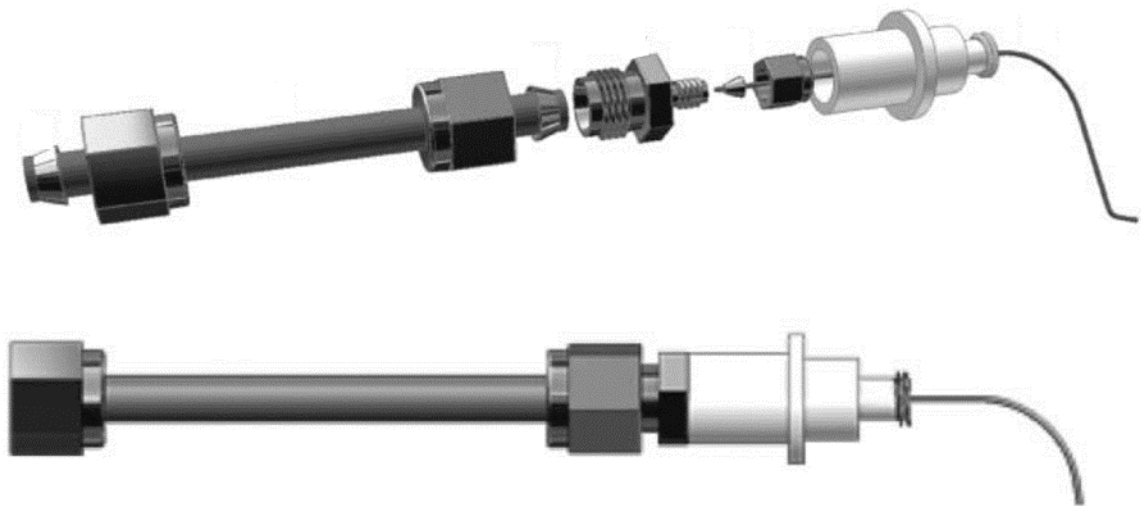


Figure 27 Three dimensional rendering of custom made capillary sampling connector and its attachment to a commercially available stainless steel thermal desorption tube; adapted from [1].

Exhaled air was sampled at 0.8 L min^{-1} . Sampling time was controlled manually, ending once the specified sample volume had been processed. This was 2 L for all experiments detailed in this thesis. TD tubes were removed from the sampling mask and capped immediately with airtight Swagelok seals, and then placed into an airtight sealed plastic box and stored at $4 \text{ }^{\circ}\text{C}$ until analysis (mean storage time equalled 51 days). After use, the breath sampling mask and its tubing were returned to the laboratory to be cleaned and prepared ready for reuse.

Environmental sampling

Environmental samples were collected by connecting TD tubes to the sample pump. A flow of 0.5 L min^{-1} was used for 4 min, collecting a total of 2 L of environmental air. These environmental blanks were collected for both ambient and filtered air supplies at all sampling locations, and analysed using the same methods as exhaled samples.

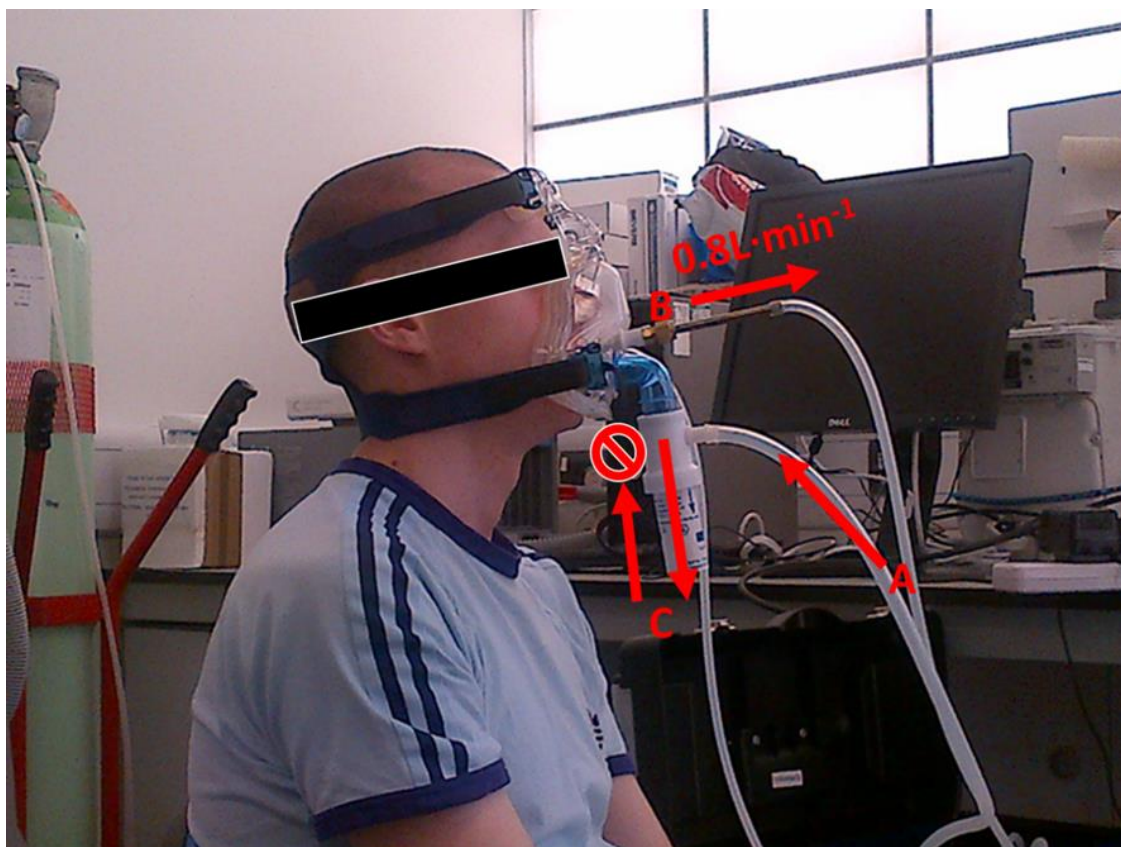


Figure 28 Image showing an individual participant providing an exhaled breath volatile sample during an experimental trial. The participant is wearing the full face mask provided with an inlet of purified air (A), with exhaled alveolar air being sampled through a thermal desorption tube controlled via an external pressure sensing device (B). The participant is isolated from environmental air through the use of a one-way non-breathing valve (C).

3.3 Exhaled VOC sample analysis

3.3.1 Analytical methods

All exhaled VOC samples collected onto adsorbent beds contained in the stainless steel TD tubes were analysed by thermal desorption-gas chromatography-mass spectrometry (TD-GC-MS). The general analysis protocol has been described in breath analysis publications from the Centre for Analytical Science (Loughborough University) [1,2]. An explanation for each step of the analysis is described and an overview of conditions is summarised in Table 6.

Pre-analysis preparation

Prior to analysis of exhaled VOCs, sample tubes were removed from storage at 4 °C and allowed to warm to room temperature. Once at room temperature, the TD tube was attached to an injector and a 20 ng toluene-D₈ (T-D₈) internal standard was loaded onto the tube. This was performed by injecting 0.1 µL of 200 µg mL⁻¹ T-D₈ solution in methanol into purified nitrogen flowing through the TD tube at a flow of 100 mL min⁻¹. The adsorbent tube remained connected to the injector for 60 s to ensure efficient transfer of the standard onto the adsorbent packing.

Thermal desorption

TD was performed using a Unity TD Unit (Markes Int, Llantrisant, UK). Tubes were fitted into the tube oven and rapidly heated to 300 °C for 5 min under a helium desorption flow of 45 mL min⁻¹. Desorbed VOCs were transferred to a general purpose hydrophobic cold trap (Markes Int., Llantrisant, UK) held at -10 °C. Flow from the sampling tube to the cold trap was splitless, with all recovered VOCs eluting into the cold trap where they were enriched. Once the 5 min primary thermal desorption was complete, the cold trap was rapidly heated to 300 °C for 5 min whilst a helium carrier gas transferred the recovered VOCs to the GC column at 2 mL min⁻¹. The secondary desorption was splitless and the transfer line to the GC was maintained at 180 °C.

Prior to analysing each sample batch, a retention index standard was analysed to assess system performance. A mixture containing a range of *n*-alkanes (C₈ to C₂₀) was used, and later utilised to allocate retention indices to VOCs isolated from samples. The cold trap was cleaned and conditioned between each sample analysis by heating to 300 °C for 5 min, with a flow of helium at 2 mL min⁻¹. Desorbed residues were analysed by GC-MS and contamination levels assessed. This conditioning assessment was repeated until levels of contamination were deemed as acceptable. This usually required one or two trap cycles between each sample analysed. A step-by-step flow chart for an example daily analysis routine, and corresponding chromatographic traces indicating an example of a retention index standard analysis and inter-sample trap blank is shown in Figure 29.

Table 6 Thermal desorption, gas chromatography and mass spectrometry conditions for the analysis of exhaled breath volatile samples; adapted from [2].

Thermal desorption conditions (Markes Unity 1)

Tube desorption:	300 °C for 5min
Desorption flow:	45 mL min ⁻¹ splitless
Cold trap:	General purpose hydrophobic
Trapping temperature:	-10 °C
Trap desorption:	300 °C for 5 min
Trap desorption flow:	2 mL min ⁻¹ splitless
Flow path temperature:	180 °C

Gas chromatograph conditions (Varian 3800)

Column:	Rxi-5ms 60 m x 0.25 mm i.d. x 0.25 µm.
Initial oven temperature:	40 °C
Oven temperature ramp:	5 °C min ⁻¹
Final oven temperature:	300 °C hold for 8 min
Carrier gas:	Helium
Carrier gas flow:	2 mL min ⁻¹

Mass spectrometer conditions (Varian 4000)

Trap temperature:	150 °C
Manifold temperature	50 °C
Transfer line temperature:	300 °C
El scan mode:	El auto
El scan frequency:	2 Hz
El scan range:	<i>m/z</i> 40-450

Note: i.d.: internal diameter; El: electron impact ionisation

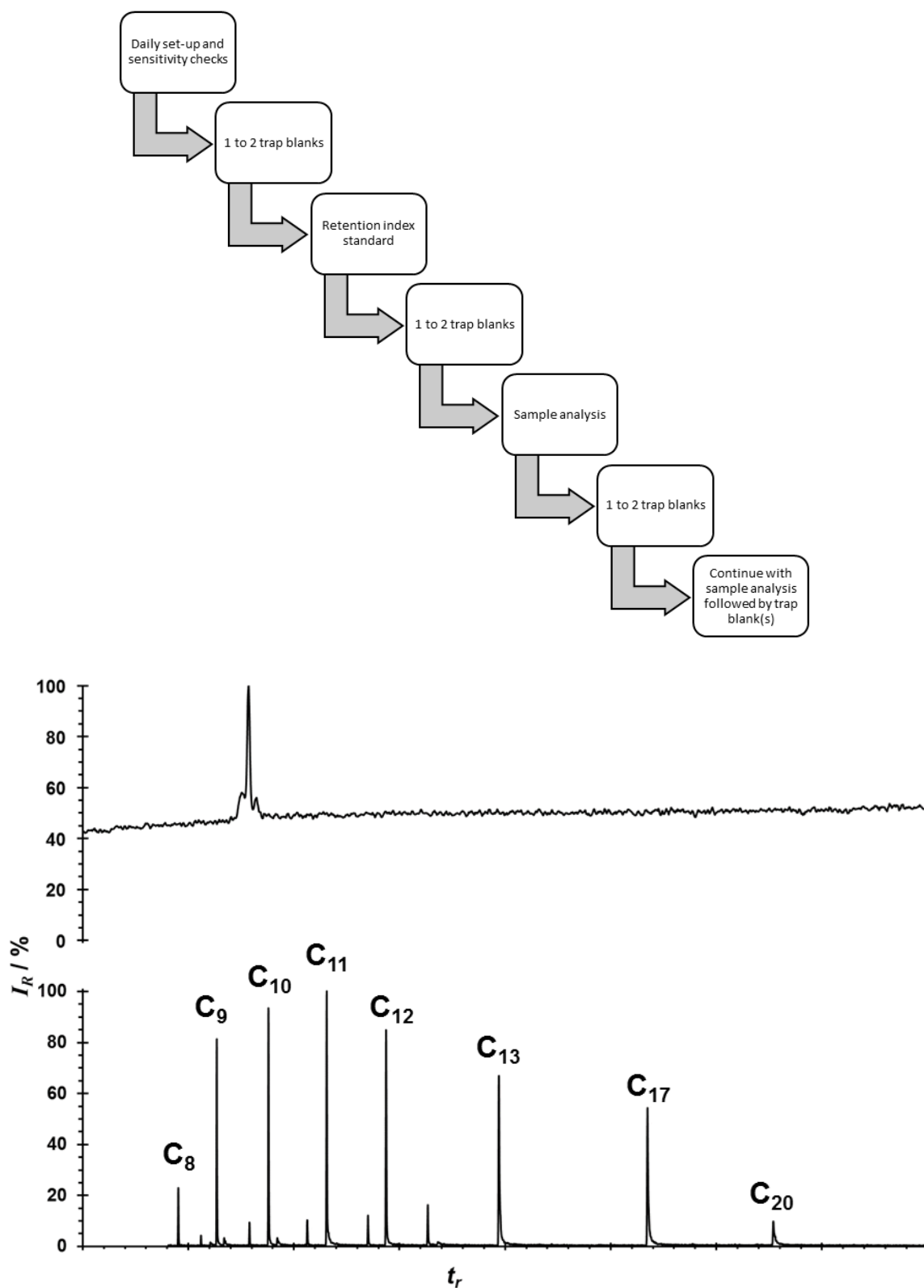


Figure 29

An example step-by-step flow chart for a daily analysis routine (top) and an example chromatogram for a retention index standard analysis (bottom, lower trace) showing *n*-alkanes with a carbon number (C#) ranging from 8 to 20 and a trap blank chromatogram for inter-sample system conditioning (bottom, upper trace).

Note: I_R = relative intensity; t_r = retention across time

Gas chromatography

Gas chromatography was performed using a Varian 3800GC series instrument (Varian Inc. – now Agilent Technologies, Palo Alto, CA, USA) fitted with a 60 m Rxi-5ms gas chromatography column (Catalogue # 13426; Restek, Bellefonte, PA, USA) (see Table 6). A carrier gas flow of helium maintained at 2 mL min⁻¹ was used. The oven was set at an initial temperature of 40 °C, with a linear temperature ramp of 5 °C min⁻¹ until reaching a maximum temperature of 300 °C. The oven was held at 300 °C for 8 min, producing a total analysis time of 60 min.

Mass spectrometry

The GC was coupled to a Varian 4000MS series quadrupole ion trap mass spectrometer (Varian Inc. – now Agilent Technologies, Palo Alto, CA, USA) by a transfer line maintained at 300 °C. An internal electron impact ionisation source (70eV) was used and the instrument operated under the conditions summarised in Table 6.

3.3.2 Daily quality control procedures

Instrument checks

Breath and environmental VOC samples were analysed in batches of five or six per day. Before batch analysis, quality control and instrument checks were performed in the following order:

- Air and water levels in the mass spectrometer were checked to ensure no leaks or excessive moisture were present. For water content, a peak at m/z 18 would be present with a corresponding peak at m/z 19 present up to an acceptance of 500 counts. For air, peaks at m/z 28 and 32 were present at low levels above baseline and large visual deviations from baseline levels would indicate an air leak. An ionisation time of 3000 μ s should be obtained.

- A mass calibration standard (perfluorotributylamine) was used to tune the instrument.
- The instrument was checked for sensitivity by ensuring a suitable responses to m/z ions 69, 131, 264, 414 and 614 were observed. For ions with m/z 69 and 131, the acceptable criterion was a peak at approximately 40,000 counts. Subsequent peaks will be present at approximately 10,000 (m/z 264), 2,500 (m/z 414) and 625 counts (m/z 614).
- The condition of the quadrupole trap was assessed by assuring that the ion storage time at rest was $> 20,000 \mu\text{s}$. (If these checks indicated contamination, the quadrupole ion trap was heated and left overnight at elevated temperature to 'bake off' residues and contaminants. If this process was unsuccessful, the instrument was vented and the stainless steel mass analyser was removed, dismantled and cleaned using a metal polish followed by solvent washes in a sonic bath, before conditioning in a vacuum oven and reassembling.)
- Once the mass spectrometer had passed its operational checks, a thermal desorption cold trap blank was performed to establish that no contamination was present. In the event that contamination were deemed too high, the process would be repeated until an acceptable threshold had been met. This was checked visually by assessing the height of the singular peak present in the chromatogram. A large peak indicated contamination within the cold trap. An example of an acceptable analysis is shown in Figure 29.
- Finally, the retention index solution was analysed. Peak elution times and intensities were assessed across the mass/volatility range of analytes. For an acceptable analysis, m/z 57 was extracted from the total ion chromatogram and all alkanes up to C_{20} should be visible in the chromatogram. An example of an acceptable analysis is shown in Figure 29. Intra-batch stability was monitored throughout analytical samples by checking the response of the post-loaded toluene- D_8 internal standard present in each of the experimental samples.

If these tests indicate a degraded instrument performance, the analytical process would be paused and the problem investigated. Completion of these tests was essential to ensure that inter-sample variation was maintained to acceptable levels, and analytical system artefacts minimised.

3.3.3 Data processing

Targeted GC-MS compounds

All targeted data processing were performed on GC-MS output files using the Varian MS Workstation (v6.9.2, Varian Inc. – now Agilent Technologies, Palo Alto, CA, USA). Chromatograms were smoothed using a mean 3-point smooth and spikes were removed using a threshold factor of 5. Target analytes' retention times and mass spectra were validated against commercially available standards. Data from standards were used to create target compound libraries that enabled analytes to be identified in an exhaled VOC sample. This was performed using an extracted ion chromatogram (EIC) for the base peak m/z ion under a clearly defined chromatographic peak, within a retention time window defined from the standards' analyses.

The library of targeted compounds enabled search parameters to be optimised to qualifier ion ratios and their peak heights and shape. Once complete, a search list was produced containing a list of sample files that were to be prospected for VOCs. The data were batch-processed and a summary report was exported to a comma separated value (.csv) file.

Metabolomic profiling of GC-MS compounds

Data were exported from the Varian operating system and converted from the .sms GC-MS output file to a .swx file suitable for import into AnalyzerPro (SpectralWorks, Runcorn, UK) for peak deconvolution. Peak deconvolution parameters were optimised via an iterative search/adjustment of parameter level against visual checks of the resultant data, to assess the level of over- or under-picking of peaks.

These parameters were applied to all breath samples and can be found in Table 7. Once optimised parameters had been defined, test runs with randomly selected sample files were performed and the resultant deconvolved data evaluated to verify that the deconvolution parameters were applicable across the sample set. If this was not the case the iterative process was repeated until satisfactory values were obtained.

Table 7 Deconvolution search parameters to identify unique peaks in exhaled breath samples using AnalyzerPro software.

Search parameter	Value
Minimum number of identified ions	2
Height threshold	0
Area threshold	1000
Peak width threshold	0.04 min
Number of scan windows	3
Smoothing points	3

Deconvolved data were exported to .csv files which were used to create a master file of all isolated chromatographic peaks, with corresponding quantifier and qualifier mass spectra ions. The master file contained information about all VOCs identified in breath and associated environmental samples. Every component entry was indexed and catalogued by:

- Sorting into retention index order.
- Consolidation of VOCs with similar/equivalent RI values and similar/equivalent mass spectra observed in different samples.
- Allocation of consolidated groups of VOC peaks to a single labelled peak and inputted into a spectrum list in the MS Workstation software (as for the targeted analysis). This was done by selecting a GC-MS file with an RI value closest to the mean value for its group (approximately at the midpoint of any minor drift of retention time across the study period). This step improved the integration and reporting of the associated compound across all sample files (Figure 30).

1	A	B	C	F	G	H	I	J	K	L	M	N
	File	RT	RI	Base Peak	Ions	Q1	Q2	Q3	Q4	Q5	BRI-RI-Q1-Q2-Q3-Q4-Q5	Grouping
19498	FM03A	10.4398	1049	43	10	43	41	71	85	70	BRI-1049-43-41-71-85-70	43-024
19499	FM20B	14.6587	1049	91	3	91	92	65	0	0	BRI-1049-91-92-65-0-0	91-010
19500	FM22C	14.6219	1049	91	2	91	92	0	0	0	BRI-1049-91-92-0-0-0	91-010
19501	FM22A	14.6298	1049	91	3	91	92	80	0	0	BRI-1049-91-92-80-0-0	91-010
19502	FM31A	14.5574	1049	91	3	91	92	65	0	0	BRI-1049-91-92-65-0-0	91-010
19503	FM22B	14.618	1049	91	2	91	92	0	0	0	BRI-1049-91-92-0-0-0	91-010
19504	FM26A	14.5448	1049	91	2	91	92	0	0	0	BRI-1049-91-92-0-0-0	91-010
19505	FM19A	14.6715	1049	91	3	91	92	65	0	0	BRI-1049-91-92-65-0-0	91-010
19506	FM24C	14.6066	1049	91	2	91	92	0	0	0	BRI-1049-91-92-0-0-0	91-010
19507	FM32B	14.5463	1049	91	2	91	92	0	0	0	BRI-1049-91-92-0-0-0	91-010
19508	WO16-PRE	9.9514	1049	71	7	71	41	57	293	84	BRI-1049-71-41-57-293-84	71-007
19509	FM01A	10.6338	1049	71	4	71	43	57	70	0	BRI-1049-71-43-57-70-0	71-007
19510	WO04-5	10.1751	1049	80	2	80	293	0	0	0	BRI-1049-80-293-0-0-0	
19511	FM11B	14.7004	1049	91	2	91	92	0	0	0	BRI-1049-91-92-0-0-0	91-010
19512	FM21C	14.6443	1049	91	2	91	92	0	0	0	BRI-1049-91-92-0-0-0	91-010
19513	FM27C	14.5774	1049	91	3	91	92	65	0	0	BRI-1049-91-92-65-0-0	91-010
19514	WO01-90	10.3775	1049	79	22	79	77	91	51	80	BRI-1049-79-77-91-51-80	79-005
19515	WO12-300	10.033	1049	204	5	204	127	95	77	51	BRI-1049-204-127-95-77-51	204-001
19516	WO5-PRE	10.1894	1050	43	3	43	71	57	0	0	BRI-1050-43-71-57-0-0	43-025
19517	FM23A	14.6473	1050	121	2	121	122	0	0	0	BRI-1050-121-122-0-0-0	121-001
19518	FM30A	14.5908	1050	122	2	122	121	0	0	0	BRI-1050-122-121-0-0-0	122-002
19519	WO01-5	10.4217	1050	111	4	111	86	44	81	0	BRI-1050-111-86-44-81-0	
19520	FM08B	14.7269	1050	91	5	91	92	65	93	63	BRI-1050-91-92-65-93-63	91-010
19521	FM11A	14.7331	1050	121	2	121	122	0	0	0	BRI-1050-121-122-0-0-0	121-001
19522	FM20A	14.6991	1050	121	3	121	122	66	0	0	BRI-1050-121-122-66-0-0	121-001
19523	FM20C	14.6901	1050	121	2	121	122	0	0	0	BRI-1050-121-122-0-0-0	121-001
19524	WO19-300	14.7273	1050	91	6	91	92	69	65	98	BRI-1050-91-92-69-65-98	91-010
19525	WO04-90	10.1876	1050	93	2	93	80	0	0	0	BRI-1050-93-80-0-0-0	
19526	WO18-510	14.7111	1050	91	5	91	92	65	63	89	BRI-1050-91-92-65-63-89	91-010
19527	WO09-5	10.138	1050	93	3	93	91	92	0	0	BRI-1050-93-91-92-0-0	
19528	WO13-90	10.0868	1050	94	4	94	91	45	89	0	BRI-1050-94-91-45-89-0	
19529	WO19-PRE	14.7373	1050	91	3	91	92	65	0	0	BRI-1050-91-92-65-0-0	91-010
19530	FM19C	14.7022	1050	121	2	121	122	0	0	0	BRI-1050-121-122-0-0-0	121-001
19531	FM05B	10.4375	1050	43	7	43	41	71	57	85	BRI-1050-43-41-71-57-85	43-025
19532	WO02-90	10.2647	1050	57	4	57	83	80	92	0	BRI-1050-57-83-80-92-0	
19533	WO08-90	10.1844	1050	79	18	79	108	91	77	107	BRI-1050-79-108-91-77-107	79-005
19534	WO19-510	14.7316	1050	91	3	91	92	65	0	0	BRI-1050-91-92-65-0-0	91-010

Figure 30 A screenshot of a section of the combined picked peaks for manual sorting and grouping to create an identifier code for each unique peak.

- Each peak was assigned an ID that consisted of ‘²BRI’ followed by its mean retention index (RI), quantification ion and qualifier ions. For example, for a VOC that eluted with a RI mean of 900, a base peak of 43 and qualifier ions (in order of magnitude) of 57, 69, 71 and 41, its ID carried forward for analysis would become BRI-900-43-57-69-71-41. This process allowed all compound IDs to contain sufficient information but yet remain unique (Figure 31).

² BRI indicates the name is derived from an averaged retention index obtained from breath samples.

	C	D	E	F	G	H	I	J
1	Original Name	Database Name	Base Peak	Q1	Q2	Q3	Q4	RI
2	57-007	BRI-972-57-41-43-71-85	57	41	43	71	85	972
3	81-006	BRI-986-81-95-67-79-123	81	95	67	79	123	986
4	71-063	BRI-1713-71-57-85-43-41	71	57	85	43	41	1713
5	40-001	BRI-641-40-44-45-0-0	40	44	45	0	0	641
6	132-001	BRI-687-132-63-81-0-0	132	63	81	0	0	687
7	71-011	BRI-1096-71-43-41-57-70	71	43	41	57	70	1096
8	43-001	BRI-646-43-45-0-0-0	43	45	0	0	0	646
9	69-021	BRI-1570-69-83-57-41-111	69	83	57	41	111	1570
10	71-030	BRI-1292-71-41-57-43-70	71	41	57	43	70	1292
11	51-001	BRI-658-51-50-62-61-0	51	50	62	61	0	658
12	77-001	BRI-643-77-48-79-95-47	77	48	79	95	47	643
13	71-008	BRI-1052-71-57-43-41-70	71	57	43	41	70	1052
14	71-014	BRI-1111-71-41-43-70-57	71	41	43	70	57	1111
15	142-003	BRI-1327-142-141-115-143-0	142	141	115	143	0	1327
16	41-044	BRI-1221-41-85-70-0-0	41	85	70	0	0	1221
17	355-005	BRI-1168-355-315-73-267-269	355	315	73	267	269	1168
18	43-021	BRI-1020-43-71-41-70-57	43	71	41	70	57	1020
19	42-003	BRI-917-42-41-40-87-85	42	41	40	87	85	917
20	97-005	BRI-1003-97-96-67-82-41	97	96	67	82	41	1003
21	91-006a	BRI-957-91-57-70-120-0	91	57	70	120	0	957
22	120-002	BRI-1207-120-92-152-0-0	120	92	152	0	0	1207
23	43-008	BRI-776-43-70-41-0-0	43	70	41	0	0	776
24	281-001	BRI-974-281-282-283-265-267	281	282	283	265	267	974
25	93-007a	BRI-998-93-108-43-41-67	93	108	43	41	67	998
26	355-002	BRI-1141-355-269-267-73-356	355	269	267	73	356	1141
27	57-031	BRI-1289-57-41-43-71-70	57	41	43	71	70	1289
28	93-008	BRI-1011-93-91-92-0-0	93	91	92	0	0	1011
29	71-034	BRI-1329-71-43-41-57-85	71	43	41	57	85	1329
30	71-020	BRI-1221-71-41-43-57-70	71	41	43	57	70	1221
31	220-002	BRI-1857-220-191-219-189-221	220	191	219	189	221	1857
32	281-004	BRI-1139-281-282-265-283-267	281	282	265	283	267	1139
33	108-004	BRI-1173-108-79-150-77-105	108	79	150	77	105	1173
34	81-014	BRI-1208-81-41-67-82-68	81	41	67	82	68	1208
35	69-013	BRI-1309-69-41-43-83-55	69	41	43	83	55	1309
36	156-001	BRI-939-156-158-0-0-0	156	158	0	0	0	939
37	57-053	BRI-1487-57-71-43-41-85	57	71	43	41	85	1487
38	71-055	BRI-1534-71-57-43-41-85	71	57	43	41	85	1534
39	57-017	BRI-1170-57-43-41-71-85	57	43	41	71	85	1170
40	43-046	BRI-1461-43-107-83-41-60	43	107	83	41	60	1461

Figure 31 A screenshot of the truncated combined picked peak list to show one line for each unique peak and its respective identifier coding.

- Integration parameters were optimised for each peak contained in the spectrum list. This was a process similar to the targeted method of data processing.
- A search list was created detailing all of the participant and environmental GC-MS data files and an analysis of the files was performed. This outputted a VOC data summary .csv file that enabled the integrated peak areas to be used to build an exhaled VOC breath matrix.
- The breath matrix designated the integration value for every VOC isolated against each sample (Figure 32).

A	HK	HL	HM	HN	HO	HP	HQ	HR	HS	HT	HU	HV	HW	HX
Sample ID	Compound184: BB-1485-49-57-71-41-85	Compound185: BB-1488-147-91-119-148-76	Compound138: BB-1477-177-220-135-0-0	Compound124: BB-1474-71-41-57-48-85	Compound242: BB-1468-118-146-30-88-43	Compound153: BB-1464-71-41-57-48-85	Compound37: BB-1461-43-107-93-41-69	Compound258: BB-1459-281-73-415-327-419	Compound125: BB-1450-57-41-71-48-85	Compound333: BB-1449-167-168-165-0-0	Compound230: BB-1448-147-91-119-148-76	Compound128: BB-1439-401-402-403-404-405	Compound71: BB-1427-91-79-93-133-147	Compound186: BB-1425-118-90-89-146-63
FM01A	18414	700469	199	41583	199	10705	199	3283000	2648	199	199	199	199	199
FM02A	12953	15305	199	14553	4159	106160	793807	199	3065	1.59E+06	5490	5719	199	199
FM04A	199	1010000	24218	29229	199	62231	409915	3488000	13631	199	1010000	199	14519	199
FM05A	199	14412	23084	23142	199	44522	244606	3701000	10540	199	1422000	199	9539	199
FM06A	7773	557	4799	6118	199	7762	51006	676278	3420	199	113735	199	6350	199
FM06A	13205	201443	13070	23730	199	24997	256603	1960000	6021	199	196175	199	199	199
FM07A	199	4337	719	199	199	5343	32003	643450	1838	199	4830	199	199	199
FM08A	10628	199	22338	14064	199	28924	24499	165002	14176	1088	553617	199	14311	199
FM09A	16304	199	25011	11117	199	33932	26687	223016	15954	199	482075	199	199	199
FM10A	1395	199	199	1832	199	199	45160	318067	3316	1530	50046	199	199	199
FM11A	4736	29203	10184	5467	95599	8875	131862	655456	5585	5268	267182	199	199	6:
FM12A	2521	199	199	2926	199	9346	41008	235351	3434	1761	104304	199	199	1
FM13A	1290	199	199	371	199	199	16536	73021	2296	922	25571	199	199	199
FM14A	6956	199	13186	5780	199	18575	51376	217376	8028	3091	1050000	199	19089	2
FM15A	2698	199	199	3093	199	9890	25044	199217	3792	199	88929	199	40149	199
FM16A	10423	199	14754	6923	199	24888	58862	295992	9136	2010	297392	199	38114	199
FM17A	5867	199	10338	6195	199	199	52909	359087	8695	1098	194356	199	8772	199
FM18A	6155	22743	6594	4654	125948	14567	61544	309342	7128	2259	328239	199	116559	7:
FM19A	9878	123756	18590	8443	41174	22742	111679	497827	10976	2040	319438	36831	199	3:
FM20A	11971	143960	18571	6292	332208	28205	67323	571553	12159	7555	868675	199	54548	18:
FM21A	1957	17026	11538	1093	30599	199	31477	208820	4958	1494	173076	199	12514	2:
FM22A	8758	199	6993	9145	199	199	61927	578821	13059	1547	573177	199	199	199

Figure 32 A screenshot showing a section of the overall breath matrix with sample identifiers (column A) against each individually picked peak and their respective peak areas.

- This breath matrix was then taken forward for multivariate statistical analyses.

A schematic outline of this process can be seen in Figure 33.

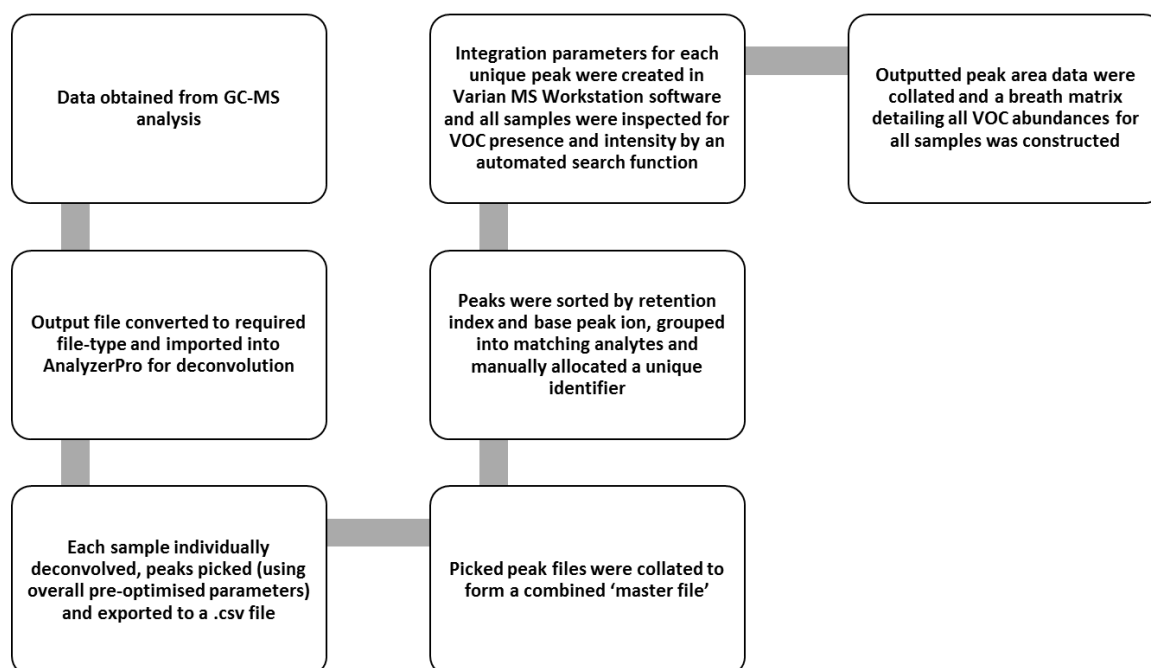


Figure 33 Step-by-step flow chart to indicate the process for producing a comprehensive breath matrix file from the original GC-MS data.

3.3.4 Statistical analyses

Targeted analyses

All targeted statistical analyses were performed using IBM SPSS Statistics (v 22.0, IBM Corp., Endicott, NY, USA). The analyses were study specific and so are described in the respective experimental chapters. Bonferroni adjustment was applied to all p values where tests for multiple comparisons were made. This adjustment is calculated by multiplying the unadjusted p value by the total number of comparisons tested.

Multivariate metabolomic profiling

A four-step multivariate statistical process was adopted for metabolomic profiling of the exhaled VOC data using SIMCA-P+ software (v 14, Umetrics, Umeå, Sweden).

Scaling

Each variable (exhaled VOC) was transformed using Pareto scaling in accordance with manufacturer recommendations. Pareto scaling is most suited to MS data due to the up-weighting of medium peaks and down-weighting of large peaks, a process done without increasing baseline noise [3]. Pareto scaling has been suggested as a compromise between unit variance (UV) and no scaling and is performed by dividing each variable (after subtracting its mean, $x - \bar{x}$) by the square root of its standard deviation (SD) (Equation 20). Where Pareto scaling lead to a negative analysis, UV scaling was investigated.

$$Par = \frac{x - \bar{x}}{\sqrt{SD}} \quad \text{Equation 20}$$

Preliminary principal components analysis (PCA)

A preliminary PCA model was created to visualise the distribution of data points with an unsupervised separation method. PCA produces a projection of the samples in a multi-dimensional space according to their loadings. If a separation of groupings was not present a further, supervised model was used.

Orthogonal partial least squares-discriminant analysis (OPLS-DA)

This supervised method prospects the data to identify components that enable pre-defined classes of data to be separated. The contribution of each component to the separation of the different classes may be evaluated by using a model contribution plot, known as S-plots. S-plots were analysed to identify variable components that showed the greatest sensitivity and selectivity in discriminating between data classes. These points present in the extreme ends (i.e. corners) of the S-plot. Identified components were then extracted from the data matrix for further analysis. Simca-P+ software automatically validates the OPLS-DA model by removing 1/7th of data and producing a model for the 6/7th of remaining data. The removed data is then predicted using the new model. This is an iterative process, with each 1/7th of the data 'left out' until all data have been predicted. Predicted data can then be

compared to the original data and the sum of squared errors calculated for the entire dataset.

3.3.5 Analysis of target components – candidate biomarkers

Individual sample values were extracted from the matrix for each of the target components and evaluated. Where time-dependent sampling occurred, the data were analysed in both raw (with IS normalisation) and normalised (i.e. ratio to maximum intra-participant reading) data formats. Any time, or group, dependent differences for individual variables were evaluated using the appropriate statistical method mentioned in the respective chapters. Multi-component contributions were scored by calculating the Euclidian distance for each individual at each time point using the Equation 21, where x refers to each participant value for the given variable and time point.

$$\sqrt{\sum (x_i^2, x_{ii}^2, \dots)}$$

Equation 21

3.4 Acknowledgments

I would like to thank Shuo Kang for the development of the portable sampler.

3.5 References

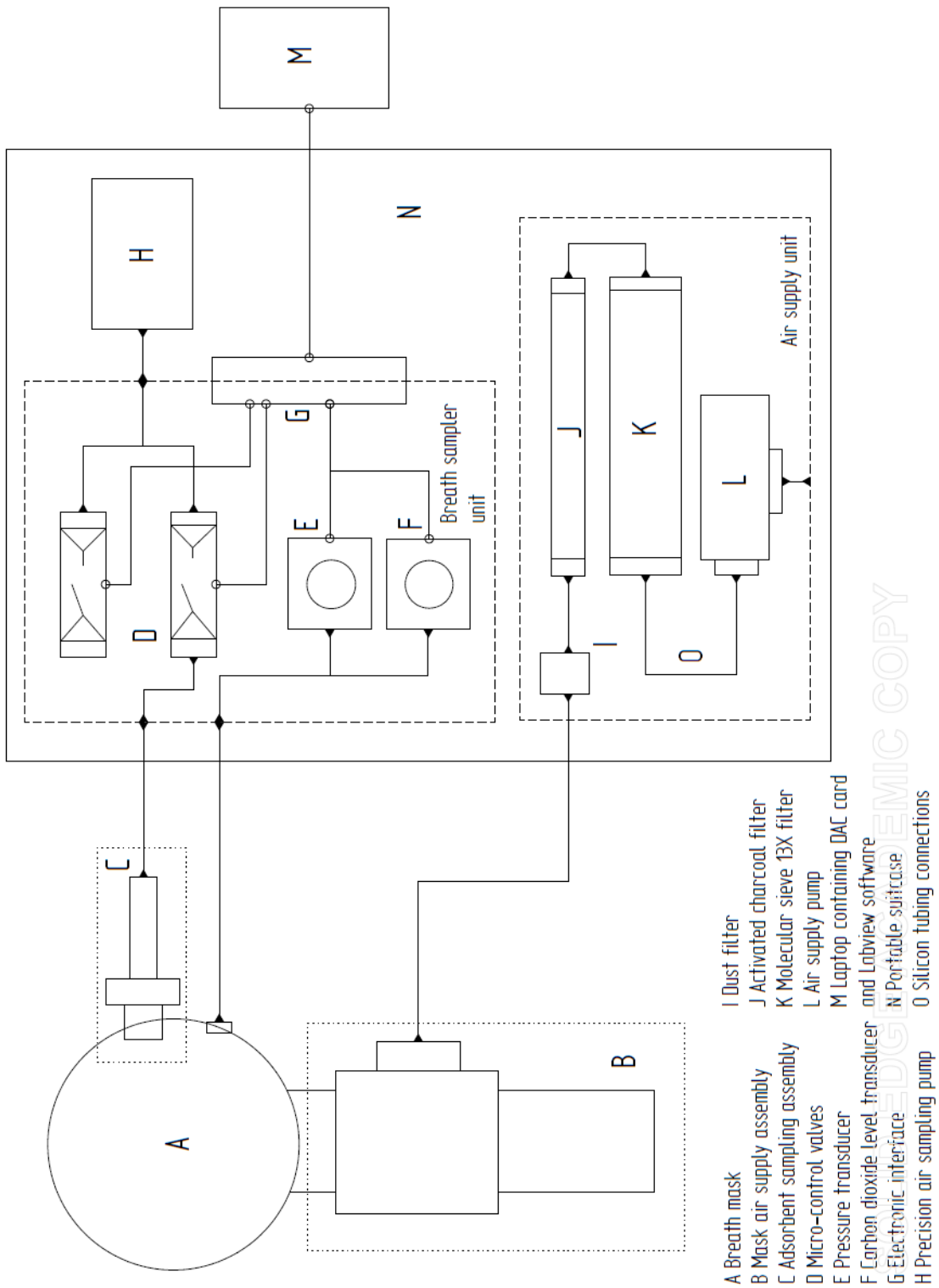
1 Basanta, Koimtzis T, Singh D, Wilson I, Thomas CLP. An adaptive breath sampler for use with human subjects with an impaired respiratory function. *Analyst* 2007;132:153-63

2 Turner MA, Guallar-Hoyas C, Kent AL, Wilson ID, Thomas CLP. Comparison of metabolomics profiles obtained using chemical ionization and electron ionization MS in exhaled breath. *Bioanalysis* 2011;3:2731-8

3 Wiklund S, Umetrics. Multivariate data analysis for omics.

http://metabolomics.se/Courses/MVA/MVA%20in%20Omics_Handouts_Exercises_Solutions_Thu-Fri.pdf (Accessed August 2015)

3.6 Appendix 1: details of portable breath sampler



Schematic code	Description
A	Breath mask (ResMed)
B	Mask air supply assembly including disposable one way valve (Clement Clarke International Ltd, Part No. 3122061), PTFE T-piece and silicon air supply line
C	Adsorbent sampling assembly including PTFE sampling valve and sorbent tube (Markes Int. Ltd)
D	Micro-control valves
E	Pressure transducer
F	Carbon dioxide level transducer
G	Electronic interface
H	Precision air sampling pump, Escort Elf personal pump, MSA
I	Dust and particulate stainless steel filter, gas filtration at 0.01 μm , Model 97S6, dimension: L79 mm, OD32 mm, maximum pressure 5000 psig at 93 °C, max temp. 204 °C, weight: 0.3 kg, seals: viton, inlet and outlet ports: 1/4", Microfiber filter cartridge grade AQ (99.9999+ %) (part number: 050-50-AQ, Parker Balston)
J	VOC purification filter consisting of stainless steel vessel (L180 mm, OD30 mm) containing granular activated charcoal 4 to 8mesh (Sigma-Aldrich, CAS:7440-44-0, Part number: C2764-500G)
K	Dehydration filter consisting of custom made stainless steel vessel (L260 mm, OD154 mm, ID150 mm) containing molecular sieve 13X, 8 to 12 mesh (Acros Organics, CAS:63231-69-6, Part number: 197310050)
L	HIBLOW linear air pump HP series, model HP-200, air flow volume: 200 L min^{-1} , weight: 9 kg, voltage: AC 220~240 V, Dimensions: L256 mm, W200 mm, H222 mm (Techno Takatsuki Co. Ltd)
M	Laptop running pcmcia card slot and containing DAQcard-6024E, with Labview software (National instruments)
N	Portable metal suitcase with 3 detachable levels
O	Silicon tubing connections, RS components

CHAPTER FOUR: EXHALED BREATH MONITORING IN HEALTHY PARTICIPANTS AFTER EXERCISE IN A SWIMMING POOL ENVIRONMENT: A TARGETED AND METABOLOMICS APPROACH

4.1 Introduction

Swimming is the most popular participant sport in the United Kingdom. Statistics (2013) report approximately three million people participating in at least one 30 min swimming session per week [1]. Three million bathers constitute a significant infection vector. Disinfection of bathing water is mostly achieved with chlorine gas and/or sodium hypochlorite solution as described in Chapter 1. The formation of volatile chlorine, and bromine, species in the swimming pool water is of growing concern. Even with careful pool user hygiene, introduction of biological matter into the swimming pool by human users induces these processes [2,3].

The pool chlorine hypothesis proposes that the inhalation, absorption and ingestion of disinfection by-products (DBPs) may cause cumulative negative health effects. For example, the reported association between swimming pool attendance throughout childhood and the development of asthmatic conditions later in life [4]. Although arguments that health benefits of swimming outweigh the potential chemical hazards that are present [5], it is important that the impact on inhaled DBPs is not ignored. Conversely, the safety of the swimmer from other potential risks associated with poor disinfection are paramount.

Uptake and elimination of DBPs has been of interest in previous years. Aggazzotti *et al.* [6] measured the elimination of chloroform (CHCl_3) on four occasions in a competitive swimmer, after a 45 min intensive training session. Samples were collected immediately, 15 min post-swimming and every 30 min for 3 hrs post-swimming, with an additional sample collected at 10 hrs post-swimming. The experiment showed a first order, one-compartment elimination of CHCl_3 from exhaled breath, with an average biological half-life ($t_{1/2}$) of 24 ± 4 min (mean \pm

standard deviation). CHCl_3 was measured in 3 out of 4 samples collected at 10 hrs post-swimming. However, 3 samples showed no detectable CHCl_3 at 105 ($n=1$) and 135 ($n=2$) min post-swimming, indicating an unexplained removal and reappearance. With the small number of observations in this experiment, it is not possible to fully understand the elimination of CHCl_3 from exhaled breath after swimming. Lindstrom *et al.* [7] collected single breath samples (1 L) of respiratory reserve volume and mapped the levels of CHCl_3 during both the exposure period (at points during swimming exercise) and the post-exposure elimination. In contrast to Aggazzotti and colleagues, elimination showed a tri-exponential model. However, the measurements were only taken on one male and one female and ceased at 150 and 180 min post-exposure, respectively. Caro & Gallego [8] collected single breath measurements using a Bio-VOC® breath sampler (Markes Int., Llantrisant, UK). This device collects the final 100 mL portion of a forced exhalation and is then pushed through an adsorbent bed contained in a stainless-steel thermal desorption (TD) tube. The authors reported that exhaled concentrations of CHCl_3 returned to pre-swimming levels at 240 min post-exposure. All of these studies collected data on a small population and used single breath measurements, with low volumes used in some cases. These sampling methods do not allow for natural breath-to-breath fluctuation of exhaled concentrations. A sensitive, multiple-breath approach would be beneficial to characterise the development and elimination of DBPs.

Furthermore, no reports in the literature describe the development of exhaled inflammatory biomarkers in conjunction with an elimination of disinfection by-products. No observational studies seeking to discover possible volatile biomarkers of lung damage have been reported.

4.2 Study aims:

4.2.1 Primary aim

Characterise the elimination of DBPs from recreational swimmers exposed to chlorinated water.

4.2.2 Secondary aim:

Test the hypothesis that swimming in chlorinated water produces a detectable change in VOC profiles following DBP exposure.

4.3 Methods

4.3.1 Ethical approval

The study was approved in its entirety by the Loughborough University Ethical (Human Participants) Sub-Committee under the reference R13-P100. All participants took part voluntarily and were informed of the experimental procedures by issue of a participant information sheet prior to consenting. All participants gave written and informed consent and were free to exclude themselves and their data from the experiment at any time without reason. Once consented, participant information and samples were anonymised and assigned a unique identifier code.

3.3.2 Characterisation of swimming pool environment

All exercise testing was performed at the Loughborough Sport swimming pool located on Loughborough University campus. The swimming pool water was, and is, drawn from the local drinking water system and is disinfected using sodium hypochlorite ($\text{NaClO}_{(\text{aq})}$) maintained at a recommended concentration of $1 \text{ mg L}^{-1}_{(\text{aq})}$ with automatic electronic dosing pumps (TEKNA EVA TPG, Crius System, Pi, UK). $\text{NaClO}_{(\text{aq})}$ has a permitted concentration range within the pool environment of between $0.5 \text{ mg L}^{-1}_{(\text{aq})}$ to $5 \text{ mg L}^{-1}_{(\text{aq})}$ and is deemed as non-hazardous. Ultraviolet light disinfection was, and is, also used.

Due to the basic nature of NaClO , a solution of hydrochloric acid (HCl) is introduced into the swimming pool water. The HCl is purchased in concentrate drums of 32-38% solution and diluted before being pumped into the pool water. The permitted concentration range for HCl in the pool water is 7.2 to 7.6 mg L^{-1} , with a recommended value of 7.4 mg L^{-1} . The pool contains approximately $2,500 \text{ m}^3$ of

water and, with the pumps running at capacity, has a turnover time of approximately 5.5 hrs. The pool water is maintained at a temperature of 27.8 ± 0.1 °C. Figure 34 shows a detailed plan of the swimming pool building highlighting the swimming and sampling areas accompanied by a photograph to visualise the complex.

4.3.2 Preliminary study

The preliminary study ($n=1$) was conducted to provide scoping data for the design of the main experiment. An estimate of the time required to eliminate exogenous DBPs from the human body after swimming in a chlorinated swimming pool was sought.

The participant arrived at the swimming pool at approximately 0830 hrs, after an overnight fast and a pre-exercise breath VOC sample was collected promptly. The exercise consisted of a 90 min continuous swim performed using the breast stroke technique. After the swim, the participant briefly showered and provided six 1 L breath samples, one every 5 min for 30 min. The experiment timeline is visualised in Figure 35.

Participant feedback suggested that 90 min continuous swimming was potentially too challenging. A shorter swimming intervention would be needed in the subsequent research.

All samples were analysed by thermal desorption-gas chromatography-mass spectrometry (TD-GC-MS) (Chapter 3) and resultant data analysed for the presence and intensity of CHCl_3 . CHCl_3 levels in breath were observed to increase 190-fold over pre-swim levels and elimination followed an approximately exponential profile, with an estimated elimination time to pre-swim levels of 600 min (Figure 36). Therefore, a period of 600 min post-exercise monitoring was specified for the following experiments.

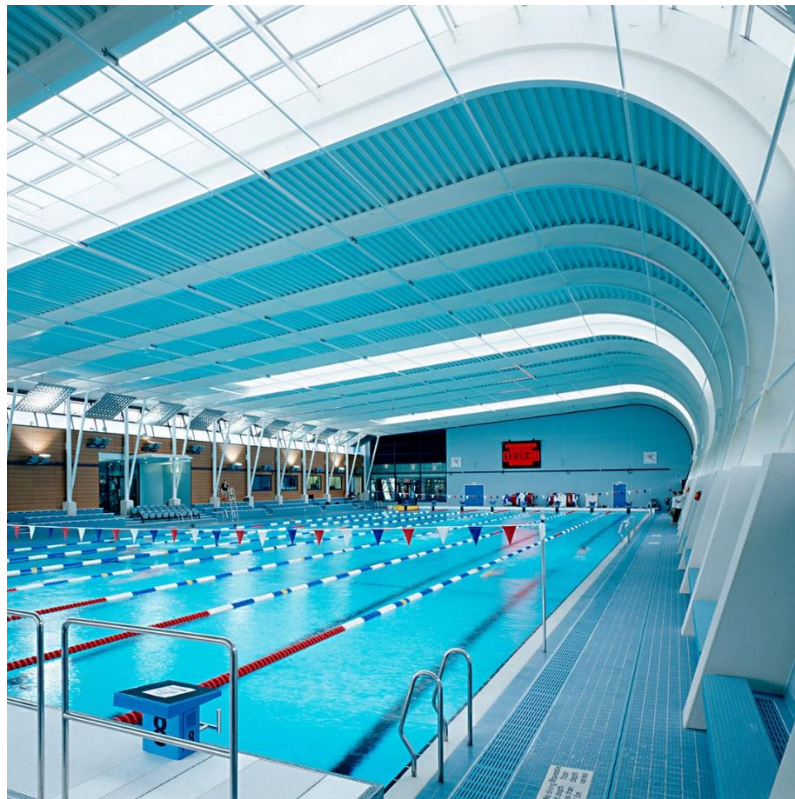
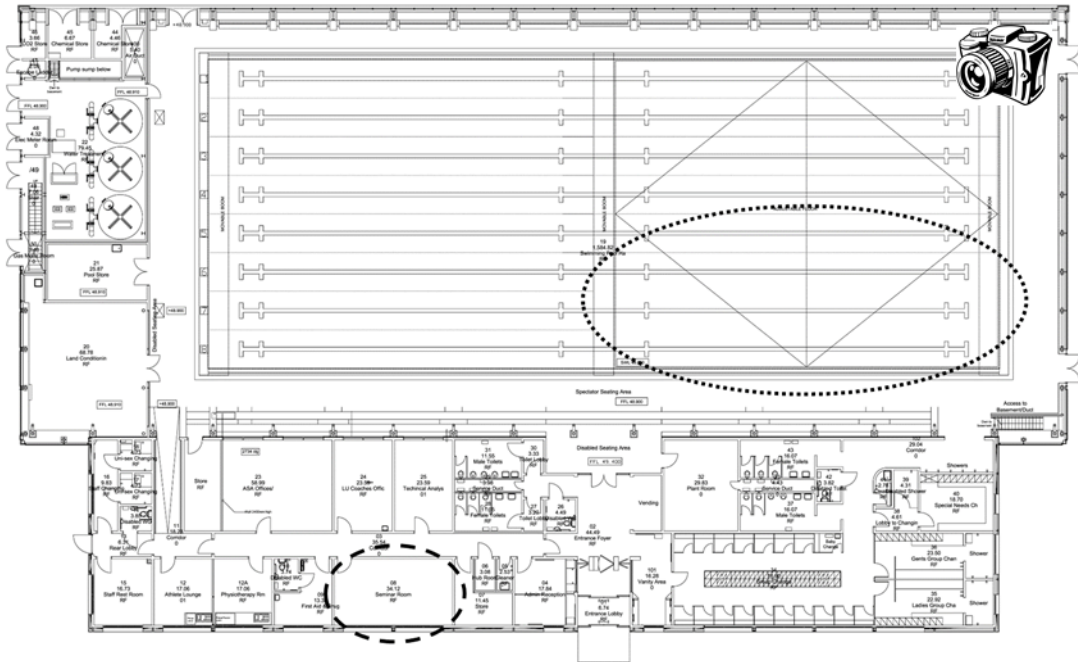


Figure 34 Detailed plan of the swimming pool building (top) highlighting swimming area (dotted oval) and room used for exhaled breath sample (dashed oval). Bottom picture of the swimming pool area corresponds to a view from the upper right section of the plan.

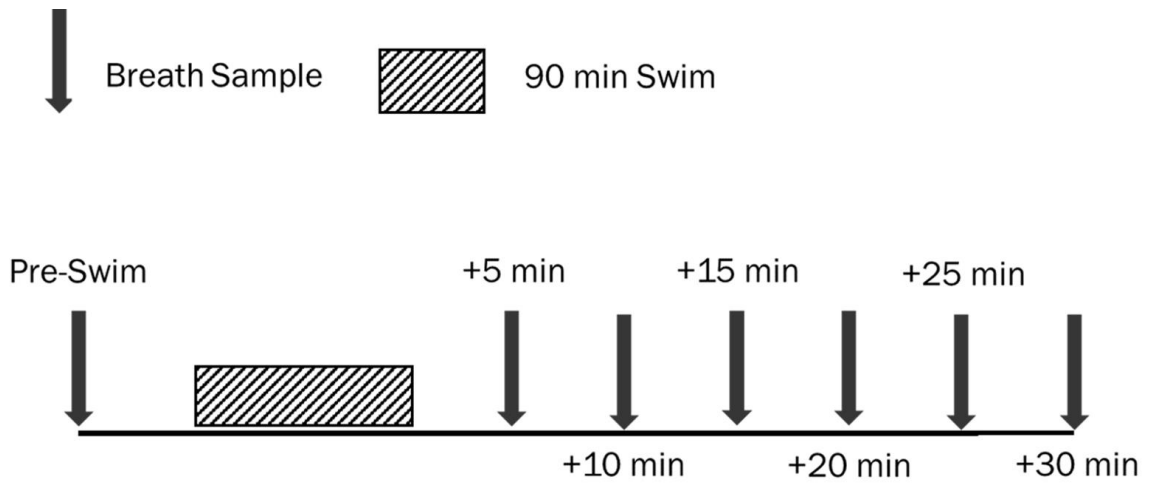


Figure 35 Schematic timeline to show sampling time points and exercise placement for an initial preliminary investigation into the exhalation of chlorine disinfection by-products post-swimming.

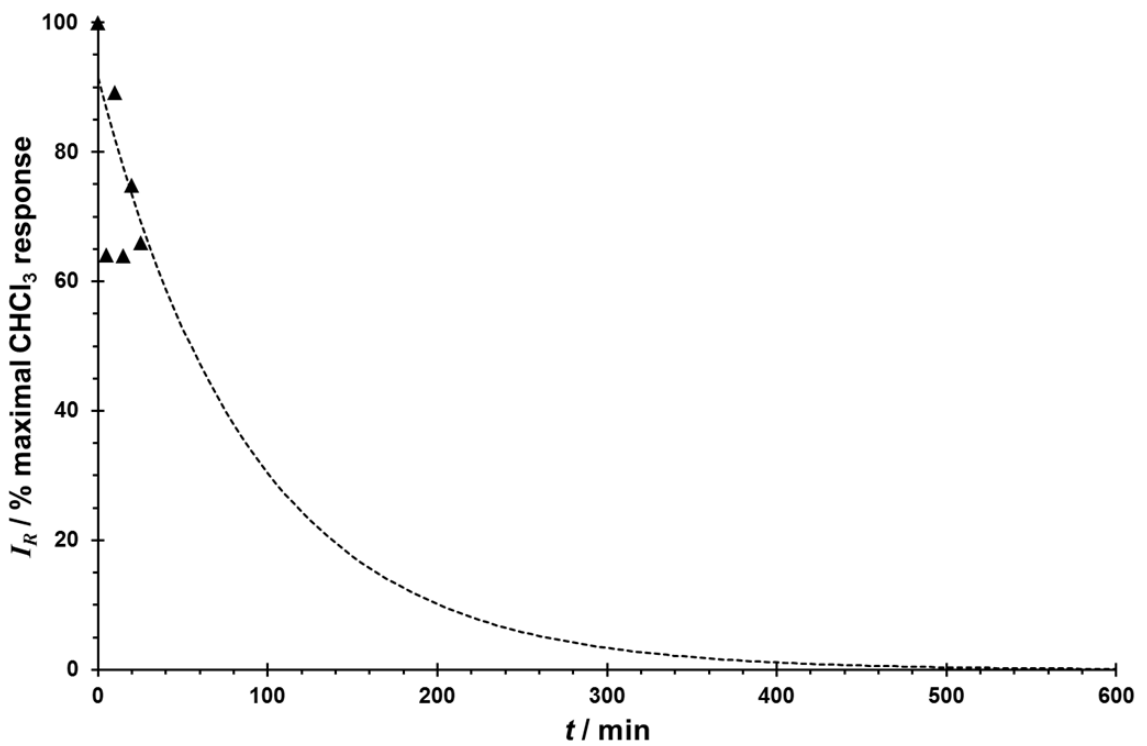


Figure 36 Elimination of chloroform as observed in exhaled breath concentrations changes in a single participant after a 90 min recreation swim in an indoor pool. Figure shows the exponential formula extrapolated for 600 min to estimate the exhaled wash out period.

4.3.2 Refinement study

A refinement experiment ($n=1$) was performed to establish if DBPs were detectable in exhaled breath 600 min after exposure through swimming, to evaluate the substantial extrapolation from the data of the preliminary study. Once again, a participant fasted overnight and provided a resting breath sample. On this occasion the exercise period was reduced to 30 min. Once the 30 min exercise was complete, the participant briefly showered and a post-exercise breath VOC sample was collected. A further eight breath VOC samples were collected, see Figure 37. All breath samples collected were 2 L and the participant was allowed to eat and follow their normal daily routine throughout the sampling period.

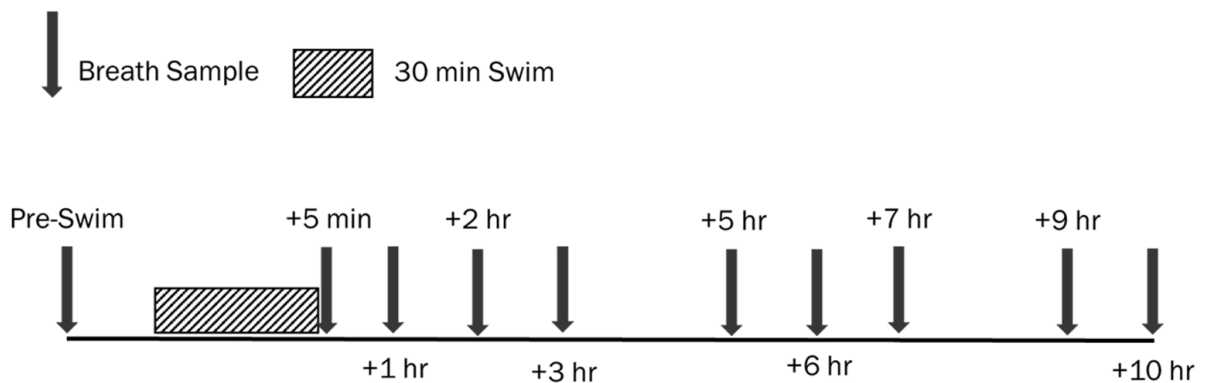


Figure 37 Schematic timeline to show sampling time points and exercise placement for a secondary preliminary investigation into the exhalation of chlorine disinfection by-products post-swimming.

Figure 38 contains example chromatographic data obtained from this preliminary study, showing a blank sample obtained from the filtered air via the portable sampler, a post-swimming exhaled breath sample and extracted ion chromatograms showing CHCl_3 , bromodichloromethane (CHBrCl_2) and carbon tetrachloride (CCl_4). Breath data were analysed for peak area intensity of CHCl_3 , CHBrCl_2 and CCl_4 at all time points. Figure 39 shows the elimination profile for each DBP. It was concluded that monitoring for 600 min post-exercise was a suitable period to provide sufficient data to characterise DBP elimination. CCl_4 did not show a rise in exhaled intensities post-swimming and remained relatively constant across the sampling period.

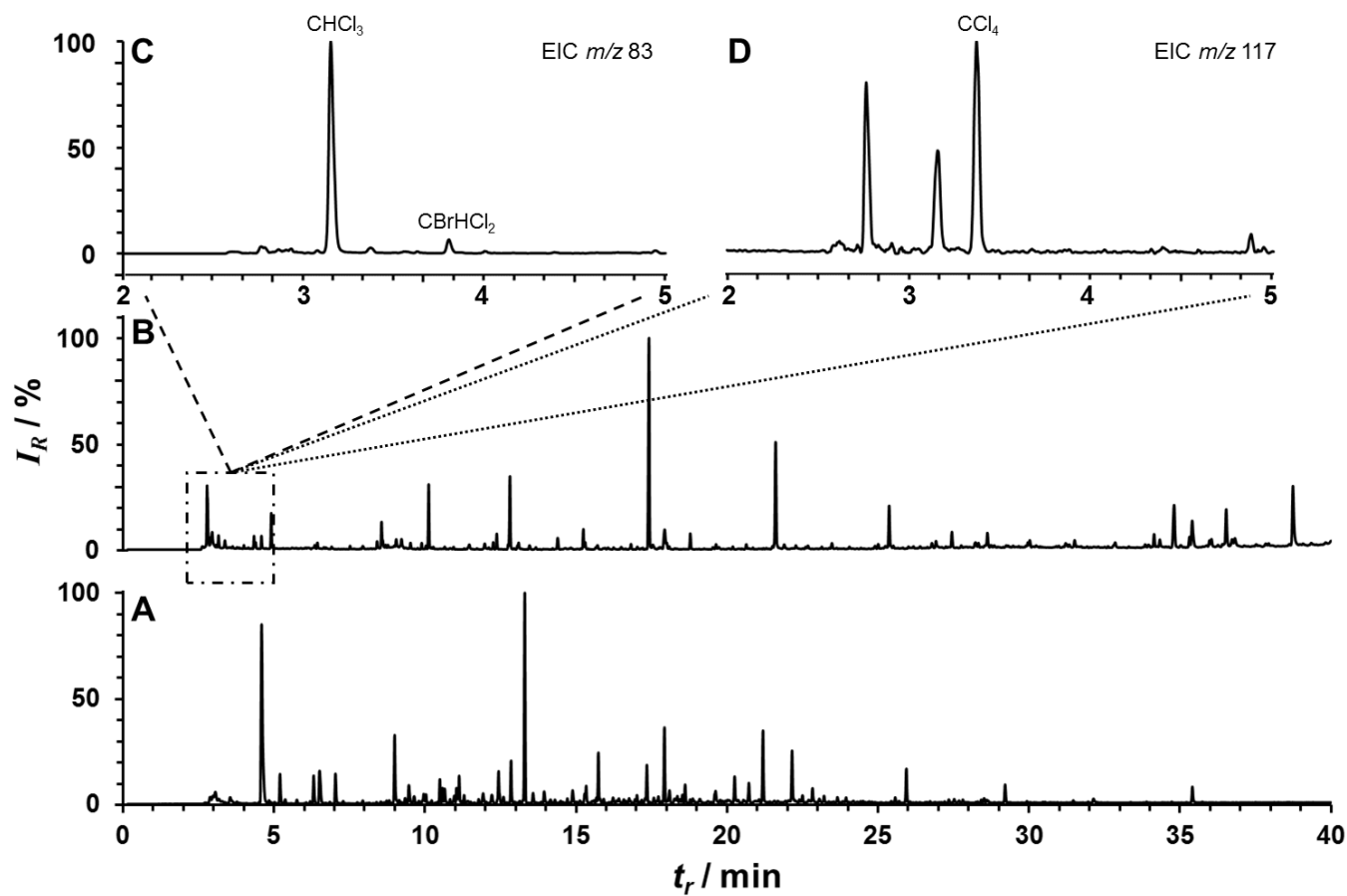


Figure 38 Example chromatograms for A) a sampling air blank, B) a post-swimming exhaled breath sample and expanded regions for the extracted ion chromatogram (EIC) of C) m/z 83 (CHCl_3 = chloroform, CBrHCl_2 = bromodichloromethane) and D) m/z 117 (CCl_4 = carbon tetrachloride).

Note: I_R = relative intensity; t_r = retention time

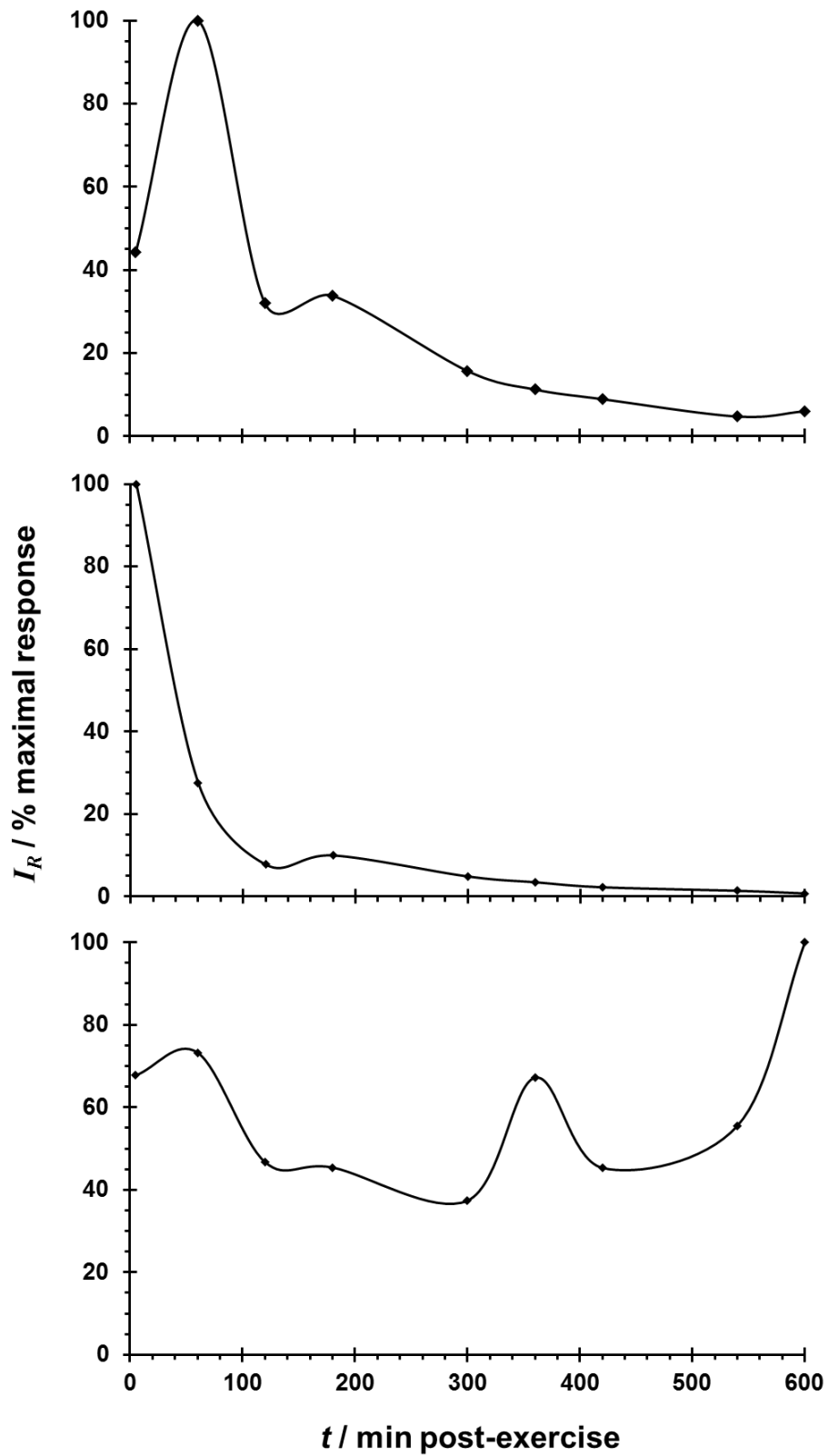


Figure 39 Single participant post-swimming wash out profiles for chloroform (top), bromodichloromethane (middle) and carbon tetrachloride (bottom) after a 30 min recreational swim.

Note: I_R = relative intensity; t = time

4.4 Main experiment

4.4.1 Experimental design

With a final sample point designated at 600 min post-exercise, a Box-Wilson central composite design (CCD) was used to allocate a total of five post-exercise sample time points [9]. The CCD depends on the number of factors in the experiment, for this instance a 1-factor design was produced using a 2-factor, or $2k$, method. The CCD contains a centre (mid) point that is augmented with a group of 'star points' that allow estimation of curvature. If the distance from the centre of the design space to a factorial point is ± 1 unit, the distance from the centre of the design space to a star point is $\pm \alpha$ with $|\alpha| > 1$ (Figure 40). For this experiment, star points are allocated by the initial and final breath VOC samples at +5 and +600 min post-exercise, respectively. See equations 22 to 26 for study time point calculations.

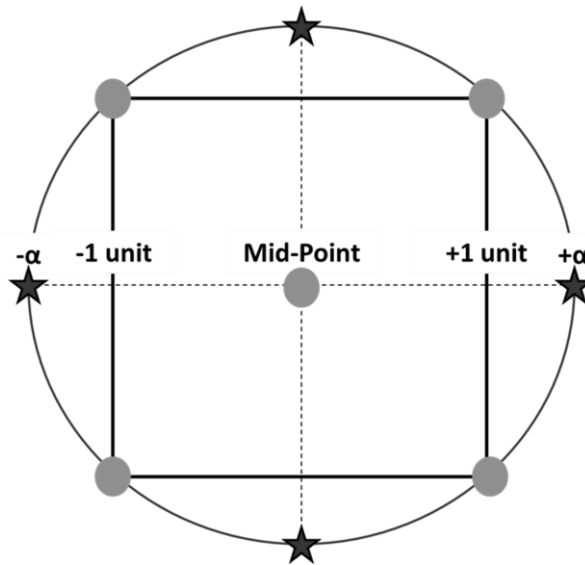


Figure 40 Graphical representation of a central composite design of experiment to estimate curvature. The design incorporates a mid-point, two outer points (± 1 units) and 2 extreme 'star' points ($\pm \alpha$)

To calculate α and maintain rotatability of the design, α depends on the number of experimental runs in the factorial portion of the CCD;

$$\alpha = [\text{number of factorial runs}]^{\frac{1}{4}} \text{ OR } \alpha = [2^k]^{\frac{1}{4}} \quad \text{Equation 22}$$

For this experiment there are two factors, therefore the factorial portion is 2^2 ;

$$2^{\frac{2}{4}} = \alpha = 1.414 \quad \text{Equation 23}$$

The mid-point is defined by the maximum and minimum factor levels;

$$\frac{600(\text{min}) - 5(\text{min})}{2} = 297.5(\text{min}) \quad \text{Equation 24}$$

Therefore the mid-point sits at;

$$5 + 297.5(\text{min}) \text{ and } 600(\text{min}) - 297.5(\text{min}) = 302.5 (\text{min}) \quad \text{Equation 25}$$

If ± 297.5 is α then ± 1 unit is derived by the following calculation:

$$\frac{297.5(\text{min})}{1.414} = 210.4(\text{min}) \quad \text{Equation 26}$$

Therefore the ± 1 unit points are at $297.5 \text{ min} \pm 210.4 \text{ min}$. This produces sampling points at; +5 min, +92.1 min, +302.5 min, +512.9 min and +600 min post-exercise. These points were simplified to; +5 (immediate), +90 (1 hr 30 min), +300 (5 hrs), +510 (8 hrs 30 min) and +600 min (10 hrs).

4.4.2 Participant information

Nineteen healthy males (mean \pm standard deviation (SD): age 25 ± 2 yrs, height 177 ± 7 cm, body mass 77.7 ± 11.2 kg, body mass index 24.8 ± 3.0 kg m⁻²) were recruited with a 100 % completion rate. All were capable, yet irregular, swimmers and free from any serious medical conditions or exercise impairing injuries.

4.4.3 Exercise protocol

Participants attended the Loughborough University Swimming Pool at approximately 0830 hrs, the morning after an overnight fast with only water permitted after waking. The participants completed a 30 min continuous swim at a challenging, yet maintainable, pace sustaining a target rating of perceived exhaustion of 15 [10]. Participants were allowed to choose and alternate swimming stroke throughout the exercise session. The exercise started at the beginning of the first length (25 m) performed and ceased after the completion of the length being performed in which the 30 min time limit expired.

4.4.4 Sampling protocol

Six exhaled breath VOC samples were collected at the times noted in Section 4.4.1.

4.4.5 Sampling methods

Exhaled breath VOCs

Exhaled breath VOCs were sampled as described in Chapter 3.

Environmental VOCs

Air samples (2 L) were collected at 0.5 L min⁻¹ onto adsorbent sample tubes identical to those used for exhaled breath sampling. Air samples were taken of the air surrounding the swimming pool and one from each sampling room (the pool complex and laboratory). A corresponding 2 L sample of the filtered air supplied to the face mask during breath sampling was also collected at 1 L min⁻¹ for each location.

VOC sample analysis

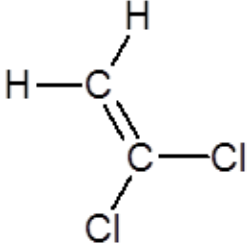
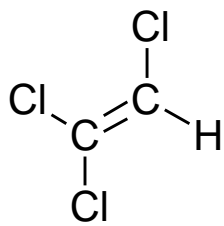
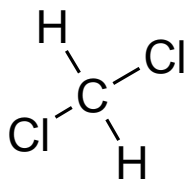
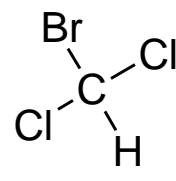
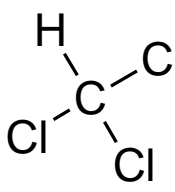
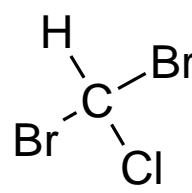
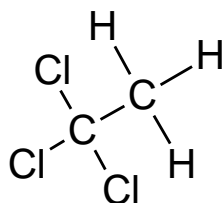
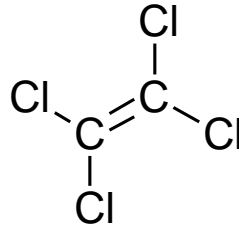
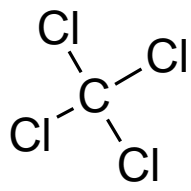
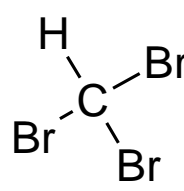
All VOC samples collected onto thermal desorption (TD) tubes were analysed by TD-GC-MS; Chapter 3. Samples were analysed at the first possibility after collection. Due to the length of the collection period (several months), each participant was analysed as a sequential batch with randomised sample order.

DBP standards were purchased from Sigma-Aldrich (Gillingham, UK) in a multi-component mixture (KDWR VOC Mix B, product code: 506583) of 100 µg mL⁻¹ of each component in methanol. A list of components included can be found in Table 8 and a copy of the certificate of analysis is included in Appendix 1.

4.4.6 Statistical analyses

All statistical analyses were performed using IBM SPSS Statistics (v 22.0, IBM Corp., Armonk, NY, USA). To assess change in post-exercise exhaled values of DBPs and candidate compounds, Wilcoxon signed rank tests were performed to compare each time point to pre-exercise values. Bonferroni correction was utilised to account for multiple comparisons, and p values refer to the Bonferroni adjusted value. Receiver operator characteristic (ROC) curves were produced and the area under the curve (AUC) calculated for the prediction of swimming. A paired subject approach was utilised to produce a ROC curve analysis using pre-swim samples as the negative state (control) and the 600 min post-exercise values as the target state. A Bonferroni adjusted p value of < 0.05 was considered statistically significant.

Table 8 Compounds present in the disinfection by-product standard mixture detailing empirical formula, estimated retention index and chemical structure.

1,1-Dichloroethene C ₂ H ₂ Cl ₂ 513		Trichloroethene C ₂ HCl ₃ 687	
Dichloromethane CH ₂ Cl ₂ 524		Bromodichloromethane CHBrCl ₂ 692	
Trichloromethane (Chloroform) CHCl ₃ 601		Dibromochloromethane CHBr ₂ Cl 768	
1,1,1-Trichloroethane C ₂ H ₃ Cl ₃ 624		Tetrachloroethene C ₂ Cl ₄ 795	
Carbon tetrachloride CCl ₄ 649		Tribromomethane (Bromoform) CHBr ₃ 849	

4.4.7 Calibration of target DBPs

A calibration curve was created ($n=10$) with on-column masses (OCM) ranging from 39 pg to 80 ng of each analyte, with a deuterated toluene internal standard (T-D₈, IS) (Table 9). Standards were prepared and used promptly by loading onto a thermal desorption tube using the same technique adopted for the T-D₈ IS (Chapter 3). Twenty ng T-D₈ was also loaded as described previously (Chapter 3). Standards were thermally desorbed and analysed by TD-GC-MS using the same parameters specified for breath and environmental samples analysis (Chapter 3).

All analytes were identified at each OCM value. Peak areas were determined and ratios were produced against the IS value. Resultant values were plotted and least squares regression was performed to create a linear calibration (Table 9).

Table 9 Calibration profiles for disinfection by-product compound standards for a range from 39 pg to 80 ng on-column mass (OCM). Calibration materials were produced by dilution of the standard mixture and OCM values refer to those calculated from the stock concentration detailed on the certificate of analysis in Appendix 1.

Disinfection by-product	On column mass (ng)	Ratio to IS	Linear fit (R ²)
1,1-Dichloroethylene	0.07	0.001	0.9996
	0.15	0.002	
	0.60	0.011	
	2.39	0.042	
	9.57	0.213	
	19.14	0.420	
	28.71	0.587	
	47.85	0.993	
	76.56	1.571	
Methylene Chloride	0.04	0.084	0.9961
	0.07	0.052	
	0.15	0.054	
	0.59	0.100	
	2.37	0.090	
	9.49	0.235	
	18.98	0.370	
	28.47	0.487	
	47.45	0.794	
75.92	1.331		
Chloroform	0.04	0.003	0.9990
	0.08	0.005	
	0.15	0.007	
	0.61	0.036	
	2.45	0.104	
	9.80	0.399	
	19.60	0.763	
	29.40	1.190	
	49.00	1.958	
78.40	3.305		
1,1,1-Trichloroethane	0.08	0.002	0.9979
	0.15	0.004	
	0.62	0.026	
	2.46	0.073	
	9.85	0.311	
	19.70	0.597	
	29.55	0.920	
	49.25	1.539	
	78.80	2.656	
Carbon tetrachloride	0.08	0.002	0.9996
	0.17	0.004	
	0.67	0.028	
	2.68	0.076	

	10.71	0.371	
	21.42	0.692	
	32.13	1.065	
	53.55	1.732	
	85.68	2.867	
Trichloroethylene	0.08	0.002	0.9999
	0.15	0.003	
	0.61	0.018	
	2.43	0.051	
	9.70	0.211	
	19.40	0.407	
	29.10	0.644	
	48.50	1.055	
	77.60	1.686	
Bromodichloromethane	0.08	0.002	0.9978
	0.16	0.004	
	0.63	0.028	
	2.50	0.073	
	10.00	0.309	
	20.00	0.581	
	30.00	0.971	
	50.00	1.586	
	80.00	2.721	
Dibromochloromethane	0.08	0.002	0.9988
	0.16	0.005	
	0.64	0.029	
	2.57	0.076	
	10.29	0.319	
	20.58	0.573	
	30.87	0.983	
	51.45	1.553	
	82.32	2.587	
Tetrachloroethene	0.08	0.003	0.9996
	0.15	0.004	
	0.61	0.027	
	2.44	0.073	
	9.75	0.287	
	19.50	0.566	
	29.25	0.882	
	48.75	1.463	
	78.00	2.406	
Bromoform	0.08	0.002	0.9974
	0.16	0.004	
	0.63	0.029	
	2.50	0.073	
	10.00	0.316	
	20.00	0.553	
	30.00	0.974	
	50.00	1.531	
	80.00	2.635	

Note: IS = internal standard

4.4.8 Data processing

Targeted compounds

DBPs were identified by confirmation of mass spectra and retention times using Varian MS Workstation (v. 6.9.2, Varian Inc. – now Agilent Technologies, Palo Alto, CA, USA), Chapter 3, and quantified against the calibration (Table 9).

Metabolomic profiling

Metabolomic profiling was undertaken as described in Chapter 3.

4.5 Results

4.5.1 Exercise performance and environmental conditions

All participants completed the 30 min of continuous swimming without the development of pains/injuries or need to pause at any time. A total of 49 ± 11 lengths (1225 ± 275 m; mean \pm SD) were completed at a pace of 0.7 ± 0.2 m.s⁻¹. The swimming pool environment temperatures were $24.5 \text{ }^\circ\text{C} \pm 0.7^\circ\text{C}$, with a humidity of 57 ± 8 % and an ambient air pressure of 756.6 ± 7.8 mmHg across the 19 participant sampling sessions.

4.5.2 DBP standard calibrations

All standards present in the calibration mixture could be detected at the measured concentrations using the analytical method described. Linear responses were observed in all analytes with an r^2 value of ≥ 0.996 (Table 9). Figure 41 shows a chromatogram of the standard calibration mixture with each analyte annotated to their respective chromatographic feature. Measured retention times and corresponding mass spectra were used as criteria to confirm the presence or absence of each analyte in the experimental samples. An automated search

function was created using Varian MS Workstation and all confirmed peaks present in the samples were quantified by peak integration. Table 10 shows a summary of all the analytes in the calibration mix and their presence across the range of samples taken throughout the experimental period.

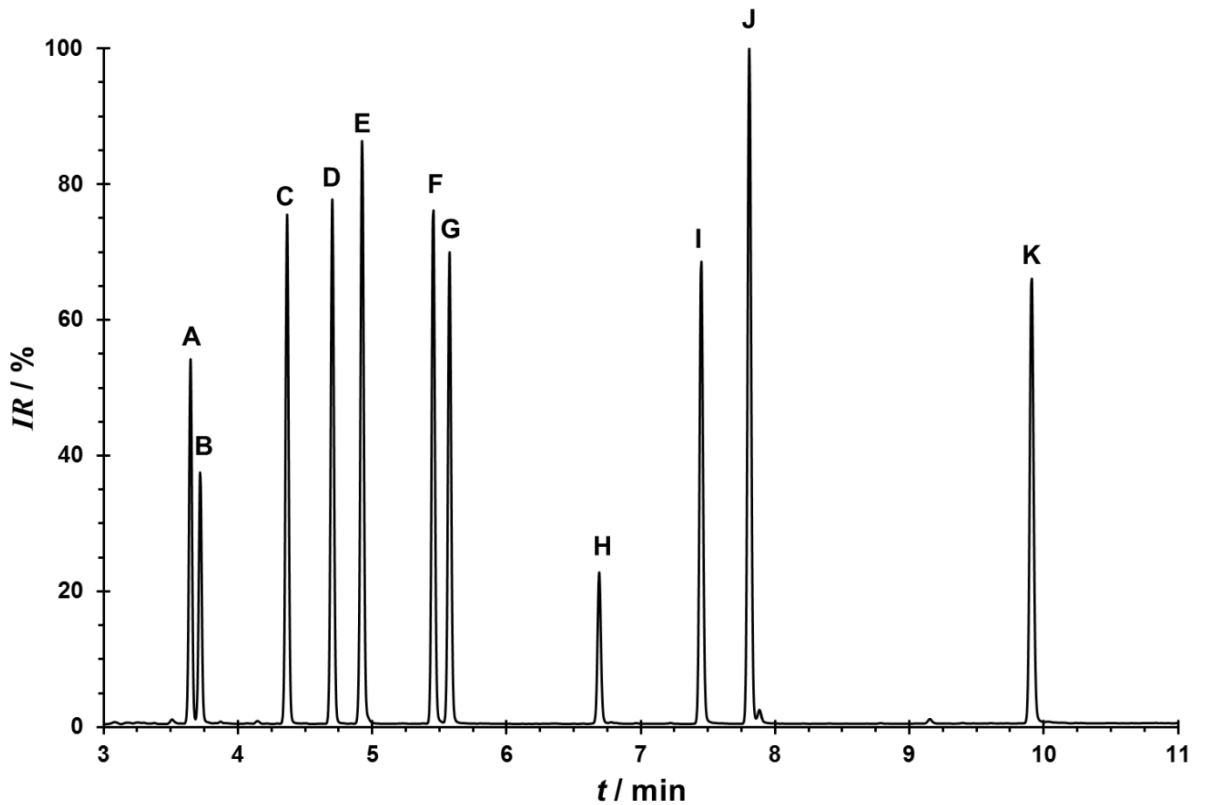


Figure 41 Example chromatogram indicating peaks A-K of the disinfection by-products standard mixture and the post-loaded internal standard. Peaks include 1,1-dichloroethene (A, OCM 76.56 ng), dichloromethane (B, 75.92 ng), trichloromethane (chloroform) (C, 78.40 ng), 1,1,1-trichloroethane (D, 78.80 ng), carbon tetrachloride (E, 85.68 ng), trichloroethene (F, 77.60 ng), bromodichloromethane (G, 80.00 ng), toluene-D8 (H, internal standard, 20.00 ng), dibromochloromethane (I, 82.32 ng), tetrachloroethene (J, 78.00 ng), tribromomethane (bromoform) (K, 80.00 ng).

Note: I_R = relative intensity; t = retention time

Table 10 Disinfection by-products in the standard mixture and their presence in exhaled and environmental volatile organic compound (VOC) samples.

Compound	Detected in samples (%)					
	Exhaled VOC samples	Pool air	Sampling room at pool complex	Filtered air at pool complex	Sampling room at laboratory	Filtered air at laboratory
1,1-dichloroethene (A)	4	5	5	0	5	0
Dichloromethane (B)	54	84	100	95	100	100
Trichloromethane (C)	89	100	16	84	100	89
1,1,1-trichloroethane (D)	6	11	37	0	53	0
carbon tetrachloride (E)	84	100	100	100	100	100
Trichloroethene (F)	2	16	5	5	0	0
Bromodichloromethane (G)	58	100	58	11	53	21
Dibromochloromethane (I)	57	100	95	16	74	37
Tetrachloroethylene (J)	74	100	79	37	100	63
Tribromomethane (K)	25	95	84	63	74	47

Note: Letters A-K refer to the chromatographic peaks present in Figure 41

4.5.3 DBPs in exhaled VOC samples

Variations in elimination profiles.

Two classifications of elimination profile were observed. More participants ($n=16$) showed a first order elimination profile with exhaled breath concentrations reducing from the maximum level observed immediately after they stopped swimming. However, 3 participants showed alternative wash out profiles for trihalomethane DBPs. Two of these participants showed maximal exhaled intensities at 90 min post-swimming, with one participant showing elevated levels at 5 min post-exercise that were maintained at 90 min post-exercise. Figure 42 shows one participant with delayed exhalation intensities for CHCl_3 with comparison to a common wash out profile.

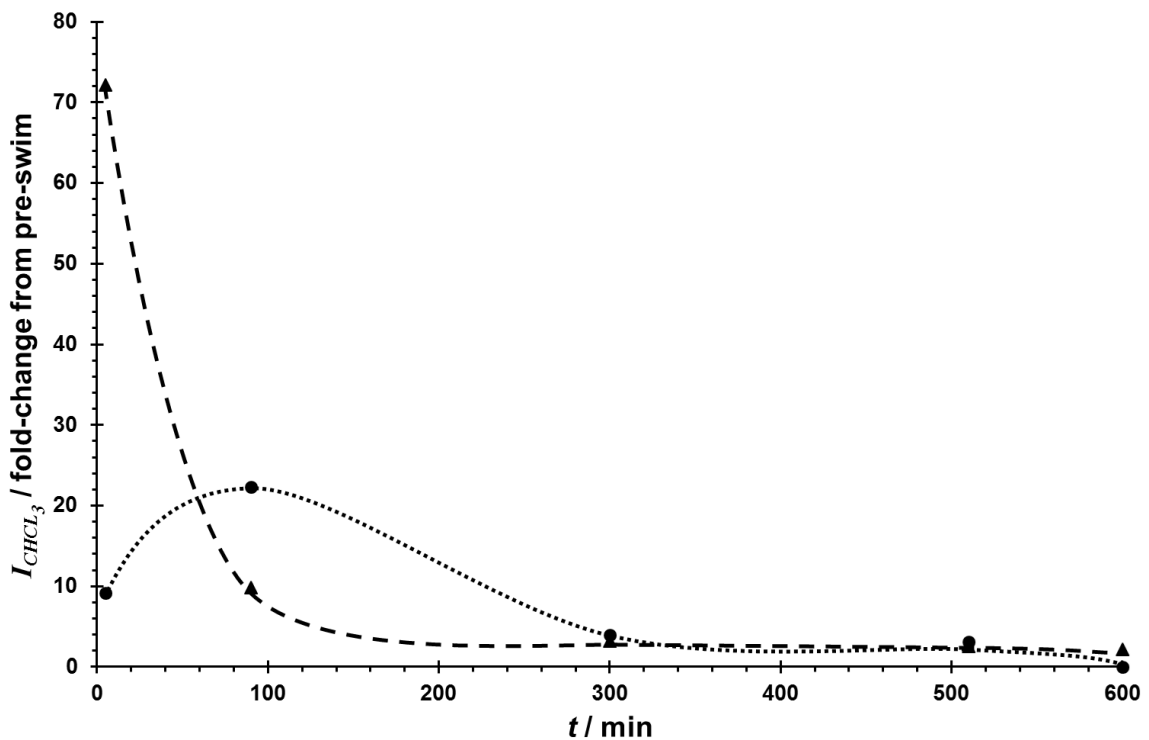


Figure 42 Comparison of one participant with delayed wash out of chloroform (circles, dotted line) overlaid against the wash out kinetics observed from another alternative participant representative of the majority of the profiles observed (triangles, dashed line).

Note: I = intensity; t = time

Delayed elimination

Participants showing delayed wash out profiles (16 %) were excluded from the main targeted analyses. However, breath data were included for non-targeted metabolomics analyses. It is unknown whether the delayed response is indicative of solely the DBPs, or indeed also of other compounds in response to swimming.

First-order elimination

All targeted DBPs were detected, with 6 DBPs observed in more than 50 % of exhaled VOC samples. These common DBPs were identified as dichloromethane, chloroform, carbon tetrachloride, bromodichloromethane, dibromochloromethane and tetrachloroethylene (see Table 10 for an overview of all target DBPs and their presence in respective samples). Three of these 6 DBPs were seen to rise post-swimming and wash out over the 10 hr recovery period. Specifically, the 3 DBPs were trihalomethane species. Figure 43 shows extracted base peak ions with matching retention times and confirmation mass spectra for each of the 3 DBPs isolated from the 5 min post-exercise exhaled breath sample of one participant. All 3 DBPs rose above pre-exercise levels in the 5 min post-exercise exhaled breath sample with chloroform showing the greatest increase (cohort median, 121-fold), followed by bromodichloromethane (4.4-fold) and dibromochloromethane (1.8-fold, $p \leq 0.002$). All DBPs median values rose above measured concentrations of the respective analyte in the sampling room environmental air, and the blank samples obtained from the supplied filtered air. None of the exhaled masses of DBP rose above the concentrations measured in the environmental air of the swimming pool hall. Table 11 summarises the exhaled on-column masses at all time points and the concentrations of environmental and blank samples for the 3 trihalomethane DBPs.

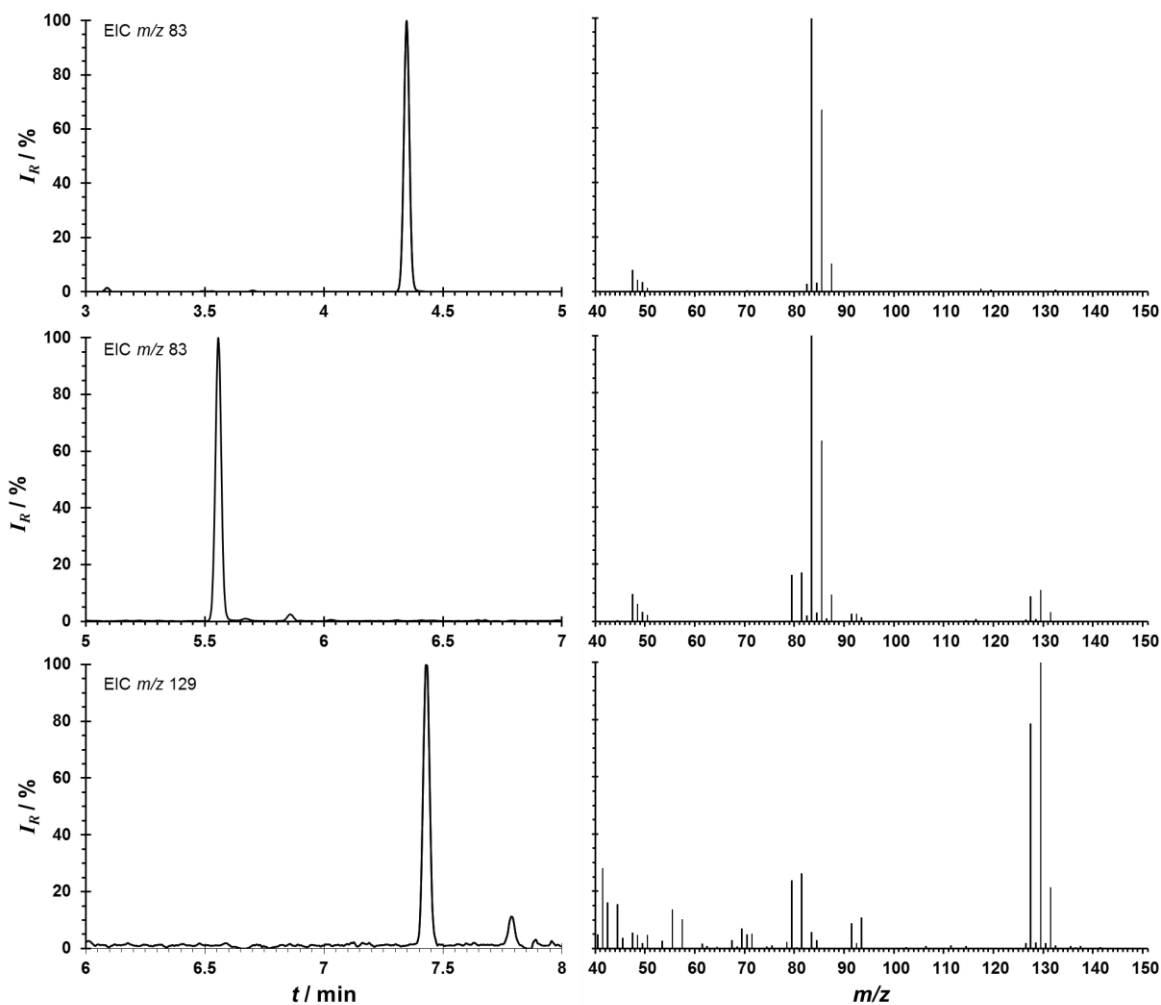


Figure 43 Example exhaled breath VOC sample extracted ion chromatograms (EIC) for base peak ions (left) and corresponding peak mass spectra (right) for trichloromethane (top), bromodichloromethane (middle) and dibromochloromethane (bottom).

Note: I_R = relative intensity; m/z = mass to charge ratio; t = retention time

Retention times do not compare with earlier preliminary experiment due to installation of new chromatography column for the main experimental campaign.

Table 11 Summary of median exhaled mass, fold change from baseline and p value of change for three trihalomethane disinfection by-products measured before and up to 600 min post-exercise in a swimming pool.

Compound	Time point / min	Median exhaled mass / ng	Fold change from baseline	p Value	
trichloromethane (chloroform)	Pre-swim	0.27 (0.00 to 1.41)			
	+5	32.49 (5.76 to 52.01)	121.0	0.005	
	+90	5.66 (2.28 to 9.96)	21.1	0.010	
	+300	1.37 (0.18 to 3.35)	5.1	0.040	
	+510	0.96 (0.16 to 1.62)	3.6	0.080	
	+600	0.72 (0.14 to 1.55)	2.7	NS	
	Concentration (ng L⁻¹)				
	Pool air		73.12 (36.68 to 223.15)		
	Sampling room 1		0.81 (0.25 to 3.91)		
	Air supply room 1		0.30 (0.17 to 1.41)		
	Sampling room 2		0.47 (0.22 to 5.55)		
	Air supply room 2		0.25 (0.19 to 3.27)		
	bromodichloromethane	Pre-swim	1.70 (0.00 to 2.71)		
+5		7.47 (2.99 to 22.74)	4.4	0.002	
+90		2.55 (1.87 to 3.67)	1.5	0.020	
+300		1.82 (1.37 to 2.39)	1.1	NS	
+510		1.73 (1.37 to 2.99)	1.0	NS	
+600		1.59 (0.00 to 3.91)	0.9	NS	
Concentration (ng L⁻¹)					
Pool air			12.49 (2.69 to 23.51)		
Sampling room 1			0.48 (0.36 to 0.96)		
Air supply room 1			0.36 (0.00 to 0.50)		
Sampling room 2			0.42 (0.36 to 0.66)		
Air supply room 2			0.37 (0.00 to 3.35)		
dibromochloromethane		Pre-swim	0.57 (0.00 to 1.09)		
	+5	1.01 (0.59 to 1.42)	1.8	0.002	
	+90	0.67 (0.58 to 0.75)	1.2	NS	
	+300	0.58 (0.00 to 0.64)	1.0	NS	
	+510	0.58 (0.00 to 0.65)	1.0	NS	
	+600	0.56 (0.00 to 0.73)	1.0	NS	
	Concentration (ng L⁻¹)				
	Pool air		1.60 (0.20 to 3.51)		
	Sampling room 1		0.16 (0.14 to 0.37)		
	Air supply room 1		0.14 (0.00 to 0.34)		
	Sampling room 2		0.15 (0.00 to 0.21)		
	Air supply room 2		0.14 (0.00 to 2.82)		

Note: a total of 2 L of breath was sampled and thus median concentrations of exhaled trihalomethanes in ng L⁻¹ correspond to the median exhaled mass divided by 2.

Median chloroform exhaled masses in breath increased 121-fold from 0.27 to 32.49 ng OCM and remained above pre-exercise levels until at least 300 min post-swimming ($p \leq 0.04$). Levels returned to baseline by 510 min post-swimming ($p = 0.08$). Similarly, median bromodichloromethane exhaled masses increased 4.4-fold from 1.70 to 7.47 ng OCM and remained above pre-exercise levels until at least 90 min post-exercise ($p \leq 0.02$). Bromodichloromethane median exhaled masses increased from 0.57 to 1.01 ng OCM, rising above pre-exercise levels at 5 min post-exercise ($p = 0.002$) and returning to pre-exercise levels by 90 min. Elimination profiles of the 3 trihalomethane DBPs can be visualised in terms of exhaled mass and fold change from pre-exercise in Figure 44 and Figure 45, respectively. Figure 46 shows an example pre-exercise exhaled breath chromatogram with overlaid and aligned extracted ion chromatograms for the 3 trihalomethane DBPs showing all post-exercise time points.

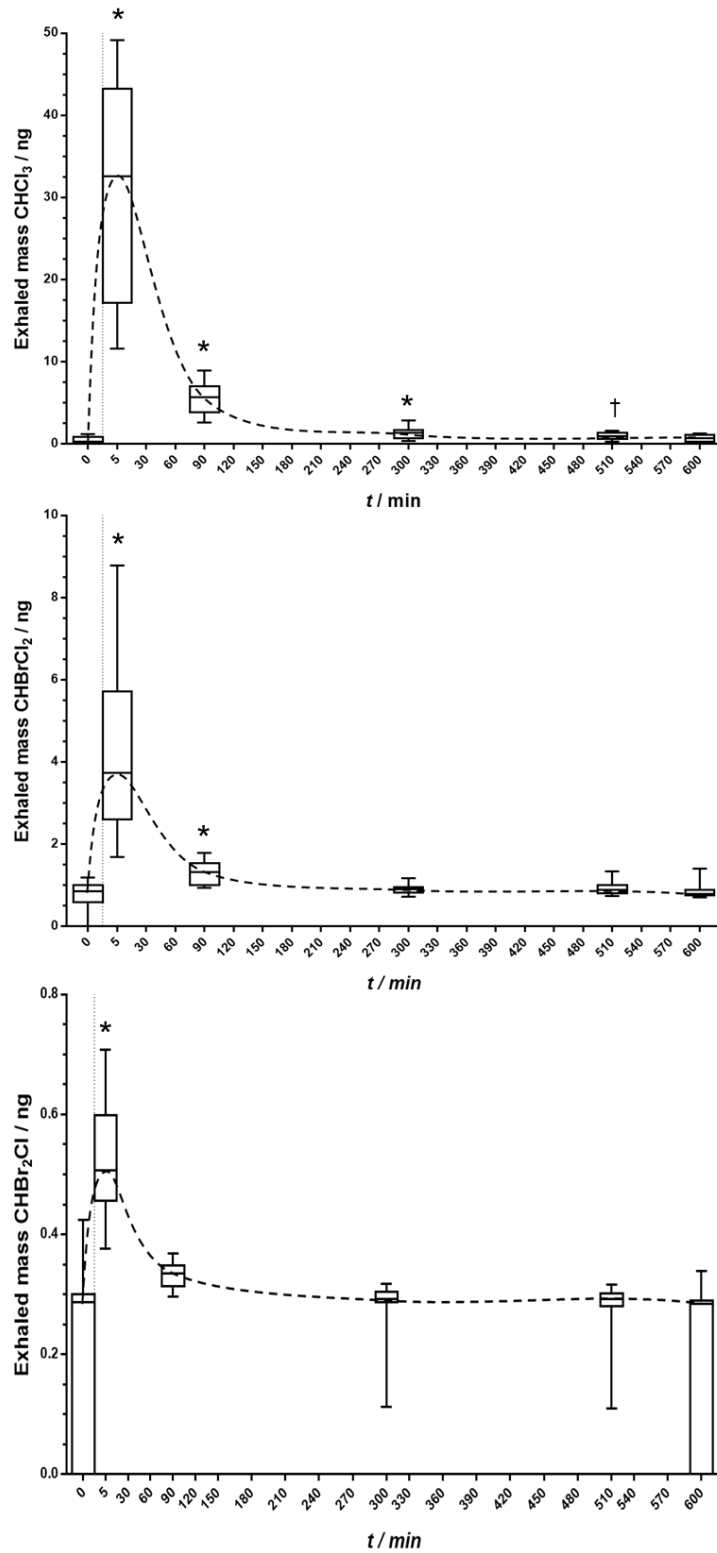


Figure 44 Box and whisker plots to show exhaled mass for chloroform (top), bromodichloromethane (middle) and dibromochloromethane (bottom) for combined participant exhaled breath samples. Boxes refer to median and interquartile range and whiskers as 10th and 90th percentiles. Compared to pre-exercise values: * $p \leq 0.040$ † $p = 0.080$.

Note: t = time

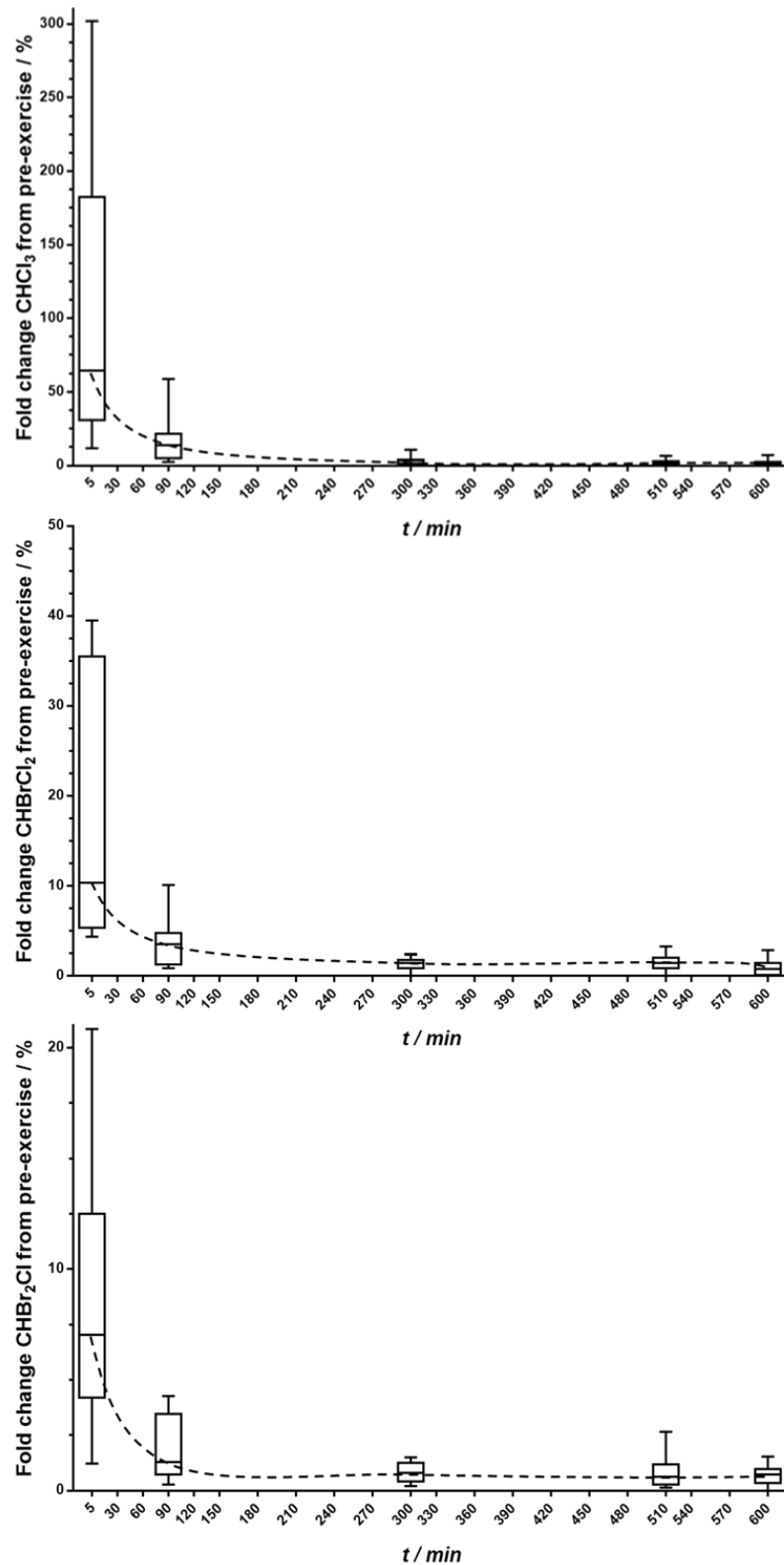


Figure 45

Box and whisker plots to show fold change from pre-exercise values for chloroform (top), bromodichloromethane (middle) and dibromochloromethane (bottom) for combined participant exhaled breath samples. Boxes refer to median and interquartile range and whiskers as 10th and 90th percentiles.

Note: t = time

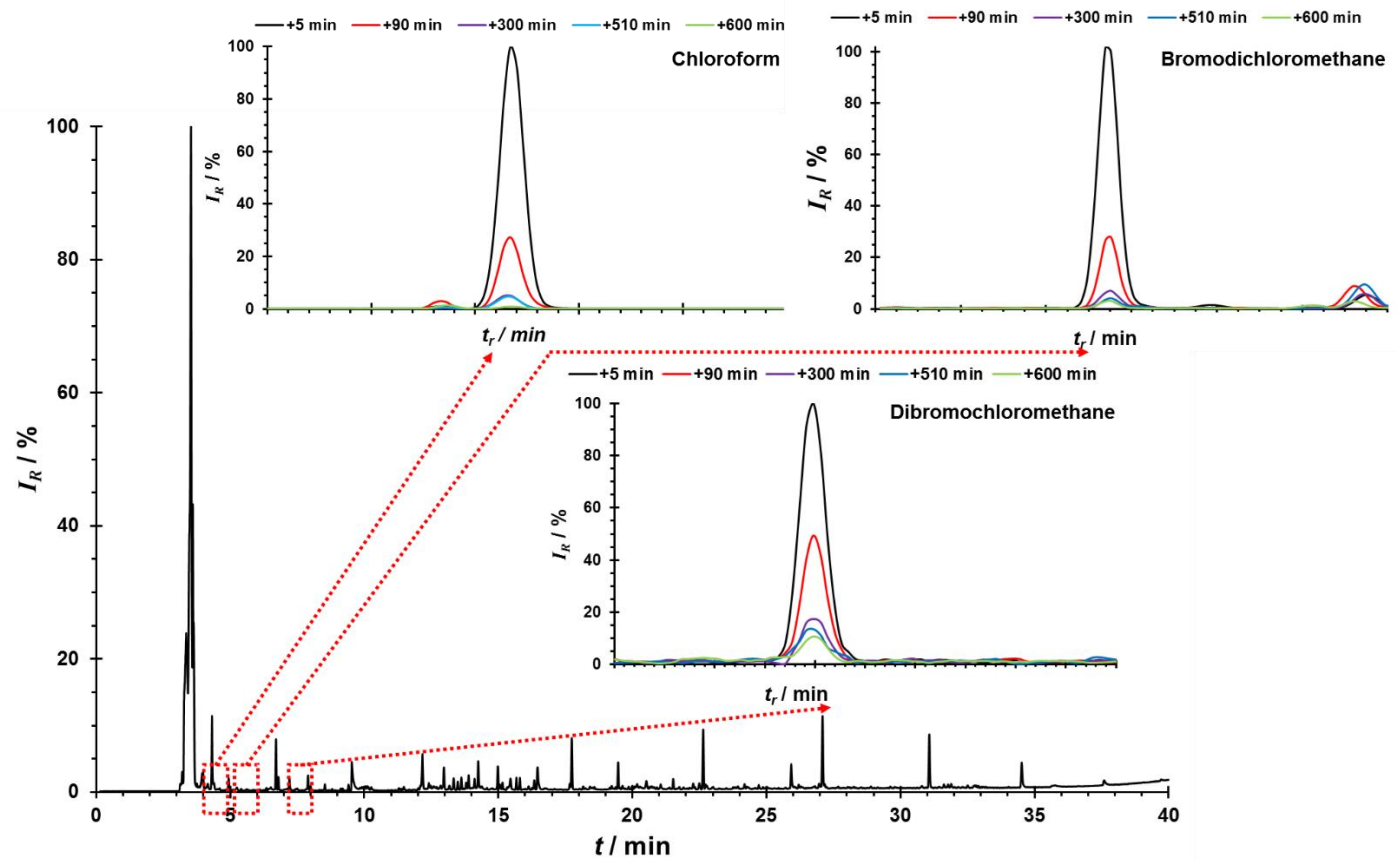


Figure 46 Pre-swim total ion chromatogram from a single participant (main body) with overlaid and aligned chromatograms across time sampling points for chloroform (extracted ion chromatogram (EIC) m/z 83, top left), bromodichloromethane (EIC m/z 83, top right) and dibromochloromethane (EIC m/z 129, bottom)

Note: I_R = relative intensity; t_r = retention time

4.5.4 Metabolomic profiling of exhaled VOCs

Identified VOCs were collated to produce a search function that prospected all samples (Chapter 3). Six hundred and three unique VOCs were isolated, with 73 VOCs distinctive to breath samples (present in > 20 % breath samples and < 20 % environment samples) with not one VOC present in > 20 % environment and < 20 % breath samples. Peak integration output values, normalised to internal standard, were organised into a matrix and imported for multivariate analysis (Chapter 3).

In order to test the secondary aim hypothesis, breath samples obtained pre-exercise and at the 600 min sample point were compared, see Chapter 3 Section 3.3.4. Data models were produced with both Pareto and UV scaling methods. Figures and candidate biomarkers discussed herein were isolated using the UV method, as Pareto scaling did not allow for discernible isolation of candidate compounds.

Orthogonal partial least squares-discriminant analysis (OPLS-DA) indicated the presence of discriminating compounds (Figure 47), and a panel of 8 candidate VOC were identified from the S-plot (Figure 48). Table 12 shows the average retention index, quantification and qualification ions for these candidates. Candidate compounds were modelled with principle components analysis (PCA) for pre- and 600 min post-exercise exhaled VOCs, yielding a near separation of time points (Figure 49).

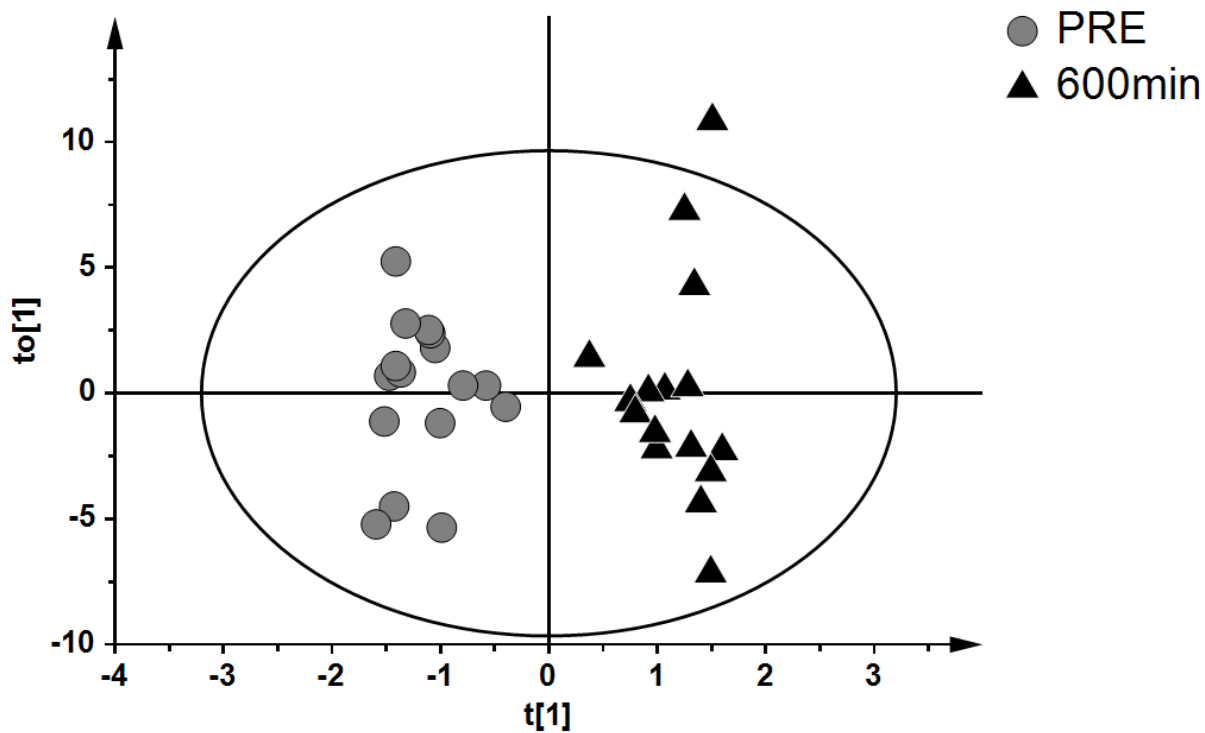


Figure 47 Orthogonal partial least squares-discriminant analysis model 2-dimensional score plot for pre- (grey circles) versus 600 min post-exercise (black triangles) breath samples.

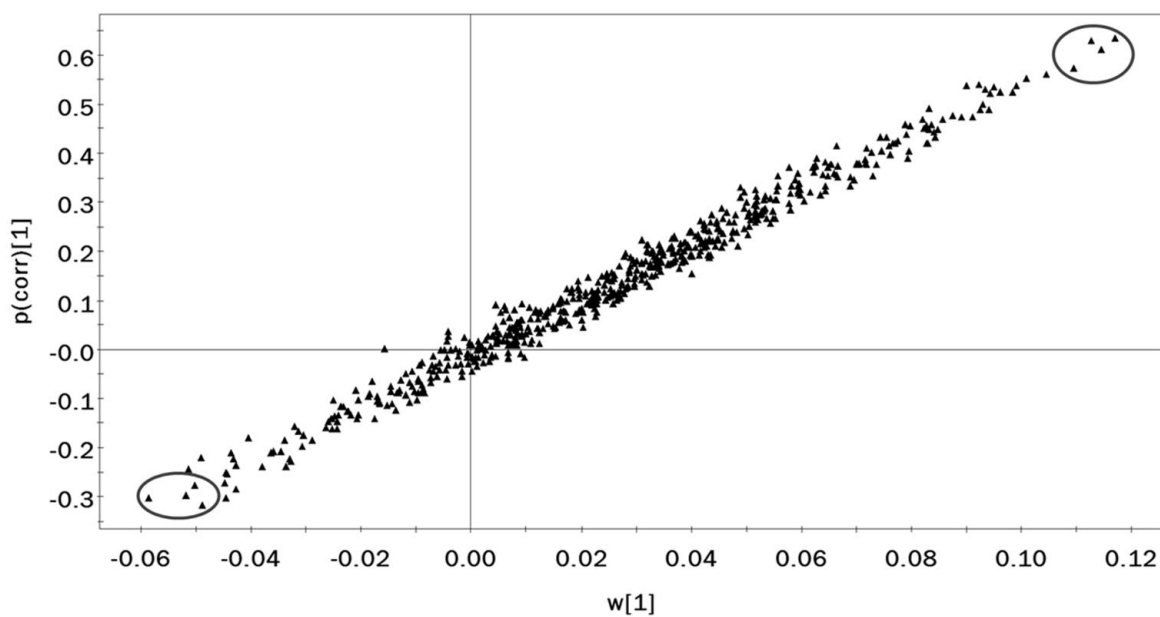


Figure 48 S-plot for modelled variables using an orthogonal partial least squares-discriminant analysis model with unit variance scaling for pre- versus 600 min post-exercise breath samples. Candidate biomarkers are highlighted in grey ovals.

Table 12 List of candidate biomarkers as identified by OPLS-DA analysis on comparison of exhaled VOC samples at pre- and 600 min post-swimming.

Experimental peak number	Mean retention index	Quantifier ion	Qualifier ion 1	Qualifier ion 2	Qualifier ion 3	Qualifier ion 4	Up/down regulated	Study ID
98	1912	73	281	429	149	282	↓	BRI-1912-73-281-429-149-282
141	1098	41	71	43	57	70	↓	BRI-1098-41-71-43-57-70
171	961	41	43	57	95	41	↓	BRI-961-41-43-57-95-41
579	927	57	71	41	43	95	↓	BRI-927-57-71-41-43-95
68	946	285	286	269	333	287	↑	BRI-946-285-286-269-333-287
118	1461	43	107	93	41	69	↑	BRI-1461-43-107-93-41-69
383	1253	415	327	416	0	0	↑	BRI-1253-415-327-416-0-0
414	1337	146	145	0	0	0	↑	BRI-1337-146-145-0-0-0

Note: ID = identification; OPLS-DA = orthogonal partial least squares-discriminant analysis

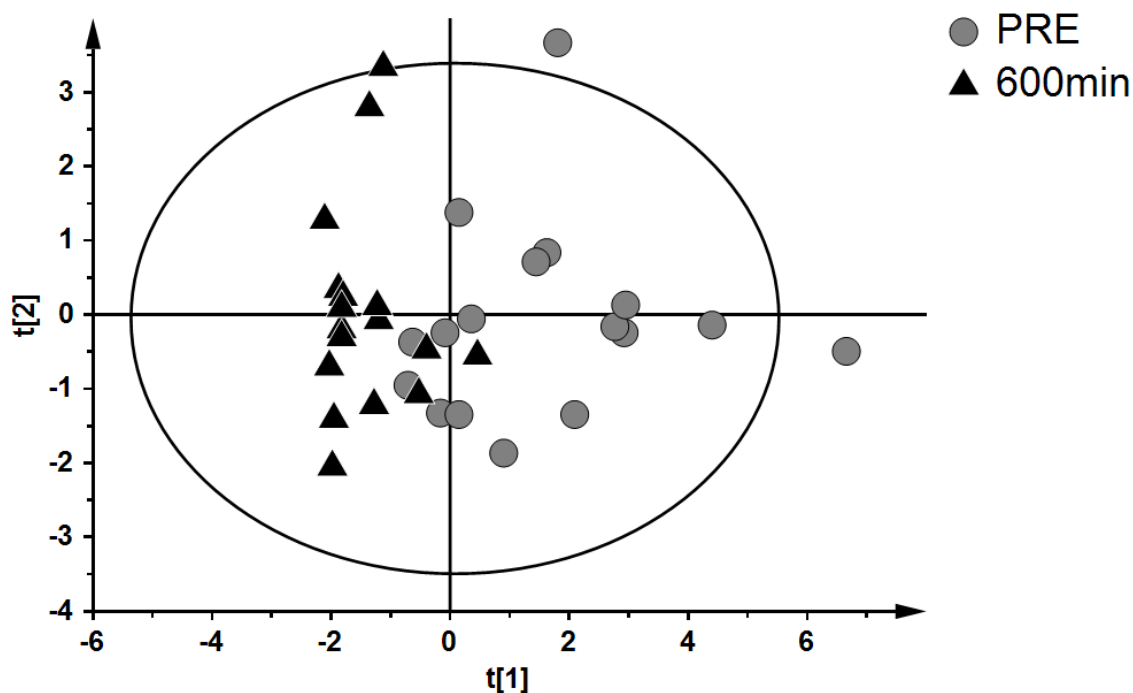


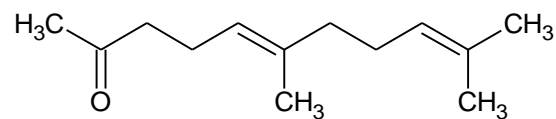
Figure 49 Principal components analysis 2-dimensional score plot constructed using candidate exhaled VOC biomarkers for pre- (grey circles) versus 600 min post-exercise (black triangles) breath samples.

Data indicate that an observed change in the breath profile could not be ruled out and the study hypothesis underlying the secondary aim of this study should be rejected. Table 13 summarises potential identifications of BRI-946-285-286-269-333-287 (1-Cyclohexyldimethyl silyloxy-pentadecane), BRI-1461-43-107-93-41-69 ((5E)-6,10-dimethylundeca-5,9-dien-2-one), BRI-1253-415-327-416-0-0 (Diethyl (2-ethoxyethoxy) octadecyloxy-silane) and BRI-1337-146-145-0-0-0 (2-benzofurancarboxaldehyde) based on spectral fit with the National Institute of Science and Technology Mass Spectral Library (NIST 14) and predicted retention index (RI) vs observed RI matches. Two upregulated compounds that were assigned as siloxanes may be associated with artefacts from the analytical system and were excluded from further study. Environmental samples were investigated for the presence of the remaining metabolites. BRI-1337-146-145-0-0-0 was identified in only 4 environmental samples. Levels of BRI-1461-43-107-93-41-69 at all time points versus the environmental samples can be visualised in Figure 52 of Appendix 2 (Section 4.11). Candidate VOCs were determined to have no influence from environmental conditions.

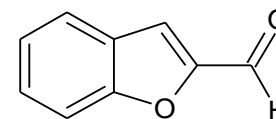
Table 13 Four post-swimming upregulated candidate biomarkers and possible identification matches using the National Institute of Science and Technology mass spectral database (NIST 14).

Candidate biomarker	Most likely hit (NIST 14)	Forward match	Reverse match	Probability (%)	Measured / predicted RI	Notes
BRI-946-285-286-269-333-287	1-Cyclohexyldimethyl silyloxy-pentadecane	517	706	8.2	946 / 2357	Large deviation in RI - possible bleed from analytical column
BRI-1461-43-107-93-41-69	(5E)-6,10-dimethylundec-5,9-dien-2-one	679	735	13.4	1461 / 1426	Good match statistics
BRI-1253-415-327-416-0-0	1-Cyclohexyldimethyl silyloxy-pentadecane, Diethyl (2-ethoxyethoxy) octadecyloxy-Silane	450	744	4.4	1253 / 2743	Large deviation in RI - possible bleed from analytical column
BRI-1337-146-145-0-0-0	2-Benzofurancarboxaldehyde	555	797	Unknown	1337 / 1296	Good match statistics - Probability unknown due to competing ions - very likely match with extra ions of 89, 63 and 90

Note: NIST = National Institute of Science and Technology mass spectral database; RI = retention index



(5E)-6,10-dimethylundec-5,9-dien-2-one



2-Benzofurancarboxaldehyde

BRI-1461-43-107-93-41-69 reported an increasing trend in the hours post-swimming. This trend was calculated to be non-significant (only once p values were adjusted for multiple comparisons). Power calculations for 80 % power with a p value of < 0.05 indicated $n=38$ would allow for this comparison to reach significance. Similarly, a ROC curve was not able to use the values for this compound at 600 min post-exercise as a predictor of swimming (AUC 0.614 (95 % CI 0.403 to 0.825, $p=0.295$). ROC curves were Figure 50 shows the plots of BRI-1461-43-107-93-41-69 with values in both a raw format (normalised to IS) and those normalised to each participant's maximal peak intensity across the 600 min time period. None of the candidates reported an individual change in values across the wash out period, likely due to large variations observed between participants.

The two candidate biomarkers were used to generate a score (Euclidean distance, Section 3.3.5) for each time point (Figure 51). Upregulation of the combined ions at 510 and 600 min post-swimming was statistically significant $p\leq 0.032$ and the ROC curve area reported as significant for the prediction of swimming (AUC 0.875 (0.730 to 1.000, $p<0.0005$). Visual interpretation of the plots for BRI-1461-43-107-93-41-69 and the Euclidean distance scoring show similar upregulated patterns, and thus it is likely that BRI-1461-43-107-93-41-69 is highly influencing the calculated scores. Furthermore, investigation in to BRI-1337-146-145-0-0-0 reported that this molecule was only characterised in 22 % of exhaled samples with 7 of the 19 participants influencing the pre- to 600 min post-exercise comparisons. The research design did not incorporate a non-swimming group that were subjected to identical environmental exposure of the swimming pool environment, therefore it was not possible to assess the impact that the exercise had on the elevation of exhaled DBPs post-exposure.

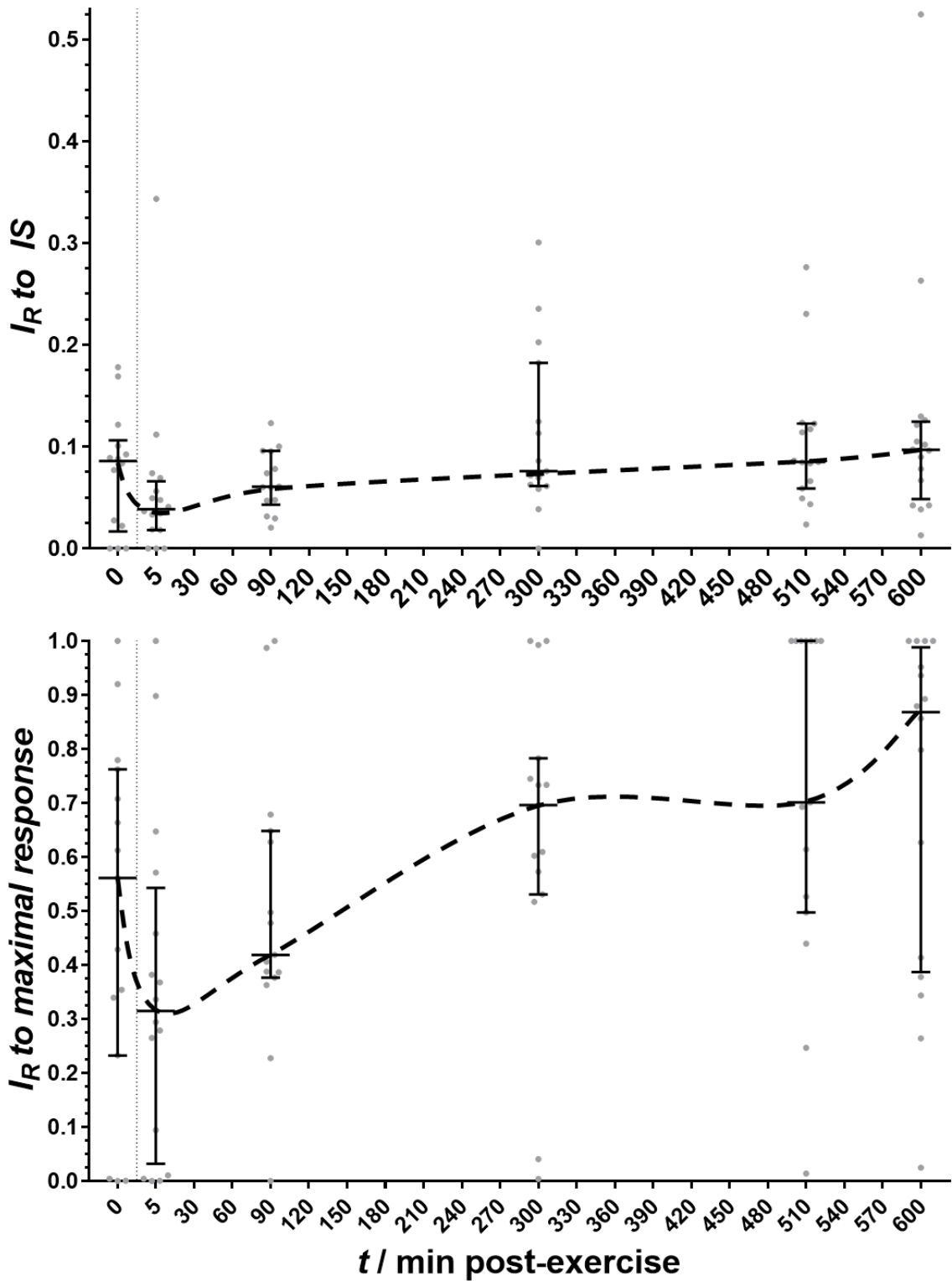


Figure 50

Individual scatter plots to visualise the change in candidate biomarker BRI-1461-43-107-93-41-69 when expressed as a response ratio to internal standard (IS) (top) and time point data normalised to each individual's maximal response (bottom). Horizontal line refers to the median and the error bars to the interquartile range.

Note: I_R = relative intensity; t = time

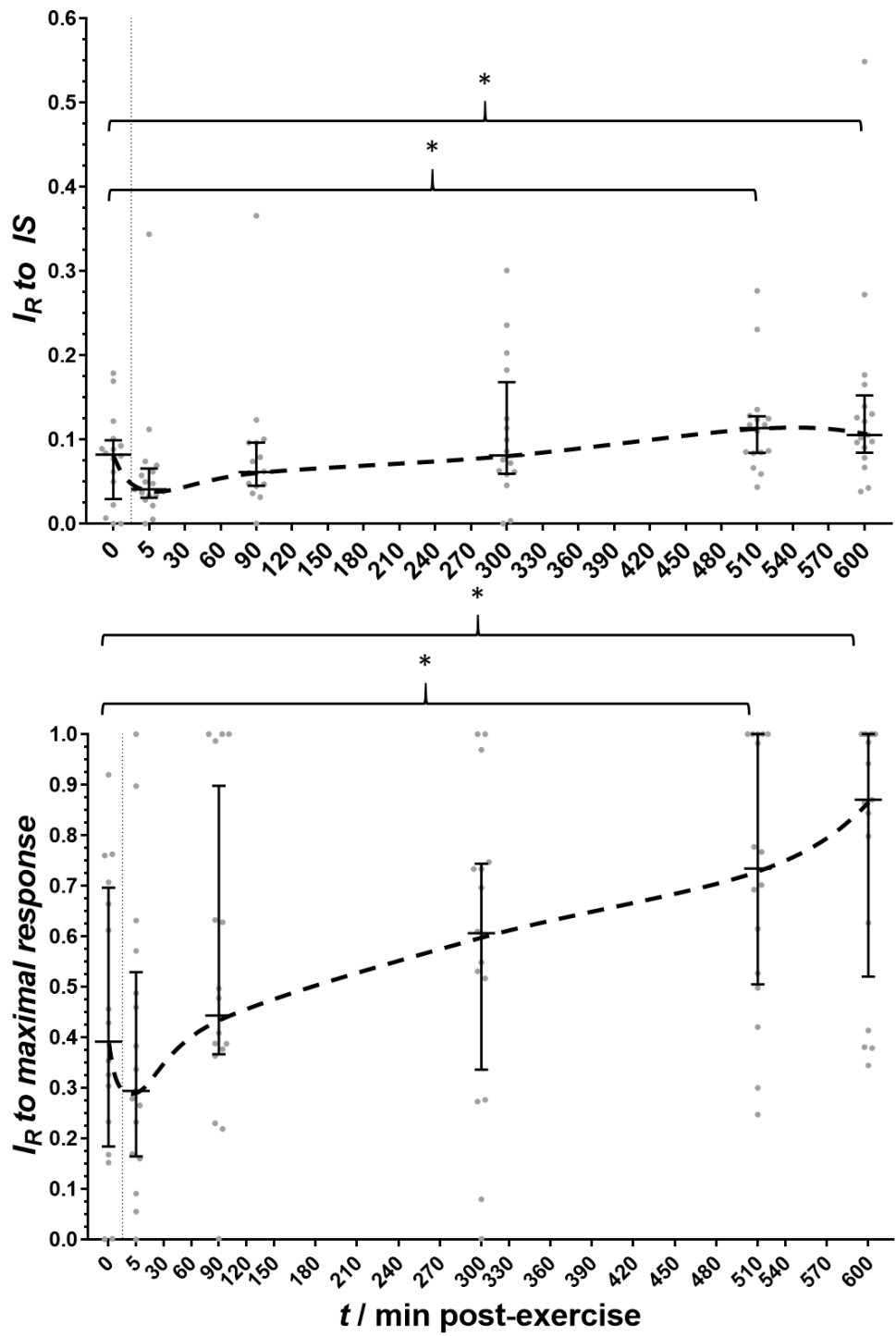


Figure 51

Scatter plots to visualise the change in the sum of Euclidean distance scores for the four upregulated candidate biomarkers expressed as a mean response ratio to internal standard IS (top) and mean time point data normalised to each individual's highest time point scoring (bottom). Horizontal line refers to the median and the error bars to the interquartile range. * denotes $p \leq 0.032$.

Note: I_R = relative intensity; t = time

4.6 Discussion

DPBs of water treatment by chlorination were detectable in the exhaled breath of participants both before and after swimming, and for up to a further 510 min after a 30 min swim. Three DPBs measured in the exhaled breath reported a pattern whereby a rapid increase in exhaled mass was observed immediately post-swimming, followed by an initially rapid washout that slowed over the 600 min time period. Two DBPs, CHCl_3 and CHBrCl_2 , were seen to be elevated in exhaled breath samples for at least 90 min after cessation of swimming exercise, with CHBr_2Cl reducing to baseline levels within 90 min. Differing exhaled wash out behaviours were noted in this cohort, with 3 participants showing delayed or maintained maximal levels of exhaled trihalomethane DBPs. Reasons for this are unknown but may be attributable to alterations in exposure. For example, a delayed wash out may indicate ingestion of swimming pool water, residing in the stomach for a period of time before being released and available to diffuse into the lungs for exhalation. It is recommended that future investigations increase the total number of participants and include more sampling time points in the first 180 min post-exercise to further understand this phenomenon. Additive information such as respiratory and heart rates, alongside exercise intensity measured by exhaled $\dot{V}\text{O}_2$, would provide valuable information for the comparison of participants. These tests were unavailable for the present investigation.

Metabolomic profiling analyses indicated that two compounds showed an upregulation from baseline levels across the experimental washout period. Combined Euclidean distance scores reported an increase in these compounds at 510 and 600 min post-swimming when compared to pre-swimming levels. ROC analysis showed that the Euclidean distance scores of the two metabolites were able to predict, at 600 min, that swimming had occurred. Although individual metabolite upregulation was not noted, one metabolite, tentatively identified as an unsaturated ketone ((5E)-6,10-dimethylundeca-5,9-dien-2-one), showed an individual trend of upregulation across the 10 hr time period when normalised to individual participant maximal response. The common name for this compound is geranylacetone (CAS: 3796-70-1) which is found in many essential oils and food flavourings. Geranylacetone is also characterised as an endogenous metabolite

[11] associated with four biological functions: cell signalling; fuel and energy storage; fuel or energy source; and, membrane integrity stability. Geranylacetone is a monoterpene that contains a chain of two isoprene units, suggestive of a connection to the mevalonate pathway. Geranylacetone could also be a breakdown product of a sesquiterpene, by oxidative cleavage of an alkene to leave the ketone. The metabolomic ontology of geranylacetone indicates that it is located within membranes and extracellular fluids.

The role that ketones play in inflammation is not fully understood. There has been interest in how ketogenic diets increase the concentration of ketones in the biological system, known as ketosis. Ketosis has been reported to reduce pain and inflammation [12], with some clinical evidence to suggest that ketogenic diets can also reduce signs of liver inflammation (through improvements in steatosis, inflammatory grade and fibrosis) in obese patients with non-alcoholic fatty liver disease [13,14]. Other data suggest that increased ketone concentrations upregulate the levels of adenosine [15,16], a neuromodulator that is known to have anti-inflammatory effects [17,18].

Ketogenic diets utilise a low carbohydrate and high fat intake that produces an upregulation of lipid oxidation which, through a cascade of reactions, produces ketone bodies such as acetone and β -hydroxybutyrate (β -HB) [19]. Acetone is a major component in an exhaled breath VOC matrix [20]. Participants in this experiment were asked to arrive following an overnight fast, producing a reduction in blood glucose levels and temporarily increasing fat oxidation. Relatively intense exercise was performed which is an action that has been reported to increase the availability of β -HB [21]. For these reasons, the rise in this unsaturated ketone may be attributable to the fasted exercise that was performed as part of the trial. However, as feeding was allowed throughout the day a continued rise throughout the 600 min post-exercise would not have been produced due to the elevated fat oxidation of a fasted state. Due to this ketone observation, acetone was investigated for exhaled samples across the time period and no differences were reported (data not shown).

It would be premature to attribute a rise in geranylacetone concentrations in breath to an inflammatory response, but the upregulated trend of this compound

across 600 min following swimming in chlorinated water is noted. Four sources for this upregulated compound have been conjectured:

- Release from damaged cellular membranes
- Generation by oxidative breakdown of a sesquiterpene-based derivative
- Release from ingested food
- Generation by ketosis following fasting and exercise.

A follow on study will be useful to establish association with inflammation using appropriate controls for ketosis and food constituents. A randomised cross-over experimental design would enable better isolation of the chlorinated pool environment as a potential causative factor.

The other potentially upregulated compound was tentatively identified as 2-benzofurancarboxaldehyde (BRI-1337-146-145-0-0-0), characterised in the Human Metabolome Database as a nutrient and food flavouring expected to be found at unquantified concentrations in cytoplasm and extracellular material [22]. It has been previously reported that aldehyde compounds are expressed in exhaled breath in response to inflammation/oxidative stress, for example malondialdehyde [23]. Furthermore, a recent publication reported the anti-inflammatory effects of benzofuran analogues [24]. As this compound was only noted throughout the experimental period in approximately one quarter of participants, it is not possible to attribute this to a post-swimming inflammatory response. However, follow on studies with a more targeted analysis and a larger sample size will reduce the sample and measurement variance enabling more reliable study statistics to inform the discussion.

All participants had detectable levels of DBPs in their breath prior to swimming. This may be due to absorption from the swimming pool environment where samples were collected within the swimming pool complex, albeit in an adjacent room with good ventilation and no direct contact with the swimming pool area. However, pre-filters were used in the sampling air supply removing DBPs from their air during sampling. This was the first study to analyse exhaled DBPs with a filtered air source, and it was also the first study to measure elevated DBP 300 min after participants had stopped swimming. Previous experiments reported a reduced post-swimming time [7], elimination of chloroform after 240 min [8] or

inconsistencies in a single participant across 600 min post-swimming [6]. The data in this study reflect the changes in sensitivity afforded by the described collection and analysis methods, with a lower limit of quantitation likely to be below an on-column mass of 38 pg.

The number of participants in this study was greater (19 versus 2 to 12) than previous washout studies (2x washouts utilising the identical environmental scenario for each participant), and inter-subject variability was observed to be a significant confounding factor to the straightforward analysis and interpretation of inter-subject data. Increased participant numbers will be required for follow-on research. Development of exhaled breath sampling instrumentation and on-line analysis to allow rapid analysis of exhaled DBPs would provide a more thorough understanding of the washout kinetics. A portable, mass spectrometer would allow the further exploration of the metabolic responses reported in this experiment.

In conclusion, this experiment characterised two distinct washout profiles of trihalomethane DBPs, lasting up to 510 min after swimming in a chlorinated pool.

4.7 Follow on research

To confirm or deny the rise in the candidate marker of swimming, geranylacetone, a follow-on study with a targeted approach should be performed. An experiment mimicking the protocol used in the investigation described in this chapter would be utilised with a targeted analytical approach to the samples. This would increase the sensitivity and selectivity of the candidate molecule and allow for more definitive information on its evolution post-exercise in a swimming pool environment. Additionally, mirroring time sampling points for participants after a prolonged period of time away from the swimming pool environment would be beneficial. This would be performed in a randomised crossover design and allow for comparison of post-swimming samples with common daily fluctuation. Furthermore, a third session whereby the participants perform exercise away from the swimming pool environment would allow for investigation as to whether the rise in exhaled levels is attributable to the environment itself, or is a metabolic response to exercise. A further session whereby participants are submerged in the pool water for an

identical time period but without swimming would allow for further understanding of the influence of exercise in the elevation and wash out of DBPs.

If exposure to chlorinated environments in swimming pools causes healthy individuals to experience inflammatory responses, or increases their susceptibility to experience inflammatory responses, the scope of studies such as this should be widened to reflect factors associated with childhood development and ageing. Participants were healthy adult males who had some, or little, history of swimming during childhood. With reports associating childhood swimming with the onset of respiratory conditions [e.g. 25] in later life, it is of interest to establish if inflammatory markers are present in childrens' breath following swimming in chlorinated pools. Lung development occurs throughout childhood and puberty and insults and injury to lung physiology may be compounded by remodelling of the developing lung. Could residual damage from an early age impact alveolar maturity? The potential of chlorination and DBPs to cause negative health outcomes for susceptible childhood phenotypes provides significant motivation to continue and develop this research. The impact of DBPs on the aging population should also be addressed. As aged populations increase and life expectancy is ever-rising there is a concomitant rise in mortality and morbidity due to lung disease [26]. Exercise has shown benefits to cardiorespiratory function in patients suffering from interstitial lung disease [27]. If inhalation of DBPs is indeed causing accelerated lung aging, consideration into the balance of exercise therapy (common in swimming pools due to the semi weight-bearing properties of water) and potential damage to the lungs needs to be addressed.

Another aspect to consider is the impact that chlorination and DBPs may have on an elite athlete's respiratory system. High-performance swimmers experience significantly higher exercise intensities than were adopted in the current study. They will place larger demands on their lungs and inhale the toxic chemicals in significantly larger amounts. The higher intensity swimming exercises also occur at high frequency; many elite swimmers training or competing every day during high season. Similar exposure frequencies may also be a factor for those who only swim recreationally, but regularly. The levels observed in this study were within irregular

swimmers, and therefore more regular attendance to a swimming pool based exercise session may cause resident elevated levels of DBPs.

Outside of exhaled breath analyses, research studies into the *in vitro* effects of DBPs on lung cell linings would be beneficial. It is important to understand whether DBPs are directly causing maladaptation to the epithelial cells and cell-based investigations will provide valuable insight into the potential causal, or simply associative, effects of pool air inhalation and development of lung tissue damage.

4.8 Acknowledgments

Louise Davies, Kevin Harty and all the staff at the Loughborough Sport Swimming Pool must be acknowledged and thanked for their knowledge and assistance provided during the experiment.

4.9 References

- 1 Sport England. Active people survey 7. http://archive.sportengland.org/research/active_people_survey/active_people_survey_7.aspx (accessed 29 November 2015)
- 2 Kim H, Shim J, Lee S. Formation of disinfection by-products in chlorinated swimming pool water. *Chemosphere* 2002;46:123-30
- 3 Judd SJ, Bullock G. The fate of chlorine and organic materials in swimming pools. *Chemosphere* 2003;51:869-79
- 4 Bernard A, Nickmilder M, Voisin C, Sardella A. Impact of chlorinated swimming pool attendance on the respiratory health of adolescents. *Pediatrics* 2009;124:1110-8

- 5 Villanueva CM, Font-Ribera L. Health impact of disinfection by-products in swimming pools. *Ann. Ist. Super Sanità* 2012;48:387-96
- 6 Aggazzotti G, Fantuzzi G, Righi E, Predieri G. Environmental and biological monitoring of chloroform in indoor swimming pools. *J. Chromatogr. A* 1995;710:181-90
- 7 Lindstrom AB, Pleil JD, Berkoff DC. Alveolar breath sampling and analysis to assess trihalomethane exposures during competitive swimming training. *Environ. Health Perspect.* 1997;105:636-42
- 8 Caro J, Gallego M. Alveolar air and urine analyses as biomarkers of exposure to trihalomethanes in an indoor swimming pool. *Environ. Sci. Technol.* 2008;42:5002-7
- 9 Box GEP, Wilson KB. On the experimental attainment of optimum conditions. *J. Roy. Statist. Soc. Ser. B* 1951;13:1-45
- 10 Borg G. Perceived exertion as an indicator of somatic stress. *Scand. J. Rehabil. Med.* 1970;2:92-8
- 11 Metabocard for geranylacetone (HMDB31846). Human metabolome database. <http://www.hmdb.ca/metabolites/HMDB31846> (accessed 14 February 2016)
- 12 Masino SA, Ruskin DN. Ketogenic diets and pain. *J. Child Neurol.* 2013;28:993-1001

- 13 Tendler D, Lin S, Yancy WS Jr, Mavropoulos J, Sylvestre P, Rockey DC, Westman EC. The effect of a low carbohydrate, ketogenic diet on nonalcoholic fatty liver disease: a pilot study. *Dig. Dis. Sci.* 2007;52:589-93
- 14 Pérez-Guisado J, Muñoz-Serrano A. The effect of the Spanish Ketogenic Mediterranean Diet on nonalcoholic fatty liver disease: a pilot study. *J. Med. Food* 2011;14:677-80
- 15 Kawamura M Jr, Ruskin DN, Masino SA. Metabolic autocrine regulation of neurons involves cooperation among pannexin hemichannels, adenosine receptors and KATP channels. *J. Neurosci.* 2010;30:3886-95
- 16 Masino SA, Li T, Theofilas P, Sandau US, Ruskin DN, Fredholm BB, Geiger JD, Aronica E, Boison D. A ketogenic diet suppresses seizures in mice through adenosine A1 receptors. *J. Clin. Invest.* 2011;121:2679-83
- 17 Kowaluk EA, Jarvis MF. Therapeutic potential of adenosine kinase inhibitors. *Expert Opin. Investig. Drugs* 2000;9:551-64
- 18 Linden J. Molecular approach to adenosine receptors: receptormediated mechanisms of tissue protection. *Ann. Rev. Pharmacol. Toxicol.* 2001;41:775-87
- 19 McPherson PA, McEneny J. The biochemistry of ketogenesis and its role in weight management, neurological disease and oxidative stress. *J. Physiol. Biochem.* 2012;68:141-51
- 20 Henderson MJ, Karger BA, Wren Shall GA. Acetone in the breath; a study of acetone exhalation in diabetic and nondiabetic human subjects. *Diabetes* 1952;1:188-93

- 21 Cotter DG, Schugar RC, Crawford PA. Ketone body metabolism and cardiovascular disease. *Am. J. Physiol. Heart Circ. Physiol.* 2013;304:1060-76
- 22 Metabocard for 2-benzofurancarboxaldehyde. Human metabolome database. <http://www.hmdb.ca/metabolites/HMDB33183> (accessed 14 February 2016)
- 23 Bartoli ML, Novelli F, Costa F, Malagrino L, Melosini L, Bacci E, Cianchetti S, Dente FL, Di Franco A, Vagaggini B, Paggiaro, PL. Malondialdehyde in exhaled breath condensate as a marker of oxidative stress in different pulmonary diseases. *Mediators Inflamm.* 2011;2011: 891752
- 24 Yadav P, Singh P, Tewari AK. Design, synthesis, docking and anti-inflammatory evaluation of novel series of benzofuran based prodrugs. *Bioorg. Med. Chem. Lett.* 2014;24:2251-5
- 25 Bernard A, Carbonnelle S, de Burbure C, Michel O, Nickmilder M. Chlorinated pool attendance, atopy, and the risk of asthma during childhood. *Environ. Health Prospect.* 2006;114:1567-73
- 26 Thannickal VJ, Murthy M, Balch WE, Chandel NS, Meiners S, Eickelberg O, Selman M, Pardo A, White ES, Levy BD, Busse PJ, Tuder RM, Antony VB, Sznajder JI, Budinger GR. Blue journal conference. Aging and susceptibility to lung disease. *Am. J. Respir. Crit Care Med.* 2015;191:261-9
- 27 Keyser RE, Woolstenhulme JG, Chin LM, Nathan SD, Weir NA, Connors G, Drinkard B, Lamberti J, Chan L. Cardiorespiratory function before and after aerobic exercise training in patients with interstitial lung disease. *J. Cardiopulm. Rehabil. Prev.* 2015;35:47-55

4.11 Appendix 2: additional figure

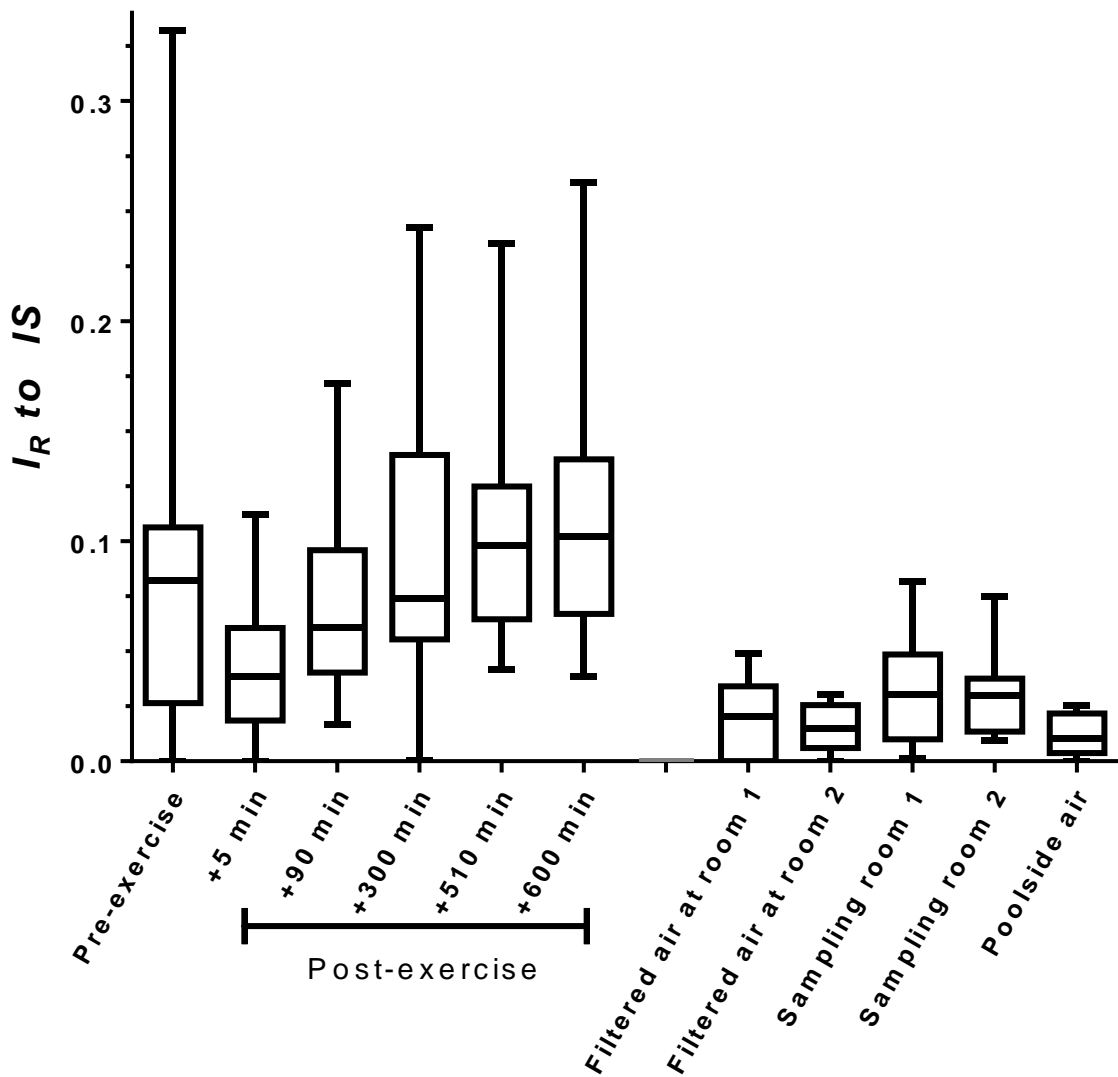


Figure 52 Box and whisker plots to show exhaled values of BRI-1461-43-107-93-41-69 and comparisons with environmental samples. Boxes refer to median and interquartile range and error bars to 10th and 90th percentiles.

Note: I_R = relative intensity; IS = internal standard

CHAPTER FIVE: EXHALED BREATH PROFILES AND INTENSE EXERCISE

5.1 Introduction

An important element in non-targeted metabolomic profiling is the selection of “healthy” controls. Indeed “healthy” is vague and difficult to define in absolute terms. Whilst a control group of participants may be recruited who are free from known health problems, and specifically free from symptoms and signs relating to a specific disease or condition under study, it is very difficult to recruit a control group who remain representative of the study population. “Healthy” controls are a far from homogenous set. A cohort of individuals with a phenotype defined strongly by a condition or disease that has reduced their exercise capacity will have had to adapt their lifestyles to using lower levels of physical activity. Individuals of potential control cohorts described as ‘fit’, and/or healthy, and/or asymptomatic are, in reality, entirely heterogeneous in their levels of physical fitness. Fit and healthy is a misleading descriptor full of discrepancy. Fit, in terms of health and disease, offers a description that an individual is free from signs and symptoms of disease. For the context of sport and exercise, ‘fit’ has a completely different connotation. An individual free from the signs and symptoms of disease, can be unfit as defined by their exercise capacity. Similarly, somebody who is defined as having a disease can possess very high exercise capacity, a notable example would be an asthmatic athlete.

It is not currently understood whether a person’s level of physical capacity, i.e. physical fitness, is manifest in their exhaled VOC profile and this was the focus of this investigation. Chapter 1 describes how exhaled breath measurement is intrinsic to characterising exercise and physical capacity. Physical exertion increases respiration from cell to tissue to organ to organism and alters the exhaled breath profile significantly [1]. Whether it be aerobic (with oxygen present) or anaerobic (in absence of oxygen), alterations in exhaled oxygen and carbon dioxide can be measured. However, there are no data that describe what, if any, changes to

exhaled VOC profiles occur as a result of changes to an individual's level of physical capacity. Further, there are few reported studies describing exercise factors in exhaled breath biomarkers. Most of such reports are concerned with exhaled breath condensate (Section 1.3.2) with reported increases in pulmonary pro-oxidative markers [2-4]. Volatile compound analyses have received less interest. King *et al.* [1] described changes in exhaled acetone and isoprene concentrations in the breath of participants exercising on a cycle ergometer. In general they showed that both compounds concentrations in breath increase with the onset of exercise. Acetone concentrations increased from approximately 700 to 1000 ng mL⁻¹ in-line with the exercise intensity to a stable level during each exercise episode. Regardless of the participants' recovery time(s) exhaled breath concentrations of acetone were correlated to carbon dioxide output. In contrast isoprene concentrations in exhaled breath increased rapidly and transiently from approximately 100 to 400 ng mL⁻¹ before reducing back to baseline levels over the course of the exercise/recovery period. A conclusion that isoprene accumulates, perhaps in the working muscles, and is then rapidly eliminated with increased blood flow and respiration was given. Repeated bouts of exercise resulted in smaller increases in isoprene concentrations on beginning exercise, relative to the first bout, with the maximum concentration levels reducing as the recovery time between exercise episodes was decreased. This was also noted by Senthilimolan *et al.* [5]. However, a slight rise in exhaled isoprene in the final stages of the 30 min exercise protocol was observed in all participants. The implication being that exhaled VOC profiles may have time-dependant components within them attributed perhaps to changes in biochemistries and metabolism in response to exercise. Methane was seen to reduce in alveolar levels during a light exercise challenge and returned to baseline levels after cessation [6]. These VOC compounds show an interaction with the change in movement during exercise, and are related to changes in physical chemistry (ventilation) and downstream metabolites of energy metabolism affected during physical exertion.

Solga *et al.* [7] differentiated between conditioned (i.e. trained) and non-conditioned rowers from changes in in exhaled ammonia concentrations after a 4000 m indoor row. Conditioned rowers exhaled ammonia increased 5-fold at around 120 min post-exercise and continued to rise at cessation of sampling. In

contrast, the non-conditioned rowers showed an increase of around 2.5-fold which plateaued during the recovery phase. A physically demanding test such as this cannot be considered as practical for monitoring fitness levels in the general population. Currently, the most widely recognised indication of physical fitness requires the participant to undergo a physical challenge at their maximal or near-maximal levels of endurance (e.g. maximal oxygen uptake test, Cooper 12 min run). Such protocols cannot be tolerated by people with incapacitating conditions such as cardiovascular disease or respiratory complications such as chronic obstructive pulmonary disease. An inability to exercise at the intensity required by the test protocol to generate maximal data requires any sub-maximal values to be extrapolated. Although maximal capacity can be predicted in a healthy population [8], inter-person variability exists and these values may not reflect the dynamics seen in critically ill patients. Athletes recovering from injury may also not be able to complete such tests. At the extreme end of the “fitness” spectrum, a fully capable high performance athlete may not have the time in their training schedule to complete, and importantly to recover from, such tests. Consequently, they have to continue their intense training without the benefit that such data would give them.

The ability to differentiate fitness levels of individuals from exhaled VOC profiles may be seen to be a potentially valuable source of information, and benefit the well and unwell alike. It would be an exciting prospect if a quick and non-invasive breath test was able to determine the current status of an individual’s physical fitness. Such a test could be used in rehabilitation clinics, and athletes would be able to track their in-season fitness levels and manage injury recovery strategies in a quantitative metabolomics-based manner.

This study, a starting point in this research, sought to test two hypotheses:

- i) the physical fitness of an individual is a factor in their exhaled breath VOC profile;
- ii) control groups of apparently ‘fit and healthy’ participants cannot be classified as homogenous phenotypes.

5.2 Methods

5.2.1 Ethical clearance

The study was approved in its entirety by the Loughborough University Ethical (Human Participants) Sub-Committee under the reference R12-P129. All participants took part voluntarily and were informed of the experimental procedures by issue of a participant information sheet prior to consenting. All participants gave written and informed consent and were free to exclude themselves and their data from the experiment at any time without reason. Once consented, participant information and samples were anonymised and assigned a unique identifier code.

5.2.2 Participant information

Thirty three healthy males (mean \pm standard deviation: age 23 ± 3 yrs, height 180 ± 6 cm, body mass 82.2 ± 10.3 kg, body mass index (BMI) 25.3 ± 2.4 kg m⁻²) were recruited and completed the research protocol. An additional participant was recruited, and although baseline measurements were taken, a malfunction in the laboratory nitrogen supply meant that the protocol could not be completed. All the participants reported active engagement in sporting behaviours, at either an individual or a team level. Although participants were deemed as 'generally fit' the cohort possessed a range of physical abilities. All participants were free from injury and were able to complete the prescribed exercise tests.

5.2.3 Experimental design

Participants were asked to arrive at the exercise laboratory at approximately 0830 hrs, after an overnight fast with only water permitted after waking. On arrival, each participant was asked to sit quietly for 5 min before the test protocol started. The test protocol consisted of (Figure 53):

- providing a reference resting sample of exhaled breath, see Chapter 3;
- being fitted with a heart rate (HR) monitor;

- undertaking a maximal oxygen uptake test, ($\dot{V}O_{2max}$ test);
- once the $\dot{V}O_{2max}$ test was complete, continuing to cycle against a low level resistance until breathing rate and HR returned closer to resting values ('warm down', approximately 5 min);
- after warm down, sitting quietly and resting for 5 min;
- after completion of the rest, providing a post-exercise exhaled breath sample;
- 60 min after exercise cessation, providing a final exhaled breath sample.

After this the participant was free to consume food and drink and leave the laboratory.

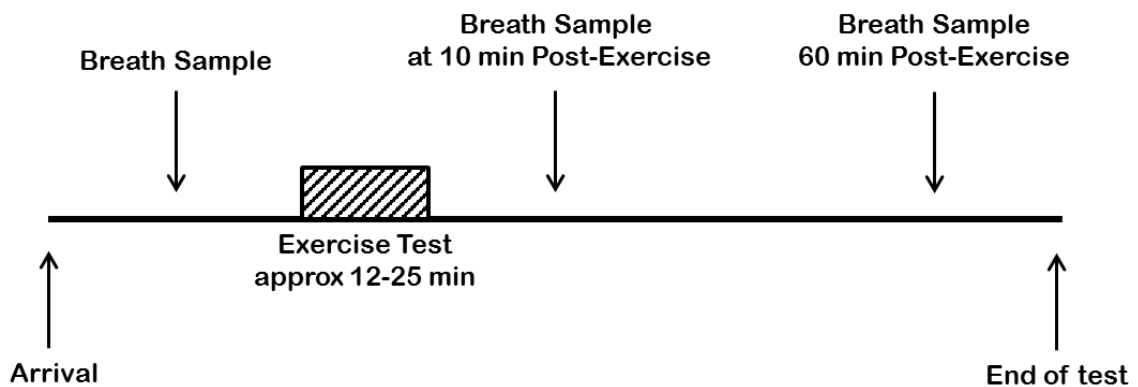


Figure 53 A schematic diagram to show the experimental protocol for each participant from arrival at the laboratory until cessation of the final exhaled breath sample.

5.2.4 Exhaled VOC collection

Exhaled breath VOCs and environmental VOCs were sampled as described previously (Chapter 3).

5.2.5 Maximal oxygen uptake ($\dot{V}O_{2max}$) test protocol

Maximal oxygen uptake was determined for all participants under identical test conditions by performing a $\dot{V}O_{2max}$ test with a cycle ergometer (Lode Excalibur Sport, Lode B.V., Groningen, Netherlands). An incremental, steady state exercise protocol

was used. Exercise intensity began with a work output of 95 W, increasing in 35 W steps every 3 min. No prior warm up was performed as the low intensity exercise in the principal 3 stages was deemed light enough to suitably prepare the lower limb muscles for the more intense stages. The cycle ergometer was electromagnetically braked so that resistance adjusted according to cadence in order to maintain a constant power output. Participants were allowed to determine cadence, and to alter this throughout the test at their own discretion. Alternative techniques where a constant cadence is maintained were not followed due to the potential of premature volitional fatigue in the lower limb skeletal muscles. Total exhaled gases were collected in an evacuated Douglas bag in the final minute of each 3 min stage. HR and rating of perceived exertion (RPE [9]) were recorded during collection. Participants were actively encouraged to continue the test for as long as possible, indicating to the investigators when they believed it was the final minute of exercise before exhaustion. Exhaled gases, HR and RPE were obtained regardless of exercise stage progression. Oxygen (O₂) and carbon dioxide (CO₂) content were measured using a gas analyser (1440 Gas Analyser, Servomex (Spectris plc), Surrey, UK) by sampling a flow of 2 L min⁻¹ of the collected exhaled gas for 2 min with O₂/CO₂ % values recorded after approximately 1 min 45 s stabilisation.

The total minute exhaled volume was measured by evacuating Douglas bags (after gas analysis was complete) using a vacuum pump and dry gas analyser (Harvard Apparatus UK, Cambridge, UK). Evacuated volume was added to the volume removed for gas analysis and total volume recorded. Oxygen uptake ($\dot{V}O_2$) was calculated using details in Chapter 1.

5.2.6 VOC sample analysis

All VOC samples were collected onto thermal desorption tubes and analysed by thermal desorption-gas chromatography-mass spectrometry (TD-GC-MS, section 3.2.2).

5.2.7 Statistical analyses

The data processing workflow described in Section 3.3.3 was followed. Deconvoluted and scaled data from participant samples were grouped according to upper and lower tertiles of fitness levels as determined by the relative, and absolute $\dot{V}O_2$ max scores (i.e. upper and lower 33% of participants split into high and low groupings). Sample pairings were initially analysed by principal components analysis (PCA) to check for unsupervised separation and subsequently investigated using the supervised method of orthogonal partial least squares-discriminant analysis (OPLS-DA). S-plots were analysed for contributor variables (Chapter 3). Discriminant components were assessed as potential biomarkers of fitness, or exercise.

Further data analyses were performed using IBM SPSS Statistics (v 22.0, IBM Corp., Endicott, NY, USA). Differences observed for high and low groupings of relative and absolute $\dot{V}O_{2max}$ were assessed using the Mann-Whitney U Test for independent samples. Isolated biomarkers were individually analysed for differences between groupings also using the Mann Whitney U Test. Predictors of relative and absolute $\dot{V}O_{2max}$ were analysed using a general linear regression model with stepwise entry. Distribution of exhaled VOC values observed across time were assessed using the Kruskal-Wallis H test for related samples. An alpha value (p) of < 0.05 was deemed as statistically significant and, where appropriate, is reported as its Bonferroni adjusted value.

Heat maps and cluster analysis were performed using GENE-E (Broad Institute, Cambridge, MA, USA) on data scaled to a \log_2 base.

5.3 Results

5.3.1 Exercise testing

All participants completed the exercise test to their self-reported maximum. Common protocol for the successful attainment of $\dot{V}O_{2max}$ include a measurement of HR within 10 beats min^{-1} of predicted maximum ($HR_{(max)} = 220 - \text{age in years}$) and a respiratory exchange ratio (RER) of ≥ 1.1 [10]. Completion of these criteria was as follows:

- 15 / 33 participants satisfied both criteria.
- 4 / 33 participants achieved a *RER* of ≥ 1.1 but HR data were unavailable.
- 10 / 33 participants achieved a *RER* of ≥ 1.1 and HR within 10 % of $HR_{(max)}$.
- 2 / 33 participants did not achieve a *RER* of ≥ 1.1 but did achieve a HR within 10 beats min^{-1} of $HR_{(max)}$.
- 2 / 33 participants achieved one of; a) *RER* of ≥ 1.1 , b) HR within 10 beats min^{-1} of $HR_{(max)}$, or c) HR within 10 % of $HR_{(max)}$.
- No participant was able to maintain a cadence of ≥ 60 in their final minute.
- Across all participants, 77 % reported a final minute RPE of ≥ 19 , with 10% and 13 % reporting RPE = 18 and RPE = 17, respectively.
- Two participants were subsequently excluded from the data analysis when their pre-exercise exhaled breath samples were discovered to contain levels of solvent molecules high enough disrupt the chromatography. See Figure 54 for example chromatograms from an environmental blank (filtered air from sampler), an 'acceptable' breath sample and an ejected breath sample from a single participant.
- An average $\dot{V}O_{2max}$ score of 46.5 $\text{mL}(\text{O}_2) \text{ kg}^{-1} \text{ min}^{-1}$ was obtained with a range of 35.3 – 58.9 $\text{mL}(\text{O}_2) \text{ kg}^{-1} \text{ min}^{-1}$.

Group differences stratified by upper and lower tertiles ($n=10$) of relative and absolute $\dot{V}O_{2max}$ are displayed in Table 14. The high relative $\dot{V}O_{2max}$ group had decreased mass, height and BMI (≤ 0.023). The high absolute group had increased mass and BMI and performed less self-reported minutes of walking per week ($p \leq 0.005$). No differences were seen for laboratory exercise conditions.

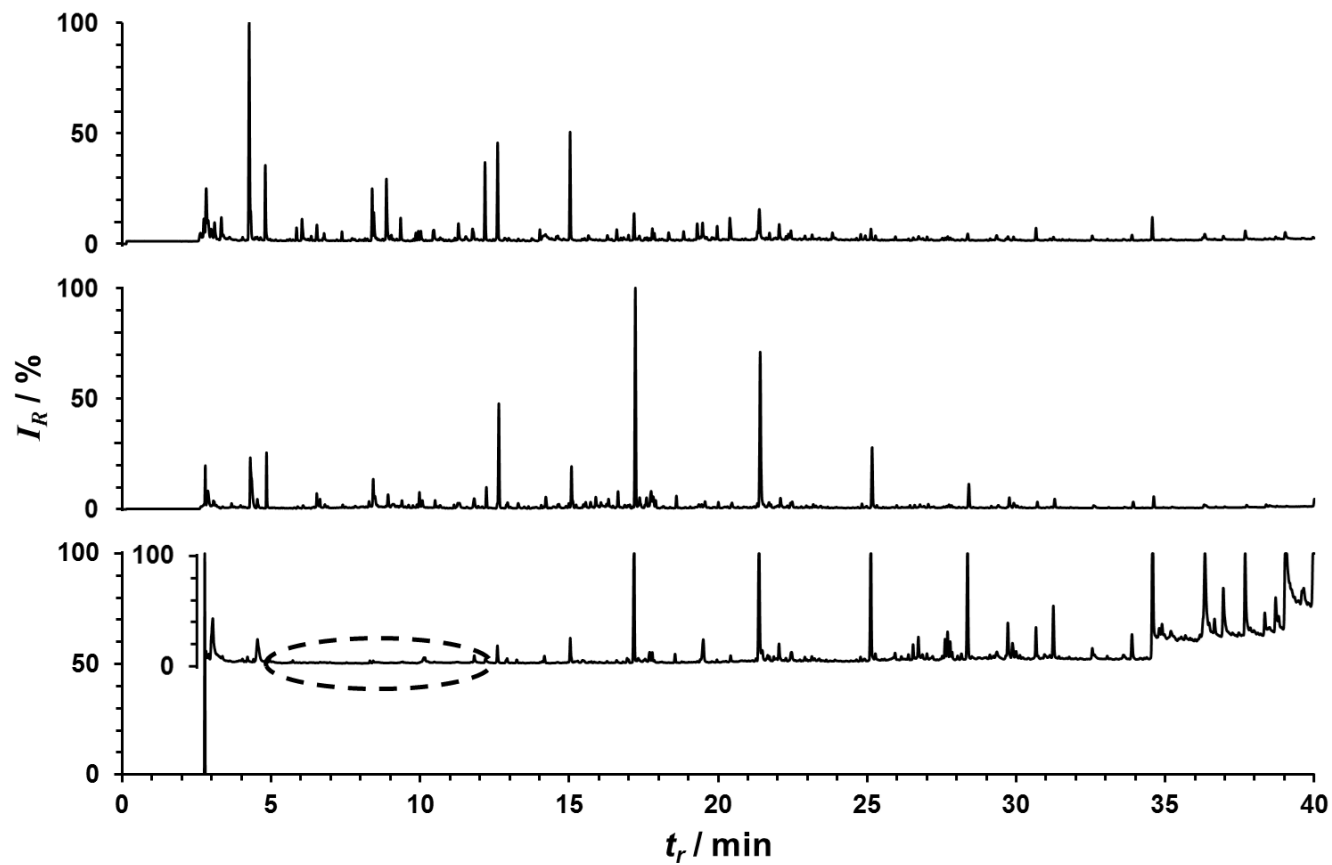


Figure 54

Example chromatograms to show i) an ejected breath sample due to excess solvent at 2.8 min (bottom) and a zoomed chromatogram for post-solvent peak responses (bottom inset) with a region of disrupted chromatography highlighted (dashed oval), ii) an acceptable exhaled breath sample from the same participant (middle), and iii) an environment blank sample taken from the filtered air supplied to the sampling mask (top).

Note: I_R = relative intensity; t_r = retention time

Table 14 Baseline and exercise characteristics of participants and environmental conditions grouped by highest and lowest 33 % values for relative and absolute maximal oxygen uptake ($\dot{V}O_{2max}$).

		Relative $\dot{V}O_{2max}$			Absolute $\dot{V}O_{2max}$		
		High	Low	p Value	High	Low	p Value
Weekly activity	Age / yrs	23 (3)	22 (3)	0.247	24 (4)	22 (2)	0.796
	Mass / kg	72.6 (6.2)	89.3 (9.1)	< 0.0005	90.2 (9.6)	75.7 (9.2)	0.005
	Height / cm	176 (7)	183 (5)	0.023	184 (6)	177 (7)	0.075
	BMI / kg m ⁻²	23.5 (1.4)	26.6 (2.4)	0.004	26.7 (2.0)	24 (1.5)	0.004
	Vigorous /min	325 (196)	230 (113)	0.353	374 (173)	228 (152)	0.052
	Moderate / min	89 (112)	144 (103)	0.143	174 (155)	168 (325)	0.218
	Walking /min	225 (99)	292 (179)	0.280	133 (84)	331 (145)	0.002
	Relative $\dot{V}O_{2max}$ / mL(O ₂) kg ⁻¹ min ⁻¹	51.9 (2.6)	40.9 (2.8)	< 0.0005	47.3 (5.9)	45.0 (5.6)	0.481
	Absolute $\dot{V}O_{2max}$ / L(O ₂) min ⁻¹	3.8 (0.4)	3.6 (0.4)	0.481	4.2 (0.2)	3.4 (0.1)	< 0.0005
	Final stage heart rate / beats min ⁻¹	191 (7)	186 (9)	0.277	185 (10)	192 (5)	0.063
	Room temperature / °C	21.1 (1.0)	21.4 (0.8)	0.247	21.1 (0.9)	21.2 (1.1)	0.796
	Room pressure / mmHg	764 (7)	760 (6)	0.218	762 (14)	764 (6)	0.353
	$F_I O_2$ (%)	21.0 (0.1)	20.9 (0.1)	0.165	21.0 (0.1)	21.0 (0.1)	0.631
	$F_I CO_2$ (%)	0.05 (0.01)	0.04 (0.01)	0.739	0.04 (0.01)	0.04 (0.01)	0.971

Note: BMI = body mass index; CO₂ = carbon dioxide; O₂ = oxygen; Fi = Fractional inhaled. All data expressed as mean (standard deviation); n=10 for both groups.

5.3.2 Metabolomic profiling analyses

After data processing, exhaled and environmental VOC features were identified and allocated a study reference as defined in Chapter 3; i.e. identified by retention index (RI) and mass spectrum. These information were used to produce a search function that prospected all samples. A total of 373 peaks were isolated, integrated and normalised to the internal standard, and imported into a multivariate analysis workflow as described in Chapter 3.

High vs low relative $\dot{V}O_{2\max}$ groups

Separation in PCA was not observed (Figure 55). OPLS-DA analysis was performed on the high vs low relative $\dot{V}O_{2\max}$ groups and showed near separation of groupings (Figure 56). However, further investigation into the corresponding S-plot yielded no suitable candidate VOCs (data not shown).

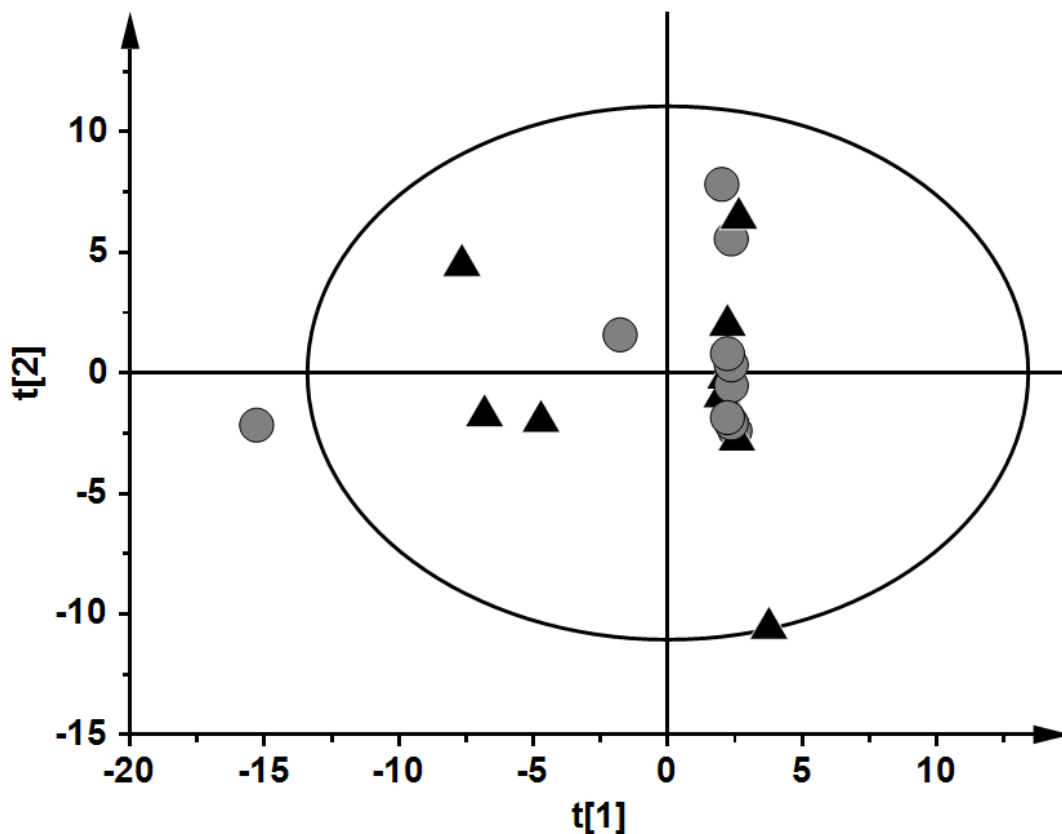


Figure 55 Principal components analysis 2-dimensional score plot constructed for breath samples for those falling into low (black triangles) and high (grey circles) relative maximal oxygen uptake groups.

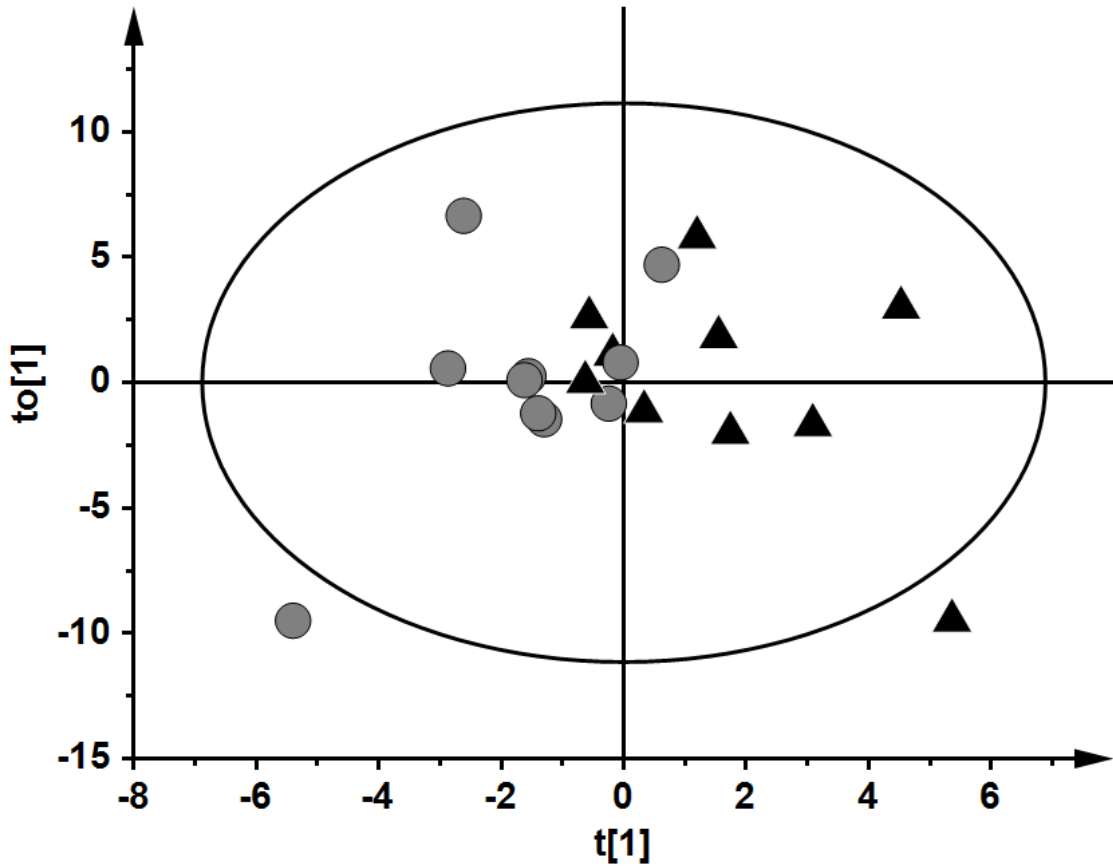


Figure 56 Orthogonal partial least squares-discriminative analysis 2-dimensional score plot constructed for breath samples for those falling into low (black triangles) and high (grey circles) relative maximal oxygen uptake groups.

High vs low absolute $\dot{V}O_{2max}$ groups

Separation in PCA was not observed (Figure 57). OPLS-DA analysis was performed on the high vs low absolute $\dot{V}O_{2max}$ groups and complete separation was achieved in the score plot (Figure 58). The S-plot was analysed and three upregulated and two down regulated compounds were selected for further investigation, see Figure 59 and Table 15.

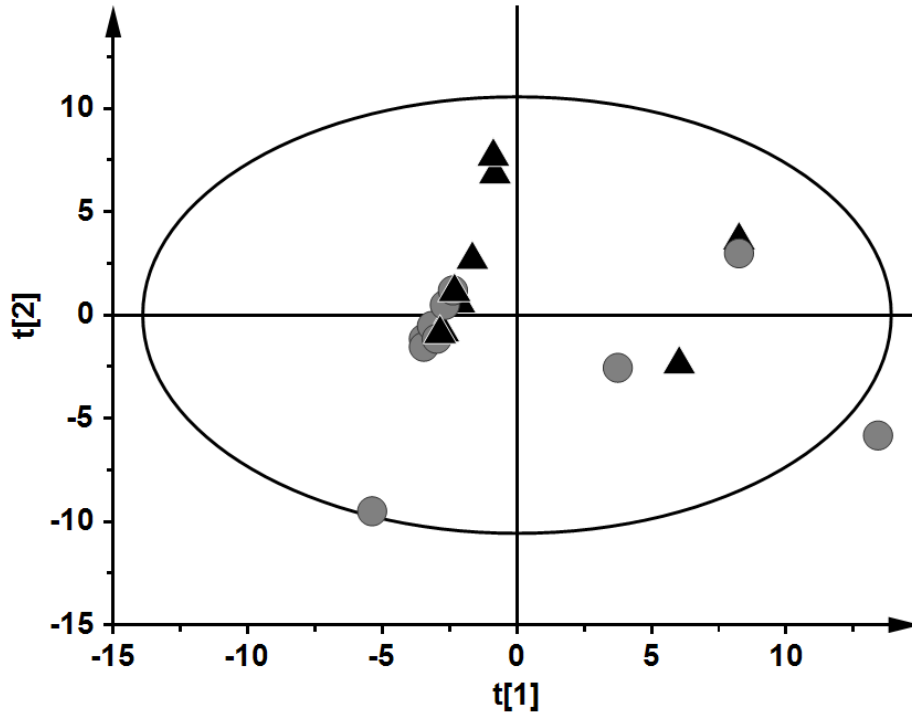


Figure 57 Principal components analysis 2-dimensional score plot constructed for breath samples for those falling into low (black triangles) and high (grey circles) absolute maximal oxygen uptake groups.

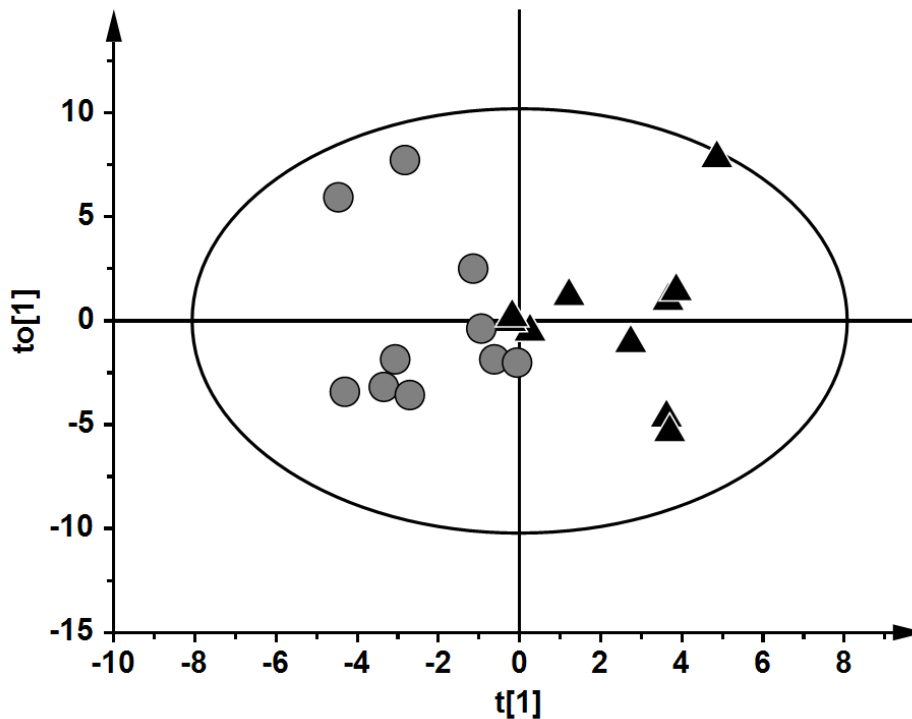


Figure 58 Orthogonal partial least squares-discriminative analysis 2-dimensional score plot constructed for breath samples for those falling into low (black triangles) and high (grey circles) absolute maximal oxygen uptake groups.

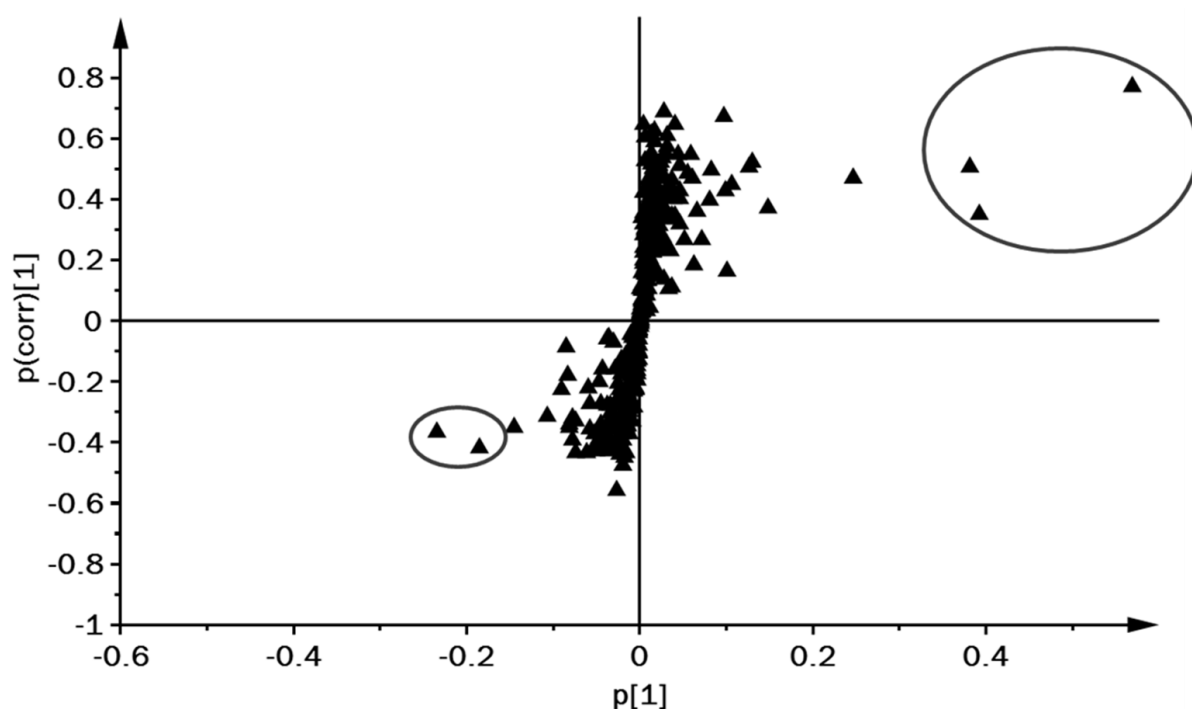


Figure 59 S-plot for modelled variables using an orthogonal partial least squares-discriminant analysis model for pre-exercise breath samples of low vs high absolute maximal oxygen uptake grouping. Candidate biomarkers are highlighted in grey ovals, no further compounds were considered as candidates.

Table 15 List of candidate biomarkers as identified by discriminant analysis on comparison of high vs low absolute maximal oxygen uptake groupings.

Ex. #	\overline{RI}	Q	Ql ₁	Ql ₂	Ql ₃	Ql ₄	Study ID
26	1141	355	269	267	73	356	BRI-1141-355-269-267-73-356
82	1295	429	325	73	341	430	BRI-1295-429-325-73-341-430
89	659	43	59	0	0	0	BRI-659-43-59-0-0-0
110	658	67	53	93	68	91	BRI-658-67-53-93-68-91
201	655	59	43	0	0	0	BRI-655-59-43-0-0-0

Note: Ex. # = experimental peak number; (\overline{RI}) = mean retention index; Q = quantifier ion m/z ; Ql1 to 4 = qualifier ions 1 to 4 m/z ; ID = identification; OPLS-DA = orthogonal partial least squares-discriminant analysis.

Candidate biomarker analysis

The five compounds in Table 15 were evaluated against the $\dot{V}O_{2max}$ scores for the two stratified groups. Outliers were excluded and BRI-659-43-59-0-0-0 and BRI-

655-59-43-0-0-0 were examined closely and ascertained as the same compound that had had altered ion statistics across the study. This information was used to combine these features. Figure 60 compares exhaled values of the two upregulated candidate biomarkers across groups. RI and NIST searches indicated that they were propan-2-one (acetone, BRI-659-43-59-0-0-0) and 2-methyl-1,3-butadiene (isoprene, BRI-658-67-53-93-68-91), two exhaled breath metabolites that have been studied in relation to exercise previously [1]. Further whole cohort analysis of correlation with these ions with absolute $\dot{V}O_{2max}$ scores showed no correlation ($p \geq 0.081$). However, a strong positive relationship was observed between candidates (Spearman's rho (r_s) = 0.693, $p < 0.0005$, Figure 61).

5.3.3 Predictors of fitness

In order to assess whether any, or a combination of any exhaled VOCs were predictive of the measured values for absolute $\dot{V}O_{2max}$, a general linear regression model with a stepwise variable entry method was performed. Three VOCs were identified in the analysis and reported an adjusted $r^2 = 0.459$ and a p value of < 0.0005 . This reported that 45.9 % of the variance seen in absolute $\dot{V}O_{2max}$ could be explained by the 3 VOCs.

When analysed for Spearman's correlations, two VOCs showed significant negative correlations with absolute $\dot{V}O_{2max}$, BRI-818-43-85-41-57-70 and BRI-1460-41-56-55-0-0 ($r_s = -0.492$ and -0.397 , $p = 0.007$ and 0.033 , respectively). BRI-732-41-69-99-100-0 did not show any correlation ($r_s = 0.109$, $p = 0.592$). Further investigation in to the data highlighted one extreme point for BRI-818-43-85-41-57-70, and when removed the VOC retained correlation ($r_s = -0.442$, $p = 0.019$). However, BRI-1460-41-56-55-0-0 lost correlation once all zero results ($n = 5$) were removed from the analysis ($r_s = -0.124$, $p = 0.565$), suggesting a skew of data from these results. Visualisation of the scatter plot for the correlation of BRI-818-43-85-41-57-70 with absolute $\dot{V}O_{2max}$ shows a negative trend with $\dot{V}O_{2max}$ but with large variation (Figure 62). Therefore, it is not possible to yet identify a model that successfully links maximal oxygen uptake with exhaled VOCs in this cohort.

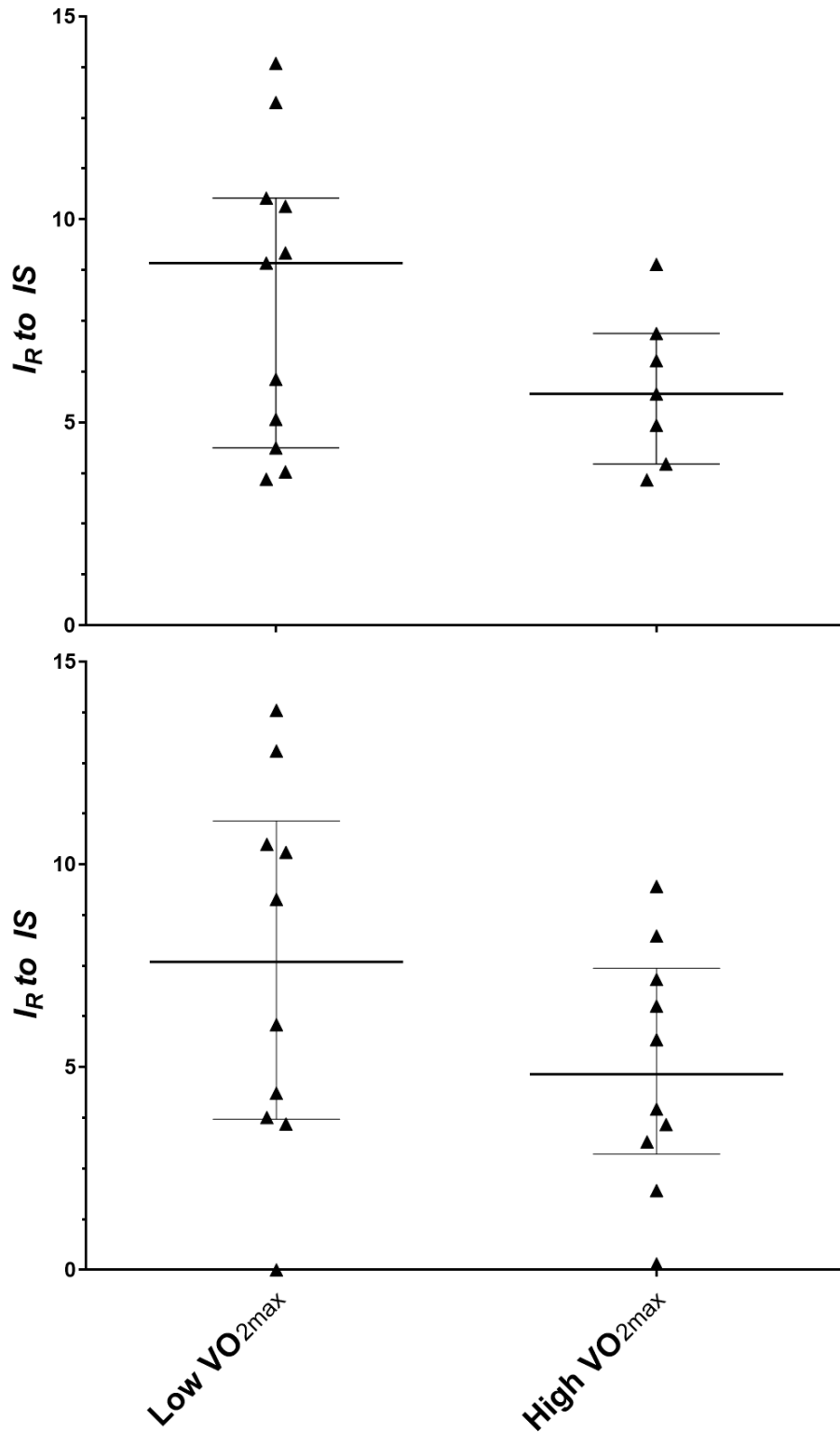


Figure 60 Plot to show the distribution of acetone (top) and isoprene (bottom) in low and high absolute $\dot{V}O_{2\max}$ groups in a pre-exercise exhaled breath sample. Horizontal line is shown at the median with errors bars indicating the interquartile range.

Note: some individuals' values are missing in acetone due to chromatographic peak splitting. I_R = relative intensity; IS = internal standard

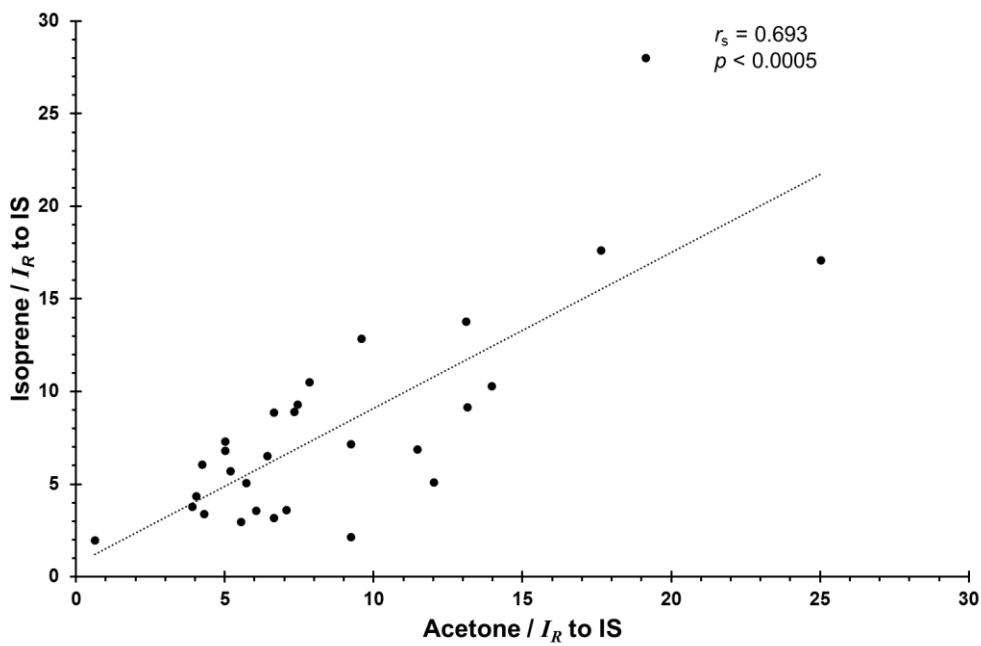


Figure 61 Scatter plot to show the relationship of acetone and isoprene values in pre-exercise exhaled samples showing a positive intra-person relationship between both compounds. Spearman's rho (r_s) and corresponding p value are reported.

Note: I_R = relative intensity; IS = internal standard

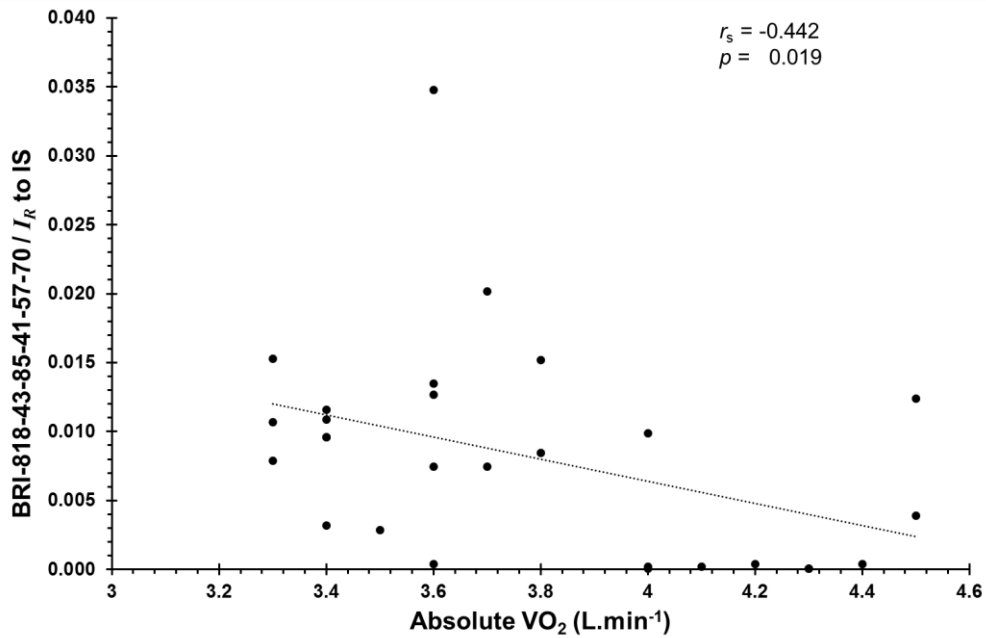


Figure 62 Scatter plot to show the relationship of absolute maximal oxygen uptake (VO₂) and BRI-818-43-85-41-57-70 values in pre-exercise exhaled samples.

Note: I_R = relative intensity; IS = internal standard

5.3.4 *Changes in exhaled VOCs after exercise*

To assess changes in VOCs caused by the maximal exercise protocol, multivariate analysis was performed across the three exercise stages. Data were visually analysed through a heat map for all measured variables across all time points prior to modelling. No signs of time point patterning were observed and cluster analysis indicated more impact was present for inter-person variability, opposed to variability across time points (data not shown due to visibility in print).

Initial analysis performed by OPLS-DA showed no separation in a 2-dimensional score plot. However, a leftward shift at 10 min followed by return toward pre-exercise sample points is present (Figure 63). When the S-plot was analysed it showed that only one VOC was providing a strong influence on the model (Figure 64). This VOC was BRI-658-67-53-93-68-91, 2-methyl-1,3-butadiene or isoprene, as identified in the previous analysis.

Further post-exercise VOC analyses were completed on the previously reported groupings of high and low relative $\dot{V} O_{2\max}$ scores. These analyses prospected for whether individuals with lower fitness levels showed alternative responses to the maximal exercise. Both at +10 and +60 min post-exercise no separation could be identified between these groups and therefore suggests that the differing fitness in the individuals did not account for a fluctuation in VOC profiling in response to the exercise-induced stress (data not shown).

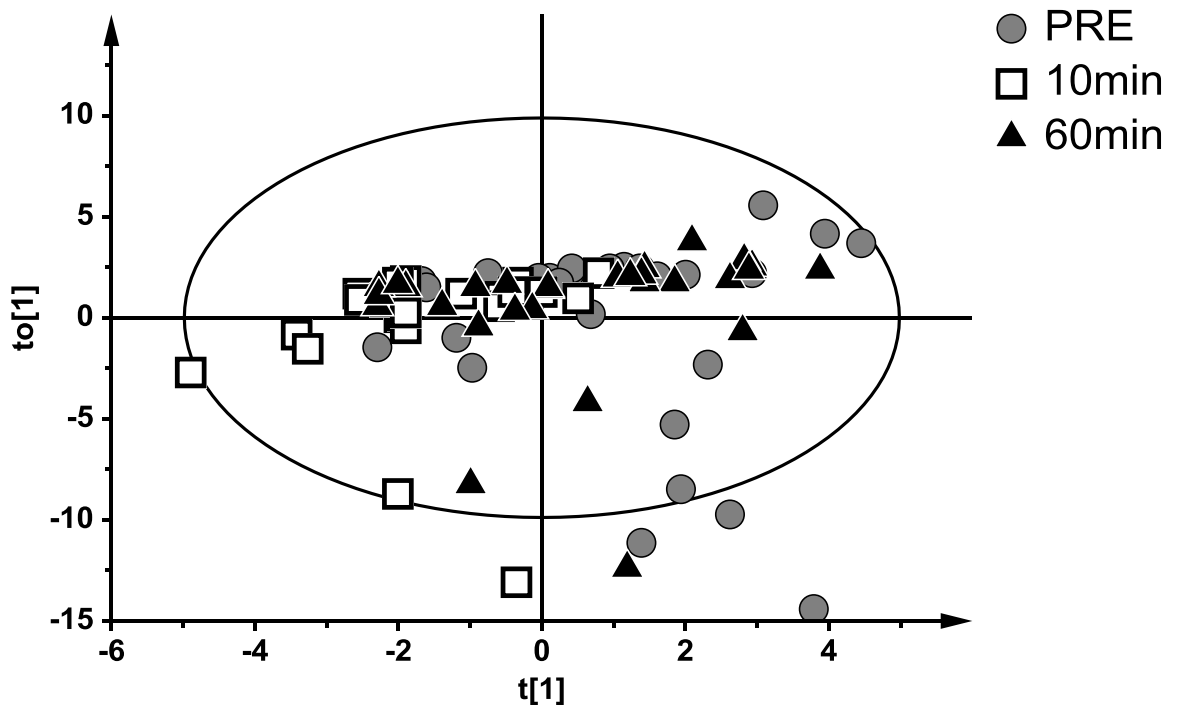


Figure 63 Orthogonal partial least squares-discriminant analysis 2-dimensional score plot showing all three breath sampling time points. Markers correspond to pre- (grey circles), +10 min post- (white boxes) and +60 min post- exercise (black triangles).

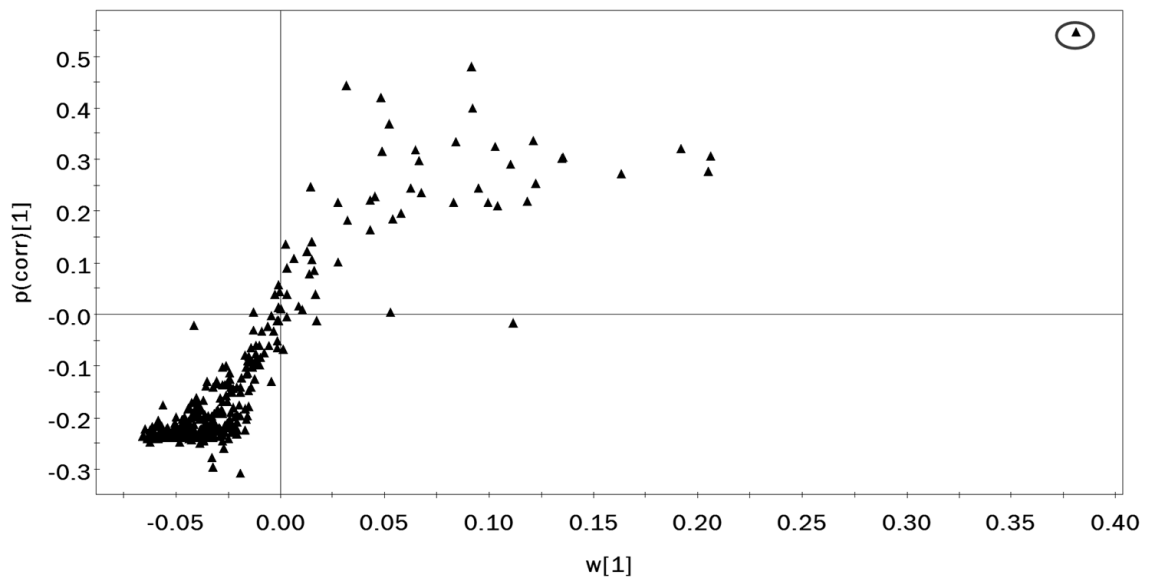


Figure 64 S-plot for modelled variables using an orthogonal partial least squares-discriminant analysis model for pre-exercise and post-exercise breath samples of low vs high absolute maximal oxygen uptake grouping. Candidate biomarker is highlighted in grey oval.

5.3.5 Isoprene across exercise stages

Isoprene was investigated and a non-automated integration was completed for all samples. Kruskal-Wallis H test indicated that there was not an equal distribution of ranks across the three time points and pairwise comparisons indicated an increase in exhaled isoprene between the 10 and 60 min post-exercise time points ($p=0.041$). A reduced trend was observed for isoprene at 10 min post-exercise when compared to baseline levels, but no statistical significance was reached. Similarly, no differences were observed between baseline values and 60 min post-exercise ($p\geq 0.269$, Figure 65).

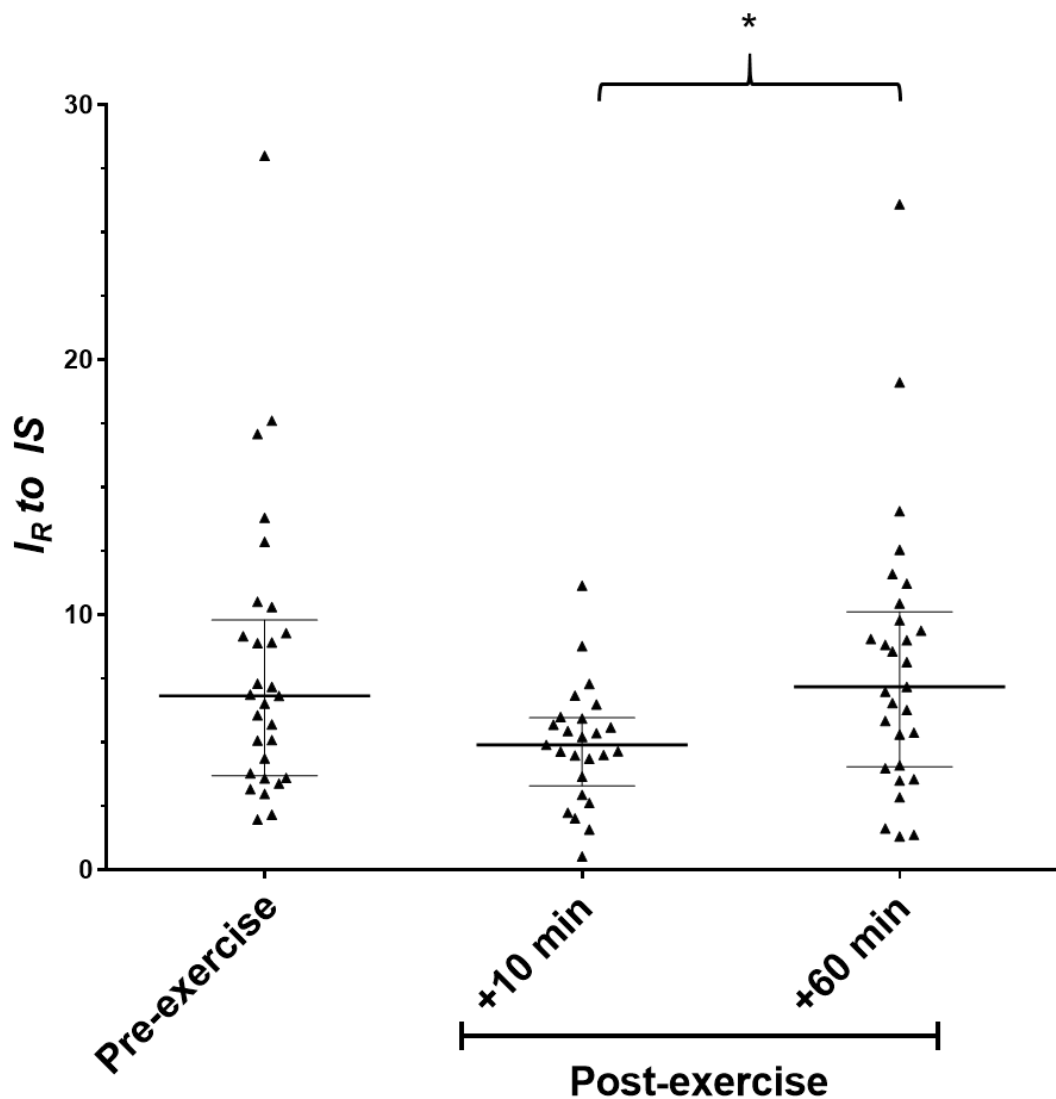


Figure 65 Box and whisker plots to display exhaled isoprene levels for all participants at pre- and post-exercise time-points. * denotes $p = 0.041$.

Note: I_R = relative intensity; I_S = internal standard

5.4 Discussion

Non-targeted metabolomics-wide analysis of exhaled breath in physically fit individuals prior to an exercise capacity test was able to provide some indication into the direction of the recorded fitness test value. Common breath metabolites acetone and isoprene showed an observed reduction for individuals with elevated absolute maximal oxygen uptake. However, a small sample size did not allow for significant differences to be observed once extraordinary values were removed from analysis, nor when manual integration of candidates was performed.

Partial separation was observed between groups when a relative $\dot{V}O_{2\max}$ score was utilised, but no suitable candidate VOCs could be isolated from the corresponding S-plot. The process of creating a test value relative to body mass may have led to the normalisation of levels for acetone and isoprene. Further correlation analyses were completed and showed no associations of acetone or isoprene with mass, height, BMI or age ($p > 0.05$, data not shown). However, near significance was recorded for isoprene and height ($r_s = -0.442$, $p = 0.051$).

Breaths analysed prior to and in stages for up to one hour post-exercise testing showed one compound fluctuating, again isoprene. A reducing trend post-exercise was observed and returned to baseline values by one hour. These data conform to the on-line analysis performed by King *et al.* [1] which showed a rise of exhaled isoprene at the onset of exercise and then a reduction across the exercise, perhaps due to the removal of an 'isoprene store' in the working muscles. Interestingly, subsequent tests showed blunted increases at exercise onset without adequate recovery, and therefore supported the idea that these 'pools' were not replenished. The data presented in this chapter support this theory as we see reduced levels after a bout of intense physical activity, which returns to baseline levels with sufficient rest time of one hour.

Breath analysis is a growing research field. Many laboratories wish to create diagnostic breath tests to capture information on developing illnesses long before they are detectable by current measures. It is important to consider the use of a control group when these experiments are conducted. Interestingly, 33 fit, young, healthy and male participants would be considered an ideal group to provide control samples for a disease versus no disease research design. However, these data

show that within this relatively homogenous group of individuals, suggestions of differences in exhaled profiles due to physical fitness are observed. This study only highlights one aspect of variation within a homogenous group, their physical fitness level, and it is not unlikely that exhaled breath profiles will differ for other aspects of natural variation. Examples of these may be height, mass, ethnicity and age, amongst many others. This raises an important question of when is a control group really a control group? Further works into the variation of normal individuals is needed to support future diagnostic research of exhaled breath VOCs.

Results reported here suggest that exhaled breath VOCs may have a potential role in fitness testing. A larger cohort size with a wider range of fitness abilities is required in further studies to develop the results from this pilot experiment. Trends seen in reduced acetone and isoprene levels, measured at rest prior to exercise, with increased oxygen uptake offer the potential to be explored further. If real associations are seen in a larger sample set, the use of on-line targeted exhaled VOC analysis for these compounds could be implemented to provide a rapid 'snapshot' of an athlete's current fitness ability, without the need for exhaustive exercise testing protocols. This would afford the athlete and coach to monitor fitness levels during competition periods, or when recovering from injury and physically unable to complete a high intensity protocol. This advantage can also be translated to a public health scenario, where individuals recovering from surgery or other debilitating illnesses/procedures are undertaking light fitness training but would not be able to push to high intensities to truly measure oxygen uptake capacity.

This experiment may be viewed as an exploratory attempt in implementing these technologies to provide answers for a non-exercising fitness test. It is important to understand that these data do not show significant associations but report trends that may be able to report differences with further exploration. Power calculations show that in order to achieve a statistical difference between the two groups, with an alpha value of 0.05 and a power of 80%, group sizes of 36 and 41 would be required for acetone and isoprene, respectively.

In conclusion, the small group of participants with a relatively narrow range of fitness values were able to report trends that showed acetone and isoprene to be

reduced in those who utilised increased volumes of inhaled oxygen, without normalisation to take into account body mass. The data does not show significant differences and further experiments with an increased sample size and wider range of maximal oxygen uptake values must be performed. Time point analyses of exhaled breath profiles reported that isoprene showed altering exhaled levels, with a trend for isoprene reduction seen post-exercise, and return to baseline within the one hour recovery period. These data reinforce the validity of the experimental conditions as they follow previously seen trends in the literature [1].

Improved and novel experiments in sport and exercise science and exhaled breath analysis ought to be completed to allow the progression of these non-invasive technologies into a sporting context.

5.5 References

- 1 King J, Kupferthaler A, Unterkofler K, Koc H, Teschl S, Teschl G, Miekisch W, Schubert J, Hinterhuber H, Amann A. Isoprene and acetone concentration profiles during exercise on an ergometer. *J. Breath Res.* 2009;3:027006
- 2 Marek E, Platen P, Volke J, Mückenhoff K, Marek W. Hydrogen peroxide release and acid-base status in exhaled breath condensate at rest and after maximal exercise in young, healthy subjects. *Eur. J. Med. Res.* 2009;14 Suppl 4:134-9
- 3 Araneda OF, Guevara AJ, Contreras C, Lagos N, Berral FJ. Exhaled breath condensate analysis after long distance races. *Int. J. Sports Med.* 2012;33:955-61
- 4 Araneda OF, Urbina-Stagno R, Tuesta M, Haichelis D, Alvear M, Salazar MP, García C. Increase of pro-oxidants with no evidence of lipid peroxidation in exhaled breath condensate after a 10-km race in non-athletes. *J. Physiol. Biochem.* 2014;70:107-15

5 Senthilmohan ST, Milligan DB, McEwan MJ, Freeman CG, Wilson PF. Senthilmohan ST1, Milligan DB, McEwan MJ, Freeman CG, Wilson PF. Redox Rep. 2000;5:151-3

6 Szabó A, Ruzsanyi V, Unterkofler K, Mohácsi A, Tuboly E, Boros M, Szabó G, Hinterhuber H, Amann A. Exhaled methane concentration profiles during exercise on an ergometer. J. Breath Res. 2015;9:016009

7 Solga SF, Mudalel M, Spacek LA, Lewicki R, Tittel FK, Loccioni C, Russo A, Ragnoni A, Risby TH. Changes in the concentration of breath ammonia in response to exercise: a preliminary investigation. J. Breath Res. 2014;8:037103

8 Fitchett MA. Predictability of VO₂ max from submaximal cycle ergometer and bench stepping tests. Br. J. Sports Med. 1985;19:85-88

9 Borg G. Perceived exertion as an indicator of somatic stress. Scand. J. Rehabil. Med. 1970;2:92-8

10 Howley ET, Bassett DR Jr, Welch HG. Criteria for maximal oxygen uptake: review and commentary. Med. Sci. Sports Exerc. 1995;27:1292-301

CHAPTER SIX: DEVELOPMENT OF AN ATMOSPHERIC PRESSURE IONISATION INTERFACE FOR ON-LINE, QUADRUPOLE MASS SPECTROMETRIC EXHALED BREATH ANALYSIS

6.1 Introduction

Mass spectrometry (MS) has the potential to obtain high resolution data and enables identification of a compound by its mass to charge ratio (m/z). Gas chromatography-mass spectrometry (GC-MS) is the gold standard technique for exhaled breath analysis [1]. However, such precision is time consuming and requires large equipment with extensive infrastructure. It is not a practicable proposition to place such instruments in the field for on-line analysis. GC-MS can offer high chromatographic resolution and is readily coupled to pre-concentration techniques such as thermal desorption (TD) [2] or needle trap devices [3], enabling trace level VOCs in breath to be concentrated up to detectable levels prior to analysis. Trapping on adsorbent tubes or storing samples in Tedlar bags enables samples to be taken at a remote location and then returned to the laboratory for analysis, and the use of GC compound libraries aids in the identification of VOCs in breath samples. However, due to the inherent complexity of breath samples the chromatographic separation often requires long run times (upwards of 30 min) making the technique ill-suited to high-throughput screening of large numbers of individuals. In addition, subtle chemical changes may occur during transport and/or storage time [4] and some information may be lost. Perhaps most importantly, the equipment required for this tends to be large, bulky, laboratory-based instruments that are operated by specialist users. When considering both medical and sporting situations, any potential use of exhaled breath VOC analysis would likely require virtually instantaneous results to present the clinician/coach with information that can answer the question in mind, and therefore impact on decisions that are subsequently made (e.g. treatment modalities or alteration of training intensities).

Furthermore, the notion of sampling and analysing at different sites creates the potential factor of maintenance of sample integrity through travel and storage.

Limitations of off-line GC-MS led to the development of real-time time analysis techniques such as proton transfer reaction mass-spectrometry (PTR-MS) [5,6] and selected ion flow tube mass spectrometry (SIFT-MS) [6] for breath analysis. These approaches are capable of monitoring highly volatile species in breath in real-time, providing instantaneous diagnostic data. Both techniques enable direct analysis of breath and, with sub- $\mu\text{g L}^{-1}$ levels of sensitivity, do not require any pre-concentration which greatly decreases the lead time to results. Both of these technologies make use of a chemical ionisation mechanism, have been successfully miniaturised (e.g. PTR-QMS 300, Ionicon, Innsbruck, Austria; and Voice 200 (SIFT-MS), Syft Technologies, Christchurch, New Zealand) and have great potential for monitoring highly volatile species. However, there is a requirement that samples are introduced in gaseous form and these technologies are therefore not well-suited to analysing some of the larger, semi-volatile, species present in breath. Furthermore, their ion chemistry limits the types of compounds that can be analysed and, although sensitive, GC-MS is capable of analysing lower exhaled concentrations. A combination of high sensitivity MS measurement in a miniaturised format is required.

The interfacing of breath sampling to MS using ambient ionisation techniques such as extractive electrospray ionisation (EESI-MS) [7-11], atmospheric pressure chemical ionisation (APCI-MS) [12] and glow discharge [13] has also been accomplished. These approaches can be used to interface volatile analysis to any mass spectrometer with an atmospheric pressure ionisation source. EESI-MS has been used off-line to analyse pre-concentrated breath samples collected on TD tubes enabling identification of breath metabolites [8], and has the potential to include a fast GC separation to give additional selectivity and remove background interferences [9]. This approach coupled to a high-resolution mass spectrometer has been shown to give increased throughput over GC-MS at the cost of chromatographic resolution. On-line extractive electrospray has been demonstrated to be capable of determining non-volatile compounds such as urea [10] and nicotine [11] in breath with $\mu\text{g L}^{-1}$ levels of sensitivity. APCI-MS has proven effective

in determining volatile species, notably being used to detect aroma compounds released from food whilst eating [12,13]. This work led to the development of the MS-nose interface where a coaxial Venturi interface was used to produce a commercial volatile analysis source for Waters mass spectrometers. Outside of food analysis, on-line breath analysis using APCI-MS has been shown to be a sensitive method for determining narcotics in breath [14]. However, a limitation of most equipment used in these studies is that they are large, expensive and require climate controlled laboratories and expert users. Therefore, they are not suitable for either patient point-of-care or in community sports-medicine applications.

Recently smaller, transportable, mass spectrometers have been developed that exploit enhanced electronics to produce smaller footprint and lower cost systems while maintaining most of their functionality. Examples of such developments include the Advion Expression Compact Mass Spectrometer (CMS) and the Waters QDa detector and Microsaic 4000 MID, and have been demonstrated for a number of different applications including on-line flow chemistry [15] and phytochemical screening [16].

6.2 Experimental objectives

The objective of this experiment was to develop an interface for a commercially available, compact and transportable mass spectrometer to enable it to be used for exhaled breath VOC sampling. In this instance an Advion Expression CMS was to be interfaced to a Venturi jet pump placed into the source nitrogen supply to enable breath samples to be drawn rapidly into the ionisation source.

The approach was tested by simulating a disease/intervention marker (i.e. a pseudo-biomarker) by inducing a controlled change in an exhaled breath profile through the use of an ingested, commercially available, peppermint oil capsule. Experiments aimed to monitor subsequent appearance and elimination of the oils components and/or metabolites over time, and enabled the evaluation of the performance of this new breath analyser in a real breath matrix.

6.3 Methods

6.3.1 Ethical clearance

This study was approved by the Loughborough University Ethical Advisory Committee using an exhaled breath generic protocol with reference G09-P5. All participants took part voluntarily and were provided with a description of the experimental procedures before giving their written consent. All participants were free to exclude themselves and their data from the experiment at any time without reason. Once consented, participant information and data were anonymised and assigned a unique identifier code.

6.3.2 Capsule details and mass spectral behaviour

For all experiments a commercially available 200 mg peppermint oil capsule was ingested (Boots, Nottingham, UK). The exact makeup of the capsule was unknown. Menthol and menthone are major components of peppermint oil [17] comprising 40.7 % and 23.4 % of the mixture, respectively (Figure 66). Initial trial runs showed that the largest response after dosing was seen relating to the menthone metabolite of the capsule (data not shown). Analysis of a 1:100 dilution of a menthone standard in water by APCI-MS demonstrated that the m/z 81, 137 and 155 ion are the main peaks in the mass spectrum (Figure 67). For this experiment an emphasis was placed on the monitoring of the ions with m/z 137 and 155. The m/z 155 is understood to be protonated menthone, the structure for the m/z 137 species is unknown but corresponds to the loss of H₂O from the molecule and is likely to be in the form of a protonated terpinene (Figure 66). The ion with m/z 81 relates to a [C₆H₈+H]⁺ ion, known to be common ion from monoterpene fragmentation [18].

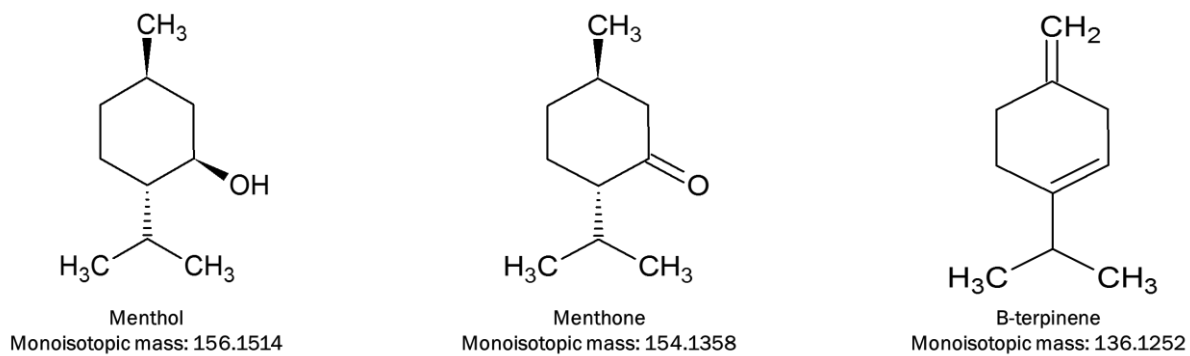


Figure 66 Chemical structures for menthol, menthone and a possible structure for the diagnostic m/z 137 ion.

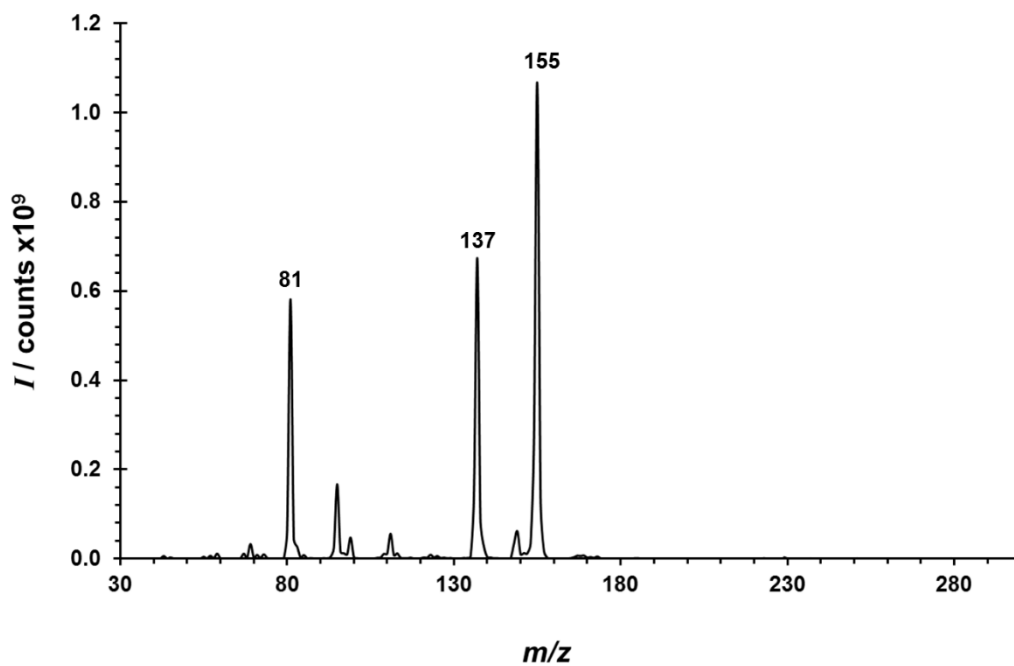


Figure 67 Atmospheric pressure chemical ionisation mass spectrum of the volatile headspace from a 1.0 % menthone solution in HPLC grade water.

Note: I = intensity; m/z = mass to charge ratio

6.3.3 Instrumentation

The same model of respiratory facemask used for collecting adaptive breath samples, Chapter 3, was interfaced into the APCI source of an Advion Expression (CMS) using a Venturi jet pump built in-house (Figure 68) that was heated to 100 °C with a thermostatically controlled rope heater (Omega, Manchester, UK). Air was supplied to the mask at 20 L min⁻¹ and the APCI gas was set at 4 L min⁻¹, generating a suction sample flow from the mask of 260 mL min⁻¹. Exhaled breath profiles were monitored with the pressure transducer system used to control sample acquisition for adsorbent bed sampling [19]. The CMS ion source parameters were optimised using a menthol vapour source, see Table 16, and the mass spectrometer instrument was operated in the positive ion mode for all these proof-of-concept experiments.

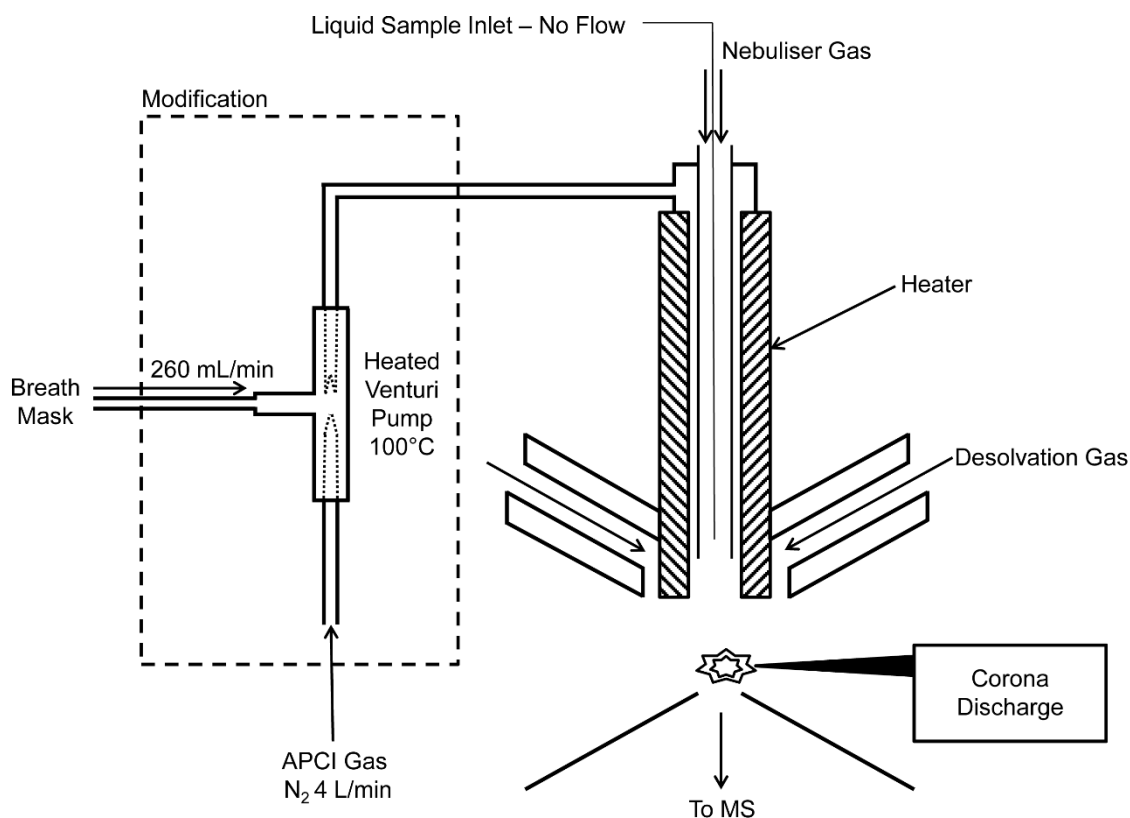


Figure 68 Schematic drawing to show the modification to the atmospheric pressure chemical ionisation (APCI) gas line to incorporate a heated Venturi pump and full face breathing mask to allow analysis of exhaled gases via APCI on a compact mass spectrometer (MS).

Table 16 A table showing the source and acquisition conditions for exhaled breath volatile analysis using atmospheric pressure chemical ionisation on a compact mass spectrometer.

Source Conditions	Level
Capillary temperature / °C	250
Capillary voltage / V	42
Source voltage / V	15
APCI gas temperature / °C	40
Corona discharge voltage / kV	5
Acquisition Conditions	
Ionisation mode	Positive
<i>m/z</i> range	30 - 300
Scan time / ms	300

6.3.4 Preliminary GC-MS characterisation

A pilot experiment was conducted in order to estimate the potential levels of menthone in exhaled breath using the method detailed in Chapter 3. Exhaled VOCs were collected from 2 L of breath prior to and at 73, 174, 415 and 600 min post-ingestion of the peppermint oil capsule. Samples were collected on a dual-bed TD tube and analysed using thermal desorption (Unity 2, Markes Int., UK)-gas chromatography (Agilent 7890, Wokingham, UK)-mass spectrometry (Agilent 5977A quadrupole mass spectrometer, Wokingham, UK) (TD-GC-MS). Sample chromatograms were processed for the presence and intensity of *m/z* 112 (base peak of menthone for electron ionisation) and an elimination curve was created. Levels of menthone and the period of wash out for these from the human biological system were assessed. Standard calibration analyses for menthone (Sigma-Aldrich, Gillingham, UK) were performed and quantitative values were obtained for each sample time point.

6.3.5 *Menthone elimination experiment with CMS*

Sixteen healthy volunteers consented and completed the experimental period (7 male and 9 female over an age range from 22 to 53 years).

Participants wore a non-vented full face mask fitted with silicone pillow (ResMed, Abingdon, UK) containing a one-way non-breathing valve and were supplied with filtered air from a laboratory compressed air source as detailed in 3.2.2. The mask contained two outlets, one connected to the previously described mask pressure monitoring device [19] and the other via silicone tubing to the Venturi pump interfaced to the CMS. All participants were issued their personal mask for their repeated measurements over a period of 6 to 10 hrs. Masks were not shared to ensure no transfer of infection material or VOC carryover contamination was presented.

Participants were encouraged to breathe in a relaxed manner with their mask on for 2 min to equilibrate with the filtered air supply. After 2 min, the data acquisition was started whilst the participants continued to breathe normally for a further 3 min. Mass spectra and breath mask pressure profiles were recorded for the full 3 min period.

To begin, continuous real-time monitoring was conducted with a single participant. The individual exhaled at a normal depth and rate into the mask for 20 min post-ingestion of a peppermint oil capsule and data was continuously acquired and the ion with m/z 137 was monitored as the most intensely released metabolite.

The main experiment was conducted where each participant gave a baseline exhaled VOC sample (0 min) before ingesting the capsule. Subsequent breath samples were acquired at 60, 120, 240 and 360 min post-ingestion for each participant. Monitoring of the intensity of menthone in the exhaled breath provided an assessment of the capability of the instrumental setup to detect changes in exhaled VOCs. Additionally, four participants repeated the experiment with sampling time points of 0 (pre-ingestion), 180, 240, 360, 480 and 600 min in order to further extend the experiment to lower concentrations (see Figure 69 for schematic). One female and three male participants from the original study with ages ranging between 26 and 36 years were recruited to complete the extended protocol.

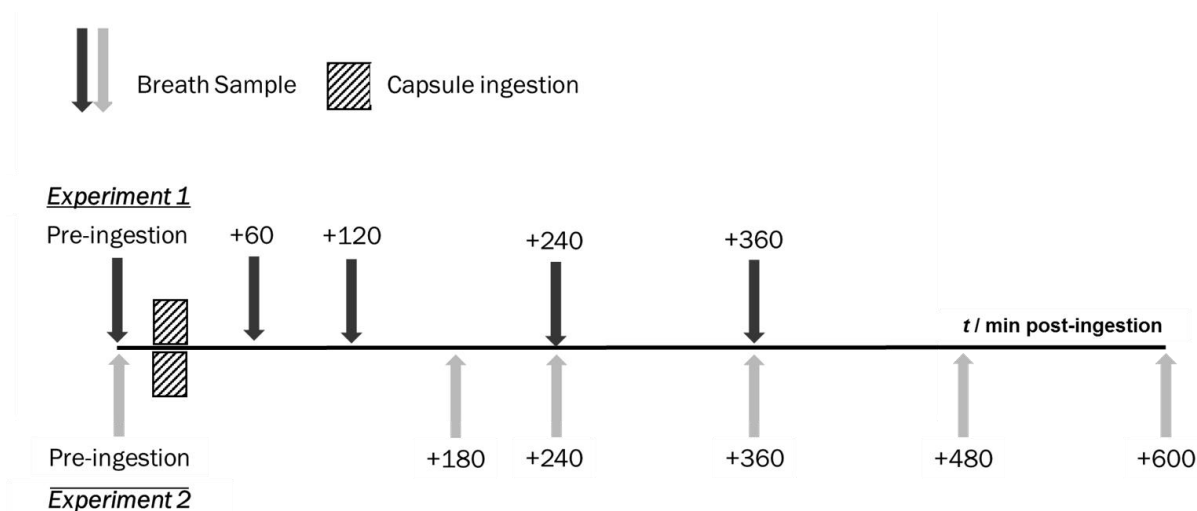


Figure 69 Schematic timeline for exhaled breath experiments for up to 360 (experiment 1) and 600 (experiment) minutes post-ingestion of a commercially available peppermint oil capsule

Note: t = time

6.3.6 Statistical analyses

Statistical analyses were performed using IBM SPSS Statistics (v 22.0, IBM Corp., Armonk, NY, USA). Wilcoxon signed rank tests were performed to assess the changes in intensity of the exhaled ion m/z 137 and 155 over time in comparison to baseline (0 min) measurements. All p values described in this manuscript refer to their Bonferroni adjusted values for multiple comparisons. An alpha (p) value of < 0.05 was deemed as statistically significant.

6.4 Results

6.4.1 GC-MS analysis of exhaled peppermint oil VOCs

A linear calibration was performed on menthone spiked onto TD tubes over a range from 0 to 8 ng on column mass (OCM) and a linear response was obtained (Figure 70). For the washout experiment performed on a single participant, Figure 71 shows that menthone was observed in the exhaled breath at all sampling time

points, including the baseline sample prior to ingestion of the capsule. The pre-ingestion sample displayed an OCM of 0.112 ng (corresponding to 56 pg L⁻¹ exhaled breath) and increased 7-fold to 0.771 ng OCM at 74 min (corresponding to 386 pg L⁻¹ exhaled breath). This concentration then dropped over time and reduced to near baseline levels of 0.166 and 0.131 ng OCM at 415 and 600 min, respectively. An overlay of the extracted ion responses for the menthone fragment ion at *m/z* 112 is shown in Figure 72 to enable visual comparison of the peak area response obtained for menthone at each time point.

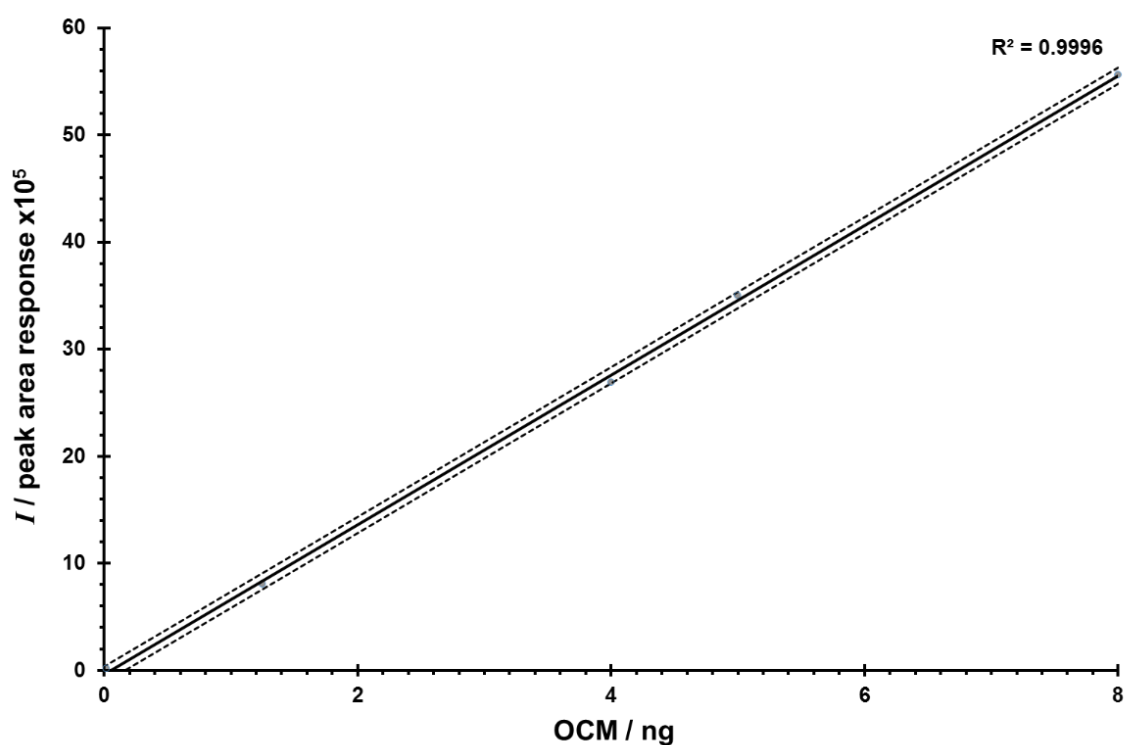


Figure 70 Calibration curve for menthone using thermal desorption-gas chromatography-electron ionisation mass spectrometry with linear fit (solid line) and 95% confidence intervals (dashed lines) plotted.

Note: *I* = intensity; OCM = on-column mass

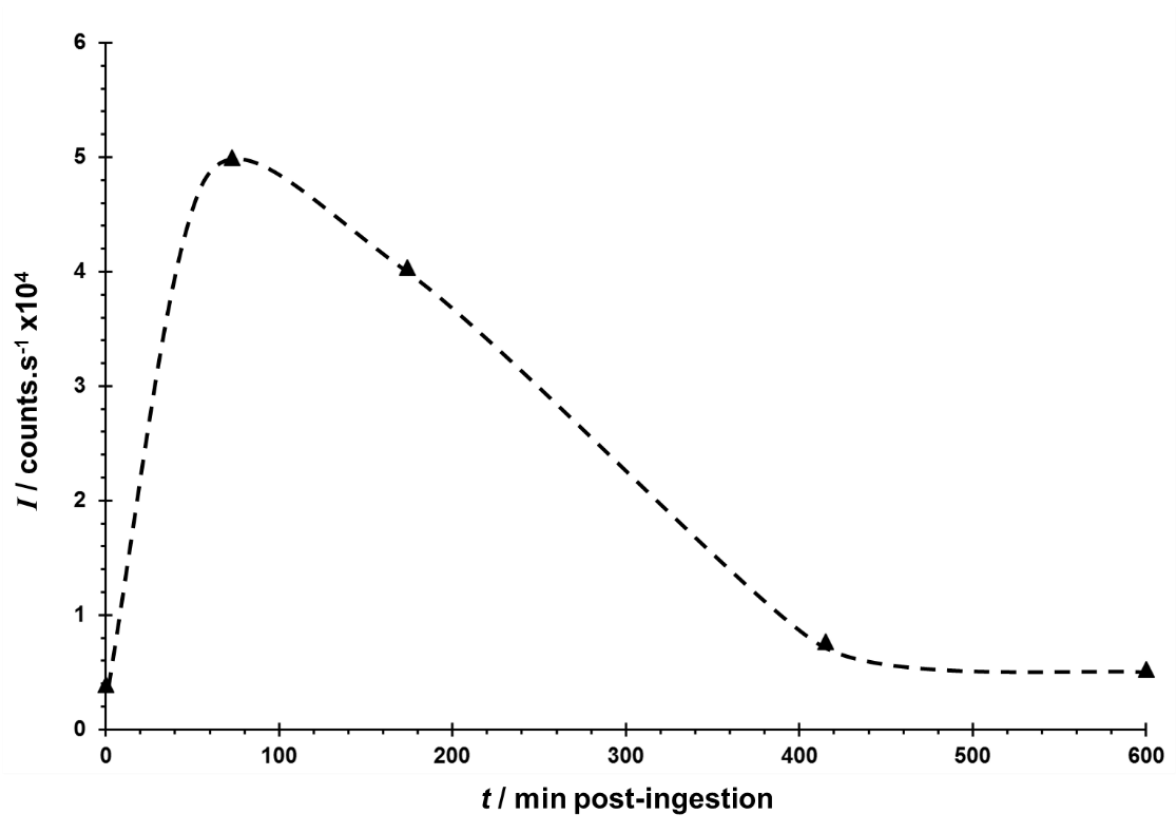


Figure 71 Figure to show the intensity of m/z 112 ion (menthone fragment) obtained by thermal desorption-gas chromatography-mass spectrometry against time over a 600 minute period post-ingestion of a peppermint oil capsule.

Note: I = intensity; t = time

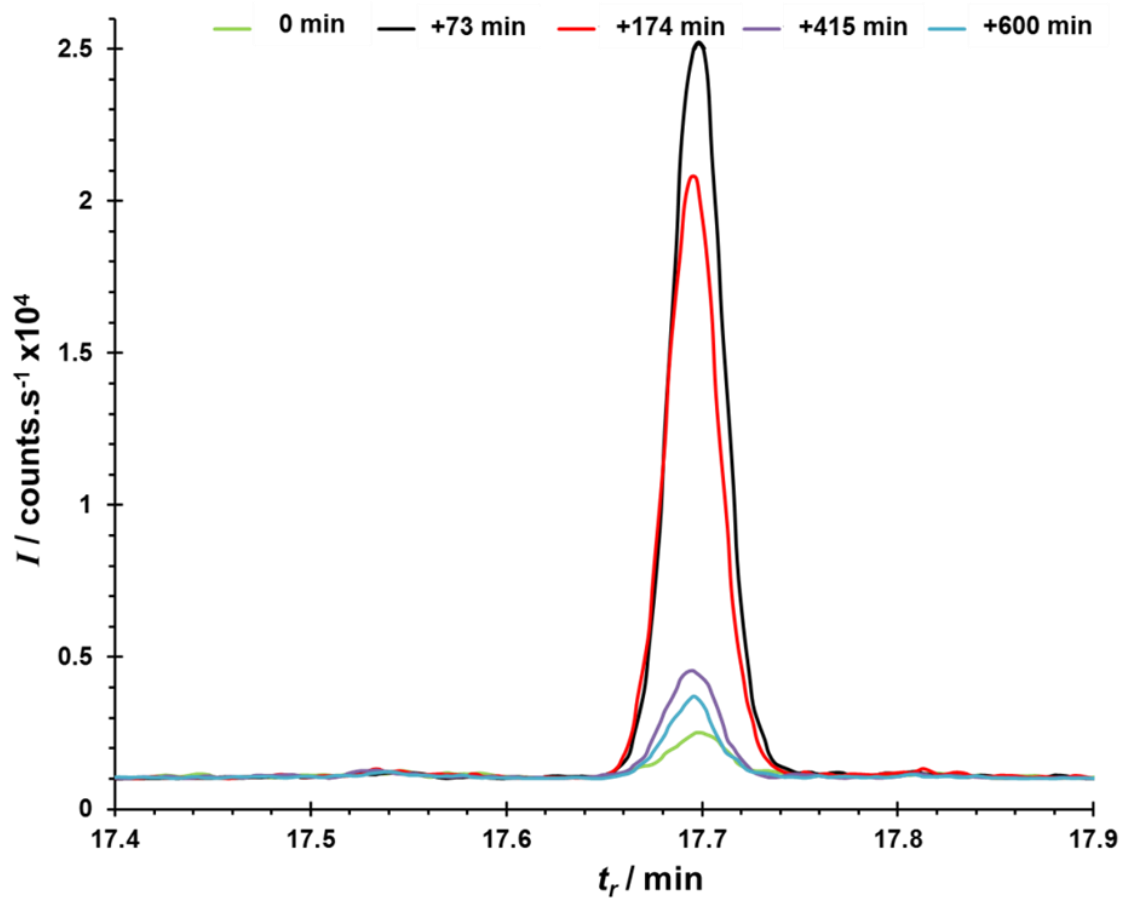


Figure 72 Overlaid extracted ion chromatograms for m/z 112 (menthone fragment) for each of the 5 sampling time points. Data obtained by analysis of exhaled breath by thermal desorption-gas chromatography-electron ionisation mass spectrometry.

Note: I = intensity; t_r = retention time

6.4.2 CMS analysis of exhaled peppermint oil VOCs

Comparison of breathing profiles using APCI-MS and breath mask pressure

Breathing profiles could be clearly observed in the total ion trace (Figure 73), where each peak demonstrated an increase in ion counts at the onset of exhalation, a plateau during steady-state exhalation and a reduced ion count at the cessation of exhalation and beginning of inhalation. This breathing profile followed an identical pattern to that seen in the pressure trace measured from the breathing mask (Figure 74).

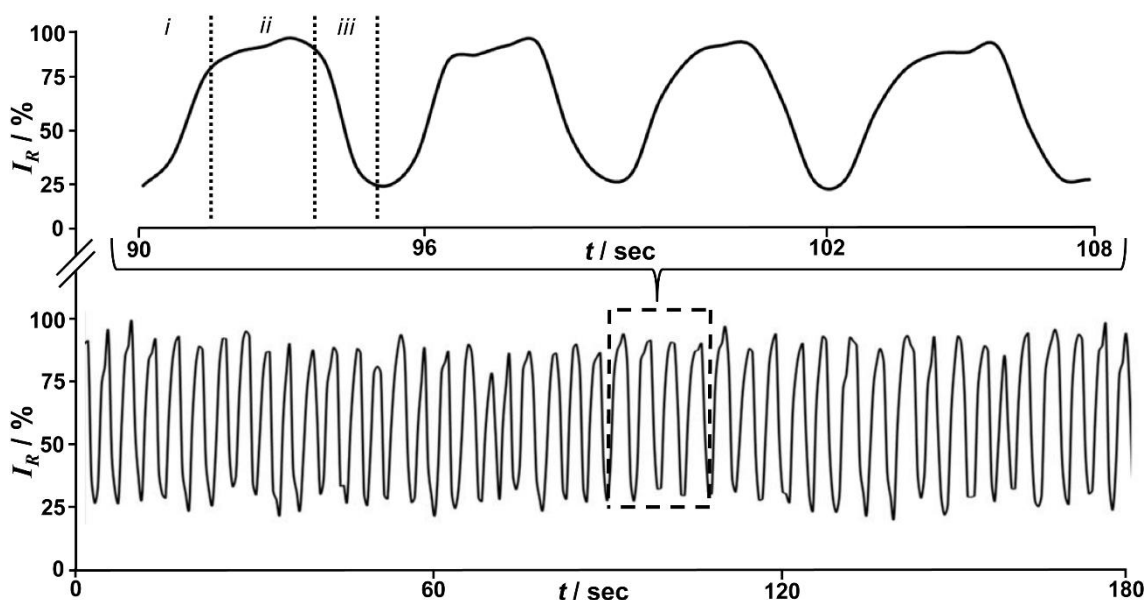


Figure 73 Example total ion trace for one participant over a 3 minute sampling period (bottom) with expanded view of four breaths (top) to show the total ion response corresponding to (i) the increased exhalation at the beginning of the breath, (ii) steady-state exhalation during the middle portion of breath and (iii) the cessation of exhalation and onset of inhalation toward the final stage of the breath.

Note: I_R = relative intensity; t = time

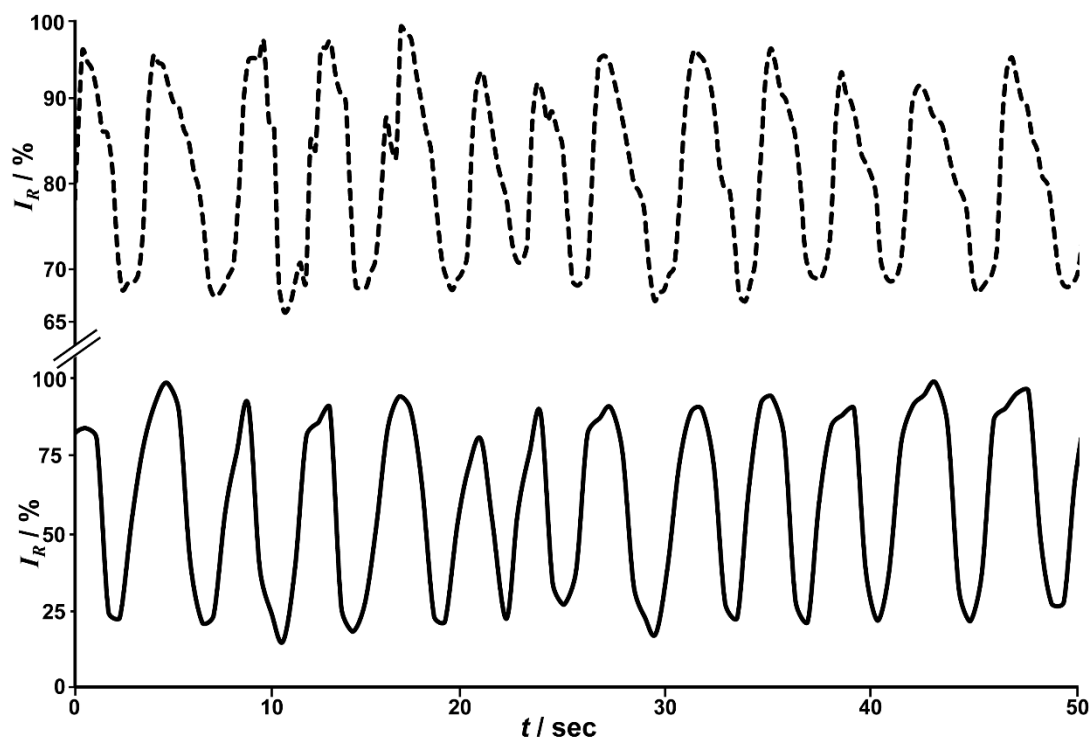


Figure 74 Example pressure trace of the full face breathing mask (top – dashed line) and the time-matched total ion response from the compact mass spectrometer (bottom – solid line). Each peak corresponds to one breath and shows a matching response of breathing profile from both sampling modalities.

Note: I_R = relative intensity; t = time

VOC profiles

Acetone in exhaled breath has been observed at concentrations ranging between 200 to 600 $\mu\text{g L}^{-1}$ in healthy individuals [20]. Exhaled breath VOC samples taken from participants before the peppermint oil was ingested all contained the acetone $[\text{M}+\text{H}]^+$ ion at m/z 59 as the base peak. Further, a proton bound dimer was also observed at m/z 117 (Figure 75).

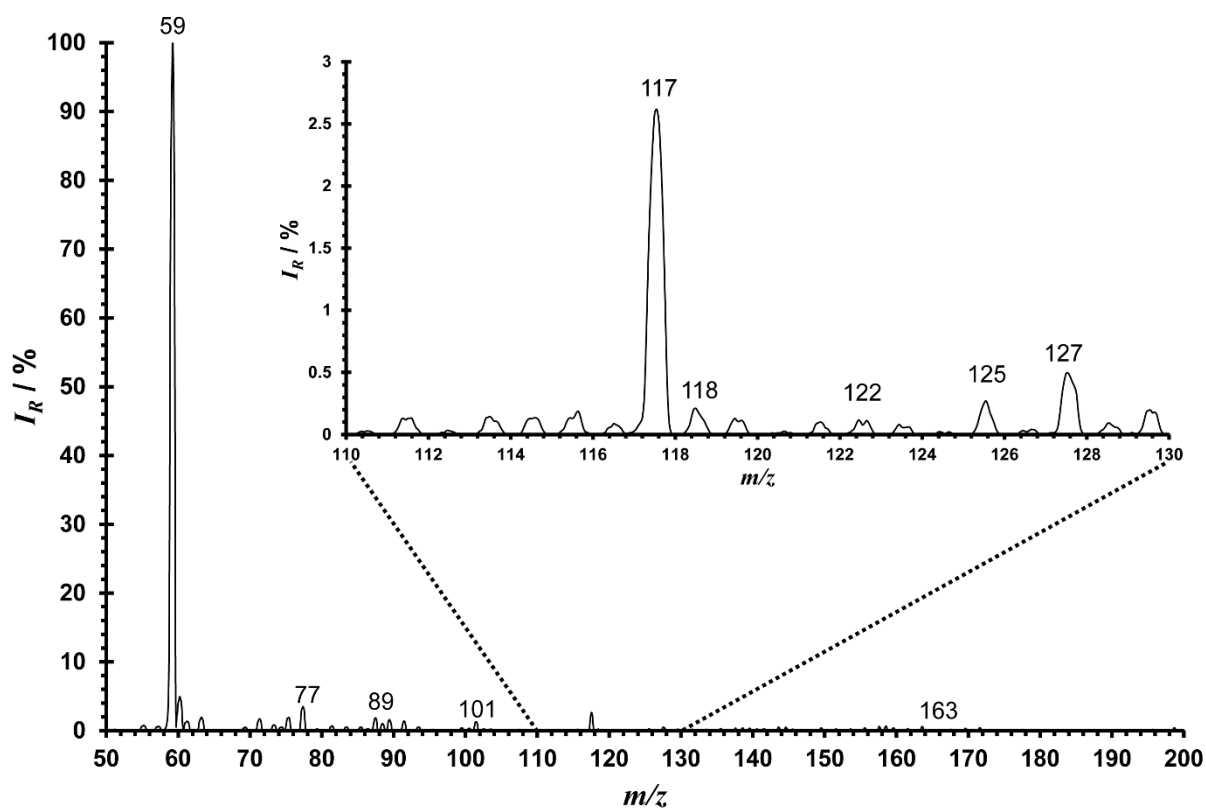


Figure 75 Averaged atmospheric pressure chemical ionisation mass spectrum for one participant prior to ingestion of a peppermint oil capsule.

Note: I_R = relative intensity; m/z = mass to charge ratio

Menthone emergence and elimination

Continuous real-time monitoring

Continuous real-time measurement of peppermint oil metabolite evolution in breath showed an increase in m/z 137 response after approximately 10-13 minutes post-ingestion. This increase can be attributed to the release of menthone from the ingested tablet as previous reported a reduction in exhaled menthone after 5 min of breathing synthetic air, remaining at the reduced levels for up to 30 min [21]. This continued to increase toward the end of the sampling period (Figure 76). The large intensity peak at 7 min corresponds to involuntary eructation producing a large response of the ion. This occurs due to the breakdown of the capsule in the

stomach, followed by an uncontrolled reflux of stomach gases containing high levels of peppermint oil components. Based on the data obtained from the 6 hr (360 min) experiments, the intensity of the m/z 137 is expected to further increase before reaching its peak intensity. This observation highlights the suitability of this method for the application of real-time breath analysis and shows the potential for on-line analysis of the metabolism of components released after digestion.

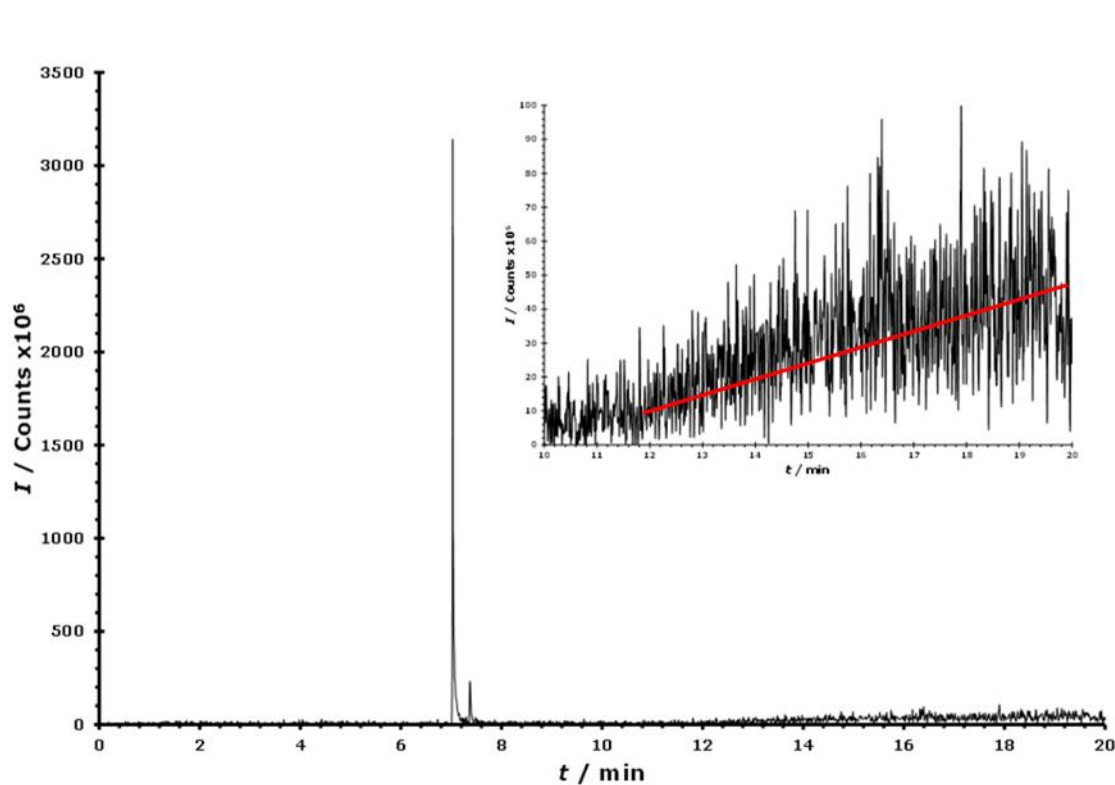


Figure 76 Extracted ion trace for m/z 137 in one participant for 20 min immediately post-ingestion of the peppermint oil capsule. Large peak intensity seen at 7 min corresponds to involuntary eructation. The inset shows the steady increase in m/z 137 observed between 10 to 20 min. A manually drawn trend line superimposed over the inset demonstrates the gradual increase in exhaled intensity over time.

Note: I = intensity; t = time

Extended protocol

The first sample time point after ingestion of the peppermint oil capsule was 60 min, see Figure 77. The three additional peaks reported from the APCI-MS menthone standard analysis were detected in the exhaled breath samples (m/z 81, 137 and 155). The most intense of the peaks resulting from peppermint oil dosing was at m/z 137.

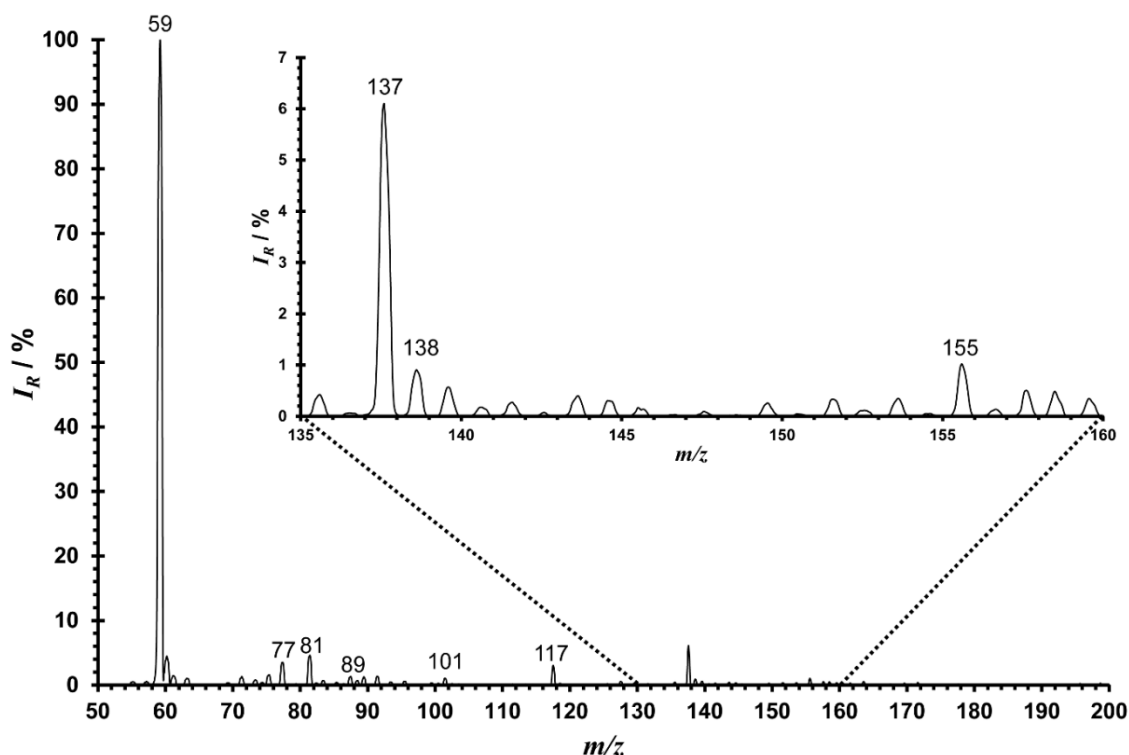


Figure 77 Averaged atmospheric pressure chemical ionisation mass spectrum for one participant at 60 minutes post-ingestion of a peppermint oil capsule.

Note: I_R = relative intensity; m/z = mass to charge ratio

The elimination of menthone was monitored by tracking the m/z 137 and 155 ion for all participants. Two distinct wash out profiles were observed. Twelve participants saw a rise in the intensity of the exhaled peppermint oil components at 60 min post-ingestion, before decreasing in an exponential manner over the sampling time period. Alternatively, delayed peak intensity was observed in 4 participants showing a maximal ion response at 120 min, reducing to similar levels

as the main group by 240 to 360 min (Figure 78 for m/z 137). For participants not showing a delayed maximal intensity, ion intensities for m/z 137 were increased at 60 min ($p=0.008$) and remained above baseline (0 min) levels for the entirety of the sampling period ($p\leq 0.009$), with ion intensities of the m/z 155 increased at 60 and 120 min ($p\leq 0.020$) and returning to baseline levels by 240 min ($p>0.05$). No statistical increases were reported in the delayed ion response group, due to underpowered analyses with $n=4$. Power calculations to report a significant difference at 60 min compared to baseline for a power of 80 % and a p value of < 0.05 indicate a sample group of $n=13$ would be required. When the two groups were combined, exhaled levels of m/z 137 remained above baseline values past 360 min post-ingestion ($p\leq 0.004$) and remained above baseline values for m/z 155 until 120 min post-ingestion (p 's=0.004) returning to baseline by 240 min post-ingestion ($p>0.05$).

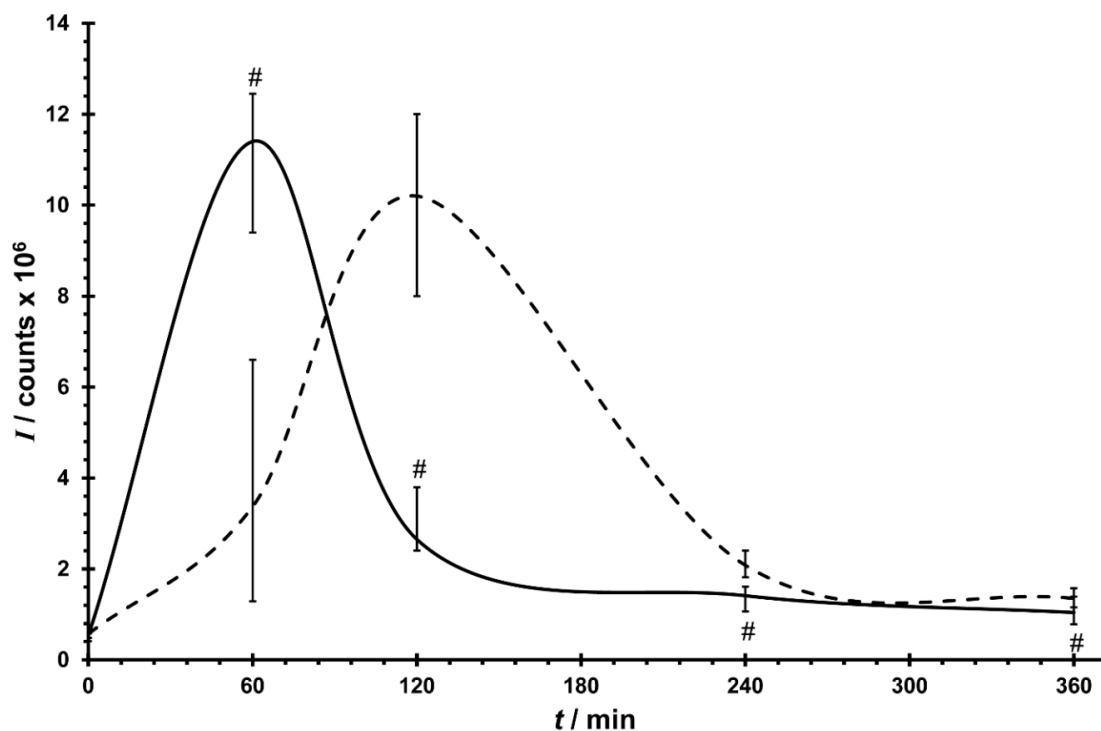


Figure 78 Extracted ion response for all participants stratified by common (solid line, $n=12$) and delayed (dashed lined, $n=4$) maximal intensities of m/z 137 from prior to and up to 360 min post ingestion of the peppermint oil capsule. Plotted points refer to the median value and error bars to the interquartile range. # $p\leq 0.009$.

Note: I = intensity; t = time

Samples collected for up to 10 hrs (600 min) after ingestion of the peppermint oil capsule showed further decrease of m/z 137 over time, with median values remaining above baseline throughout (data not shown). Statistically different levels were not observed in this cohort, again due to underpowered analyses with $n=4$. Final elimination of the peppermint oil compounds and a return to baseline values was predicted at approximately 10.5 to 11 hrs post-ingestion.

6.5 Discussion

The previously validated breath monitoring and sampling system interfaced to an APCI-CMS was shown to provide sensitive analysis of exhaled VOCs. Data obtained were ready for processing and evaluation directly from instrument without any further requirement for pre-processing preparation. Single breath measurements were demonstrated for metabolites, such as acetone, commonly measured in concentrations in the $\mu\text{g L}^{-1}$ down to ng L^{-1} levels. The introduction of a controlled and artificial change in breath profile was demonstrated by dosing with a peppermint oil capsule, indicating the potential use of the instrument to monitor real-time changes in metabolism (e.g. drug metabolism, responses to exercise etc.).

The full 3 min of data were averaged to give the spectra, and acetone and its dimer were detectable from a single breath in all participants without any prior pre-concentration, highlighting the sensitivity of this approach for the analysis of low molecular weight VOCs. The performance of the CMS in full scan mode compares favourably for this application with a quadrupole time-of-flight instrument which required pre-concentration of 2.5 L of breath on thermal desorption tubes to achieve a roughly comparable level of sensitivity, albeit with accurate mass measurement [9].

With refinement of the engineering, the CMS instrument is capable of in-situ breath analysis such as on a clinical ward or at pitch-side during a sporting event. The analysis time is compatible with embedding the procedure into training protocols for use by athletes and coaches. Further research is required to identify exhaled VOCs that are altered through events such as heavy training, injury or illness. Here is an opportunity to provide elite sports with a tool to assess the

athlete's health status. The identification of VOCs that are increased/decreased with the onset of an upper respiratory tract infection, or other common illnesses such as gastrointestinal disturbances may be seen as a priority research goal. Training or competing during the development of an illness increases the stress on the individual, and the probability of injury accompanied by a reduction in their performance. The impacts are a loss of training and competition time with follow-on consequences that last significantly longer than the episode of ill-health. Psychological impacts should not be discounted either, and for the top performers financial impacts may be substantial. Success here would allow coaches to protect the athlete from exacerbation of the health impacts from training and/or competition when it was medically inappropriate to do so. The longer term benefit is intended to be reduced recovery times and an overall increase in the opportunities for effective training/competition.

Additionally, with the development of breath-by-breath measurements it could be possible to monitor exercise-induced stress markers that enable personalised and stratified optimisation of training sessions, reducing over-training and realising the full potential of a training session.

The ability to transport the device for rapid analysis of exhaled VOCs in community settings for individuals for whom travel to a clinic is problematical, and frail or vulnerable patients in long term care, is attractive. In hospital, preliminary applications may be the monitoring of metabolism responses to drug therapy and research into such exhaled biomarkers is logical continuation of the research described here.

Comparison with the obtained calibration indicated that the concentration of menthone in the breath at the 360 min time point was approximately 21 ng L⁻¹. This cannot be compared directly with the APCI-MS system since there is no separation occurring before ions are detected on the APCI-MS system. Other peppermint oil species, such as α - and β -pinene and isomenthone, or metabolite species may possibly be contributing to the m/z 137 response. As menthone is one of the major components of peppermint oil (23.4 %, [17]), this suggests that the mass spectrometer is capable of detecting species in the sub- μ g L⁻¹ levels. This

observation highlights that the CMS with direct APCI analysis has potential as an in-clinic breath analyser

In conclusion, it has been shown here that a CMS is capable of being interfaced with an exhaled breath sampling device for a rapid, non-invasive on-line measurement of exhaled VOCs. Further development is required to achieve full mobilisation of the instrument and its true value to future sporting or medical situations will only be fully appreciated as exhaled VOC biomarkers are discovered through further research.

6.6 Acknowledgments

I would like to acknowledge Jim Reynolds, Matt Turner, Dorota Ruszkiewicz, Kayleigh Arthur and Andria Hadjithekli for their assistance during the experimental sampling period.

6.7 References

- 1 Kim KH, Kabir SAE. A review of breath analysis for diagnosis of human breath. *TrAC Trends Anal. Chem.* 2012;33:1-8
- 2 Turner MA, Bandelow S, Edwards L, Patel P, Martin HJ, Wilson ID, Thomas CLP. The effect of a paced auditory serial addition test (PASAT) intervention on the profile of volatile organic compounds in breath: a pilot study. *J. Breath Res.* 2013;7:017102
- 3 Trefz P, Roesener L, Hein D, Schubert JK, Miekisch W. Evaluation of needle trap micro-extraction and automatic alveolar sampling for point-of-care breath analysis. *Anal. Bioanal. Chem.* 2013;405:3105-15
- 4 Beauchamp J, Herbig J, Gutmann R, Hansel A. On the use of Tedlar® bags for breath-gas sampling and analysis. *J. Breath Res.* 2008;2:046001

5 Trefz P, Schmidt M, Oertel P, Obermeier J, Brock B, Kamysek S, Dunkl J, Zimmermann R, Schubert JK, Miekisch W. Continuous real time breath gas monitoring in the clinical environment by proton-transfer-reaction-time-of-flight-mass spectrometry. *Anal. Chem.* 2013;85:10321-9

6 Smith D, Španěl P, Herbig J, Beauchamp J. Mass spectrometry for real-time quantitative breath analysis. *J. Breath Res.* 2014;8:027101

7 Chen HW, Venter A, Cooks RG. Extractive electrospray ionization for direct analysis of undiluted urine, milk and other complex mixtures without sample preparation. *Chem. Comm.* 2006;19:2042-4

8 Reynolds JC, Blackburn GJ, Gullar-Hoyas C, Moll VH, Bocos-Bintintan V, Kaur-Atwal G, Howdle MD, Harry EL, Brown LJ, Creaser CS, Thomas CLP. Detection of volatile organic compounds in breath using thermal desorption electrospray ionization-ion mobility-mass spectrometry. *Anal. Chem.* 2010;82:2139-44

9 Reynolds JC, Jimoh MA, Gullar-Hoyas C, Creaser CS, Siddiqui S, Thomas CLP. Analysis of human breath samples using a modified thermal desorption: gas chromatography electrospray ionization interface. *J. Breath Res.* 2014;8:037105

10 Chen H, Wortmann W, Zhang R, Zenobi R. Rapid in vivo fingerprinting of nonvolatile compounds in breath by extractive electrospray ionization quadrupole time-of-flight mass spectrometry. *Angew. Chem. Int. Ed. Engl.* 2007;46:580-3

11 Ding J, Yang SP, Liang DP, Chen HW, Wu ZZ, Zhang LL, Ren Y. Development of extractive electrospray ionization ion trap mass spectrometry for in-vivo breath analysis. *Analyst* 2009;134:2040-50

12 Taylor AJ, Linforth RST, Harvey BA, Blake A. Atmospheric pressure chemical ionisation mass spectrometry for in vivo analysis of volatile flavour release. *Food Chem.* 2000;71:327-38

13 Taylor AJ, Linforth RST. Direct mass spectrometry of complex volatile and non-volatile flavour mixtures. *Int. J. Mass Spectrom.* 2003;223-224:179-91

14 Berchtold C, Meier R, Zenobi R. Evaluation of extractive electrospray ionisation and atmospheric pressure chemical ionisation for the detection of narcotics in breath. *Int. J. Mass Spectrom.* 2011;299:145-50

15 Browne DL, Wright S, Deadman DJ, Dunnage S, Baxendale IR, Turner RM, Ley SV. Continuous flow reaction monitoring using an on-line miniature mass spectrometer. *Rapid Commun. Mass Spectrom.* 2012;26:1999-2010

16 Joshi A, Bhoje M, Sattarkar A. Phytochemical investigation of the roots of *Grewia microcos* Linn. *J. Chem. Pharm. Res.* 2013;5:80-7

17 Schmidt E, Bail S, Buchbauer G, Stoilova I, Atanasova T, Stoyanova A, Krastanov A, Jirovetz L. Chemical composition, olfactory evaluation and antioxidant effects of essential oil from menthe x piperita. *Nat. Prod. Commun.* 2009;4:1107-12

18 Steeghs MML, Crespo E, Harren FJM. Collision induced dissociation study of 10 monoterpenes for identification in trace gas measurements using the newly developed proton-transfer reaction ion trap mass spectrometer. *Int. J. Mass Spectrom.* 2007;263:204-12

19 Basanta, Koimtzis T, Singh D, Wilson I, Thomas CLP. An adaptive breath sampler for use with human subjects with an impaired respiratory function. *Analyst* 2007;132:153-63

20 Wang ZN, Wang CJ. Is breath acetone a biomarker of diabetes? A historical review on breath acetone measurements. *J. Breath Res.* 2013;7:037109

21 Maurer F, Wolf A, Fink T et al. Wash-out of ambient air contaminations for breath measurements. *J. Breath Res.* 2014;8:024107

CHAPTER SEVEN: GENERAL DISCUSSION

This thesis proposes that exhaled breath analyses have a potential role in enhancing competitive sport and general exercise, and as such there is a basis for further research. Breath as a sampled medium in exercise, most notably sports training and competition, has yet to be properly explored. The ability to make rapid and non-invasive measurements that provide previously unobtainable information on the athletes' metabolism and condition would be advantageous. The ability to enhance training and competition would be of great interest to athletes, coaches and non-professional sports players. This research sought to prospect the use of exhaled breath analysis in exercise-as-medicine and sports performance contexts.

7.1 Review of swimming impacts on breath profiles

7.1.1 *Summary of findings*

In Chapter 4, exhaled breath monitoring was used to assess potential lung health impacts associated with swimming in a chlorinated pool environment. Known disinfection by-products (DBPs) were monitored in exhaled breath both before and for several hours after a 30 min recreational swim. Rapid rises in the exhaled breath concentrations of 3 trihalomethane DBPs were observed, with peak concentrations reported immediately post-swimming. The largest rise was observed with chloroform (median = 121-fold increase across 19 male participants), followed by bromodichloromethane (4.4-fold) and dibromochloromethane (1.8-fold). Three participants showed a delay in the build-up of peak exhaled intensity, with highest concentrations noted at 90 min post-swimming. Previous reports have not observed this modified wash out profile. Although reasons for delayed kinetics are unknown, ingested pool water may have provided DBPs that were released only after further processing in the digestive tract. General wash out kinetics, i.e. rapid increase with a decline slowing over an extended period, are in-line with previous studies [1-4].

This research was able to define wash out characteristics in a larger cohort than previous reports, allowing for the identification of delayed responders. Although this better defines the nature of wash out kinetics, further investigation is required to support these observations.

A novel approach used to assess chlorine-based swimming pool insults was the metabolomic treatment of the data. Analyses isolated exhaled compounds that reported an increased trend in exhaled concentration over 10 hrs post-swimming. These were BRI-1461-43-107-93-41-69 (geranylacetone, CAS: 3796-70-1) and BRI-1337-146-145-0-0-0 (2-benzofurancarboxaldehyde, CAS: 4265-16-1). This is the first report to identify these molecules in response to exercise. Geranylacetone is associated with cell signalling, fuel storage and membrane integrity stability [5]; therefore its presence provides a plausible link to an inflammatory response. It is neither possible to attribute, nor rule out, this as a response to chlorine-induced inflammation. The identification of a ketone body suggests possible emergence of a marker to reflect biological stress, whether it be oxidative or inflammatory. Further work is required to either eliminate or support this finding. The study involved young (mean 25 (95 % confidence intervals (CI) 24 to 26) yrs) but fully matured males. An important aspect for future study would be to investigate the impact to chlorinated swimming pool exposure in the adolescent lung. The complexity of the human lung increases during maturation, and exposure to these chemicals could cause transient problems during developments stages. The effect of potential early residual damage should be investigated more thoroughly.

This is the first report of non-targeted metabolomics for exhaled breath volatiles using a wide-range mass to charge (m/z) scan performed in conjunction with any mode of exercise.

7.1.2 Recommendations for follow on studies

Relocate on-site sampling station

Two samples, pre- and 5 min post-swimming, were collected within the swimming pool complex. Although not directly connected to the swimming pool and adequately

ventilated, contamination with DBPs was still present and environmental artefacts may have been present during breath sampling. However, blank samples of the filtered air supply were shown to contain levels lower than those measured in the breath (Table 11, Section 4.5.3). Experimental design would be improved if all samples were taken off-site, with an adjacent building or a mobile laboratory providing suitable alternatives.

Management of exercise intensity

Participants exercised for 30 min at a pace to push their own limits, but not so that they were unable to complete the full exercise duration. As with any exercise, swimming requires a combination of physical fitness and technical ability. Although none of the participants were regular swimmers, a range of swimming ability meant that certain individuals were able to swim further distances. Heart rate and respiration levels were not possible during the exercise meaning accurate levels of respiratory exposure were not monitored. Nevertheless, variability was addressed through selection of phenotypically matched participants (19 healthy males; mean body mass index (BMI) 24.8 (95 % CI 23.3 to 26.2) kg m⁻², age 25 (24 to 26) yrs). Inclusion of pool-capable on-line measurements of expired oxygen, heart rate and breathing rate would be beneficial for future investigations. The removal of the need to swim is a potential design modification. More specifically, alternative exercise modalities could be performed in the swimming pool, such as aqua jogging. This would remove the requirement for technical swimming ability whilst maintaining a pool-based protocol. Nonetheless, the nature of variability in VOC profiles between matched phenotypes was observed throughout the samples collected in this research, regardless of exercise ability.

In addition, inclusion of control conditions would benefit the experimental conclusions and provide more robust comparisons. Each participant would serve as their own control, using a 4-way randomised crossover research design. The 3 protocols would consist of:

- i) exercise in a swimming pool environment;
- ii) exposure to a swimming pool environment without exercise;

- iii) matched exercising intensity performed in an alternative location;
- iv) a time-matched period without exercise.

7.2 Review of fitness prediction breath test

7.2.1 *The prospect of rapid assessment of physical fitness*

Data obtained in Chapter 5 indicate the potential to categorise individuals into levels of absolute maximal oxygen uptake ($\dot{V}O_{2\max}$) using exhaled concentrations of acetone and isoprene (median ratios to internal standard (interquartile range (IQR)) for low versus high absolute $\dot{V}O_{2\max}$ group; acetone 8.93 (4.38 to 10.53) versus 5.71 (3.98 to 7.19); isoprene 7.60 (3.72 to 11.08) versus 4.83 (2.86 to 7.44). Furthermore, a general linear model with stepwise entry isolated exhaled compounds that were significantly related to the measure of absolute $\dot{V}O_{2\max}$ values. This technique takes the inputted independent variables and adds one variable per iteration in a stepwise manner, until a model is produced that contains all of the dependent variables independent predictors. One molecule (BRI-818-43-85-41-57-70) displayed a significant negative correlation ($r_s = -0.442$, $p=0.019$) with absolute $\dot{V}O_{2\max}$. However, variability observed across participants highlighted the requirement for a larger sample power to confidently assign an association. The prospect of acetone and isoprene monitoring as a targeted measurement for the rapid assessment of physical fitness is attractive. These are ubiquitous breath analytes, related to metabolism, that are at concentrations high enough to be analysed with relative ease [6]. The scope for this application is wide, from the monitoring of incapacitated persons to the support of an elite athlete. In sporting contexts, this test offers condition monitoring without added physical exertion.

Participants were young (mean age 23 (95 % CI 22 to 24) yrs), healthy (BMI 25.3 (24.5 to 26.2) kg m^{-2} , $\dot{V}O_{2\max}$ 46.5 (44.6 to 48.4) $\text{mL}(\text{O}_2) \text{kg}^{-1} \text{min}^{-1}$, self-reported vigorous exercise 307 (245 to 370) min.wk^{-1}) and disease-free, and would be suitable a control set in diagnostic investigations. Nevertheless, data suggest that, even within this set of 'control' participants, exhaled VOC differences are present. Multivariate discriminant analyses were able to separate participants

categorised as high (median 4.3 (IQR 4.0 to 4.4) L(O₂) min⁻¹) and low (3.4 (3.3 to 3.4) L O₂ min⁻¹) absolute $\dot{V}O_{2max}$. Further investigation reported that acetone and isoprene were 2 of the major discriminants. Statistical significance was not met for these molecules, however clear trends for reduced levels in higher absolute $\dot{V}O_{2max}$ levels were observed. This raises an interesting question; what would the defining characteristics of a control cohort be? For example, acetone and isoprene have been related to disease states (e.g. in critically ill patients and diabetes [7]). All participants were informed to arrive at the laboratory in a fasted state, normalising the effect of rises in acetone during starvation [8]. Under the assumption that protocol was followed, any differences cannot be attributed to the fasted state. Acetone levels showed a decrease with increased oxygen capacity, and suggest that previously reported disease associations may be related the measurement of inactive individuals.

7.2.2 Recommendations for future studies

Incorporate a longitudinal research design

A major limitation in this study was the relatively narrow range of physical fitness within participants. A longitudinal study tracking changes in exhaled VOCs throughout an exercise training intervention would contribute further understanding to the field. This fitness contrast could be assessed and VOCs mapped against rises in maximal oxygen uptake.

Baseline repository

The fasted, resting breath samples from a cohort of young and healthy male participants that were captured in this study forms a valuable resource. This cohort of participants forms the basis of a well-defined and phenotypically matched group of 'control' participants with corresponding exercise capacity data. This information is envisaged to be beneficial to the wider research community. Future plans to release this cohort as freely accessible will allow for researchers to compare like-for-

like data against these participants, and adjust for physical fitness where appropriate.

VOC profiles from a maximally exercised metabolism.

It was anticipated that maximal levels of physical exertion would induce changes in metabolism and be reflected in the exhaled breath profiles. This was not observed. Isoprene was identified to change in exhaled concentration across the three sampling time points. An expected reduction in concentration post-exercise was observed. This confirmed a previous report where it was proposed that a 'store' of isoprene, perhaps in the working muscles, was being released during exercise [6]. Isoprene concentrations returned to baseline levels after one hour. The methodology was not able to record the rate of return or concentration dynamics.

The need for on-line measurements

The measurement procedure was limited by the total number of samples that were accessible. On-line measurements were needed and not available. Transient short-lived changes could not be monitored during or immediately after exercise, nor could rates of change in concentration. This limitation could be overcome with further development of on-line breath analyses using a compact mass spectrometer, as described in Chapter 6.

The experimental design was not able to monitor breath profiles over an extended period. Changes in metabolism and associated VOC markers may take several hours to manifest themselves, and future experiments would benefit from a longer follow-up period.

7.3 Increased cohort size

Difficulties encountered from the observed variability in exhaled VOCs would be reduced with increased sample sets. Chapter 5 utilised only male participants who were all sport-active and within a narrow age range (18 to 30 yrs). Future

investigations would benefit by repeating the experimental design, with the addition of (an) older age group(s) (e.g. 30 to 50 and 50 and over). This would allow for greater understanding of whether observed changes translate to another age group and cohort. Importantly, critically ill patients who cannot perform physical exercise tests are often older individuals, and comparing exhaled data to those from young adults may not be appropriate. The addition of female participants would allow investigation of gender-specific reactions. Female metabolism may be partly regulated by the menstrual cycle, therefore the timing of sampling must be taken into consideration during future investigations.

Studies would also benefit from an extended platform of analytical tests. For example, the introduction of ion mobility spectrometry may allow further delineation of exhaled VOCs. A multiplex approach would allow for a more comprehensive analysis of obtained data.

Stratification of participants by high/low $\dot{V}O_{2\max}$ values, inevitably produced a reduced cohort size for comparison, and therefore reduced statistical power for tests of difference. Power calculations for a power of 80% and a p value < 0.05 reported that group samples sets of 36 and 41 would be required to record statistical differences in acetone and isoprene, respectively. Therefore, for future investigations it is advised that a minimum cohort of 80 individuals is used for each grouping to be investigated; i.e. 80 young males, 80 young females, 80 older males etc. The larger group size would allow for adequate stratification at the median, and produce more robust correlation analyses.

7.4 An on-line breath analyser for breath-by-breath monitoring

A sampling interface was developed to allow the adaptation of a compact mass spectrometer, in order to enable on-line measurement of exhaled volatiles. This modification enabled the provision of instant readings, a requisite feature for the elite sporting community. The concept was tested using an ingested peppermint oil capsule enabling breath-by-breath concentrations of exhaled menthone to be tracked for up to 10 hrs. In addition to the on-line breath-by-breath approach, data

can be collected on ion accumulation over a short (3 min) period, and analysed instantly.

Important operational aspects that have yet to be resolved satisfactorily are the provision of portable air and nitrogen supplies. This requires the construction of a custom built trolley with these items incorporated. More significantly, if breath analyses are to be performed with participants during or immediately after exercise, then the breath sampling system needs to be redesigned. Participants require sufficient air to breathe at ventilatory rates of up to 200 L min⁻¹ (data not shown from $\dot{V}O_{2\max}$ exercise test collections). This is significantly higher than the 30 L min⁻¹ supplied to the current system. Future studies, including those that are outlined in this thesis, would benefit greatly from the development and application of this system for use in exercise research.

7.5 Concluding remarks

The research presented in this doctoral thesis describes initial investigations into the integration of exhaled breath VOC analyses into a performance-based sports monitoring context. This is the principle report to show exhaled metabolites as a potentially functional analysis for reporting physical capability. The findings are of interest, but with the requirement for future developments and validation. This thesis has investigated the use of exhaled breath in two domains:

- i) health based monitoring, whether it be within athletes/exercising individuals or those suffering or recovering from health complications;
- ii) performance based monitoring for athletes.

The research describes the analysis of potentially harmful chlorinated DBPs and their delayed removal from the biological system. Tentative identifications of metabolites that show an up-regulated trend, and that may be attributable to a post-contamination inflammatory response, were proposed. Furthermore, it describes an initial use of exhaled breath volatiles as a potential non-invasive analytical test to monitor physical fitness and exercise capacity. Finally it described preliminary advances in allowing analyses using a portable mass spectrometer to be done in real-time.

The advancement of this research would progress the field, by offering the possibility of a wider scope of health and fitness monitoring. Our understanding of the possibility of lung injuries, and accumulative damage of repeat exposure to swimming pool environments, remains poor. Swimming is a form of exercise promoted as beneficial to those with respiratory complaints such as asthma. However, an unequivocal rebuttal to swimming-exacerbated respiratory problems is not possible, nor is it supported by the findings from this research. Swimming is the most recreationally popular activity in the United Kingdom [9] and promoted heavily within primary schools. It is important to assess possible health impacts that may occur in the developing lung and ascertain whether chlorine exposure and inhaled DBPs are causing detrimental effects. The answers to such questions will require the implementation of highly sensitive exhaled breath assays within scaled and properly stratified cohorts.

The capability to monitor physical performance through exhaled breath analysis would benefit athletes and health professionals alike. The impact of an assay that could adequately monitor the fitness of individuals prescribed exercise rehabilitation would be substantial. Cardiovascular rehabilitation, after events such as stroke, myocardial infarction and heart failure, would enjoy notable benefit from advances in this field. It would also allow physicians to develop a better understanding of if, and how, an exercise regime is benefitting an individual. Furthermore, these innovations would advance the movement toward personalised precision medicine. In the context of sport, the ability to monitor, or acutely assess, fitness capabilities would enable athletes to reduce their exhaustive testing burden, allowing them to focus on their applied training in their respective sports. In addition, this aspect of monitoring would likely be of interest to the military services, allowing for the regular monitoring of fitness levels in serving personnel. These advances are not without their difficulties, but the preliminary data described in this thesis show initial steps toward these difficult but rewarding goals.

7.6 Conclusion

In conclusion, the research described in this thesis has demonstrated, for the first time, the possibility of exhaled breath monitoring in an exercising and sporting context. It has also yielded insights into potential health impacts and personalised and/or stratified training. The experiments are not without flaws and their shortcomings stimulated the development of a new, on-line, at-track/pool/clinic instrument. This has since been developed further and is due to be released as a commercial product in Q2 2016 by Advion. These first studies engender a hope that they could be repeated and developed, so that the techniques they employed become common practice in the future.

7.7 References

- 1 Aggazzotti G, Fantuzzi G, Righi E, Predieri G. Environmental and biological monitoring of chloroform in indoor swimming pools. *J. Chromatogr. A* 1995;710:181-90
- 2 Lindstrom AB, Pleil JD, Berkoff DC. Alveolar breath sampling and analysis to assess trihalomethane exposures during competitive swimming training. *Environ. Health Perspect.* 1997;105:636-42
- 3 Aggazzotti G, Fantuzzi G, Righi E, Predieri G. Blood and breath analyses as biological indicators of exposure to trihalomethanes in indoor swimming pools. *Sci. Total Environ.* 1998;217:155-63
- 4 Caro J, Gallego M. Alveolar air and urine analyses as biomarkers of exposure to trihalomethanes in an indoor swimming pool. *Environ. Sci. Technol.* 2008;42:5002-7

5 Metabocard for geranylacetone (HMDB31846). Human metabolome database. <http://www.hmdb.ca/metabolites/HMDB31846> (accessed 14 February 2016)

6 King J, Kupferthaler A, Unterkofler K, Koc H, Teschl S, Teschl G, Miekisch W, Schubert J, Hinterhuber H, Amann A. Isoprene and acetone concentration profiles during exercise on an ergometer. *J. Breath Res.* 2009;3:027006

7 Amann A, Costello Bde L, Miekisch W, Schubert J, Buszewski B, Pleil J, Ratcliffe N, Risby T. The human volatilome: volatile organic compounds (VOCs) in exhaled breath, skin emanations, urine, feces and saliva. *J. Breath Res.* 2014;8:034001

8 Statheropoulos M, Agapiou A, Georgiadou A. Analysis of expired air of fasting male monks at Mount Athos. *J. Chromatogr. B* 2006;832:274-9

9 Sport England. Active people survey 7. http://archive.sportengland.org/research/active_people_survey/active_people_survey_7.aspx (accessed 29 November 2015)